Production of self-inactivating lentiviral vectors by constitutive packaging cell lines for gene therapy clinical applications

Khaled Sanber

Thesis submitted to University College London

for the degree of Doctor of Philosophy

2015

Cancer Institute

University College London

DECLARATION

I, Khaled Sanber, confirm the work presented in this thesis is my own. Where information has been derived from other sources, I confirm that this has been indicated in the thesis.

ABSTRACT

Lentiviral vectors (LVs) are useful experimental tools for stable gene delivery and have been used to treat human inherited genetic disorders and hematologic malignancies with promising results. Because some of the LV components are cytotoxic, transient plasmid transfection has been used to produce the large batches needed for clinical trials. However, this method is costly, poorly reproducible and hard to scale up.

Generation of stable packaging cell lines (PCLs) that continuously produce LVs can potentially overcome these limitations. The WinPac-RDpro cell line was developed between Collins and Takeuchi laboratories in Division of Infection and Immunity, UCL by inserting a codon-optimized HIV-1 *Gag-Pol* expression cassette in a continuously expressed locus in 293FT cells using Cre recombinase-mediated cassette exchange (RMCE). Subsequently HIV-1 *Rev* and *RDpro* envelope expression cassettes were serially transfected. In this thesis, WinPac-RDpro cells were used to generate model producer cells by stably transfecting a plasmid expressing a SIN GFP-encoding LV. Vector titers in excess of 10^6 293T transducing units (TU)/ml could be repeatedly harvested from the final producer clones in a volume of >0.5 L even under reduced serum conditions. Titers could be increased to around 1 x 10^8 293T TU/ml by concentration using scalable tangential flow filtration (TFF). Additionally, these LVs efficiently transduced human T cells and CD34+ cells at low multiplicities of infection (MOI). Titers in excess of 10^6 TU/ml were achieved using an RMCE-based strategy that was aimed at introducing a SIN LV expression cassette at a pre-selected locus. Similar titers were also achieved by using a promoterless selectable marker cloned *in cis* to the vector genome expression cassette.

Furthermore, the Cocal Virus G protein (COCV-G) was stably expressed in WinPac cells to generate WinPac-CVG cells. These packaging cells were able to support the production of COCV-G pseudotyped SIN LVs at high titers (up to 10^6 TU/ml) following transient supplementation of a SIN LV expression plasmid. The efficient and stable expression of SIN LV genomes in these cells is expected to facilitate high-titer production of vectors with favorable characteristics.

In conclusion, the work presented here provides significant improvements to available LV production methods. This will be of use to all basic and clinical investigators

who wish to produce large batches of LVs, and addresses an important issue that has hindered large-scale LV clinical testing and application.

ACKNOWLEGDEMENTS

I am truly grateful to Prof. Mary Collins and Dr. Yasuhiro Takeuchi for supervising this PhD. Mary's unwavering support since I first joined the lab has been a great asset. Her insight and direction towards achieving significant long-term goals kept me focused throughout this PhD. Yasu's friendly advice and guidance were and will always be sincerely appreciated. His trust in my abilities motivated me to work hard to meet his expectations.

I was lucky to be part of the Collins and Takeuchi labs, where I was exposed to a very stimulating environment. This allowed me to build my research skills and knowledge especially with the kind help of Mehdi Baratchian and Ilaria Nisoli, to whom I am most obliged. I also enjoyed working alongside other dear friends and colleagues in the lab including Kanayo Doi, Juan Ribes, Christopher Bricogne and Kam Zaki.

I have to thank Sean Knight and Sam Stephen who had started the work on which this thesis integrally depended. Sean's help at the beginning of my PhD was vital and greatly beneficial. I wish Maha Tijani, with whom I enjoyed working, all the best in carrying this project forward.

I was also fortunate enough to work at the Wohl Virion Centre, where I was warmly welcomed throughout the majority of my PhD work by Robin Weiss, Ariberto Fassati and Clare Jolly. The feedback and excellent advice I received during joint lab meetings have been invaluable. The Wohl was also a second home where I made long-lasting friendships. Edward Tsao's, Alice Len's, Gordon Cheung's and Aksana Labokha's help, advice and friendship will always be fondly remembered.

I am eternally indebted to my parents whose kindness and wisdom equipped me with the tools I needed to get to where I am today. Their unconditional love and support allowed me to pursue my passions without hesitation. Additionally, my brother's steadfast belief in me and his encouragement have kept me determined to surmount all challenges during the last three years.

Last but not least, I wish to thank my friends who have been thousands of miles away and yet so close. They have never failed me in times of need, and have always made the good times merrier and blissfully memorable.

TABLE OF CONTENTS

LIST OF FIGURES

LIST OF TABLES

ABREVIATIONS

A	Active state
aa	Amino acid
APC	Antigen presenting cell
A3G	APOBEC3G
ADA-SCID	Adenosine deaminase deficiency-SCID
ALD	Adrenoleukodystrophy
APOBEC	Apolipoprotein B mRNA editing enzyme, catalytic polypeptide-like
BCA	Bicinchoninic acid
BlaS	Blasticidin S
BPlPuH	Blasticidin S + phleomycin + puromycin + hygromycin
BPuH	Blasticidin S + puromycin + hygromycin
BSA	Bovine serum albumin
bsr	Blasticidin resistance gene
°C	Degrees Celsius
CA	Capsid protein
CAI	Codon adaptation index
CAR	Chimeric antigen receptor
cDNA	Complementary DNA
CGD	Chronic granulomatous disorder
CHAV	Chandipura Virus
CHAV-G	Chandipura Virus protein G
CIS	Common integration site
CMV	Cytomegalovirus
CO	Codon-optimized
COCV	Cocal Virus
COCV-G	Cocal Virus glycoprotein G
cPPT	Central polypurine tract
CS	10-layer cellSTACK
CypA	Cyclophilin A
D1	DMEM + 1% FBS
D10	DMEM + 1% FBS

DC	Dendritic cells
ddH_2O	Double distilled water
DMEM	Dulbecco's modified Eagle's medium
DNA	Deoxyribonucleic acid
dNTP	Deoxynucleotide triphosphate
DNMT	DNA methyltransferase inhibitor
DTT	Dithiothreitol
ECL	Enhanced chemiluminescence
EDTA	Ethylenediaminetetraacetic acid
EIAV	Equine Infectious Anemia Virus
eGFP	Enhanced green fluorescent protein
EMBL	European Molecular Biology Laboratory
EBI	European Bioinformatics Institute
F	Forward primer
FBS	Fetal bovine serum
FIV	Feline immunodeficiency virus
GAPDH	Glyceraldehyde-3-phosphate dehydrogenase
GFP	Green fluorescent protein
GPI	Glycosylphosphatidylinositol
GRV	Gamma-retroviral vector
GOI	Gene of interest
HSCT	Hematopoietic stem cell transplant
HF	HYPERFlask
HIV-1	Human immunodeficiency virus type 1
HmB	Hygromycin B
HRP	Horseradish peroxidase
HSC	Hematopoietic stem cell
Hyg	Hygromycin resistance gene
I	Inactive state
Ig	Immunoglobulin
IL-2RG	Interleukin-2 receptor gamma chain
IM	Insertional mutagenesis
ISHV	Isfahan Virus
ISHV-G	Isfahan Virus protein G

kb	Kilobase
kDa	Kilodalton
LB	Lysogeny broth
LDL	Low-density lipoprotein
LDL-R	Low-density lipoprotein receptor
LEDGF/75	Lens epithelium-derived growth factor
LPS	Lipopolysaccharide
LTR	Long terminal repeat
LV	Lentiviral vector
M	Molar
MA	Matrix protein
MAR	Matrix attachment region
MARAV	Maraba Virus
MARAV-G	Maraba Virus protein G
MFI	Mean fluorescence intensity
min	Minute
MLD	Metachromatic Leukodystrophy
MOA	Mechanism of action
MOI	Multiplicity of infection
mRNA	Messenger RNA
MWCO	Molecular weight cut-off
N	Native state
OD	Optical density
OE-PCR	Overlap extension-PCR
OP	OptiPro
OP1	OptiPro + 1% fetal bovine serum
OP10	OptiPro + 10% fetal bovine serum
pac	Puromycin N- acetyl-transferase (puromycin resistance gene)
PAGE	Polyacrylamide gel electrophoresis
pb	Polybrene
PBS	Phosphate-buffered saline
PCL	Packaging cell line
PCR	Polymerase chain reaction
PES	Polyethersulfone

PFA	Paraformaldehyde
PIRYV	Piry Virus
PIRYV-G	Piry Virus protein G
PMSF	Phenylmethanesulfonyl fluoride
PRR	Pattern recognition receptors
PS	Phosphatidylserine
PVDF	Polyvinylidene difluoride
Q-PCR	Quantitative PCR
RABV	Rabies Virus
RABV-G	Rabies Virus protein G
RC	Reverse primer
RCL	Replication-competent lentivirus
RF	Restriction factor
RMCE	Recombinase-mediated cassette exchange
RNA	Ribonucleic acid
rpm	Revolutions per minute
RRE	Rev response element
RT	Reverse transcriptase
RT-Q-PCR	Reverse transcription-Q-PCR
RV	Retroviral vector
sa	Surface area
SAMHD1	Sterile α motif domain- and histidine-aspartate (HD) domain-containing protein 1
SCID	Severe combined immune deficiency
SD	Standard deviation
SDS	Sodium dodecylsulphate
SEM	Standard error of the mean
SFFV	Spleen focus-forming virus
Sh ble	Phleomycin resistance gene
SIN	Self-inactivating vector
siRNA	Small interfering RNA
SIV	Simian Immunodeficiency Virus
SVCV	Spring Viremia of Carp Virus
SVCV-G	Spring Viremia of Carp Virus protein G

SRH	STAR-RDpro-HV
SV40 T Ag	Simian Vacuolationg Virus 40 large T antigen
TCR	T cell receptor
TEMED	Tetramethylethylenediamine
TFF	Tangential flow filtration
TLR	Toll-like receptor
TRIM	Tripartite motif
TU	Transduction unit
U	Unit
UCOE	Ubiquitous chromatin opening element
UV	Ultraviolet
v	Volume
VCM	Vector containing medium
VLP	Virus-like particle
VSV	Vesicular Stomatitis Virus
VSV-G	Vesicular Stomatitis Virus glycoprotein G
VSIV	Vesicular Stomatitis Indiana Virus
VSNJV	Vesicular Stomatitis New Jersey Virus
WAS	Wiskott Aldrich Syndrome
WRH	WinPac-RD-HV
WT	Wild-type
X-CGD	X-linked Chronic Granulomatous Disease

CHAPTER

1

INTRODUCTION

1 Introduction:

1.1 Gene therapy: a brief history

Gene therapy is the vector-mediated introduction of exogenous therapeutic nucleic acids into cells to prevent, halt or reverse a pathological process. This can be achieved through gene addition, gene editing or gene deletion (Kay, 2011). The vectors are either administered *in vivo* or *ex-vivo* into target cells that are then infused/transplanted back into the patient.

The notion of using 'exogenous "good" DNA' transfer techniques to treat human diseases was beginning to be discussed in the early 1970s (Friedmann and Roblin, 1972). This was instigated by the identification of a growing number of disorders that were caused by genetic defects as well as the advent of techniques that allowed the isolation of functional DNA segments (Shapiro et al., 1969) and the synthesis of double-stranded DNA encoding whole genes (Agarwal et al., 1970). The ability of oncogenic viruses to transform mammalian cells through the transfer of part of its genetic materials was at the root of idea of using viruses as vectors of genetic material (Sambrook et al., 1968). The growing knowledge of the biology of retroviruses later led to the derivation of efficient gene transfer vectors from these viruses (Mann et al., 1983). This paved the way for the first clinical trial of gene transfer in humans whereby the neomycin resistance gene was expressed in tumor infiltrating lymphocytes (TILs) using a Murine Leukemia Virus (MLV)- based gamma-retroviral vector (GRV) (Rosenberg et al., 1990).

To exploit viruses' natural ability to efficiently infect mammalian cells, other viral vectors were also developed including lentiviral vectors (LVs), adenoviral vectors and adeno-associated virus (AAV) vectors. Retroviral vectors, including those derived from lentiviruses, have been extensively used for *ex vivo* modification of autologous hematopoietic stem cells (HSCs) and T cells which are then administered to the patient. This thesis will focus on Human Immunodeficiency Virus Type 1 (HIV-1)-based lentiviral vectors (LVs). HIV-1 is an example of the lentivirus genus of orthoretrovirinae, whereas MLV is a gammaretrovirus. RD114, the envelope of which is used in this thesis, is a cat endogenous retrovirus (Reeves et al., 1985). RD114 is a recombinant between *Felis catus* endogenous retrovirus (FcEV) and Baboon endogenous virus (BaEV) with BaEV supplying the envelope (van der Kuyl et al., 1999).

1.2 Retrovirus structure and life cycle

An outline of the retroviral life cycle is shown in Figure 1.1. Retroviruses produce enveloped particles that containing two copies of the (+) strand RNA genome. On budding the virus particle has an immature morphology, processing by the retroviral protease enzyme converts the particle into a mature conformation. All retroviruses encode *gag-pol* and *env*, in HIV-1 there are also the regulatory genes *tat* and *rev*, as well as the accessory genes *nef*, *vif*, *vpr* and *vpu* (Coffin et al., 1997b).

Retroviruses enter the host cell by fusion of the viral envelope with the cellular plasma membrane and release of the virion core into the cytosol. The retroviral envelope surface glycoprotein (SU) binds to a cellular receptor, which leads to a conformational change that exposes a fusion peptide (normally rich in hydrophobic amino acids) in the transmembrane envelope glycoprotein (TM), following which viral and cellular membranes fuse. SU and TM are synthesized as a single precursor and cleaved by cellular proteases in the endoplasmic reticulum (Decroly et al., 1994).

The cell surface receptors used by gammaretroviruses are multiple membrane spanning proteins, the viruses use these receptors for both attachment and fusion. The receptor for BaEV and RD114 is ASCT-2, a neutral amino acid transporter, which is used by other retroviruses such as HERV-W and some betaretroviruses (Overbaugh et al., 2001). BaEV can in addition use a similar transporter ASCT-1 as a receptor (Marin et al., 2000). HIV-1 infects helper T cells, dendritic cells and macrophages that express the CD4 receptor and one of the co-receptors (Klasse, 2012). The HIV envelope SU gp120 binds to CD4 and the co-receptor, which induces a conformational change in HIV envelope TM gp41, leading to release of the gp41 ectodomain in an extended conformation, and insertion of the N-terminal fusion peptide (FP) into the target cell membrane. gp41 then folds into a hairpin structure that induces the fusion of viral envelope and cellular membrane, releasing the viral capsid into the cytosol (Ashkenazi and Shai, 2011).

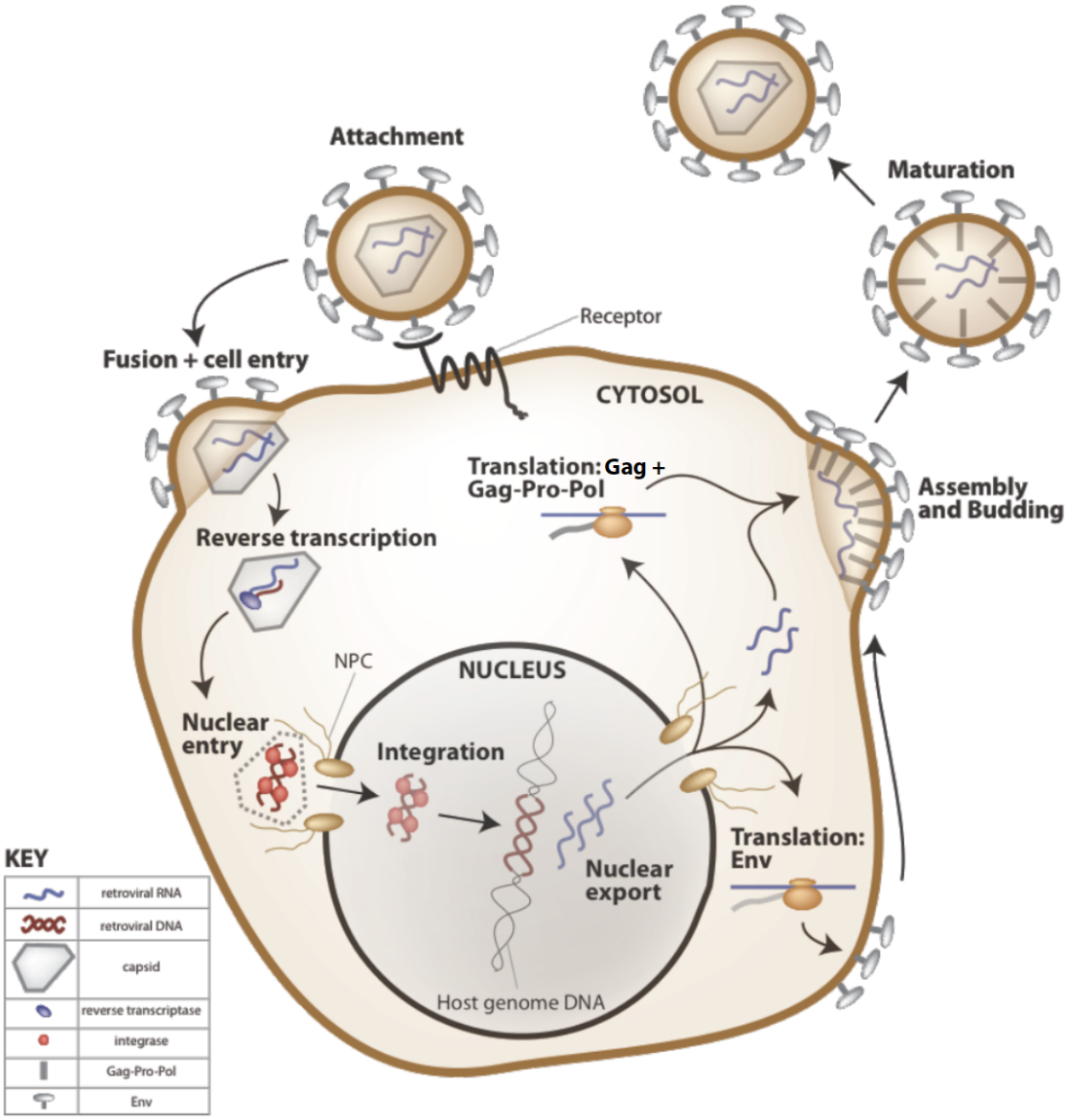

Figure 1.1. Retrovirus lifecycle.

The steps of the retrovirus lifecycle are shown. Only a basic retroviral virion is shown. The retroviral proteins are only shown where relevant, and some are not shown at all (e.g. protease and accessory proteins). A key in the bottom left panel shows the retroviral components illustrated in the diagram. The relevant cellular components are labeled in the diagram. NPC, nuclear pore complex. Adapted with modifications from (Knight, 2011).

After entry into the cell reverse transcription occurs, where the RNA (+) strand genome is converted into a double stranded DNA provirus. The virion core released into the cytoplasm at cell fusion forms the reverse transcription complex (RTC). The HIV-1 capsid is thought to remain reasonably intact during reverse transcription. Firstly, a cellular restriction factor for HIV-1, rhesus macaque TRIM5α, accelerates capsid un-coating and inhibits reverse transcription (Black and Aiken, 2010). Secondly the HIV-1 capsid protein is required to target the RTC to cytoplasmic components of the nuclear pore (Schaller et al., 2011). Reverse transcription does not generally occur in the virion, despite the annealing of the tRNA primer to the primer binding site (PBS) and the presence of reverse transcriptase (Mougel et al., 2009). The exposure of the RTC to a significant concentration of dNTPs in the cytoplasm is probably necessary (Goff, 2001). The RTC makes contacts with the cellular cytoskeleton, facilitating movement through the cytoplasm (Naghavi and Goff, 2007).

An outline of reverse transcription is shown in Figure 1.2. The retrovirus particles contain two genomic RNA transcripts, both of which are used in a single round of reverse transcription; this can generate genetic diversity and compensate for RNA genome damage. Reverse transcription begins from a tRNA primer bound to the PBS. Different tRNAs are used by different retroviruses, tRNAlys3 is used by lentiviruses and betaretroviruses, in contrast to tRNApro that is mainly used by gammaretroviruses. *In vitro* studies with HIV-1 have shown that initiation of DNA synthesis of the DNA (-) strand using tRNALys3 as a primer occurs at a slow rate for addition of the first 6 nucleotides, during which HIV-1 reverse transcriptase dissociates rapidly from the primer/template duplex. There is some specificity in this step, as HIV-1 reverse transcriptase cannot be substituted for non-homologous reverse transcriptases (such as from MLV). Following this, elongation of the 5' R and U5 DNA (-) strand ensues, which is non-specific, as it can be performed by non-homologous reverse transcriptases (Isel et al., 2010).

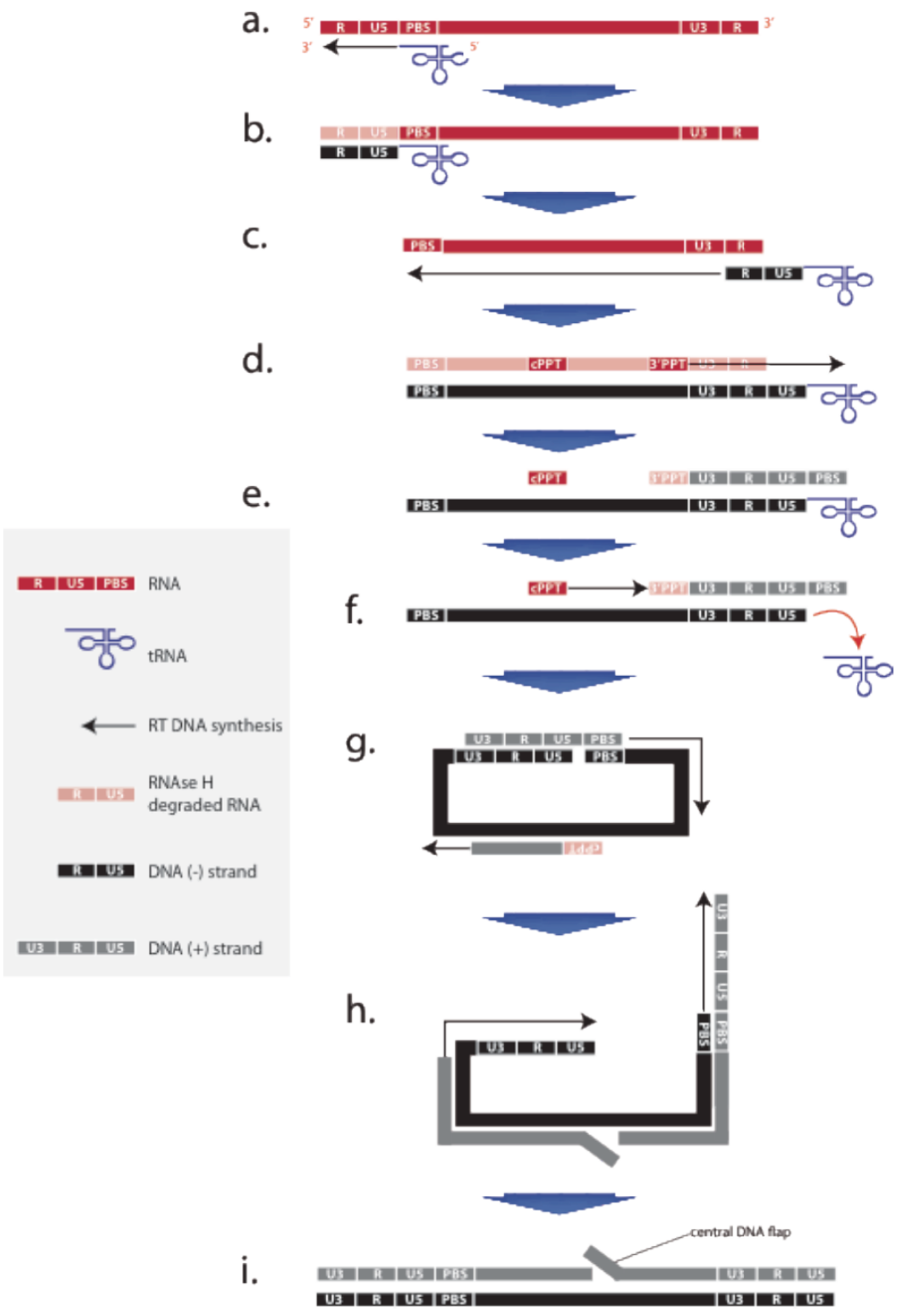

Figure 1.2. Reverse transcription of HIV-1.

(a.) RNA genome is shown in red, bound to tRNA primer. Reverse transcriptase initiates DNA synthesis of the DNA (-) strand (shown in blank). (b.) RNAse H function of RT degrades RNA (degraded RNA shown in light red). (c.) DNA (-) strand, consisting of R,

U5 and tRNA primer, is transferred to the 3' end of RNA genome. This can be intramolecular or intermolecular, as two RNA genomes are in each virion. DNA synthesis of the DNA (-) strand then occurs using the RNA genome as a template. (d.) RNAse H domain of RT degrades the RNA genome except in two places, namely the 3'PPT and cPPT (in other retroviruses such as the gammaretroviruses, only the 3'PPT is not degraded). DNA synthesis of the DNA (+) strand (grey coloured) ensues from the 3'PPT. (e.) RNAse H domain of RT degrades 3'PPT primer. DNA synthesis initiated from the 3'PPT terminates when RT encounters a methylated nucleotide in the T4C-loop in the tRNA primer. (f.) The tRNA primer is cleaved by RNAse H domain, when RT pauses at position 19. DNA synthesis of the DNA (+) strand initiated from the cPPT. (g.) DNA (+) strand elongated from the 3'PPT primer is transferred to the 3' side of the DNA (-) strand. (h.) DNA (+) strand synthesis by RT occurs from the strand transferred, as well as the cPPT. DNA (-) strand is completed by elongation from PBS to 5'LTR. (i.) A double strand DNA provirus is produced, with a central flap (caused by cPPT primed DNA synthesis). Retroviruses lacking the cPPT do not have a central flap. PPT, polypurine tract. Adapted with modifications from (Knight, 2011).

The RNA-DNA hybrid formed as a consequence of initial DNA (-) strand synthesis is degraded by the DNA 3' end directed RNAse H activity of reverse transcriptase. The nicks and gaps in the RNA template strand are too infrequent to be sufficient for complete removal of the RNA in the RNA/DNA hybrid, and probably function to initiate RNA 5' end-directed cleavage that is DNA synthesis independent. On completion of RNA template degradation, the single DNA (-) strand, consisting of the tRNA primer joined to the newly synthesised R and U5 DNA remains (termed 'strong stop' DNA). Strand transfer then occurs, whereby strong stop DNA binds to the R region at the 3' end of the genome and primes the DNA synthesis of the whole of the remaining RNA genome. DNA 3' end directed RNAse H cleavage occurs about once every 100 -120 nucleotides with HIV-1 reverse transcriptase, which correlate with pause sites, where the reverse transcriptase encounters RNA secondary structure. The polypurine tract (PPT) in the RNA genome is left intact as an RNA/DNA hybrid.

PPT then primes DNA synthesis of the (+) strand LTR using the DNA (-) strand 3' LTR strong stop sequence as a template. After 12 nucleotides, the reverse transcriptase pauses and cleaves the PPT-U3 junction. When the reverse transcriptase reaches the junction with the tRNA primer, it uses the first 18 nucleotides as a template for DNA synthesis. After reaching a methylated nucleotide at position 19, the reverse transcriptase pauses, allowing the RNAse H domain to cleave the tRNA one nucleotide from the tRNA/DNA junction. This leaves a ribonucleotide at the 5' end of the DNA (-) strand. The 18 nucleotide DNA (+) strand 3' hangover, generated by tRNA removal forms base pairs with the first 18 nucleotides of the 5' PBS, transferring the DNA (+) strand to the 5' end, where DNA synthesis leads to extension of the entire DNA (+) strand, reconstituting the 5' U3 region. Lentiviruses have an additional PPT, called the cPPT, from which DNA synthesis of the DNA (+) strand is also initiated. When the 3' end of the DNA (+) strand reaches the 5' end of the cPPT, DNA synthesis proceeds to displace the DNA (+) strand elongated from the cPPT primer, before reaching a termination sequence in the DNA (-) strand. This leads to the formation of a 99bp triple strand DNA structure in the center of the proviral DNA that has been referred to as the 'central flap'.

Entry into the nucleus is an obligatory step in the retroviral lifecycle required for accessing the host cell genome for provirus integration. Many retroviruses, including most gammaretroviruses are dependent on the dissolution of the nuclear membrane that occurs in mitosis to access host cell DNA and thus are only able to infect dividing cells.

However, lentiviruses use the nuclear pore to enter the nucleus and therefore are able to infect both dividing and non-dividing cells. The HIV-1 nucleoprotein complex enters the nucleus by capsid interaction with the nuclear pore protein NUP358. This targets the viral DNA for integration at transcriptively active regions. Mutants that fail to interact with NUP358 are still infectious but show a different integration pattern (Hilditch and Towers, 2014).

Once inside the nucleus, the provirus integrates into host cell DNA mediated by the retroviral protein integrase (IN). Integration can be divided into 3' processing, strand transfer and gap repair. 3' processing involves removal of two nucleotides at the 3' end of each DNA strand in the double stranded DNA provirus by IN. Following nuclear entry, and binding to host cell DNA, strand transfer occurs, whereby the recessed 3' ends attack opposite strand phosphodiester bonds, separated by 4 to 6 bases (5 in HIV). This forms a gap at the 5' end of each DNA strand of the provirus that is repaired by the host cell DNA repair system in the final step of integration, leading to duplication of the 4 – 6 host DNA bases flanking the provirus. The cellular protein LEDGF/p75 has been shown to bind to HIV IN and acts as a chromatin tether. Depletion of LEDGF/p75 causes a change in the integration site pattern of HIV (Marshall et al., 2007).

Transcription in most retroviruses is initiated from the long terminal repeats (LTRs). The U3 segment of the LTR contains transcription factor binding sites, and a TATA box for assembly of general transcription factors and RNA polymerase II complex. The transcription start site defines the beginning of the 'R' segment of the LTR. In general, simple retroviruses transcribe a spliced mRNA transcript encoding env and an unspliced mRNA transcript that serves as the RNA genome and the gag-pol mRNA transcript. In contrast complex retroviruses have two phases of transcription, the first involves expression of multiply spliced regulatory genes, followed by expression of singly and unspliced RNAs. In HIV-1 two NF-KB sites in the enhancer region are important in transcription initiation (Nabel and Baltimore, 1987). The nuclear factor of activated T cells (NFAT) family is also important, as is SP1. In HIV-1, the viral protein Tat increases elongation of mRNA transcripts. In the absence of Tat, transcription initiation is unaffected, but mRNA transcripts are not readily elongated past the TAR loop in the R/U5 region of the LTR (Kao et al., 1987).

In eukaryotic cells, splicing removes introns from pre-mRNA by two trans-esterification reactions mediated by the spliceosome, which is a complex of small nuclear

ribonucleoproteins (snRNPs) (Sperling et al., 2008). Then 3' end processing occurs directed by the polyadenylation sequence (PAS) and a U/GU rich region known as the downstream sequence element (DSE). PAS is bound by cleavage and polyadenylation specificity factor (CPSF). DSE is about 30 nucleotides downstream of the cleavage site and is bound by cleavage stimulation factor (CstF). The endonuclease responsible for RNA cleavage resides within CPSF, the site of cleavage occurs preferentially after a CA dinucleotide between PAS and DSE. Then polyadenylation of the 3' end of the cleaved RNA is carried out by polyadenylation polymerase (PAP) (Millevoi and Vagner, 2010).

After 3' end processing, the mature mRNA is exported out of the nucleus into the cytoplasm. The central nuclear transport receptor involved in this process is TAP in which associates with nucleoporins to mediate nuclear export. Subunits of the adaptor complex TREX associate with RNAP2 elongation complexes and bind to exon-junction complexes on successfully spliced exons. TREX association with TAP and subsequent nuclear export of mRNA is tightly regulated to ensure that only mature mRNA transcripts are exported (Iglesias and Stutz, 2008). As HIV-1 also needs to export unspliced RNAs from the nucleus, it encodes the Rev protein. Rev N terminus binds to the Rev responsive element (RRE) sequence that is present in all un-spliced and single spliced HIV-1 transcripts. Nuclear export then occurs via an interaction between the carboxy terminus of Rev and the nuclear export factor CRM1 (Hakata et al., 2002). Rev must therefore be supplied in lentiviral vector packaging cells and the viral vector genome must contain the RRE.

Un-spliced retroviral mRNAs can be used as a template for translation of gag-pol genes. The two main proteins translated from this mRNA transcript are Gag and Gag-Pro-Pol (which is processed to make Gag proteins, protease, reverse transcriptase and integrase). About 10 – 20 Gag proteins are made for every Gag-Pro-Pol protein, and retroviruses use different mechanisms to regulate translation of these proteins (Coffin et al., 1997b). One method, adopted by MLV, involves read-through of the stop codon after Gag. In HIV-1 pol is in a different reading frame to gag, and ribosomal frame-shifting accounts for Gag-Pro-Pol synthesis. HIV un-spliced mRNA forms a stable stem loop structure downstream of gag that is preceded by a heptanucleotide 'slippery sequence' (Gaudin et al., 2005).

Following translation of viral proteins, retroviruses assemble into virions and exit the cell by budding through a cellular membrane. Assembly and budding occur as

simultaneous processes in some retroviruses, including HIV-1 and MLV. Expression of Gag alone is sufficient to induce assembly of particles that bud through the plasma membrane in some cell lines (Bieniasz, 2009). In HIV-1, Gag accumulates at the plasma membrane where particle assembly occurs. The interaction between Gag and the plasma membrane is dependent on attachment of a myristyl group to the N-terminal glycine residue in MA (Bryant and Ratner, 1990). Gag-Pro-Pol associates with the plasma membrane in the same way as Gag. The frameshift mechanism of Gag-Pro-Pol synthesis ensures that the correct ratio of Gag:Gag-Pro-Pol is incorporated into virus particles. Gag binds viral RNA in the cytoplasm as a monomer or low-order multimer and subsequent assembly into virus particles only occurs at the plasma membrane (Kutluay and Bieniasz, 2010). Once Gag associates with the plasma membrane, it multimerises to form the immature virus particle (Ganser-Pornillos et al., 2008). Retroviral genomic RNA is packaged into budding virus particles by association of the nucleocapsid (NC) portion of Gag, which binds to the dimer linkage structure formed by the packaging sequence (Amarasinghe et al., 2000). Translation of Env follows the same pathway as that for secreted and membrane bound proteins. Envelope proteins are incorporated into budding virus particles by a mechanism that is incompletely understood. Clearly this is not highly specific, as envelope proteins from many other viruses can be incorporated into HIV virions.

In HIV-1 some of the accessory proteins, which have essential roles in host-pathogen interactions, are packaged into virus particles. These are incorporated through different mechanisms; Vpr is recruited through p6 in Gag (Martin-Serrano and Neil, 2011), whereas Nef associates with lipid rafts and presumably is incorporated passively into virions. In contrast, Vif incorporation is dependent on interaction with HIV-1 genomic RNA (Khan et al., 2001). Although Gag multimerisation is important in initiating virus budding, it is not sufficient to mediate membrane scission and particle release. To accomplish membrane scission, the p6 domain of Gag recruits cellular endosomal sorting complexes required for transport (ESCRTs), which are normally involved in the cellular process of multi-vesicular body (MVB) formation. Two peptide sequences in p6, PTAP and YPLTSL, bind the cellular proteins Tsg101 (a component of ESCRT-I) and ALIX (an ESCRT-I and –III binding protein) respectively and recruit ESCRT-III, which mediates membrane scission. Mutation of the p6 PTAP motif severely impairs HIV budding (Martin-Serrano and Neil, 2011).

1.3 HIV-1 restriction factors and mechanisms of evasion

Restriction factors (RFs; reviewed in (Malim and Bieniasz, 2012) and (Harris et al., 2012)) are cellular proteins that directly and dominantly attenuate viral replication and infectivity without the need for other cellular cofactors. The antiviral activity of these factors tends to be species specific, and they are therefore considered to be important determinants of the host cell range of viruses and a major barrier to cross-species transmission. Moreover, their expression is usually inducible by interferon (IFN), which is a key component of innate immune response against pathogens.

Central to its ability to efficiently infect and replicate in human cells, HIV-1 has evolved so that it can avoid or antagonize these restriction factors in human cells often through the activity of some of its accessory proteins such as *Vif* and *Vpu*. As a result of selective pressure exerted through these host-pathogen interactions, restriction factors tend to exhibit evidence of rapid evolution.

Since HIV-1-based LVs are devoid of most of HIV-1's accessory proteins (see Section 1.3.1), they may be more susceptible to some of the restriction factors in primary human cells. Therefore, restriction factors that have been shown to have a potent suppressive effect on HIV-1 replication *in vivo* will be briefly discussed here. The relevance of each of these factors to the use of lentiviral vectors for gene therapy applications will also be mentioned. It should be noted that other host cell factors that might contribute to HIV-1 restriction as suggested by recent studies such as IFTIMs (Compton et al., 2014) and TIMs (Li et al., 2014) but these are yet to be better characterized.

1.3.1 TRIM5α and TRIMCyp

TRIM5α belongs to the family of tripartite-motif (TRIM)-containing proteins (reviewed in (Nisole et al., 2005)). Similar to other viral restriction factors, TRIM5α proteins have species-specific anti-viral activity. Although, HIV-1 is relatively insensitive to the human TRIM5α, it is susceptible to TRIM5α proteins from some Old World monkeys such as the African green monkey and Rhesus macaques (Stremlau et al., 2004), and this restriction is dependent on CypA-CA interaction (Berthoux et al., 2005). The human TRIM5α however, is a potent inhibitor of N-tropic MLV.

TRIM5α is generally ubiquitously expressed and its expression is inducible by IFN. It consists of amino terminal RING domain (that has E3 ubiquitin ligase activity) and B-box domain (that mediates multimerization), a central coiled coil domain (that mediates dimerization) as well as a C-terminal PRYSPRY (also known as B30.2) domain. The latter is responsible for CA recognition and carries hypervariable regions that determine the protein's anti-viral specificity. In owl monkeys and certain macaque species the CypA pseudogene has been inserted via retrotransposition events in TRIM5α gene locus creating chimeric gene that is expressed as a TRIMCyp fusion protein (Malim and Bieniasz, 2012) in which the PRYSPRY domain is replaced by CypA. As a result TRIMCyp is able to restrict HIV-1 whose capsid is recognized by CypA. In this protein the CypA domain replaces the PRYSPRY domain of TRIM5α, allowing it to restrict lentiviruses whose CA is recognized by CypA including HIV-1.

TRIM5α and TRIMCyp inhibit HIV-1 replication immediately after entry and before reverse transcription. The exact molecular mechanism of restriction of HIV-1 by these proteins is still unclear. They seem to bind the viral CA and target it for ubiquitination and proteasomal degradation resulting in a block in reverse transcription (Rold and Aiken, 2008). However, inhibition of the proteasome rescued reverse transcription but failed to relieve the restriction on viral replication (Anderson et al., 2006). Additionally, these proteins can act as pattern recognition receptors (PRRs) that recognize the incoming viral CA and induce an NF-κB-dependent innate immune response. This in turn, contributes to viral restriction (Pertel et al., 2011a).

Since HIV-1 is insensitive to restriction by human TRIM5α, this restriction factor is unlikely to have significant effects on HIV-1-based-LV transduction in human cells. However, TRIM5α-mediated restriction should be taken into account when considering the use of primate models for pre-clinical testing of these vectors. In addition to that, artificial fusion proteins such human TRIM5-Cyp and human TRIM21-Cyp made from human components have been exploited as a tool for anti-HIV-1 gene therapy in pre-clinical studies (Chan et al., 2012; Neagu et al., 2009).

1.3.2 SAMHD1

The sterile α motif domain- and histidine-aspartate (HD) domain-containing protein 1 (SAMHD1) is an HIV-1 restriction factor found in myeloid cells (Hrecka et al., 2011; Laguette et al., 2011) and resting T cells (Baldauf et al., 2012).

SAMHD1-mediated viral restriction is exerted at the level of reverse transcription. It has been proposed that the dNTP triphosphohydrolase activity of SAMHD1 leads to the depletion of cellular dNTPs needed for cDNA synthesis by the viral reverse transcriptase (Lahouassa et al., 2012). However, recent evidence suggests that SAMHD1's dNTPase activity may be dispensable for its HIV-1 restriction, and that its RNase activity mediates viral restriction by degrading the HIV-1 RNA (Ryoo et al., 2014).

The Vpx proteins of HIV-2 and SIV can recruit SAMHD1 to an E3 ubiquitin ligase complex leading to its polyubiquitination and proteasomal degradation (Ahn et al., 2012). However, HIV-1 does not appear to be able to counteract SAMHD1.

SAMHD1-mediated restriction is a major hurdle against targeting antigen-presenting cells (APCs) such as dendritic cells (DCs) using HIV-1-based vectors. These vectors can induce an interferon response in these cells through Toll-like receptors (TLRs) (Breckpot et al., 2010), with can lead to the upregulation of SAMHD1 expression. Overcoming this restriction may facilitate the development of effective LV-based vaccines. The use of Vpx virus-like particles (VLPs) offers one way to improve the efficiency of *in vitro* DC transduction (Pertel et al., 2011b). However, for *in vivo* applications packaging the vector particles with Vpx in order to antagonize SAMHD1 might be needed (Durand et al., 2013; Sunseri et al., 2011).

1.3.3 APOBEC3 proteins

The APOBEC (apolipoprotein B mRNA editing enzyme, catalytic polypeptide-like) family of proteins in humans includes eleven members (reviewed in (Malim, 2009)). Of these, APOBEC3G (A3G) has the most potent activity against HIV-1 (Sheehy et al., 2002). Other members such as APOBEC3F and APOBEC3H (haplotype II) might also have physiologically relevant *in vivo* activities (Malim and Bieniasz, 2012).

A3G was initially identified in resting human T cells and is expressed in many hematopoietic cells including T cells, dendritic cells and macrophages (Koning et al., 2009). In the absence of *Vif*, A3G can be packaged into virions by binding with the viral gRNA and interacting with the NC part of Gag (Bogerd and Cullen, 2008). When these virions infect target cells, A3G associated with the reverse transcriptase complex catalyzes the deamination of cytidine residues in the nascent single-stranded negative sense complementary DNA (cDNA) to uridine residues (C to U). This results in G to A mutations in the viral plus strand. Since up to 10% of cytidine residues can be

deaminated, the resulting hypermutation in the viral genome can have deleterious consequences on its replicative potential. Moreover, A3G reduces the synthesis of viral cDNA in target cells likely by impeding reverse transcriptase translocation along the viral RNA template (Bishop et al., 2008).

HIV-1 uses its accessory protein *Vif* to counteract the antiviral activity of A3G. *Vif* binds A3G and uses the T cell differentiation factor CBFbeta to recruit a cellular E3 ubiquitin ligase complex leading to the polyubiquitnation and proteasomal degradation of A3G (Zhang et al., 2012). Another member of the family A3F also causes HIV-1 mutation and is counteracted by *Vif* (Ara et al., 2014). The cPPT is also thought to play a role in protecting against A3G possibly by reducing the duration of reverse transcription and thereby the time during which the viral single-stranded DNA is susceptible to A3G (Hu et al., 2010). The packaging of A3G into virions is essential for its anti-HIV activity. Although HIV-1 *Vif* can efficiently counteract physiological levels of A3G, *Vif*-deficient HIV-1-based lentiviral vectors are susceptible. Therefore, it is important to use cells that do not express A3G for the production of LVs (Miller and Metzger, 2011). Otherwise, the G to A hypermutation in target cells may impair transgene expression, or lead to the expression of a mutated version that might be inactive, immunogenic or have other unforeseen consequences.

1.3.4 MX2

Myxovirus resistance 2 protein (MX2) is another recently reported IFN-inducible HIV-1 restriction factor. MX-2-mediated restriction can be averted by cyclophylin A (CypA) depletion or by some CA mutants (Goujon et al., 2013; Kane et al., 2013; Liu et al., 2013). Although the exact mechanism of restriction is still unclear, MX2 seems to interact directly with HIV-1 CA (Fribourgh et al., 2014) to block HIV-1 replication at two steps: nuclear import and post-import trafficking and/or integration (Matreyek et al., 2014).

1.3.5 Tetherin

Tetherin (also known as BST2 or CD317) is a dimeric type II membrane glycoprotein that has an N-terminal cytoplasmic tail, a transmembrane helix, a coiled-coil extracellular domain, and a C-terminal glycosylphosphatidylinositol (GPI) anchor (reviewed in (Neil, 2013)). It is expressed in multiple cell types including myeloid and lymphoid cells, and its expression is inducible by IFN and other cytokines.

Two alternatively translated isoforms of tetherin exist: long- and short-tetherin (Cocka and Bates, 2012). Both isoforms can physically trap nascent HIV-1 virions at the surface of infected cells (Perez-Caballero et al., 2009) and prevent their release by virtue of their dual anchorage to the viral envelope membrane and the plasma membrane of infected cells (Neil et al., 2008). However, the longer isoform has a tyrosine-based motif in its cytoplasmic tail that can also activate NF-KB signaling after virion retention, which induces an anti-viral state in the infected cells (Cocka and Bates, 2012).

The HIV-1 accessory protein, *Vpu,* interacts with and antagonizes tetherin. This is thought to occur by redirecting the trafficking of tetherin/*Vpu* complexes through the trans golgi network (TGN) leading to their endosomal degradation and preventing tetherin from reaching the sites of virus budding at the plasma membrane (Janvier et al., 2011). The HIV-1 accesory protein *Nef* also antagonizes tetherin among other activities (Serra-Moreno et al., 2013). Tetherin can potentially prevent the release of budding HIV-1-based lentiviral vectors. Thus, it is important to ensure that cell lines used for vector production have minimal tetherin expression, which is the case for 293T cells (Neil et al., 2008). However, it is important to remember that tetherin expression in this cell line is interferon-inducible.

1.4 Retroviral vectors

1.4.1 Derivation and design of retroviral vectors

Viral vectors are naturally adapted to infect host cells and their genomes can be manipulated to make them replication-defective and less pathogenic. This makes them attractive tools for the efficient delivery of therapeutic genes to target cells. Retroviral vectors (RVs) were among the earliest viral vectors to be developed and quickly became popular laboratory tool for gene transfer. Such vectors were initially derived from gammaretroviruses such as the Moloney Murine Leukemia Virus (Mo-MLV) (Miller et al., 1983). Later on, lentiviral vectors (LVs) based on HIV-1 were developed (Poznansky et al., 1991). Other lentiviral vectors were also derived from Simian Immunodeficiency Virus (SIV), Equine Infectious Anemia Virus (EIAV) and Feline Immunodeficiency Virus (FIV).

To make retroviral vector particles, producer cells need to express the structural and enzymatic components of the particle (packaging functions) and the vector genome carrying a transgene of interest (transfer vector function). For lentiviral vectors, the

packaging functions underwent iterative improvements in design, including a reduction in the number of encoded lentiviral genes and their splitting into multiple plasmids, leading to the development of the so-called third generation vectors (Dull et al., 1998; Sakuma et al., 2012). In these vectors, the packaging functions are provided by 3 separate plasmids. The first encodes the *Gag-Pol* genes (consisting of *Gag*, *Pro* and *Pol* open reading frames with a deleted packaging signal), which provide the structural, and enzymatic components of the particles. The second plasmid encodes *Rev,* which is a necessary for export of the full-length viral gRNA from the nucleus. All HIV-1 accessory genes as well as *Tat* were excluded. *Tat* is unnecessary in lentiviral vector packaging cells, because the HIV-1 U3 region can be replaced by a strong heterologous promoter, to drive expression of the vector genome in a *Tat* independent manner. However, *Rev* is necessary for nuclear export of the RRE containing vector genome as described in section 1.2. The accessory proteins *Vif*, *Vpu* and *Nef* can be omitted if the cell line chosen does not express the restriction factors A3G and tetherin (see section 1.3). The final accessory protein Vpr has not been described to exert any effect of HIV-1 replication in cell culture, so is also omitted. The envelope function is provided by the third plasmid, which consists of a heterologous envelope glycoprotein most commonly that of the Vesicular Stomatitis Virus (VSV-G). Although early vectors were provided with HIV-1 *Env* restricting their tropism to CD4+ cells, vector pseudotyping with heterologous envelopes was a major breakthrough in the development of widely applicable lentiviral vectors (Naldini et al., 1996).

In parallel, the design of the transfer vector (or vector genome) underwent significant improvements too. Thus, the third-generation vectors were made Tat-independent by replacing the 5' LTR promoter/enhancer sequences with a heterologous promoter (Dull et al., 1998). The state-of-the-art vector design also includes the viral packaging signal (Ψ), the Rev Response Element (RRE) and the central Polypurine Tract (cPPT), which improved transduction efficiency by facilitating reverse transcription and nuclear import (Riviere et al., 2010). A sequence from Woodchuck hepatitisvirus, the Woodchuck post-transcriptional regulatory element (WPRE) (Donello et al., 1998), was initially found to improve transgene expression in retroviral and lentiviral vectors (Zufferey et al., 1999) (Ramezani et al., 2000) and a version lacking any coding or promoter sequences (Schambach et al., 2006) is now included in many vectors. Because the U3 region of the 3' LTR is copied to the 5' LTR during reverse transcription (Figure 1.2), it is possible to delete the promoter/enhancer sequences in the 3' LTR of the vector in the producer cell. This results in self-inactivating (SIN) vectors (Zufferey et al., 1998),

which have a reduced risk of vector mobilization in target cells (Hanawa et al., 2005a) and a potential for insertional gene activation (Knight et al., 2010).

Retroviral vectors (RVs) have several advantageous characteristics that make them well-suited for use as gene transfer tools. They can carry large genetic payloads (up to ≈9kb), induce a minimal immune response when administered *in vivo* (Nayak and Herzog, 2010) and can integrate into the host cell genome and persist in daughter cells allowing long-term transgene expression. Additionally, they can be pseudotyped with alternative envelope proteins that govern their tropism as well as other important properties such as their mechanical stability and sensitivity/resistance to serum proteins (Friedmann and Yee, 1995; Strang et al., 2004).

Although the above properties are shared between gammaretroviral vectors (GRVs) and LVs, there are some key differences between the two types of vectors. Importantly, GRVs cannot efficiently transduce non-dividing cells. LVs on the other hand, can transduce non-dividing cells including quiescent HSCs (Case et al., 1999; Naldini et al., 1996; Uchida et al., 1998) since its PIC can cross the intact nuclear membrane (see section 1.2.3). However, transduction efficiency increases when quiescent cells are stimulated into the G_0/G_1 phase of the cell cycle (Ailles et al., 2002; Cavalieri et al., 2003; Sutton et al., 1999). The development of these vectors expanded the range of cell types that can be targeted for gene therapy applications to include neurons (Palfi et al., 2014), hepatocytes (Cantore et al., 2015) and retinal cells (Kong et al., 2008). Moreover, they allowed more efficient transduction of HSCs with shorter *ex vivo* culture times and milder stimulation requirements (Uchida et al., 2011). This is considered to be advantageous since it helps preserve the phenotypic and functional characteristics of target cells including their engraftment potential (Ailles et al., 2002; Cavalieri et al., 2003; Mazurier et al., 2004), which may account for the relatively high levels of multi-lineage gene marking in recent LV-mediated HSC gene therapy clinical trials even when corrected cells do not possess a growth/survival advantage (Naldini, 2011). Moreover, it reduces the chances of overgrowth of modified cells in which vector integration imparts a proliferative/survival advantage and this may help limit the risk of IM (Howe et al., 2008; Sellers et al., 2010; Shou et al., 2006).

In addition to that, HIV-1-based LVs have been found to target actively transcribed areas of the genome, and to integrate uniformly along the length of transcriptional units without a preference for transcriptional start sites (TSSs), both in transformed human cell

lines (Schroder et al., 2002; Wu et al., 2003) and in human primary cells in human HSCs and PBMCs (Cattoglio et al., 2007; Mitchell et al., 2004). On the other hand, MLV-based γ-RVs preferentially target TSSs in HeLa cells (Wu et al., 2003) as well as in human HSCs, in which a preference for 'hotspots' enriched in proto-oncogenes and genes regulating cell growth and proliferation was also found (Cattoglio et al., 2007). This suggests that HIV-1-based LVs have a safer integration profile compared to γ-RVs, which may contribute, at least in part, to their lower oncogenic potential as demonstrated by comparing LVs and γ-RVs using *in vitro* and *in vivo* IM assays (Modlich et al., 2009; Montini et al., 2009). These assays have also demonstrated the lower oncogenic potential of self-inactivating (SIN) LVs (which have a deletion in the U3 region of the viral LTR (Zufferey et al., 1998)), especially when physiological internal promoters were used (Modlich et al., 2009; Montini et al., 2009; Montini et al., 2006; Zychlinski et al., 2008). Data from recent LV-mediated clinical trials is in line with these predictions as discussed in Section 1.3.2. However, it is imperative to note that the risk of IM is not completely eliminated with LVs (Cavazzana-Calvo et al., 2010), and *in vitro* IM assays have been utilized to map and eliminate potential splice acceptor/donor sites that can induce host gene deregulation through aberrant splicing events in order to improve vector safety (Cesana et al., 2012; Knight, 2011; Moiani et al., 2012).

1.4.2 Retroviral vectors for clinical gene therapy applications

Retroviral vectors have been the vectors of choice for early gene therapy clinical trials targeting hematopoietic stem cells (HSCs) as well as T cells to treat a range of disorders (Table 1.1). A selection of key clinical trials will be discussed in the following sections.

1.4.2.1.1 Hematopoietic stem cells:

HSC-based gene therapy has largely used retroviral vectors as *ex vivo* gene transfer tools. In most clinical trials to date, autologous HSCs ($CD34^+$ cells) are obtained from the patient's bone marrow or mobilized peripheral blood. These cells are then expanded, stimulated and transduced with the retroviral vectors *ex vivo* before being transplanted back into the patient (Naldini, 2011). In addition to being available to all patients (including those without HLA-matched HSC donors), autologous HSCT minimizes the risk of immunologic complications including graft-versus-Host disease (GvHD) and graft

rejection. It also often involves low-dose chemotherapeutic pre-conditioning regimens rather than ablative regimens, thus reducing chemotherapy-associated side effects.

In the early trials, γ-retroviral vectors (GRVs) derived from the murine leukemia virus (MLV) were used to treat several PIDs including X-linked severe combined Immunodeficiency (SCID-X1), adenosine deaminase deficiency (ADA-SCID), X-linked Chronic Granulomatous Disorder (X-CGD), and Wiskott-Aldrich Syndrome (WAS). Notably, the SCID-X1, ADA-SCID, and WAS trials resulted in clinical benefits that are comparable to those of the gold standard allogeneic HSCT (Braun et al., 2014; Gaspar et al., 2011b; Hacein-Bey-Abina et al., 2010). However, insertional mutagenesis (IM) arose as serious side effect of retroviral integration in the vicinity of proto-oncogenes in the SCID-X1, X-CGD, and WAS trials (Braun et al., 2014; Hacein-Bey-Abina et al., 2008; Howe et al., 2008; Stein et al., 2010). Poor engraftment of transplanted HSCs and silencing of integrated vectors were also documented as complications that can potentially compromise treatment efficacy (Mukherjee and Thrasher, 2013; Stein et al., 2010).

Importantly, these trials helped identify critical factors in determining efficacy and safety of RV-mediated gene therapy. Optimization of *ex vivo* HSC culture and transduction conditions was important to ensure adequate gene transfer, preserve the engraftment potential and 'stemness' of transplanted HSCs, and possibly limit the risk of IM (Howe et al., 2008; Sellers et al., 2010). Disease-specific considerations related to the nature of 'corrected' cells and whether or not they gain a survival/growth advantage were noted. These issues may govern the risk of IM (Shaw and Kohn, 2011), as well as the degree of chemotherapeutic pre-conditioning regimens needed to ensure adequate long-term engraftment of transplanted cells (Grez et al., 2011). Additionally, the use of endogenous or lineage specific promoters was highlighted as attractive option to ensure adequate transgene expression and reduce off-target/ectopic expression (Chiriaco et al., 2014).

Largely driven by concerns related to the risk of IM as well as *ex vivo* HSC manipulation, third generation SIN LVs have been increasingly used in more recent trials targeting HSCs ((Naldini, 2011); Table 1.1; see section 1.3.2). Thus, clinical trials for adrenoleukodystrophy (ALD) (Cartier et al., 2009), metachromatic leukodystrophy (MLD) (Biffi et al., 2013), β-thalassemia (Cavazzana-Calvo et al., 2010), and Wiskott Aldrich Syndrome (WAS) (Aiuti et al., 2013; Hacein-Bey Abina et al., 2015) have been undertaken with encouraging initial results published (summarized in Table 1.2). There are also phase

I/II clinical trials for the treatment of other PIDs including X-CGD, ADA-SCID, and SCID-X1 that have started more recently (Cicalese and Aiuti, 2015), while clinical trials for other disorders such as Fanconi's Anemia are being planned (Tolar et al., 2012).

In light of the above overview, the following sections will address disease-specific concerns and clinical trial outcomes, as this is essential to understand the current standing in the field and to drive future endeavors.

1.4.2.1.1.1 Primary immunodeficiencies

Primary immunodeficiencies (PIDs) are a heterogeneous group of monogenic disorders that are characterized by defects in the innate and/or adaptive immune system and are caused by mutations affecting an expanding repertoire of genes (Al-Herz et al., 2011; Al-Herz et al., 2014). This results in disorders with a wide spectrum of clinical manifestations and severity. For milder disorders supportive care in the form of antibiotics and immunoglobulins may be adequate. However, for more severe forms allogeneic HSCT is the main treatment option. With HLA-identical transplants, long-term survival rates exceeding 80% can be achieved. However, when no HLA-matched donors (related or unrelated) are available, survival rates are drastically lower with a high burden of side effects due to chemotherapeutic conditioning regimens and the incidence of Graft versus Host Disease (GvHD).

1.4.2.1.1.1.1 Adenosine deaminase deficiency

Severe Combined Immunodeficiency (SCID) represents a group of PIDs with severe manifestations resulting from defects in all lymphocyte compartments including T, B and NK cells. ADA-SCID is an autosomal recessive form of SCID is caused by a deficiency in the Adenosine Deaminase (ADA) enzyme. ADA is ubiquitously expressed in human cells and is part of the purine salvage pathway. It catalyzes the deamination of adenosine and deoxyadenosine to inosine and deoxyinosine respectively. Impaired ADA activity leads to the accumulation of deoxyadenosine, which is converted to the toxic metabolite deoxyadenosine triphosphate. This results in the SCID phenotype as well as other systemic manifestations (Hershfield, 1998).

Like other severe PIDs, HLA-identical HSCT (ideally from a sibling donor) is the gold standard of treatment. Other options include HLA-haploidentical HSCT and enzyme replacement therapy (ERT) with polyethylene glycol-conjugated bovine ADA (PEG-

ADA). However, responses with ERT are not complete with a decline in T and B cell function over time are usually seen and treatment can be complicated by the incidence of antibodies against bovine ADA and autoimmune manifestations

ADA-SCID was the first disorder to be treated by gene therapy using retroviral vectors. In the early 1990s, a group of five trials were initiated in different centers for the treatment of this disorder using LTR-intact GRVs carrying a normal human ADA gene. Although all of these trials did not show long-term clinical, they did provide an opportunity to identify pitfalls and devise improved gene therapy protocols.

In three of these trials peripheral blood lymphocytes (PBL) from patients receiving ERT were transduced (Aiuti et al., 2002; Blaese et al., 1995; Bordignon et al., 1995; Onodera et al., 1998). Multiple infusions of transduced PBLs were administered without yielding any significant long-term clinical benefit. However, follow up studies showed that PEG-ADA administration can impair the selective advantage of the 'corrected' T cells (Aiuti et al., 2002). More importantly, it was recently demonstrated by tracking retroviral integration sites (RISs) that the transduced T memory stem cells persisted for up to 12 years following the last infusion with preserved differentiation potential. Additionally, no evidence of clonal dominance was seen although further follow-up is warranted (Biasco et al., 2015).

In the other two trials $CD34^+$ cells either derived from umbilical cord blood (Kohn et al., 1998) or from bone marrow (Hoogerbrugge et al., 1996). Both of these trial did not demonstrate long-term clinical trials and this was largely attributed to low gene marking largely attributed to inefficient transduction and engraftment potential of the transplanted cells, which was thought to be to suboptimal *ex vivo* culture and stimulation protocols used in these early trials. ERT was also continued in these trials after the patients underwent transplantation.

This lead to significant improvements in protocols used for later gene therapy trials targeting ADA-SCID as well as other disorders. Thus, $CD34^+$ cells were cultured and transduced on fibronectin-coated surfaces following stimulation with an optimized cytokine cocktail that acts on hematopoietic stem and progenitor cells. Preconditioning regiments with low-dose chemotherapy were also employed with or without the discontinuation of PEG-ADA (Kohn, 2008). Three trials were conducted using these revised protocols and LTR-intact GRVs in Italy (Aiuti et al., 2009), the UK (Gaspar et al.,

2011b) and the US (Candotti et al., 2012). Substantially better results were seen in the three trials with sustained immune reconstitution, multi-lineage gene marking, metabolic detoxification and discontinuation of ERT in 31 out of a total of 42 patients that have been treated worldwide (≈74%) (Cicalese and Aiuti, 2015).

The survival rate in these ADA-SCID clinical trials is 100% without any documented serious side effects. Remarkably, although analysis of RISs in these trials revealed a preference for integration near transcriptional start sites (TSSs), there were no signs of clonal dominance or malignant transformation even when integration occurred in the vicinity of known proto-oncogenes (Aiuti et al., 2007). This is in stark contrast to the malignant transformation events documented in several SCID-X1 patients treated using similar LTR-intact GRVs as discussed in Section 1.3.3.1.1.1.2). There is no clear explanation for this difference yet, but one contributing factor might be that the ADA enzyme only offers a survival advantage (without any proliferative signals) to corrected cells with a potential for cross-correction of uncorrected ones (Shaw and Kohn, 2011).

Given the safety concerns associated with LTR-intact GRVs in general, SIN LVs with a moderately-active short-form elongation factor-1α promoter driving the expression of a codon-optimized ADA gene has been developed (Carbonaro et al., 2014) and used in two phase I/II clinical trials in the UK and the US (Cicalese and Aiuti, 2015). Five patients aged between 1.2 and 4.5 years have been treated to date in these trials with low-dose busulfan (5mg/kg) pre-conditioning resulting in improved T cell numbers and function after a mean follow-up of around 1 year.

1.4.2.1.1.1.2 X-linked severe combined immunodeficiency

X-linked SCID (SCID-X1) is the most common variant of SCID. It is caused by loss-of-function mutations in the IL2RG gene that lead to a deficiency of the interleukin (IL)-2 receptor common gamma-chain, which is a subunit of the receptors for IL-2, IL-4, IL-7, IL-9, IL-15 and IL-21. This leads to a defect in T- and NK-cell development and poorly functional B cells resulting recurrent life-threatening infections. HLA-matched allogeneic HSCT preferably from a related donor is the treatment of choice with lower survival rates seen with unrelated or mismatched donors. Interestingly, immune reconstitution secondary to spontaneous reversion of disease-causing mutations has been documented suggesting that corrected cells gain a selective advantage over uncorrected ones (Cicalese and Aiuti, 2015).

Two gene therapy trials using LTR-intact GRVs expressing the IL2RG gene without chemotherapeutic pre-conditioning were conducted in France and the UK to treat SCID-X1 patients who lacked an HLA-matched donor (Gaspar et al., 2011a; Hacein-Bey-Abina et al., 2010). A total of 20 patients were treated resulting in polyclonal reconstitution of the T cell compartment in the majority of patients and improved B cell function leading to discontinuation of intravenous immunoglobulin in around half of the patients. This has resulted in a survival rate of 85% after more than 10 years of follow-up (Williams and Thrasher, 2014), which is comparable to outcomes seen with related HLA-matched HSCT.

However, T cell leukemia occurred in a total of five patients (25%) (Cicalese and Aiuti, 2015). One patient died from chemotherapy-refractory leukemia, while four went into remission after treatment with chemotherapy, and one of those four underwent subsequent HLA-matched HSCT. In all of these cases the primary culprit leading to malignant transformation is thought the aberrant expression of proto-oncogenes (either LMO2 or CCND2) situated in the vicinity of the vector integration site secondary to the effect of the viral LTR. Secondary genomic aberrations, which might have accrued during *ex vivo* manipulation of the $CD34^+$ cells, were documented in all cases (Howe et al., 2008). This might have been compounded by the proliferative advantage gained by the corrected cells too.

The robust T cell reconstitution seen in the French and UK trials is thought to be largely a consequence of a functional thymus. Notably, treatment of three adolescent SCID-X1 patients (aged 10, 11 and 14) in a US clinical trial resulted in improved T cell count and function only in the youngest patient. Failure of treatment in older patients has been at least partly attributed to a decline in thymic function over time highlighting the importance of early treatment (Chinen et al., 2007; Thrasher et al., 2005).

In an attempt to maintain efficacy and avoid adverse events, a SIN GRV has been developed in which the IL2RG gene is under the control of the moderately active human elongation factor 1α (EF1α) short promoter (Thornhill et al., 2008)and used in more recent multicenter clinical trial conducted in France, the UK and the US (Hacein-Bey-Abina et al., 2014). Nine patients have been treated in this trial and the inclusion criteria included the lack of an HLA-identical sibling donor or drug-resistant disseminated infections. One patient died due to a pre-existing adenoviral infection, while 7 of the

surviving 8 showed polyclonal reconstitution of the T cell compartment after up to 2 years of follow-up.

Furthermore a SIN LV expressing IL2RG under the control of the EF1α promoter has been developed and used in another US clinical trial, which will treat children with typical SCID-X as well as adolescents and children with atypical presentations who will be given a pre-conditioning regimen of busulfan at 6mg/kg. Preliminary results from two adolescents show improved B cell function, NK cell counts and clinical improvement (Cicalese and Aiuti, 2015).

1.4.2.1.1.1.3 X-linked chronic granulomatous disorder

Chronic granulomatous disorder (CGD) is caused by mutations in any of five subunits of the NADPH oxidase complex of phagocytes. The inability to form reactive oxygen species impairs the killing of a multitude of bacterial and fungal pathogens by phagocytes leading to severe invasive fungal and bacterial infections and early death. Around two thirds of CGD cases are caused by mutations in the X-linked gene encoding gp91phox (X-CGD). Conventional treatment includes lifelong antimicrobial prophylaxis and IFN-γ therapy but is not curative. Allogeneic HSCT can be curative for patients with HLA-matched donors.

Most recent trials for X-CGD used LTR-intact GRVs with nonmyeloablative conditioning. This resulted in initial transient improvement in phagocyte function what was associated with clinical improvement and clearance of severe infections. However, low levels of long-term engraftment of 'corrected' cells and silencing of transgene expression due to promoter methylation limited the efficacy of the treatment. Several factors have been proposed to contribute to the observed failure to achieve long-term engraftment including the ectopic expression of the therapeutic gene gp91phox in HSCs as well as an immune response against the 'corrected' cells. In addition to that there was a high incidence of clonal dysregulation associated with integration in one of three proto-oncogenes, namely PRDM16, SETBP1, and MDS-EVI1. The latter was associated with the development of myelodysplastic syndrome in three patients.

1.4.2.1.1.1.4 Wiskott Aldrich syndrome

Wiskott-Aldrich syndrome (WAS) is an X-linked recessive PID disorder caused by mutations in the Wiskott-Aldrich syndrome protein (WASP) gene (Notarangelo et al.,

2008). WASP is exclusively expressed in hematopoietic cells and is involved in the transduction of signals between the cell surface and actin cytoskeleton. Mutations that prevent WASP expression or result in the expression of a truncated protein cause the classical, most severe phenotype of the disease, which is characterized by a triad of recurrent severe infections, thrombocytopenia and eczema as well as an increased risk for autoimmune disorders and malignancies. These patients tend to have T and B cell dysfunction, impaired NK cell synapse formation and impaired migration of all leukocyte subsets. Allogeneic HSCT is the mainstay of treatment and the outcome depends on multiple factors including the patient's age and HLA-matching with survival rates of up to 85-90% with HLA-matched unrelated donor transplants (Cicalese and Aiuti, 2015). However, gene therapy with autologous HSCT of 'corrected' cells is emerging as an option for the treatment patients who lack an HLA-matched donor. The selective advantage conferred by WASP expression in 'corrected' cells is expected to aid in successful engraftment and immune reconstitution with this approach (Notarangelo et al., 2008).

In the first gene therapy clinical trial conducted in Germany, an LTR-intact GRV expressing WASP was used to treat a total of 10 patients. Low-dose chemotherapeutic pre-conditioning was used in this trial (Braun et al., 2014). Successful engraftment and WASP protein expression in was seen in 9/10 patients resulting in partial or complete immune reconstitution, cessation of the bleeding diathesis and improvement in autoimmune disorders. Analysis of RISs revealed initial polyclonal reconstitution of the hematopoietic system. However, the clinical course was later complicated by the development of acute leukemia in 7/10 patients (1 AML, 4 T-ALL, 2 primary T-ALL with secondary AML) associated with the malignant transformation of a dominant clone with retroviral integration at the LMO2 (6 T-ALL), MDS1 (2 AML) or MN1 (1 AML) loci. Retroviral integrations in the MDS-Evi1 locus were also reportedly implicated in the development of secondary myeloid malignancies (Williams and Thrasher, 2014).

Other investigators have developed a SIN LV expressing the WASP gene under the control of its endogenous promoter in an attempt to recapitulate the clinical efficacy seen in the first trial while reducing the risk of dysregulation of host gene expression and insertional mutagenesis. Initial results from two trials, one in Italy and another in France and the UK, are summarized in Table 1.2. In these trials similar, clinical improvement in immune function and other disease manifestations was seen as in the earlier trials.

Importantly this was associated with high-level engraftment and gene marking as well as a significant number of shared RISs between multiple lineages after a follow up times of more that 2 years in some patients (Aiuti et al., 2013; Hacein-Bey Abina et al., 2015).

1.4.2.1.1.2 Lysosomal storage disorders

Lysosomal storage disorders (LSDs) represent a group of progressive metabolic disorders affecting the white matter of the central nervous system with or without the involvement of the peripheral nervous system. They are usually caused by genetic defects affecting glial cells, which are responsible myelin sheath formation and/or maintenance (Parikh 2015). Some of these disorders have been successfully treated using HLA-matched HSCT. This approach was based on preclinical studies showing that cells derived from donor HSCs are able to cross the blood-brain barrier and differentiate into perivascular microglia capable. These cells can then produce and secrete lysosomal enzymes, which can be taken up by neighboring cells with possible cross-correction of oligodendrocytes and neurons (Biffi et al., 2011a).

1.4.2.1.1.2.1 Adrenoleukodystrophy

Adrenoleukodystrophy is an X-linked recessive LSD caused by mutations of the ABCD1 gene encoding the ALD protein. This protein is an adenosine triphosphate (ATP)–binding cassette transporter in the membrane of peroxisomes and required for the degradation of very-long-chain fatty acids (VLCFAs) in oligodendrocytes and microglia, which are responsible for myelin maintenance in the central nervous system (CNS). Its deficiency leads to accumulation of VLCFAs in these cells leading to impaired myelin maintenance. Consequently patients suffer from a progressive demyelination of the CNS resulting in progressive motor and cognitive deficits with death before reaching adolescence in most patients. Allogeneic HSCT is the mainstay of treatment and outcomes depend on HLA-matching as well as the patients' age

Two patients have been treated in the ALD trial using a SIN LV expressing the normal ABCD1 gene under the control of the MND promoter (a synthetic promoter that contains the U3 region of a modified Mo-MLV LTR with myeloproliferative sarcoma virus enhancer). Stable engraftment with polyclonal reconstitution of hematopoiesis was documented in both patients with around 10% gene marking in peripheral blood mononuclear cells (PBMCs) and shared RISs between lymphoid and myeloid lineages. Clinical and radiological progression was halted in both patients, an outcome comparable

to that seen with allogeneic HLA-matched HSCT (Table 1.2; (Biffi et al., 2011a; Cartier et al., 2009)). Results from two more patients, who were treated in this trial, are awaited.

1.4.2.1.1.2.2 Metachromatic leukodystrophy

Metachromatic leukodystrophy (MLD) is an autosomal recessive LSD caused by mutations that lead to a deficiency in the enzyme arylsulfatase-A (ARSA) or rarely its activator protein saposin-B (Biffi et al., 2008). ARSA normally metabolizes sulfatides, and its deficiency leads to the accumulation of these substrates in oligodendrocytes, macrophages and some neuronal subtypes in the CNS, in Schwann cells and macrophages in the peripheral nervous system (PNS), and in some visceral organs. This results in progressive demyelination and neurodegeneration, which is ultimately manifested as progressive motor and cognitive impairment with developmental delay or psychomotor regression. PNS involvement can lead to diffuse muscle atrophy and weakness with areflexia.

The disease severity and age at onset depend on whether the causative mutation results in absent or minimal residual ARSA activity. The late infantile (LI) form is the most severe and most frequent form of MLD. Patients with the LI variant show symptoms within the second year of life, have the most severe manifestations of the disease, and die within a few years of symptom onset. Treatment is supportive as there are no effective interventions available. Even allogeneic HSCT proved to be ineffective in children with the late infantile disease and generally in all patients with evident neuropsychological and/or neurological signs. Enzyme replacement therapy was recently developed and is currently being tested in clinical trials. LV-mediated gene therapy is a viable option since ARSA can be expressed at supra-physiologic levels and progeny of the 'corrected' transplanted HSCs can migrate to the CNS and cross-correct abnormal cells to varying degrees (Biffi et al., 2011a).

In the first gene therapy phase I/II trial, a SIN LV expressing the ARSA gene under the control of a human phosphoglycerate kinase 1 promoter (PGK) to transduce HSCs *ex vivo*. 8 patients have been recruited (Kaufmann et al., 2013) and preliminary results from 3 patients have been published (Table 1.2 (Biffi et al., 2013)). These 3 patients carried mutations associated with LI MLD with biochemically confirmed ARSA deficiency, and had one or more older siblings with LI MLD onset within 2 years of age. Patients were

given a myeloablative busulfan conditioning regimen before the cells were transplanted back into the patients.

High-level (45-80%) stable engraftment of the transduced HSCs was observed in the bone marrow and peripheral blood of all patients at all times tested. ARSA activity was reconstituted at supra-physiologic levels. Analysis of RISs revealed highly polyclonal reconstitution of hematopoiesis without evidence of aberrant clonal expansion. Additionally, several integration sites were shared among progenitors as well as differentiated myeloid and lymphoid (both B- and T-cells), indicating efficient transduction and engraftment of HSCs. 2/3 patients did not manifest any clinical or imaging abnormalities 7 and 10 months beyond the expected age of disease onset (based on age at onset in affected siblings). The third patients remained asymptomatic and pre-existing imaging and lab-based abnormalities stabilized at 20 months beyond expected age of disease onset. These results are unprecedented in patients with LI MLD.

Importantly, in the LV-mediated trials targeting ALD, MLD and WAS polyclonal hematopoiesis without clonal dominance has been observed. Moreover, no enrichment of integrations near common insertion sites (CISs) (Suzuki et al., 2002; Wu et al., 2006) was noted in comparison to neighboring genes, suggesting that the detection of these CISs was merely due to the intrinsic tendency of LVs to integrate in genomic regions that harbor these CISs rather than a growth/survival advantage imparted by vector integration (Aiuti et al., 2013; Biffi et al., 2011a; Biffi et al., 2011b; Biffi et al., 2013). Notably, impressive gene marking in the recent MLD and WAS trials has been partly attributed to improved LV manufacturing and HSC *ex vivo* transduction techniques (Aiuti et al., 2013; Biffi et al., 2013), which highlights the importance of optimizing these processes.

1.4.2.1.1.3 Hemoglobinopathies

To achieve stable high level expression of the human β globin gene, large segments of its locus control region had to be used. However, in the context of GRVs, since these regulatory regions contain multiple elements such as splice sites and polyadenylation signals that can lead to low titer GRV production and multiple rearrangements in the transmitted proviruses(Leboulch et al., 1994). Lentiviral vectors are better-suited for delivering such complex genetic payloads since they can achieve efficient *Rev*-mediated nuclear export and packaging of unspliced genomic RNA containing multiple splice sites and faithfully transmitting it into target cells (May et al., 2000). LVs facilitated the

development of gene therapies for hemoglobinopathies, which are among the most common monogenic disorders worldwide (Chandrakasan and Malik, 2014) including beta-thalassemia and sickle cell anemia.

1.4.2.1.1.3.1 β-thalassemia

The hemoglobin (Hb) molecule is tetramer consisting of two α-globin and two β-globin chains. β-thalassemia is caused by mutations that impair β-globin gene expression leading to decreased (β^{+}) or absent (β^{0}) β-globin production. This leads to a relative excess of free α-globin chains that precipitate in the erythroid precursors leading to their intramedullary destruction and that ineffective hematopoiesis that underlies all β-thalassemias (Thein, 2005). The anemia seen in these disorders is a consequence of ineffective hematopoiesis as well as peripheral red blood cell destruction.

The first gene therapy clinical trial for β-thalassemia recruited two patients (Table 1.2; (Cavazzana-Calvo et al., 2010)). The HSCs failed to engraft in the first patient because they were reportedly compromised during *ex vivo* handling. The second patient was 18 years old at treatment. He had severe β^{E}/β^{0} thalassemia and had been transfusion-dependent since the age of 3 years with a poor response to conventional therapy. He did not have an HLA-matched donor available.

Autologous HSC were transduced with a SIN LV expressing a mutated adult β-globin ($\beta^{A(T87Q)}$) under the control of the endogenous locus control region of the β-globin gene. This vector also carried two copies of the 250-bp core of the cHS4 chromatin insulator in the U3 region. The $\beta^{A(T87Q)}$ had anti-sickling properties and could be distinguished from normal adult β-globin by high performance liquid chromatography (HPLC) analysis. A transduction efficiency of around 30% was reported in this trial.

Following a myeloablative busulfan conditioning regimen, the HSCs were transplanted back into the patient and successfully engrafted resulting in a gradual increase in gene marking up to around 10% both in bone marrow erythroid precursors and in PBMCs. Although the ineffective erythropoiesis persisted, the patient became transfusion independent with a total Hb level of 9-10 g/dl, one third of which consisted of Hb-$\beta^{A(T87Q)}$.

Analysis of RISs revealed a gradual expansion of an IS in the third intron of the high mobility group AT-hook 2 (HMGA2) gene in erythroblasts and granulocytes-

monocytes but not lymphocytes. The dominant clone harboring this IS accounted for up to 45% of vector bearing erythroblasts and granulocytes-monocytes, which represented only 2% and 8% of total erythroblasts and granulocytes-monocytes, respectively. Around 10000-fold upregrulation of HMGA2 expression was only detectable in erythroblasts. This was mediated by the loss of let-7 microRNA binding sites on a truncated transcript formed by aberrant splicing between the third intron of HMGA2 and a cryptic splice acceptor site in the cHS4 insulator core and cleavage/polyadenylation within the R region of the left LTR of the vector. At the time of reporting, both the frequency of the dominant clone in the erythroblast compartment and the HMGA2 expression levels had been stable since around 18 months post-transplant and up to around 33 months post-transplant (Cavazzana-Calvo et al., 2010). It was later reported that at 6 year post-transplant, the clone bearing the vector at the HMGA2 IS was no longer dominant and that the level of therapeutic $\beta^{A(T87Q)}$ expression remained high enough for the patient to be transfusion-independent of blood transfusions (Leboulch, 2013).

It is noteworthy that integration within the HMGA2 locus has been detected in the LV-mediated WAS trial (Aiuti et al., 2013) and GRV-mediated SCID-X1 trial (Wang et al., 2010) without the incidence of any adverse events. The HMGA2 protein is also commonly associated with a benign tumor phenotype (Cleynen and Van de Ven, 2008). However, it was recently reported that the HMG2A transcript can contribute to lung cancer progression by competing for the let-7 microRNA (Kumar et al., 2014).

Improvements in vector design have been made and there are plans to start new clinical trials with this second generation for the treatment of patients with β-thalassemia as well as sickle cell disease (Negre et al., 2015).

1.4.2.1.2 T Cells

Most gene therapy clinical trials targeting T cells have used GRVs (Table 1.1) since data from clinical trials using SIN GRVs showed clinical efficacy without any documented events of clonal dominance or malignant transformation in gene-modified T cells (Scholler et al., 2012). This is thought to be partly due to tight immune regulation of differentiated T cells. Moreover, the availability of stable PCLs for large scale GRV production is another reason limiting a move towards using LVs in this field. Despite that there are some groups are moving towards utilizing LVs

1.4.2.1.2.1 Cancer

Adoptive T cell therapy using engineered T cells entails re-directing T cells against tumor cells by expressing either T cell receptors (TCRs) or chimeric antigen receptors (CARs) targeting tumor-associated antigens (June et al., 2015; Rosenberg and Restifo, 2015). Several malignancies were targeted with this approach (listed in Table 1.1) including neuroblastoma, lymphoma/leukemia, colorectal cancer (Parkhurst et al., 2011), melanoma, and synovial sarcoma. Notably, significant clinical responses were documented and no events of IM or clonal expansion related to retroviral integration were documented. The latter is consistent with pre-clinical data suggesting that mature T cells are relatively resistant to malignant transformation (June et al., 2009; Newrzela et al., 2008; Scholler et al., 2012). However, further work is needed to improve efficacy and limit serious off-target side effects of this promising approach for cancer immunotherapy (Di Stasi et al., 2011; Linette et al., 2013; Morgan et al., 2010; Park et al., 2011; Parkhurst et al., 2011).

Following the promising results achieved using γ-RVs in T cell-based gene therapy against cancer (especially B cell malignancies (Kochenderfer and Rosenberg, 2013)), recent trials have utilized LVs since they can mediate more efficient gene transfer with milder *ex vivo* stimulation conditions and have a generally more favorable safety profile. Outcomes form two trials using CAR-engineered T cells directed against CD19 to treat B cell malignancies are summarized in Table 1.3.

1.4.2.1.2.2 HIV-1 infection

The first gene therapy clinical trial using LVs was directed against HIV-1 infection by engineering CD4 T cells to express an antisense gene targeting the HIV-1 Env (Levine et al., 2006). A recently published follow-up report on this trial demonstrated the safety of this approach, which used a conditionally replicating LV with intact LTRs (Tebas et al., 2013). Various gene therapy strategies to treat HIV-1 infection have targeted HSCs or T cells with the aim of replacing HIV-susceptible cells with resistant ones by either eliminating host cell cofactors or expressing anti-viral genes using γ-RVs or LVs (Deeks et al., 2012; Rossi et al., 2007).

1.4.2.1.3 Other target cell types:

There is interest in developing LVs as therapeutic vaccines against pathogens and tumor cells by targeting professional antigen presenting cells (APCs) (Collins and Cerundolo, 2004). Recently, a phase I/II clinical trial was initiated to test an *in vivo* lentiviral therapeutic vaccine against HIV-1 infection based on pre-clinical studies done in cynomolgus macaques (Beignon et al., 2009). In this trial, patients are planned to receive iterative injections of VSV-G-pseudotyped LVs expressing an HIV-1 antigen (derived from fragments of HIV-1 Gag, Pol, and Nef) under the control of a promoter that is preferentially active in APCs. This is then expected to induce a strong T cell-mediated immune response against HIV-1 infected cells in these patients.

In addition to that, a clinical trial for the treatment of Parkinson's disease (Palfi et al., 2014) used EIAV-based lentiviral vectors to target neuronal and demonstrated that this approach was well tolerated but had limited efficacy.

Table 1.1 List of selected recent RV-mediated gene therapy clinical trials

Target cells	Disease Group	Disease	Vector	Env	Production Method	References
HSCs ($CD34^+$)	PIDs	ADA-SCID: ADA	γ-RV	MLV-A	Gp+Am12	(Aiuti et al., 2009)
			γ-RV	GALV	PG13	(Gaspar et al., 2011b)
			γ- RV	GALV	PG13	(Candotti et al., 2012)
		X-SCID: IL2RG	γ- RV	MLV-A	ψCRIP	(Hacein-Bey-Abina et al., 2010)
			γ- RV	GALV	PG13	(Gaspar et al., 2011a)
			γ- RV	GALV	PG13	(Chinen et al., 2007)
		X-CGD: gp^{phox91}	γ- RV	GALV	PG13	(Ott et al., 2006; Stein et al., 2010)
			γ- RV	GALV	PG13	(Bianchi et al., 2009)
			γ- RV	MLV-A	293-derived /Vamp	(Kang et al., 2010; Kang et al., 2011)
		WAS: WASP	γ- RV	GALV	PG13	(Boztug et al., 2010)
			LV	VSV-G	293T: transient	(Aiuti et al., 2013)
			LV	VSV-G	293T: transient	(Hacein-Bey Abina et al., 2015)
	Hereditary anemias	B-thalassemia: $\beta^{A(T87Q)}$	LV	VSV-G	293T: transient	(Cavazzana-Calvo et al., 2010)
	Storage disorders	ALD: ABCD1	LV	VSV-G	293T: transient	(Cartier et al., 2009)
		MLD: ARSA	LV	VSV-G	293T: transient	(Biffi et al., 2013)
T cells	Cancer	Neuroblastoma	γ- RV	GALV	PG13	(Louis et al., 2011; Pule et al., 2008)
		Lymphoma/ Leukemia	γ- RV	NS	NS	(Kochenderfer et al., 2012; Kochenderfer et al., 2010)
			γ- RV	NS	NS	(Kochenderfer et al., 2015)
			γ- RV	GALV	PG13	(Brentjens et al., 2011)
			γ- RV	GALV	PG13	(Brentjens et al., 2013; Davila et al., 2014)

		γ- RV	NS	NS	(Lee et al., 2015)
		LV	VSV-G	293T: transient	(Kalos et al., 2011; Porter et al., 2011)
		LV	VSV-G	293T: transient	(Grupp et al., 2013; Maude et al., 2014)
	Melanoma	γ- RV	GALV	PG13	(Morgan et al., 2006)
		γ- RV	NS	NS	(Johnson et al., 2009)
	Synovial sarcoma	γ- RV	GALV	PG13	(Robbins et al., 2011)
	Colorectal cancer	γ- RV	RD114	293: transient	(Parkhurst et al., 2011)

HSCs, hematopoietic stem cells; PID, primary immunodeficiency; ADA-SCID, adenosine deaminase deficiency; SCID-X1, X-linked severe combined immunodeficiency; X-CGD, X-linked chronic granulomatous disorder; WAS, Wiskott Aldrich syndrome; WASP, WAS protein; ALD, adrenoleukodystrophy; MLD, metachromatic leukodystrophy; IL2RG, interleukin-2 receptor common gamma chain; ARSA, arylsulfatase-A; LV, lentiviral vector; γ- RV, γ-retroviral vector; Env, envelope; MLV-A, amphotropic murine leukemia virus; GALV, gibbon ape leukemia virus; VSV-G, vesicular stomatitis virus G protein; NS, not specified.
Gp+Am12, PG13, ψCRIP and Vamp are stable gammaretroviral packaging cell lines.

Table 1.2 Summary of LV-mediated gene therapy clinical trials targeting CD34+ HSCs

Disease	Int prom; Transgene	Titer; MOI; VCN; cell dose	Chemotherapeutic conditioning	Patient no✚: Age	Outcome	References
ALD	MND; ABCD1	- Titer: $9.41x10^7$ TU/ml - MOI: 25 - VCN: 0.6-0.7	Full myeloablation (busulfan)	2 (4): 7-8 years	- Halted progression (both clinically and on MRI) - PC recons, shared RISs + - %VBC: 10-11% PBMC	(Cartier et al., 2009)
MLD	PGK; ARSA	- Titers (genomic): Initial: $1\text{-}2x10^7$ TU/ml Final: $2\text{-}7x10^8$ TU/ml - MOI: 100 (x2 cycles) - VCN: 2.5-4.4 $7\text{-}11x10^6$ cells/kg	Full myeloablation (busulfan)	3: 7-16 months	- Based on clinical examination and imaging: onset prevented in two patients, pre-existing defects stabilized in one patient. - ARSA expression ≥10 fold NC - PC recons, shared RISs + - %VBC: 45-80% BM	(Biffi et al., 2013)
β-thalassemia	human β-globin promoter/$\beta^{A(T87Q)}$ with cHS4 insulator	Titer: $1.1x10^8$ TU/ml VCN: 0.6 Cell dose: $3.93x10^6$ $CD34^+$ cells/kg	full myeloablation (busulfan)	2★: 18 years	- Transfusion independent (10mg/dl total Hb with 1/3 from $\beta^{A(T87Q)}$) but persistent hypererythroid state (requiring monthly phlebotomies). - Clonal dominance with spontaneous resolution - %VBC: 11% PBMC, 3% PB EB, 10% BM EB	(Cavazzana-Calvo et al., 2010; Leboulch, 2013)
WAS	1.6-kb h WAS prom/WASP gene	- Titer: 1 x 10^8 TU/ml - MOI: 100 (x2 cycles) - VCN: 2.3 ± 0.6 - Cell dose: $3\text{-}4x10^6$ $CD34^+$ cells/kg	low intensity regimen (anti CD20 mAb + busulfan + fludarabine)	3: 1-6 years	- Infection free with improved lymphocyte functional assays, improved platelet counts, resolution of eczema - PC recons, shared RISs + - %VBC: 25-50% BM	(Aiuti et al., 2013)

WAS	1.6-kb h WAS prom /WASP gene	Titer: 1 x 10^8 TU/ml MOI: 100 (x2 cycles)? VCN: 0.6 – 2.8 Cell dose: 2-15 x 10^6 $CD34^+$ cells/kg	Low intensity busulfan (4 mg/kg/d) and fludarabine (40 $mg/m^2/d$) for 3 days ± anti-CD20 Ab	7: 3 -15.5 years	- 6/7 alive after mean f/u 28 mo 6/6 infection free 6/6 resolution of eczema 5/5 autoimmunity improved no severe bleeding episodes - PC recons, shared RISs+ - %VBC in PB: 34%-84% T cells, 14%-85% NK cells, 13%-55% B cells	(Hacein-Bey Abina et al., 2015; Merten et al., 2011)

✚Patient number with published details. The number between brackets refers to total number of patients enrolled (total)
★P1 failed to engraft reportedly secondary to technical issue in cell handling during *ex vivo* culture/transduction. Data from P2 only is presented in this table.

Shared RISs +, shared retroviral integration sites detected between lymphoid and myeloid cells (implying successful correction and engraftment of HSCs); PC recons: polyclonal reconstitution (deduced from large number of RISs isolated and sequenced); VCN, vector copy number (copies per cell); GM, Gene marking; NC: normal control; MRI: magnetic resonance imaging; MND, myeloproliferative sarcoma virus enhancer, negative control region deleted, *d*l587rev primer-binding site substituted promoter; PGK, human phosphoglycerate kinase 1 promoter; 250bp cHS4: 250bp core of cHS4 chromatin insulator; $\beta^{A(T87Q)}$, mutated adult beta chain with anti-sickling properties; Ab, antibody; 1.6-kb h WAS prom, 1.6-kb human WAS endogenous proximal promoter; f/u, follow up; mo, month

Table 1.3 Summary of LV-mediated CAR-engineered T cell clinical trials

Disease	Patient no (median age)	Vector; CAR design	Cell dose; VCN; Tduct eff	Pre-conditioning	outcome	References
CLL (advanced chemotherapy-resistant)	3; 65 years	LV; 2nd gen CD3-zeta 4-1BBL	Cell dose: 1-1.6 x 10^7 CAR^+ T cells/kg; VCN: 0.1-0.275; Tduct eff: 5-23%	Pentostatin or bendamustine ± cyclophosphamide	- 2CR with -ve MDR ≥10 mo, 1PR (7mo) - persistence for ≥ 6 mo in PB and BM - CAR^+ effector and memory T cells - Adverse events: 3 CRS, 3 B cell aplasia	(Kalos et al., 2011; Porter et al., 2011)
ALL (18 post-allo-HSCT)	30; 14 years	LV; 2nd gen CD3-zeta 4-1BBL	Cell dose: 0.076-1.73 x 10^7 CAR^+ T cells/kg	None or fludarabine + cyclophosphamide	27 CR with 22 MRD^- 30 CRS: 22 mild-moderate + 8 moderate to severe	(Grupp et al., 2013; Maude et al., 2014)

CLL chronic lymphocytic leukemia, ALL, acute lymphoblastic leukemia; CAR, chimeric antigen receptor, allo-HSCT, allogeneic hematopoietic stem cell transplantation; VCN, vector copy number; Tduct eff, transduction efficiency; CR complete response, PR partial response, MDR minimal residual disease (detected by multi-parameter flowcytometry), PB peripheral blood, BM bone marrow; CRS, cytokine release syndrome; Yr: years, Mo: months. Titers of vector preparations were not specified.

1.5 Aims of thesis

The efficacy and safety data emerging from recent small-scale clinical trials targeting debilitating and/or life-threatening disorders such as leukemias and primary immune deficiencies highlight the limitation imposed by the lack of affordable, large-scale and cGMP-compliant production platforms for SIN LVs.

The research and investment dedicated to contriving the means and technologies that facilitate the delivery of new and effective therapies to patients, has often lagged behind the development of such therapies. This disparity has been sorely recognized as an avoidable cause of failure of treatment for serious disorders such as HIV infection and tuberculosis (Farmer, 2013). Therefore, it is imperative to couple the development of promising gene therapies with research that is aimed at establishing affordable and robust production and delivery platforms at an early stage. I hypothesized that this would help prevent a 'delivery gap' from developing in the budding field of gene therapy, and would ensure that these life-saving therapies become available to all patients who need them at a reasonable cost.

The work presented in this thesis aims to address these issues by testing methods to improve vector production and processing. Accordingly, the broad aims of this work were to:

1. Generate and characterize monoclonal SIN LV producer cell lines derived from the WinPac-RDpro packaging cell line as a proof of concept. Subsequently, a protocol that facilitates the reproducible generation of such producer cell lines was to be established.

2. Establish protocols for large-scale LV production and downstream processing of pseudotyped LVs.

3. Use alternative envelope glycoproteins to establish WinPac-derived packaging cell lines that can support high titer production of vector pseudotypes with favorable characteristics that would facilitate downstream processing and vector handling.

CHAPTER

2

MATERIALS AND METHODS

2 Materials and methods

2.1 Molecular biology techniques

2.1.1 Molecular buffers and bacterial media

All buffers and bacterial media used are listed in Table 2.1. They were all prepared in double distilled water (ddH_2O).

Table 2.1. Buffers and bacterial media

Application	Buffer/Medium	Composition
gDNA extraction	Lysis buffer	10mM Tris-Cl (pH7.4) 10mM EDTA 10mM NaCl 0.5% SLS 1mg/ml Proteinase K
RNA extraction	RLT buffer with 1% β-mercaptoethanol	RLT buffer composition is confidential (Qiagen) 1% β-mercaptoethanol
Western blotting	Phosphate-Buffered Saline (PBS) (pH 7.4)	137 mM NaCl 2mM KCl 10 mM Sodium hydrogen phosphate (dibasic) 1.5 mM Potassium hydrogen phosphate (dibasic)
	PBS-T	PBS 0.1% Tween20

	Laemmli buffer	50 mM Tris (pH 6.8) 2% Sodium dodecylsulphate (SDS) 10% Glycerol 5% 2-Mercaptoethanol 0.2 mg/mL Bromophenol blue 0.1 M DTT
	11% polyacrylamide gel	11% Acrylamide/bis 125 mM Tris.HCl (pH 8.8) 10% SDS 0.1% TEMED 1% ammonium persulphate (APS)
	4% stacking gel	4% Acrylamide/bis 125 mM Tris.HCl (pH 6.8) 10% SDS 0.1% TEMED 1% APS
	Running buffer	25 mM Tris (pH 8.5) 200 mM glycine 0.1% SDS
	Transfer buffer	100 mM Tris 200 mM Glycine 20% Methanol

	Blocking buffer	5% semi-skimmed milk 0.1% Tween 20 in PBS
	Stripping buffer	62.5 mM Tris-HCl (pH6.8) 2% SDS 100mM 2-Mercaptoethanol
Preparation of competent bacterial cells	Transformation (TFB)-I	30mM potassium acetate 100mM rubidium chloride 10mM CaCl2 50mM MgCl2 15% glycerol acetic acid to pH 5.5
	TFB-II	10mM MOPS 75mM calcium chloride 10mM rubidium chloride 15% glycerol KOH to pH 6.5
Bacterial Amplification	Luria-Bertani (LB) Broth	1% bacto tryptone 0.5% bacto yeast 0.5% NaCl (pH 7.5)
	Luria-Bertani (LB) Agar	LB Broth 15g/L bacto-agar

		(pH 7.5)
Elution buffers	AE	10 mM Tris-HCl (pH 9.0) 0.5mM EDTA
	EB	10 mM Tris-HCl (pH 8.5)
Gel electrophoresis	Tris-acetate EDTA (TAE)	40 mM Tris (pH 7.8) 20 mM sodium acetate 1 mM EDTA
	6x gel loading buffer	0.25% bromophenol blue 0.25% xylene cyanol FF 30% glycerol in water (pH 6.8)
Flowcytometry	Fixing solution	PBS 1% Paraformaldehyde (PFA)

2.1.2 Plasmid transformation, amplification and purification

2.1.2.1 Preparation of competent bacterial cells

XL1 Blue E. Coli cells (Invitrogen, CA, Carlsbad) were used for all transformations. These cells encode the mutated genes *recA1* (to avoid recombination events between plasmid and genomic DNA), *endA1* (to avoid DNA degradation) and *lacZΔM15* (needed for blue/white colony screening).

XL1 Blue cells from a glycerol stock were picked and streaked on an agar plate with 10 μg/ml tetracycline. The streaked plate was incubated overnight at 37 °C. A single colony was picked and used to inoculate 4 ml LB broth with 10 μg/ml tetracycline. This culture was incubated overnight at 37 °C. 1ml of this culture was then used to inoculate 100 ml LB broth (without any antibiotics). This culture was incubated at 37 °C in a shaker

until an OD600 of 0.3-0.6 was reached (2-2.5 hours). The culture was then cooled on ice for 5 min, centrifuged for 10 min at 6000 x g at 4 °C. The supernatant was decanted and the pellet resuspended in 50 ml Buffer TBF-I and incubated on wet ice for 5 min. The resuspended mixture was centrifuged again at 6000 x g for 10 min at 4 °C. The supernatant was decanted and the pellet resuspended in 4 ml Buffer TBF-II and incubated for 15 min on wet ice. The cells were dispensed in 100 µl aliquots into RNase and DNase free microcentrifuge tubes (Sarstedt) on wet ice and stored at -80 °C.

2.1.2.2 Transformation of competent bacterial cells

For transformation, competent bacteria were thawed on ice for 15-20 minutes 50-100 ng of plasmid DNA or 5 µl of ligation reaction was added to 50µl of competent cells and incubated on ice for 15-30 minutes. The cells were heat-shocked for 2 minutes at 37°C and then incubated on ice for 5 minutes. Transformed cells were then streaked on LB agar plates containing the appropriate antibiotic, usually ampicillin (Sigma, St Louis, MO) at 100 µg/mL, and incubated overnight at 37 °C.

2.1.2.3 PCR colony screening

PCR assays were used to screen the antibiotic-resistant colonies obtained from the competent cells transformed with ligation reactions. A master mix was prepared according to table 2.2 using the GoTaq G2 Hot Start Green MasterMix (Promega, Madison, WI) and the appropriate pair of primers that allowed detection of the correct construct (typically one primer that bound to the insert and another that bound to the plasmid backbone). 25 µl per reaction was dispensed into a PCR tube. A Single colony was picked using a pipette tip, streaked onto a labeled LB agar plate containing 100 µg/ml ampicillin and then transferred to a labeled PCR tube containing the PCR mix. PCR cycling conditions were as listed in Table 2.3. PCRs were run in a Hybaid thermal cycler.

Table 2.2. Master mix preparation for PCR colony screening

Reagent	Stock concentration	Volume per reaction (µl)
Nuclease-free water	-	7.5
Forward primer	10 µM	2.5
Reverse primer	10 µM	2.5
GoTaq G2 Hot Start Green MasterMix	2x	12.5

Table 2.3. Cycling conditions for PCR colony screening

Step	Temperature (°C)	Time
Initial heat activation	98	2 min
3-step cycle repeated 40 times:		
Denaturation	98	15 sec
Annealing	≈ lower Tm - 3	15 sec
Extension	72	1 min/kb
Final extension	72	4 min

2.1.2.4 Preparation of plasmid DNA

Single colonies were picked from LB agar plates and used to inoculate 5 mL (for minipreps) or 100 mL (for midipreps) of LB broth with ampicillin (100 µg/mL). The cultures were then grown overnight at 37 °C with shaking at 250 rpm in Innoca Incubator Shaker. Plasmid DNA was purified using the QIAGEN Plasmid Mini or Midi kits (Qiagen, Hilden, Germany) according to the manufacturer's instructions. DNA concentrations were determined using a Nanodrop 3300 spectrophotometer (Thermo Scientific, Wilmington, DE).

2.1.3 Restriction endonuclease enzyme digestion

All restriction enzymes used were from New England Biolabs (NEB, Ipswich, MA) or Promega. Digestion reactions were typically performed by mixing the following components: 1-5 μg DNA to be digested, 5 U of enzyme per μg of DNA, 1x of the appropriate buffer with/without bovine serum albumin (both according to manufacturer's instructions) and nuclease free water (Eppendorf, Hamburg, Germany) to bring the final volume to 30 μl. The reaction mix was incubated at 37 °C for at least 3 hours.

2.1.4 Ligation reaction reactions

T4 DNA ligase (Promega or NEB) was used where indicated for cloning DNA plasmids according to the manufacturer's instructions. In a typical reaction, 100 ng of backbone DNA was mixed with insert DNA at 1:3 molar ratio of backbone to insert DNA in a final concentration of 1x Ligase buffer (supplied by the manufacturer) made up to a final volume of 10 μl with nuclease free water (Eppendorf).

2.1.5 DNA phosphorylation reactions

The T4 polynucleotide kinase (NEB) was used for DNA phosphorylation reactions according to the manufacturer's instructions. Briefly, 1-2 μg of DNA was added to 1x T4 ligase buffer (NEB) and T4 polynucleotide kinase (NEB). The mix was made up to a final volume of 50μl with nuclease free water and incubated at 37°C for 45 min. DNA was purified using the QIAquick PCR purification kit (Qiagen) following the manufacturer's instructions.

2.1.6 DNA dephosphorylation reactions

The calf intestinal alkaline phosphatase (CIAP, Promega) was used for DNA dephosphorylation following the manufacturer's instructions. DNA was then purified using the QIAquick PCR purification kit (Qiagen) following the manufacturer's instructions.

2.1.7 Agarose gel electrophoresis

1-2% agarose gels were prepared by dissolving agarose (Invitrogen) in Buffer TAE by heating and stirring. The solution was allowed to cool and Ethidium Bromide (Dutscher Scientific, Essex, UK) was added at a final concentration of 0.25 μg/ml.

DNA was electrophoresed in the agarose gels with a 1kb plus DNA ladder (Invitrogen). Higher gel percentages were used for separation of fragments with a small size difference. DNA fragments of interest were excised and purified form the gel using a QIAquick Gel Extraction Kit (Qiagen) following the manufacturer's instructions.

2.1.8 Polymerase chain reaction (PCR)

Phusion polymerase (NEB), which possesses 3' to 5' proof-reading activity and generates blunt-ended products, was used for PCRs run for cloning purposes. A typical reaction setup is shown in Table 2.4. The PCRs were run in a Hybraid thermal cycler using the cycling conditions shown in Table 2.5. Primer Tm and annealing temperature used were determined using the NEB Tm calculator: http://tmcalculator.neb.com/#!/

Table 2.4. Master mix preparation for a typical PCR

Reagent	Stock concentration	Volume per 20 µl reaction (µl)	Volume per 50 µl reaction (µl)
Nuclease-free water	-	To 20 µl	To 50 µl
Phusion HF Buffer	5x	4	10
Forward primer	10 µM	1	2.5
Reverse primer	10 µM	1	2.5
Template DNA	Variable	Variable (<250 ng)	Variable (<250 ng)
Phusion polymerase	-	0.2	0.5

Table 2.5. Cycling conditions for a typical PCR

Step	Temperature (°C)	Time
Initial heat activation	98	30 sec
3-step cycle repeated 25 times:		
Denaturation	98	10 sec
Annealing	≈ lower Tm + 3	15 sec
Extension	72	30 sec/kb
Final extension	72	5 min

2.1.9 Quantitative polymerase chain reaction (Q-PCR)

2.1.9.1 Q-PCR for determination of DNA copy numbers of vector components in packaging/producer cells

Q-PCR was used to determine the number of DNA copies of the expression cassettes of the different vector components in packaging/producer cells. This was done using the QuantiTect SYBR Green PCR Kit (Qiagen). The SYBR green dye binds non-specifically to double stranded DNA and consequently fluoresces. As the target DNA sequence is amplified with each PCR cycle the amount of fluorescence increases until it reaches a detectable level. The number of the PCR cycle at which a signal is first detected is referred to as the Ct value. Thus, the Ct value is inversely related to the initial amount of DNA present in the samples tested. To convert Ct values to DNA copy numbers, a standard curve of Ct value against initial DNA copy number was plotted using a set of five serially diluted standards containing known copy numbers of the target sequence.

The standards and primers used in the Q-PCR assays are summarized in Table 2.6. The primer pairs were designed to specifically amplify a target DNA sequence. For *Gag-Pol,* primers Q-gagpol-F and Q-gagpol-R were primers designed to anneal at the frameshift region between *gag* and *pol* genes. For vector genome, primers GT248 and GT249, which anneal to and amplify the HIV-1 leader region were used. For *Rev*, primers Q-Rev-F and Q-Rev-R were used, whereas primers Q-RD-F and Q-RD-R were used for

RDpro. The standards used were as follows: p8.91 for Gag-Pol and Rev; pHV for HIV-1 leader region; for β-actin and RDpro, the standards were made by cloning the PCR product from HB-actin-F and RC or Q-RD-F and RC respectively, into pGEM T easy (Promega). The concentrations of the standards used in all Q-PCR assays were 10^5, 10^4, 10^3, 10^2, and 10^1 plasmids (copies)/µl.

To calculate the DNA copy number per cell, the human β-actin gene (an endogenous gene) was quantified in every gDNA sample used and divided by 6 to get an estimate of the total number of cells per reaction. This was based on two assumptions: 293FT cells are triploid, and the primer pair used (HB-actin-F and HB-actin-RC) (Knight, 2011) detect the β-actin gene (on Chromosome 7) and β-actin pseudogene (on Chromosome 11). The latter is based on an alignment of the primers' nucleotide sequences against the human genome using NCBI's online Basic Local Alignment Search Tool (BLAST: http://blast.ncbi.nlm.nih.gov/Blast.cgi) confirming that these primers would amplify the human β-actin gene as well the β-actin pseudogene on Chromosome 11.

Initially, genomic DNA (gDNA) was extracted as detailed in Section 2.6.1. Working stocks were prepared at 50 ng/µl from each gDNA sample.

A master mix was prepared based on the total number reactions to be performed as outlined in Table 2.7. Reactions were performed in 96-well plates by dispensing 20 µl of the master mix into each of 12 wells to be used for standards and no-template controls (typically 5 x 2 wells for standards and 1 x 2 wells for controls). Nuclease-free water (volume added = 3 µl x number of remaining reactions) was added to the remaining master mix resulting in a final composition as listed in Table 2.8. 23 µl of the master mix were dispensed into each well which to be used for samples. Finally, 5 µl of standards, 5 µl nuclease-free water or 2 µl the 50 ng/µl samples (total 100 ng) were added to the corresponding wells. All reactions were performed in duplicates.

All Q-PCR reactions were performed under the conditions outlined in Table 2.9 using the ABI 7500 Real-Time PCR system (Applied Biosystems, Warrington, UK). A melting curve was run following each assay to determine the Tm of the PCR product and confirm a single Tm is detected corresponding to a single PCR product.

Table 2.6. Primers and standards used in Q-PCR and Q-RT-PCR assays

Component	Standard	Primer Name	Primer Sequence
HIV-1 Gag/Pol	p8.91	Q-gagpol-F	AAGAGAGCTTCAGGTTTGGG
		Q-gagpol-RC	TGCCAAAGAGTGATCTGAGG
HIV-1 Rev	p8.91	Q-rev-F	TGTGCCTCTTCAGCTACCAC
		Q-rev-RC	CAATATTTGAGGGCTTCCCA
RDpro envelope	RDpro	Q-RD-F	AACTCCCAACAGGAATGGTC
		Q-RD-RC	TTAAGTAGGCCGTCTTGCCT
HIV-1 leader sequence	pHV	GT248	TGTGTGCCCGTCTGTTGTGT
		GT249	GAGTCCTGCGTCGAGAGAGC
Human β-Actin	HB-actin	HB-actin-F	TGGACTTCGAGCAAGAGATG
		HB-actin-RC	TTAAGTAGGCCGTCTTGCCT
GFP	pHV	GT139	CAACAGCCACAACGTCTATATCAT
		GT140	ATGTTGTGGCGGATCTTGAAG

Table 2.7. Master mix preparation for Q-PCR (standards and controls)

Reagent	Stock concentration	Volume per reaction (µl)
Nuclease-free water	-	2.5
Forward primer	20 µM	2.5
Reverse primer	20 µM	2.5
Quantitect MasterMix	2x	12.5

Table 2.8. Master mix for Q-PCR (unknown samples)

Reagent	Stock concentration	Volume per reaction (µl)
Nuclease-free water	-	5.5
Forward primer	20 µM	2.5
Reverse primer	20 µM	2.5
Quantitect MasterMix	2 x	12.5

Table 2.9. Cycling conditions for Q-PCR

Step	Temperature (°C)	Time
Initial heat activation	95	15 min
3-step cycle repeated 40 times:		
Denaturation	95	15 sec
Annealing	55	30 sec
Extension	72	30 sec
Melting curve	-	-

2.1.9.2 Q-PCR assay for detection of cell-derived and plasmid DNA contaminants

Detection of cell-derived SV40 TAg-encoding DNA (Bergsagel 1992) and plasmid DNA (Sastry 2004) was done using previously reported primer pairs. PCR reactions were prepared and conducted as detailed in section 2.6.1 using 2 µl of untreated VCM as a template per reaction. Reactions were performed at 95 **°C** for 15 min, followed by 40 cycles of 95 **°C** for 15 seconds, 57 **°C** (SV40 TAg) or 60 **°C** (AmpR) for 30 seconds, 72 **°C** for 60 seconds. A melting curve was run following each assay. Q-PCR reactions were performed in triplicates.

Details of primers and standards used for each target are listed in Table 2.10. The concentrations of the standards used in the Q-PCR assays were 10^5, 10^4, 10^3, 10^2, and 10^1 plasmids (copies)/ µl .

Table 2.10. Primers and standards used in Q-PCR assays for detection of cell-derived and plasmid DNA contaminants

Target Sequence	Standard	Primer Name	Primer Sequence
SV40 T Ag	pBABE-puro SV40LT	SV40TAg F	TGAGGCTACTGCTGACTCTCAACA
		SV40TAg RC	GCATGACTCAAAAAACTTAGCAATTCTG
AmpR	pHV	Amp F	GTTGCCATTGCTACAGGCATC
		Amp RC	ACTCGCCTTGATCGTTGGG

SV40 T Ag: Simian Virus 40 large T antigen, AmpR: ampicillin resistance gene

2.1.10 Reverse transcription quantitative polymerase chain reaction (RT-Q-PCR)

RT-Q-PCR was used for determination of RNA copy numbers of vector components in packaging/producer cells as a measure of the expression levels of the different components.

RNA was extracted as explained in Section 2.6.2. The extracted RNA was quantified by spectrophotometry and concentration was adjusted to 100 ng/ml.

cDNA was synthesized using the Quantitect Reverse Transcriptase kit (Qiagen) following the manufacturer's instructions. 2 µl of the synthesized cDNA was used as template for each Q-PCR reaction using the QuantiTect SYBR Green PCR Kit (Qiagen) and ABI 7500 Real-Time PCR system (Applied Biosystems) as explained in section 2.1.9.1.

RNA copy number for each gene was normalized to β-actin RNA copy number (a constitutively expressed endogenous gene), which was determined in every cDNA sample used. The primers and standards used were identical to those used for Q-PCR (Table 2.6). The concentrations of the standards used in all RT-Q-PCR assays were 10^7, 10^6, 10^5, 10^4, and 10^3 plasmids (copies)/µl.

2.1.11 Plasmid construction

Primers used for cloning DNA plasmids are listed in Table 2.11.

Table 2.11. Primers for cloning DNA plasmids

Vector	Primer name	Primer sequence
pLFA	Ba(XbNh)Ap F	GATCCATTCTAGATAGTTCTACAGT ACAGTACTGTACGCTAGCATGGGCC
	Ba(XbNh)Ap RC	CATTCTAGATAGTTCTACAGTACAG TACTGTACGCTAGCATG
pCVGLFA	CVi XbaI F	TCTAGATCGAAGCTTACATGTGGTA CCGA
	CV NheI RC	GCTAGCTCACTTCCTGAAGCGGCT
pFBIL2RGF12 & pFBIL2RGcoF13	ApaI CMVp F	AGAGGGCCCAAGCTTGGCCATTGC ATACGTTG
	SnaBI RC	GCGATGACTAATACGTAGATGTACT GCCAAG
	EcoRV F	CTTTCGAATTCGATATCAAGCTG
	ApaI RC	TCTGGGCCCAAGATGACATGAACTA CTACTGCTAGAG
SIN pHVC	BamHI mCherry F	CTTGGATCCGCCACCATGGTGAGCA AGGGCGAG
	SalI mCherry RC	CTTGTCGACCCTCGAGTTTACTTGT ACAGCTC

2.1.11.1 SIN pHV

This plasmid was generated by Sean Knight(Knight, 2011). To construct SIN PHV, the SIN lentiviral LTR from UCOE-gamma-C was cloned into pHV in place of the wild type lentiviral LTR. Briefly, pHV was digested with BamHI (Promega) and ApaI (NEB). The 2 fragments of DNA resulting from this were separated by electrophoresis on a 1% agarose gel. The ≈5.7kb fragment was extracted and kept as a backbone, the ≈2.2kb band was digested with Sac II and the resulting ≈1.2 kb fragment extracted from a 1.5% agarose gel after electrophoresis. The SIN LTR from UCOE-gamma-C was amplified by PCR using KOD polymerase (Novagen) by primers Sac WPRE-F and ApaI UCOE RC. This PCR product was then cut with SacII (Promega) and ApaI (present on either side of SIN LTR). The 1.2kb fragment of pHV cut with SacII and BamHI and the SIN LTR cut with SacII and ApaI were cloned into the backbone cut with BamHI and ApaI using T4 DNA ligase (Promega) overnight at 4 ℃.

2.1.11.2 pCVGLFA

pRDproLF plasmid (Ikeda et al., 2003a) was cut with ClaI (NEB) and BamHI (NEB). The digestion products were separated by electrophoresis on a 1% agarose gel and the ≈5.3kb fragment was extracted.

pLFA plasmid was generated by insertion of two unique restriction sites, namely XbaI and NheI, into the 5.3kb fragment. To achieve this, two complementary oligos (Ba(XbNh)Ap F and Ba(XbNh)Ap RC) were annealed resulting in a double-stranded DNA fragment with BamHI and ClaI sticky ends flanking the XbaI and NheI restriction sites. This DNA fragment was then phosphorylated using T4 polynucleotide kinase (NEB) at 37 ℃ for 30min. The phosphorylated fragment was subsequently ligated with the 5.3kb fragment using T4 DNA ligase (Promega) overnight at 4 ℃.

pLFA plasmid was then cut with XbaI (NEB) and NheI (NEB). The digestion products were separated by electrophoresis on a 1% agarose gel and the ≈5.3kb fragment was extracted. This DNA fragment was dephosphorylated.

The Cocal Virus G protein (CV-G) was amplified by PCR from pMD2Cocal.G plasmid using the primers CVi XbaI F and CV NheI RC. This PCR product was ligated into the pJET cloning plasmid (Themo Scientific) using T4 DNA ligase (Themo Scientific) for 5min at room temperature. The resulting plasmid, pJET CVG, was

amplified and then cut with XbaI (NEB) and NheI (NEB). The digestion products were separated by electrophoresis on a 1% agarose gel and the ≈ 2.2 kb fragment was extracted.

This 2.2 kb fragment was then ligated into the 5.3 kb fragment from pLFA plasmid using T4 DNA ligase (Promega) overnight at 4°C to generate pCVGLFA.

2.1.11.3 pFBIL2RGF12

pCCL.EFS.IL2RG was kindly provided by Adrian Thrasher.

The 5' end of the expression cassette of pCCL.EFS.IL2RG (443 bp, identical to that in pCCL.EFS.IL2RGco) was amplified by PCR using the primers ApaI CMVp F and SnaBI RC. The PCR product was cut with ApaI.

The 3' end of the expression cassette of pCCL.EFS.IL2RG (345 bp, identical to that in pCCL.EFS.IL2RGco) was amplified by PCR using the primers EcoRV F and ApaI RC. The PCR product was cut with ApaI.

pFBCF (made by Sean Knight) was cut with ApaI (NEB) and BamHI (NEB). The digestion products were separated by electrophoresis on a 1% agarose gel and the ≈ 4.5 kb fragment was extracted.

A 3-piece ligation was carried out to ligate the cut PCR products into the 4.5 kb pFBCF backbone. Colonies derive from competent cells transformed with the ligation reaction were screened by PCR. The plasmid pFBF 53Gc4 was amplified and the sequence and orientation of the ligated PCR products were confirmed (GATC Biotech, Cologne, Germany).

pFBF.53Gc4 was cut with SnaBI (NEB) and EcoRV (NEB). The digestion products were separated by electrophoresis on a 1% agarose gel and the ≈ 5 kb fragment was extracted. The fragment was dephosphorylated.

pCCL.EFS.IL2RG was cut with SnaBI (NEB), EcoRV (NEB) and SspI. The digestion products were separated by electrophoresis on a 1% agarose gel and the ≈ 4 kb fragment was extracted.

The 5 kb backbone derived from p pFBF.53Gc4 was ligated with 4kb fragment derived from pCCL.EFS.IL2RG. Colonies derive from competent cells transformed with

the ligation reaction were screened by PCR. The plasmid pFBIL2RGF12 was amplified and its sequence and orientation were confirmed (GATC Biotech, Cologne, Germany).

2.1.11.4 pFBIL2RcoF13

pCCL.EFS.IL2RGco was kindly provided by Adrian Thrasher.

pCCL.EFS.IL2RGco was cut with SnaBI (NEB), EcoRV (NEB) and SspI. The digestion products were separated by electrophoresis on a 1% agarose gel and the ≈ 4 kb fragment was extracted.

The 5 kb backbone derived from p pFBF.53Gc4 was ligated with 4kb fragment derived from pCCL.EFS.IL2RGco. Colonies derive from competent cells transformed with the ligation reaction were screened by PCR. The plasmid pFBIL2RGcoF13 was amplified and its sequence and orientation were confirmed.

2.1.11.5 SIN pHVC2

SIN pHV was cut with BamHI (NEB) and SalI (NEB) and the digestion products were separated by electrophoresis on a 1% agarose gel and the ≈ 5 kb fragment was extracted.

The mCherry gene was amplified by PCR from plasmid pDual PD1 mCherry (made by Christopher Bricogne) using the primers BamHI mCherry F and SalI mCherry RC. The ≈ 700 bp PCR product was cut with BamHI and SalI.

The 5 kb backbone derived from SIN pHV was ligated with the cut 700 bp PCR product. SIN pHVC2 was amplified and its sequence was confirmed (GATC Biotech, Cologne, Germany).

2.2 Cell Culture

HEK293T, HEK293FT (Genethon, Evry, France), HeLa, HT1080, WinPac, STAR, and FLY cells were cultured in DMEM (Dulbecco's Modified Eagle Medium) containing Glutamax (GIBCO, Carlsbad, CA), supplemented with 50 U/ml Penicillin, 50 mg/ml Streptomycin (GIBCO) and 10% FBS (Sigma-Aldrich / GIBCO) at 37**°C** and 5% CO_2. When indicated, antibiotics were added to the culture medium (Antibiotics and their working concentration are listed in the Supplementary Table S4). The lot numbers of all

reagents added to 293FT cells and all cell lines derived from it potentially for future clinical use have been documented.

2.2.1 Cell lines

HEK 293T cells are derived from HEK 293 cells by stable transfection of the SV40 T-Antigen. HEK 293 cells were originally derived from normal human embryonic kidney (HEK) cells following transformation with sheared adenovirus 5 DNA (adenoviral sequences corresponding to the early region 1 (E1) transforming sequences were mapped to chromosome 19 in these cells) (Graham et al., 1977) (Stacey and Merten, 2011). Although they were originally thought to be of an epithelial origin, evidence suggests that they are derived from cells of neuronal origins that were transformed by the adenoviral DNA in the original HEK cell culture (Shaw et al., 2002).

HEK 293FT cells are a traceable cell line derived from HEK 293F cell line (a "fast growing" clone of HEK 293 cell line) by stable transfection of a plasmid encoding SV40 T-Antigen under the control of the hCMV promoter (Stacey and Merten, 2011).

STAR cells are a lentiviral vector packaging cell line derived from 293T cells by transduction with MLV vectors expressing HIV-1 gag-pol, rev and tat. Stable transfection of a plasmid encoding the RDpro envelope into STAR cells gave rise to STAR-RDpro cells. Transduction of STAR-RDpro cells with a lentiviral vector expressing GFP yielded STAR-RDpro-HV cells (Ikeda et al., 2003a).

HeLa cells are an epithelial cell line derived from human cervical adenocarcinoma, whereas HT1080 cells are a human fibrosarcoma-derived cell line. FLY cells are a HT1080-derived cell line expressing the Murine Leukemia Virus (MLV) gag- (Cosset et al., 1995).

2.2.2 Antibiotics

In this thesis antibiotics were used to select for cells expressing genetically-linked vector components. These anibiotics are puromycin (Invivogen), hygromycin (Invivogen), phleomyin (Invivogen) and blasticidin (Invivogen).

Table 2.12. Antibiotics used in mammalian cell culture

Antibiotic	MOA	Working concentration (μg/ml)	Vector component selected for
Puromycin	Inhibition of protein synthesis	1	Gag-Pol
Hygromycin	Inhibition of protein synthesis	100	Rev
Phleomycin	DNA cleavage	30	Env
Blasticidin	Inhibition of protein synthesis	5-10	Vector Genome

MOA: Mechanism of action, Env: Envelope glycoprotein (RDpro or CV-G)

2.2.2.1 Puromycin (Puro)

Puromycin is an aminonucleoside derived from *Streptomyces alboniger*. Puromycin inhibits protein synthesis by two mechanisms. First, it can be incorporated at the C-terminal ends of growing polypeptide chains resulting in the premature release of incomplete chains. It can also result in the dissociation of polyribosomes during protein synthesis (Bread et al., 1969).

Resistance to puromycin is conferred by the puromycin N-acetyltransferase (PAC) activity of the enzyme encoded by the *pac* gene (Cundliffe, 1989).

2.2.2.2 Hygromycin B (HmB)

Hygromycin B is an aminoglycoside antibiotic produced *Streptomyces hygroscopicus*. It binds to the small ribosomal subunit and specifically inihibits translocation during translation elongation. This is thought to result from steric hindrance of the movement of tRNA between the ribosomal A and P sites and the confinement of tRNAs at these sites (Borovinskaya et al., 2008).

Resistance to hygromycin B is imparted by hygromycin phosphotransferase (HPH) activity (*Hyg* gene), which phosphorylates hygromycin B resulting in its inactivation (Cundliffe, 1989).

2.2.2.3 Phleomycin (Phleo)

Phleomycin is a mixture of copper-containing glycopeptides isolated from *Streptomyces verticillus*. It binds and intercalates into the DNA double helix and results in single-stranded DNA breakage most likely via a mechanism involving the production of free-radicals (Fox et al., 1987; Sleigh, 1976).

Resistance to phleomycin is conferred by the *Sh ble* gene, which encodes a 14kDa acidic protein that binds and sequesters phleomycin (Cundliffe, 1989).

2.2.2.4 Blasticidin (BlaS):

BlaS is nucleoside analog produced by S*treptomyces griseochromogenes*. It consists of a cytosine linked with a pyranose ring and an N-methyl-guanidine tail.

At working concentrations, BlaS inhibits protein synthesis by inhibiting translation termination and, to a lesser extent, translation elongation. This is mediated through binding to the P site of the 50S ribosomal subunit and bending the CCA end of the P-site tRNA toward the A site. This is hypothesized to result in steric hindrance to the binding of release factors and the aminoacyl-tRNA at the ribosomal A site. Moreover, altered positioning of the peptidyl-tRNA at the P site might impair the nucleophilic attack by aminoacyl-tRNA during translation elongation and by a water molecule during translation termination (Svidritskiy et al., 2013).

Resistance to BlaS can be imparted by the *bsr* gene which encodes Blasticidin S deaminase (Yamaguchi et al., 1975). This enzyme catalyzes the deamination of the cytosine moiety of blasticidin S resulting in its inactivation.

2.3 Stable transfection

Stable transfection was employed to achieve stable expression of vector components in PCLs. This process involves the transfection of a plasmid DNA expressing the vector component of interest as well as a gene that confers antibiotic resistance on the same construct or a second co-transfected one. The plasmid can undergo stable integration at sites of double-strand breaks in the cell genome. Cells with stable integrations were then selected for using the antibiotic to which resistance is conferred.

2.3.1 Stable transfection of a SIN LV in WinPac-RD cells

A GFP-expressing SIN LV encoding plasmid, SIN pHV, was co-transfected at a 10:1 molar ratio to pSelect Blasti MCS, which expresses the *bsr* gene (confers resistance to blasticidin).

Briefly, WinPac-RD cells were passaged 1:6 in 10 cm plate. After 24 hours, 34.6 μg SIN pHV and 1.5 μg pSelect Blasti MCS (molar ratio 10:1) were co-transfected using FuGENE 6 (Promega) and Optimem (GIBCO). After 48 hours cells were passaged 1:20 and then 5 serial 3-fold dilutions were made. Each dilution was used to seed a 10cm plate in DMEM with 10 μg/ml blasticidin S (Invivogen).

2.3.2 Stable transfection of Cocal Virus G-protein in WinPac cells

Winpac cells were seeded at $6x10^6$ per 10 cm plate. After 48 hours, 3 μg of pCVGLFA was transfection was performed by using 20μl of FuGENE 6 (Promega), 200 μl of Optimem (GIBCO) and 3 μg of plasmid (which encode RDpro, RDTR, GALVTR, CV and RRV envelope genes) carrying the phleomycin resistance gene. 24 hr after the transfection the old media was replaced with 8ml of new complete media. 48 hr after the transfection, the cells were trypsinized and six-fold dilutions were seeded in 10 cm plates in 12 ml DMEM supplemented with phleomycin 15 to 30 μg/ml.

2.4 Recombinase-mediated Cassette Exchange (RMCE)

C61 cells were thawed out and sequentially selected in puromycin, hygromycin and phleomycin for >10 days. Cells were seeded at $1x10^6$ cells/well in a 6-well plate. 48 hours post-seeding, cells were co-transfected with 3 μg pFBCF and 9 μg pCflpe plasmids (molar ratio of 1:4) using FuGENE 6 (Promega). 72 hours post-transduction, cells were harvested and six 1:10 dilutions were prepared. Each dilution was plated into a $10cm^2$ plate in complete medium with blasticidin (5 μg/ml).

Over the next 14 days, medium with blasticidin was changed every 3-4 days and the plates were monitored for the growth of distinct colonies of cells. Individual colonies were picked and transferred to a 96-well plate. Cell cultures were scaled up and re-selected with blasticidin, puromycin, hygromycin and phleomycin. Single cell clones were then isolated by limiting dilution in 96-well plates.

2.5 Limiting dilution in 96-well plates

A cell suspension at $2x10^4$ cells/ml was prepared. 100ul of medium was added to each well in a 96-well plate except well A1 (leave empty). 200µl of the cell suspension was added to well A1. 100µl from well A1 was quickly transferred to well B1 and mixed by gentle pipetting. These 1:2 dilutions were repeated down the entire column. 100µl was discarded form well H1. An additional 100µl of medium was added to each well in column 1 to bring the final volume to 200µl/well. Then 100µl were transferred from the wells in column 1 (A1 – H1) to the corresponding wells in column 2 (A2 – H2) and mixed by gentle pipetting. These 1:2 dilutions were repeated across the entire plate, and 100µl from the wells in the last column (A12 – H12) were discarded. The final volume in all wells was brought to 200µl by adding 100µl medium to each well. The plates were then incubated at 37°C with 10% CO_2. Wells were monitored for growth of single colonies over the next two weeks. These colonies were then transferred into 24-well plates.

2.6 Nucleic Acid Extraction from mammalian cells

2.6.1 Extraction of genomic DNA (gDNA)

$2\text{-}4x10^6$ cells were centrifuged, resuspended in PBS (Gibco) and centrifuged again. The supernatant was decanted and the cell pellets stored at -80°C. gDNA was extracted from the cells using DNeasy Blood and Tissue Kit (Qiagen) following the manufacturer's instructions. DNA concentrations were determined using a Nanodrop 3300 spectrophotometer (Thermo Scientific, Wilmington, DE) and 50ng/µl working stocks were prepared from each sample.

2.6.2 Extraction of RNA

$2\text{-}5x10^6$ cells were centrifuged, resuspended in PBS (Gibco) and centrifuged again. The supernatant was decanted and the cell pellet was resuspended and mixed well (by pipetting/vortexing) in 350ul buffer RLT (Qiagen) and 1% β-mercaptoethanol (Sigma). This ensures lysis and homogenization of cells while the highly denaturing guanidine-thiocyanate–containing RLT buffer and β-mercaptoethanol inactivate RNases to ensure purification of intact RNA. The samples were then frozen at -80°C. The sample were later thawed out on ice and RNA was extracted from the cells using RNeasy Mini Kit (Qiagen) following the manufacturer's instruction. RNA concentrations were determined using a

Nanodrop 3300 spectrophotometer (Thermo Scientific, Wilmington, DE) and 100 ng/µl working stocks were prepared from each sample.

2.7 LV production, concentration and titration:

2.7.1 LV production

2.7.1.1 Stable LV production

Cells were seeded at a density of 2.1–2.3 x 10^5 (for WinPac-RDpro-HV cells) or 3.1-3.2x 10^5 (for WinRD-F1-derived cells) cell/cm^2. After 72 hours, cells were washed with medium and 0.08–0.1 ml/cm^2. of medium was replaced except for HYPERFlasks for which 0.33 ml/cm^2. medium was used. 24 hours later, vector-containing medium (VCM) was collected, passed through 0.45 µm filter and stored at -80 °C. Fresh medium was added to the cells for collection after 24 hours. This process was repeated for up to six times.

Typically, vectors were harvested in regular culture medium: DMEM containing Glutamax (GIBCO), supplemented with 50 U/ml penicillin, 50 mg/ml streptomycin (GIBCO) and 10% FBS (Sigma-Aldrich/GIBCO). Alternatively, no FBS was included or only 1% FBS was used with or without 20 mM HEPES buffer (Sigma-Aldrich). Other harvesting media used included OptiPro (GIBCO) supplemented with 4mM L-glutamine (GIBCO) with/without supplementation with FBS (Sigma-Aldrich/GIBCO). The harvesting medium used in all experiments is indicated in the text.

2.7.2 Transient LV production

2.7.2.1 Transient LV production from unmodified cell lines (293T cells)

Three-plasmid co-transfection into HEK293FT cells was used to make pseudotyped LV as described previously (Zufferey et al., 1997). Briefly, 6x10^6 293FT cells were seeded in 10 cm^2 plates. 24 hours later, they were transfected using FuGENE 6 (Promega) with the following plasmids: SIN pHV (vector plasmid), p8.91 (Gag-Pol and Rev expression plasmid (Zufferey et al., 1997), and either pMD.G (VSV-G env expression plasmid (Naldini et al., 1996)) or pRDproLF (RD114-derived env expression plasmid (Ikeda et al., 2003a)). Medium was changed after 24 hours and then VCM was collected over 24-hour periods for 3 days. Following collection, VCM was passed through 0.45 µm filter and stored at -80 °C.

2.7.2.2 Transient LV production from packaging cell lines

Packaging cell lines were transiently transfected with DNA plasmids expressing the missing LV components as a functional test to compare the isolated cell populations/clones.

Briefly, WinPac-CVG cells were seeded at $2x10^6$ cells/well in a total volume of 3ml/well in three wells of a 6-well plate. 48 hours after seeding, the cells were transfected with SIN pHV plasmid. This was performed by adding 4 µl fugene 6 (Promega) to 50 µl Optimem (GIBCO). Then 1 µg SIN pHV was added to the mix and incubated at room temperature for 15 minute. 1.5ml of medium was carefully pipetted off the cells and the DNA-fugene 6 mix was added to the cells dropwise. The cells were incubated at 37°C. After 24 hours, the cells from one well were tripsinized, fixed in 1% PFA and analysed by flowcytometry for GFP expression as a measure of transfection efficiency. For the remaining two wells, the medium was replaced with 1ml of fresh complete medium. At three consecutive 24 hour intervals, VCM was harvested, passed through 0.45µm filter and stored by freezing at -80°C until titrated (Table 2.13).

Table 2.13. Transient LV production protocol from packaging cell lines

Day	Step/Procedure
0	seeded $2x10^6$ cells/well in three wells of a 6-well plate (A, B and C)
2	Transfected cells with SIN pHV
3	Well C: trypsinized cells, fixed in 1% PFA and analyzed by flowcytometry Wells A & B: Replaced medium with 1ml fresh medium
4	Harvested VCM, passed it through 0.45µm filter and stored it by freezing at -80°C until titrated. Replaced 1ml of fresh medium onto cells.
5	As for day 4
6	As for day 5

1% PFA: 1% Paraformaldehyde in phosphate-buffered saline, VCM: Vector-containing medium

2.7.3 LV Concentration

WinPac-RD-HV, RDpro LV and VSV-G LV preparations were concentrated by centrifugation in a Heraeus Megafuge (Thermo Scientific, Waltham, MA) at 4000*g* for18 hours at 4 °C, or by ultracentrifugation in 35 mL ultracentrifugation tubes (Beckman-coulter, Brea, CA) using a Sorvall Discovery M120SE Micro-Ultracentrifuge and a SureSpin 630 (36ml) rotor (Thermo Scientific) under the following conditions: for RDpro psuedotypes 37 000*g* for 2 hours at 4 °C; for VSV-G psedudotypes 37 000*g* for 2 hours at 4 °C. The pellet was re-suspended in ice cold X-VIVO10 (Lonza, Walkersville, MD) and stored at -80°C. Alternatively, vector preparations were concentrated by tangential flow filtration (TFF) using a KrosFlo Research IIi System and PES hollow fiber modules (Spectrum Labs, Rancho Dominguez, CA). TFF protocols were developed partly based on a previous work (Cooper et al., 2011) and described in detail in the Results section.

2.7.4 LV Titration

The functional titer of each vector preparation was determined by flow cytometric analysis for eGFP expression following transduction of 293T cells. Briefly, 293T cells were seeded in 12-well plates at $6x10^5$ cells/well in 250µl medium with 8 µg/ml polybrene (Sigma-Aldrich). 5-fold serial dilutions of the vector preparations were made using medium supplemented with 8µg/ml polybrene. 250 µl of each dilution was added per well to bring the total volume to 500µl/well at transduction. Where indicated, vectors were spinoculated onto 293T cells (1200*g*, 2 hours, 25°C). 24 hours post-transduction, medium was replaced with fresh medium. 48 hours post-transduction, cells were trypsinized, fixed in 1-2% Paraformaldehyde (Sigma-Aldrich) in PBS (GIBCO) and analyzed for eGFP expression by flow cytometry using FACSCalibur (BD Biosciences, San Jose, CA) and Flowjo software. Titers were calculated from virus dilutions where 1–20% of the cell population was eGFP-positive using the following formula:

Titer (TU/ml)= (no. of cells at transduction x % of GFP positive cells ÷ 100) ÷ (vector input volume (ml) x dilution factor)

Vector preparations harvested from STAR-RDpro cells were used as a control in titration experiments.

2.8 Isolation and transduction of human primary cells

2.8.1 Isolation and transduction of human primary T cells

For T cell isolation, whole blood was collected from donors following their signed informed consent under sterile conditions. PBMCs were isolated by Ficoll (GE Healthcare, Little Chalfont, UK) gradient centrifugation, re-suspended in X-VIVO 10 (Lonza, Basel, Switzerland), stimulated overnight with 0.5 μg/ml OKT3 (anti-CD3, Miltenyi Biotech, Auburn, CA) and 0.5 μg/ml anti-CD28 (Miltenyi Biotech). IL-2 (Proleukin, Chiron, Emeryville, CA) was added at a concentration of 100 international units (IU)/ml following overnight stimulation. On the next day, T cells were harvested, seeded at 3 x 10^5 cells per well, and spun at 1000*g* for 40 min at room temperature on 24-well plates previously coated with the CH-296 fragment of fibronectin (Retronectin, Takara, New York, NY) and preloaded with TFF-concentrated vector supernatant at MOI 1 or 5 (based on 293T transduction units). After 72 hours incubation, T cells were harvested and re-suspended in fresh XVIVO 10 medium supplemented with 100 TU/ml IL-2. 72 hours later (6 days post-transduction). Transduced cells were analyzed for GFP expression by flow cytometry (FACSCalibur, BD Biosciences).

2.8.2 Isolation and transduction of human CD34+ cells

Human CD34+ cells were isolated from G-CSF mobilized peripheral blood of a healthy donor after their signed informed consent using the Diamond CD34 Isolation Kit (Miltenyi Biotec). Cells were cultured in X-VIVO 10 plus 1% human serum albumin (HSA), supplemented with stem cell factor (hSCF) at 100 ng/ml; human Flt3-ligand (hFlt-3L) at 100 ng/ml; thrombopoietin (hTPO) at 100 ng/ml; and human interleukin 3 (hIL3) at 20 ng/ml (all from Peprotech, London, UK) for three days before transduction.

For CD34+ cell transduction, 24-well plates were coated with Retronectin (Takara); each well was incubated with 0.5 ml of Retronectin 125 x diluted with PBS at 4 °C overnight. Concentrated GFP-encoding LVs (WinPac-RD-HV1 or VSV-G LV) were preloaded (by centrifugation at 1200*g* at 32 °C for 40 min) onto the retronectin-coated plates and the supernatant was discarded (Kuhlcke et al., 2002). 1 x 10^5 hCD34+ cells were transduced overnight at MOI 0.5 or 5 (based on 293T transduction units). 96 hours post-transduction, CD34+ cells were analyzed for GFP expression by flow cytometry (FACSCalibur, BD Biosciences).

2.9 Western Blot

To prepare cell lysates, 2-3x10^6 cells were washed with ice-cold PBS and lysed using 1% Triton-X100 in PBS-T (0.1% Tween20 in PBS) in the presence of 1 x protease inhibitor. An equal amount of protein (20-25 μg) from each sample was mixed with 1x Laemmli Buffer, heated at 90 °C for 5 min and then loaded onto 10% SDS-polyacrylamide gel. To prepare vector lysates, equal volumes of vector-containing medium (VCM) was mixed with 1x Laemmli Buffer, heat inactivated at 95 °C for 5 min, and loaded onto 10% SDS-polyacrylamide gel.

To prepare vector lysates, equal volumes of vector-containing medium (VCM) was mixed with 1x Laemmli Buffer, heat inactivated at 95 °C for 5 min, and loaded onto 10% SDS-polyacrylamide gel.

Samples were electrophoresed on the gel and then blotted onto Hybond ECL nitrocellulose membrane (Amersham). The membranes were blocked with 5% skimmed milk in PBS-T (Blocking Buffer), incubated with primary antibodies, washed with PBS-T, incubated with a secondary antibody conjugated with Horseradish peroxidase, washed with PBS-T, and then incubated with LimiGLO chemiluminescent substrate (Cell Signaling Technology) at room temperature for 1 minute. Lastly, the membranes were exposed to Hyperfilm ECL (Amersham) for signal detection. The antibodies used are shown in Table 2.14.

To prepare cell lysates, 2–3 x 10^6 cells were washed with ice-cold PBS and lysed using 1% Triton-X100 in PBS-T (0.1% Tween20 in PBS) in the presence of 1 x protease inhibitor. Following 10–15 min incubation on ice, whole cell lysates were clarified by centrifugation at 13,000 rpm and 4°C for 20 min on Eppendorf Centrifuge 5415D. Total protein concentration was measured using the Pierce BCA Protein Assay Kit (Thermo Scientific).

An equal amount of protein (20–25 mg) from each sample was mixed with Laemmli Buffer, heated at 90 °C for 5 min. Samples were separated by electrophoresis on 10% SDS-polyacrylamide gel at 120 volts for 2 hours, and then electrotransferred at 40 volts for 1.5 hour onto Hybond ECL nitrocellulose membrane (GE Healthcare). The membranes were blocked with 5% skimmed milk in PBS-T (blocking buffer) for 1 hour, and then incubated with the primary antibody (diluted in blocking buffer) overnight at 4°C. After that, the membranes were washed with PBS-T for 5 min five times, incubated

with the HRP-conjugated secondary antibody (diluted in blocking buffer) for 1 hour at room temperature, washed as before, and then incubated with LimiGLO chemiluminescent substrate (Cell Signaling Technology, Beverly, MA) at room temperature for 1 minute. Lastly, the membranes were exposed to Hyperfilm ECL (GE Healthcare) for signal detection. For detection of APOBEC3G, polyclonal rabbit anti-APOBEC3G (kind gift from Michael Malim, King's College London) was used as primary antibody, and polyclonal swine anti-rabbit IgG (P0399, Dako, Glostrup, Denmark) was used as secondary antibody. For detection of α-tubulin, mouse anti-α-tubulin (T6199, Sigma-Aldrich) was used as primary antibody, and polyclonal rabbit anti-mouse IgG (P0260, Dako) was used as secondary antibody.

Table 2.14. Antibodies used for western blotting

Antibody	Host	Cataglogue number, Manufacturer/Source	Dilution
Polyclonal anti-APOBEC3G	Rabbit	Prof. Michael Malim (KCL)	1:3000
Monoclonal anti-α-tubulin	Mouse	T6199, Sigma-Aldrich	1:2000
HRP-conjugated polyclonal Anti-rabbit IgG	Swine	P0399, Dako	1:3000
HRP-conjugated polyclonal anti-mouse IgG	Rabbit	P0260, Dako	1:1000

APOBEC3G: HRP:

2.10 Infection assay for evaluation of role of Low Density Lipoprotein Receptor (LDL-R) in pseudotyped LV entry

To determine whether the human LDL-R plays a role in mediating infection of pseudotyped LVs, an infection assay was performed in the presence or absence of soluble LDL-R (sLDL-R).

293T cells were seeded at a density of $2x10^6$ cells per well in 24-well plates and incubated for 1 hour in the presence or absence of the soluble LDL-R (tested at two concentrations: 1 or 3 μg/ml). The cells were then transduced at two MOIs (0.1 or 0.5) with VSV-G-, CV- or RDpro-pseudotyped lentiviruses (MOI 0.1 and 0.5) in a total volume of 275 μl. After 24 hours, the medium was replaced with 1ml of fresh medium. 48 hours post-transduction cells were trypsinized and fixed using 1-2% PFA. Transduced cells were analyzed for GFP expression by flow cytometry (FACSCalibur, BD Biosciences) to determine the percentage of GFP positive cells. This experiment was done in triplicates for each condition tested.

2.11 Sequence and phylogenetic analysis of rhabdoviral G-proteins

The nucleotide sequences of the codon-optimised CV-G was kindly provided by Hans-Peter Kiem (Trobridge et al., 2010). The nucleotide sequences of the wild-type CV-G and VSV-G were obtained from GenBank (Table 2.15). Pairwise sequence alignments of nucleotide sequences were calculated using Clustal Omega online tool on the EMBL-EBI website at default settings:

http://www.ebi.ac.uk/Tools/msa/clustalo/

The amino acid sequences of the rhabdoviral G proteins were obtained from Uniprot (Table 2.15). Multiple alignments of rhabdoviral G proteins of rhabdoviruses were calculated using Clustal Omega online tool on the EMBL-EPI website at default settings. Alignments were visualized using Jalview v2 (Waterhouse et al., 2009).

To generate the phylgenetic tree, Vesiculoviral G proteins as well as that of the Rabies Virus (a related rhabdovirus) were included in the analysis. The BEAST v1.8.1 software (Drummond and Rambaut, 2007) was used to perform bayesian analysis of the amino acid sequences. This is entirely orientated towards rooted, time-measured phylogenies inferred using molecular clock models. The tree was visualized after bootstrapping with FigTree v1.4.2.

Table 2.15. Accession numbers of Rhabdoviral G proteins

Rhabdovirus	UniProtKB/Swiss-Prot accession number	Genbank Accession number
Cocal Virus (COCV)	O56677	AF045556
Vesicular Stomatitis Indiana Virus (VSIV) - San Juan	P03522	M35219
Vesicular Stomatitis New Jersey Virus (VSNJV) - Ogden	P04882	V01214
Maraba Virus (MARAV)	F8SPF4	HQ660076
Chakanguya (CHPV)	P13180	J04350
Isfahan Virus (ISFV)	Q5K2K4	AJ810084
Piry Virus (PIRYV)	Q85213	D26175
Spring Viremia of Carp Virus (SVCV)	Q91DS0	AJ318079
Rabies Virus (RABV)	P08667	M13215

2.12 Statistical Analyses

All data were analyzed using the GraphPad Prism v5.0 statistical software package. Details of statistical tests applied to individual data sets are indicated in the corresponding figure legends.

CHAPTER

3

Characterization and Validation of a Stable Packaging Cell Line for Clinical Self-inactivating Lentiviral Vector Production

3 Characterization and validation of a stable packaging cell line for clinical self-inactivating lentiviral vector production

3.1 Introduction

As detailed in Chapter 1, LVs have been used by many investigators to modify cells *in vitro* and *in vivo* because they can integrate a transgene or shRNA into the genome of most cell types (Sakuma et al., 2012). This work has extended to clinical trials using LV to modify bone marrow stem cells from patients with inherited genetic disorders; subsequent transplantation of the modified cells has resulted in clinical benefit for several life-threatening conditions such PIDs and hemoglobinopathies (Naldini, 2011). LV-modified autologous T cells have also been used in clinical trials to treat malignancies yielding encouraging results (Kochenderfer and Rosenberg, 2013).

As LVs are replication defective, they need to be produced by co-expression of their constituents in one producer cell. These constituents are usually provided in three or four separate plasmids. The Gag-Pol expression cassette encodes HIV structural proteins and enzymes. Another cassette encodes Rev, which is an HIV accessory protein necessary for vector genome nuclear export (Pollard and Malim, 1998). A third cassette encodes a heterologous envelope protein, often that of the G protein from vesicular stomatitis virus (VSV-G) (Naldini et al., 1996), that allows LV particle entry into target cells. Another cassette encodes the vector genome itself, which carries signals for incorporation into particles as well as an internal promoter driving transgene expression. The construction of stable packaging cell lines expressing all these components at high levels has been challenging. Notably, the HIV Gag-Pol cassette has proved impossible to express continuously at high level by stable plasmid transfection. The cytotoxicity of the HIV-1 protease has been suggested as a possible cause for this problem (Kaplan and Swanstrom, 1991; Nie et al., 2002; Sainski et al., 2011). The commonly used VSV-G envelope is also cytotoxic (Friedmann and Yee, 1995; Hoffmann et al., 2010). Therefore, most LV batches, including those used in published clinical trials to date, have been produced by transient transfection of HEK293T cells with multiple plasmids (Table 1.1). Such transfection is expensive, hard to reproduce at large scale, and results in contamination of the LV preparation with plasmids and cellular debris (Pichlmair et al., 2007).

LV production using stable packaging cell lines (PCLs) would avoid some of these problems and will be particularly necessary to produce batches of LV for larger clinical trials and future gene therapies that may be approved for use in the clinic (Table 3.1). If robust PCLs become available, they might become widely adopted for clinical LV production similar to GRV PCLs. As an alternative to continuous, constitutive vector production, inducible PCLs have been developed wherein inducible cassettes are used to express packaging functions. Only one of the reported inducible HIV-based PCLs, named GPRG, has been proposed for the production of therapeutic vectors for use in clinical trials targeting SCID-Xl (Greene et al., 2012; Throm et al., 2009). Another inducible EIAV-based LV producer cell line has been developed to make therapeutic vectors for use in clinical trials targeting Parkinson's disease (Stewart et al., 2011; Stewart et al., 2009). However, the scaling-up of inducible systems necessary for clinical-grade LV production is problematic, and additional purification steps of the vector preps to eliminate inducing agents are required. Furthermore, vector production rapidly declines as a result of instability of producer cell clones following induction (Broussau et al., 2008; Farson et al., 2001; Ni et al., 2005). Additional concerns regarding the GPRG cell line (Throm et al., 2009)(238)(238)(238)(238)(238)(237)(237)(236)(235)(236)(235)(Throm et al., 2009)(Throm et al., 2009)(Throm et al., 2009)(Throm et al., 2009)(Throm et al., 2009)(Throm et al., 2009)(Throm et al., 2009)(Throm et al., 2009)(Throm et al., 2009)(Throm et al., 2009)(Throm et al., 2009) include the risk of mobilization of packable full length transcripts from SIN GRVs (Xu et al., 2012) used to express the various packaging components including HIV-1 Gag-Pol, as well as the possible instability of concatemers consisting of multiple SIN LV expression cassettes ligated in tandem.

Continuous, high-titer LV packaging cells called STAR (Ikeda et al., 2003a) were previously constructed in our lab. To avoid the problem of VSV-G toxicity, the RDpro envelope glycoprotein was used. This envelope is derived from that of the gammaretrovirus RD114 by replacing the R peptide cleavage site with that found in HIV-1 Gag (between the matrix (MA) and capsid (CA) proteins) (Ikeda et al., 2003a; Strang et al., 2004). This mediates particularly efficient transduction of human hematopoietic stem cells (HSCs) and T cells (Brenner et al., 2003; Relander et al., 2005; Sandrin et al., 2002), which are important targets for gene therapy clinical applications. Gammaretroviral vectors (GRVs) were used to express a codon-optimized HIV-1 Gag-Pol and Rev in STAR cells. This resulted in the insertion of HIV-1 Gag-Pol in chromosomal loci that allowed its high-level, stable expression (Ikeda et al., 2003a). However, Gag-Pol and Rev

expression could be lost in these cells as they were not maintained under antibiotic selection. There was also a possibility of packaging a GRV encoding Gag-Pol and Rev within LV particles making the vectors unsuitable for clinical application. Clone F was also constructed (by Giorgia Santilli in Adrian Thrasher's lab) in a similar way to STAR cells except that SIN GRVs were used to express Gag-Pol and Rev in a traceable 293FT cell line ((Sanber et al., 2015); Table 3.0). However, this cell line was abandoned since RNA expression levels and titers achieved were suboptimal.

Another constitutive PCL, named RD2-MolPack, was recently reported (Stornaiuolo et al., 2013). In this cell line, SIN LVs were used to introduce HIV-1 tat and an RD114-derived envelope. However, this may raise safety concerns since full-length transcripts might be packaged into LV particles if expressed in the packaging cells (Hanawa et al., 2005b; Logan et al., 2004). It also has Gag-Pol and Rev in a single construct, which is another safety concern as it reduces the number of recombinations required to generate wild-type HIV-1. Furthermore, the method used to express LTR-intact LV in RD2-MolPack by transduction is not applicable to SIN LV, which are the gold standard for most gene therapy applications.

A long-standing goal of the Collins/Takeuchi lab was to establish a method that solves all these problems for generation of stable LV packaging and producer cell lines. These efforts lead to the construction of the WinPac-RDpro packaging cell line. Former lab members, mainly Sam Stephen and Sean Knight, carried out the initial part of this project. In order to present a clear and complete picture of the work I carried out using this packaging cell line, I attempted to summarize the work they did in sections 3.3.1 and 3.3.2 of this chapter.

3.2 Aims

The work done in this chapter was aimed at generating stable producer cell lines for the continuous production of self-inactivating lentiviral vectors at high titers. The packaging/producer cell lines and the stably produced vectors were then extensively tested and characterized. Furthermore, an optimized protocol for large-scale vector production and processing using the stable producer cell lines was established.

Table 3.0 Summary of published lentiviral packaging cell lines.

PCL	Parental cell line	Vector gen, design, transgene	Exp of transfer vector	Exp of packaging functions	Env	Titer¶ (TU/ml x 10^6)	Prod type, days in culture (PPPI)	Comments	Refs
WinPac-RDpro	293FT	3rd gen, HIV-1 SIN, eGFP	Tfect	GRV tagging + Cre RMCE (Gag-Pol) Tfect (Rev & Env)	RDpro	0.5-7	Constitutive, 150 with selection✚	co Gag-Pol, scaled up in cellSTACKs & HYPERFlasks	(Sanber et al., 2015)
Clone F	293FT	3rd gen, HIV-1 SIN, eGFP	Tfect	Tduct with SIN GRV (Gag-Pol) Tfect (Rev & Env)	RDpro	<0.1	Constitutive, 70	co Gag-Pol, risk of mobilization of SIN vector	(Sanber et al., 2015)
STAR	293T	3rd gen, HIV-1 LTR-i, eGFP	Tduct	Tduct with SIN GRV (Gag-Pol & Rev), Tfect (Env)	RDpro GALV/TR MLV-A	8.5 1.6 2-80	Constitutive, 120	co Gag-Pol, risk of mobilization of SIN vectors	(Ikeda et al., 2003a)
		3rd gen, HIV-1 SIN, eGFP	Tfect	Tduct with SIN GRV (Gag-Pol & Rev), Tfect (Env)	MLV-A	0.06-10	Constitutive, 120◆		
RD2-MolPack	293T	2nd gen, HIV-1 LTR-i, GFP	Tduct	Tduct with baculo-AAV vector + Rep 78 (Gag-Pol & Rev), Tduct with SIN LV (Tat & Env)	RD/TR	0.1-1, CD34+ OR SupT1 cells■	Constitutive, 87	Gag-Pol and Rev expressed from single construct, Tenofovir to block autotransduction, risk of mobilization of SIN vectors	(Stornaiuolo et al., 2013)
GPRG	293T/17	3rd gen, HIV-1 SIN, eGFP	CAT	Tduct with SIN GRV	VSV-G	30	Inducible, 90 (7)	co Gag-Pol, scaled up in wave bioreactors, risk of mobilization of	(Greene et al., 2012; Throm et al.,
		3rd gen, HIV-1				50			

3.3 Results

3.3.1 Constitutive HIV-1 Gag-Pol expression via recombinase mediated cassette exchange (Work done by Sam Stephen)

Traceability of clinical vector producer cell lines is likely to be required in the current good manufacturing practice (cGMP) regulations. Traceable 293FT cells with well-documented culture history (Stacey and Merten, 2011) were therefore used for packaging cell development. A strategy was designed to introduce a codon-optimized HIV-1 Gag-Pol by recombinase-mediated cassette exchange (RMCE) (Araki et al., 1997; Turan and Bode, 2011). This strategy takes advantage of GRV's ability to integrate within chromosomal loci that can support constitutive, high-level expression of HIV-1 Gag-Pol but minimizes GRV derived sequences remaining in the final packaging cells (Figure 3.1A). An MLV-based GRV encoding a Hyg-eGFP hybrid protein with an LE mutant LoxP site cloned into its 3' U3 region, pSLS51 (Figure 3.1A: top panel), was used to transduce 293FT cells at low MOI and the cells were then selected in hygromycin (Figure 3.1A: middle panels). Among the hygromycin resistant clones, clone 2G had a single vector copy per cell as determined by qPCR and stably expressed eGFP at a relatively high MFI for more than 50 passages (Figure 3.1B). The vector integration site was identified by inverse PCR as nucleotide position 10619185 in the first intron of midline 1 gene (MID1) on the X chromosome, the vector was integrated in reverse orientation to the MID1 gene (Sanber et al., 2015).

Subsequently, a plasmid encoding a codon-optimized H87Q Gag-Pol mutant driven by CMV promoter and flanked by RE mutant LoxP sites was constructed, pSLS94 (Figure 3.1A: middle panel). The H87Q mutant is a naturally occurring capsid mutation that enhances transduction of mouse and monkey cells without compromising transduction of human cells (Chatterji et al., 2005; Ikeda et al., 2004; Kootstra et al., 2007). This can facilitate pre-clinical testing using these vectors. Additionally, there was a more extensive optimization in this current construct according to codon optimization indices, compared to our previous HIV-1 Gag-Pol construct used in STAR cells (Tables 3.1 and 3.2). A promoter-less puromycin resistance gene with a downstream polyA signal was also cloned downstream from the 5' RE mutant LoxP site. This plasmid (pSLS94) was co-transfected with a Cre-recombinase encoding plasmid resulting in recombination between the integrated LE mutant LoxP sites and the RE mutant LoxP sites in pSLS94 (Figure 3.1A: bottom panel). As a result, the Gag-Pol expression cassette was integrated between

a double (LE + RE) mutant LoxP site and a wild type LoxP site. Since Cre-recombinase has low affinity to the former, the cassette will remain stably integrated (Araki et al., 1997). Puromycin-resistant clones were then tested for successful Cre-mediated recombination by the absence of GFP expression (by flow cytometry) and HIV-1 Gag-Pol expression levels (by HIV-1 RT ELISA). Clone 57 was chosen for further experiments as it had high level Gag-Pol expression and had lost GFP expression (Figure 3.1C).

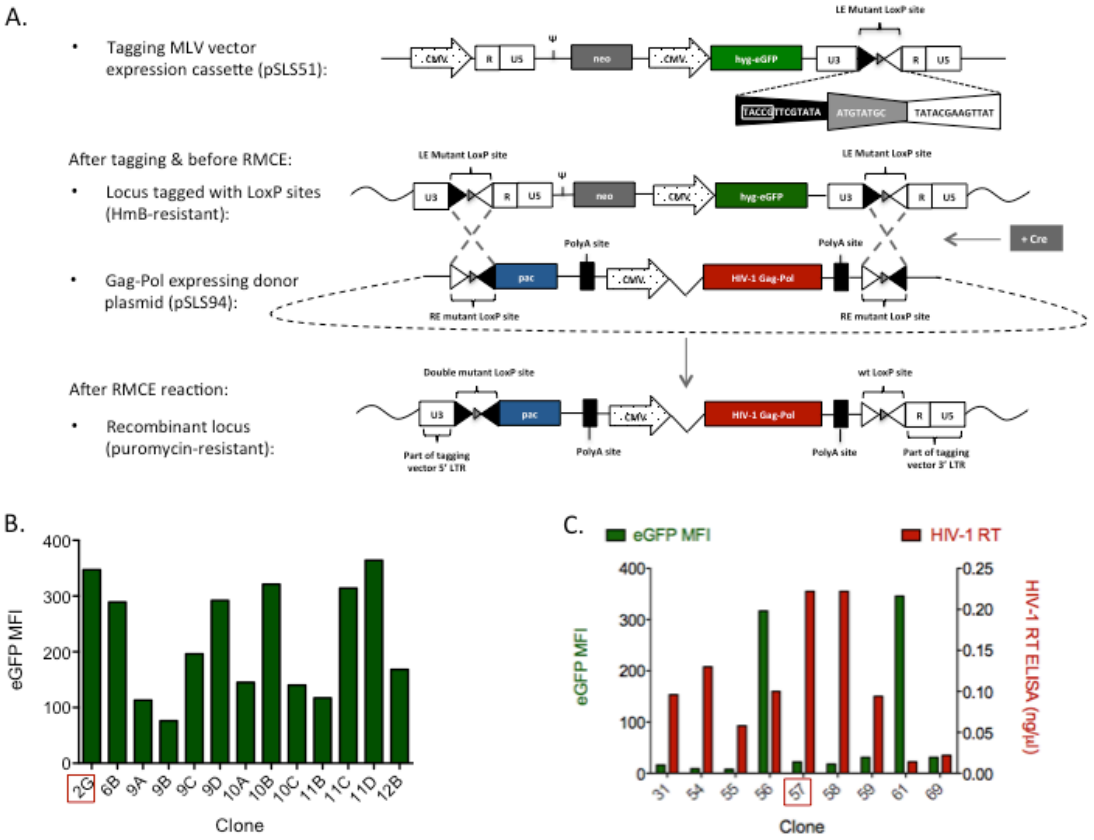

Figure 3.1. Stable expression of HIV-1 Gag-Pol in 293FT cells via Cre recombinase-mediated cassette exchange (Cre RMCE).

(A) Schematic representation of Cre RMCE to introduce codon-optimized HIV-1 Gag-Pol at a transcriptionally active chromosomal locus in 293FT cells. neo, neomycin resistance gene; CMV, cytomegalovirus promoter; hyg-eGFP, hygromycin-resistance gene and eGFP fusion transgene; pac, puromycin N-acetyltransferase (puromycin resistance gene). **(B)** eGFP mean fluorescence intensity (MFI) as determined by FACS analysis of hygromycin-resistant clones following transduction with the lox-P tagging MLV vector. The median MFI was 195 (range: 78 – 359). Clone 2G (boxed in red) was chosen for further experiments based on the relatively high MFI, superior stability of MFI over 50 passages, and a single copy of the tagging vector by Q-PCR (data not shown). eGFP, enhanced green fluorescent protein; MFI, mean fluorescence intensity. **(C)** Levels of HIV-1 RT in culture supernatant of puromycin-resistant clones following the co-transfection of the Cre recombinase-encoding plasmid (pCAGGS Cre) and pSLS94 containing the HIV-1 Gag-Pol donor cassette. The median RT was 0.095 ng/ml (range: 0 - 0.23). eGFP MFI as determined by FACS analysis of puromycin-resistant clones is also shown. Clone 57 was chosen for further experiments based on highest RT levels and loss of eGFP expression following RMCE reaction.

Table 3.1. Codon adaptation indices of the HIV-1 *Gag* gene

HIV-1 *Gag* Gene	Codon Adaptation Index
Wild Type	0.725
Codon Optimized - WinPac	0.862
Codon Optimized - STAR	0.852

codon adaptation indices (Carbone et al., 2003; Sharp and Li, 1987) were determined using CAIcal (Puigbo et al., 2008)

Table 3.2. Codon adaptation indices of the HIV-1 *Pol* gene

HIV-1 *Pol* Gene	Codon Adaptation Index
Wild Type	0.703
Codon Optimized - WinPac	0.895
Codon Optimized - STAR	0.843

codon adaptation indices (Carbone et al., 2003; Sharp and Li, 1987) were determined using CAIcal (Puigbo et al., 2008)

3.3.2 Establishment of a WinPac-RD packaging cell line: introduction of HIV-1 Rev and an RDpro envelope (Work done by Sean Knight)

The remaining vector components were introduced by a series of plasmid DNA transfection, antibiotic selection, cell cloning and clone screening (Knight, 2011; Sanber et al., 2015). Firstly, HIV-1 Rev, which is required for nuclear export of vector genomes containing Rev response element (RRE), and secondly, RDpro envelope (Ikeda et al., 2003a), were introduced. Cell clones at each step were screened for both RNA expression and vector production by transient transfection of missing vector components. The best performing clones, WinPac and WinPac-RD respectively, were selected for further study (Table 3.2).

Table 3.3. Construction steps of WinPac-RD packaging cell line.

Step	Construct	Selectable marker	Clones screened	Screening assays	Selected clone
Tagging with MLV vector	pSLS51	hyg-eGFP	40	eGFP MFI (FACS)/ VCN (Q-PCR)	Clone 2G
RMCE for HIV-1 Gag-Pol	pSLS94	pac	67	HIV-1 p24 (ELISA)/ hyg-eGFP loss (FACS)	Clone 57
HIV-1 Rev transfection	pCEP4-Rev	hyg	15	HIV-1 Rev RNA (RT-Q-PCR) / transient vector production	WinPac
RDpro transfection	pRDproLF	Sh ble	12	RDpro RNA (RT-Q-PCR)/ transient vector production	WinPac-RDpro

MLV, murine leukemia virus; HIV-1, human immunodeficiency virus type 1; RDpro, RD114-derived envelope; hyg, hygromycin resistance gene; pac, puromycin N-acetyltransferase (puromycin resistance gene); MFI, mean fluorescence intensity, VCN, vector copy number.

3.3.3 Establishment of continuous vector producer cells

WinPac-RD cells constitutively expressed all packaging functions, Gag-Pol, Rev and envelope, to package HIV-1 vector genomes. The final step to establish continuous LV producer cells was to express vector genomic RNA. SIN LVs contain a deletion within

the LTR U3 region. This deletion makes them less genotoxic (Modlich et al., 2009; Montini et al., 2009; Zufferey et al., 1998) and more likely to be widely used for clinical applications. Therefore, I transfected a GFP-expressing SIN LV, SIN-pHV (Figure 3.2A), into WinPac-RD cells. I aimed to produce culture supernatants with LV titers of at least 10^5 293T transduction units (TU)/ml, since the final product for clinical use after vector concentration and purification may be required to have a titer of more than 10^7 TU/ml.

Before transfection of the SIN LV, WinPac-RD cells were cultured in the presence of puromycin, hygromycin and phleomycin for 9 days to ensure the majority of cells express all the packaging functions that are genetically linked to different antibiotic resistance genes (Table 2.12). Subsequently, SIN pHV was co-transfected with pSELECT Blasti MCS (encoding the blasticidin resistance gene, Bsr) at a molar ratio of 10**:**1. Fifteen cell clones (WinPac-RD-HV shortened to WRH) were obtained from a blasticidin-resistant bulk population of cells which produced SIN-pHV at titers $>10^4$ TU/ml (Table 3.3). One of these clones (WRH26) produced LV titers higher than $1x10^5$ TU/ml (Figure 3.2B, Blasticidin selected). Because the stable transfection of a new vector component may be associated with a reduction in expression of pre-existing packaging functions (Knight, 2011), the clones were also re-selected with puromycin and hygromycin to ensure that the packaging components were expressed at relatively high levels. Three more clones (WRH1, WRH2, and WRH29) with titers of ≈ 1 x 10^5 TU/ml were identified (Figure 3.2B, BPuH selected). To confirm that re-selection with antibiotics can reproducibly increase LV titers, unselected WRH clones were thawed out and re-selected in a stepwise manner with the four antibiotics (blasticidin, puromycin, hygromycin, and phleomycin). Functional titers were determined after the addition of each of the antibiotics (Figure 3.2C). Importantly, selection of WRH clones with antibiotics raised titers to ≈ 1 x 10^5 TU/ml. Moreover, these titers were stable for ≥4 weeks of culture following removal of antibiotics. To further demonstrate the stability of WinPac-derived producer cells, clone WRH1 was kept in culture with or without antibiotics and transduction titers were determined at 2–4 week intervals. Titers were relatively stable over a period of around 4 months in the absence of antibiotics, and for around 5 months in the presence of antibiotics (Figure 3.2D). It should be noted that the all titers shown in Figure 3.2 represent sub-optimal values as vectors were harvested from small numbers of cells in order to screen multiple clones and to test a number of antibiotic selection procedures.

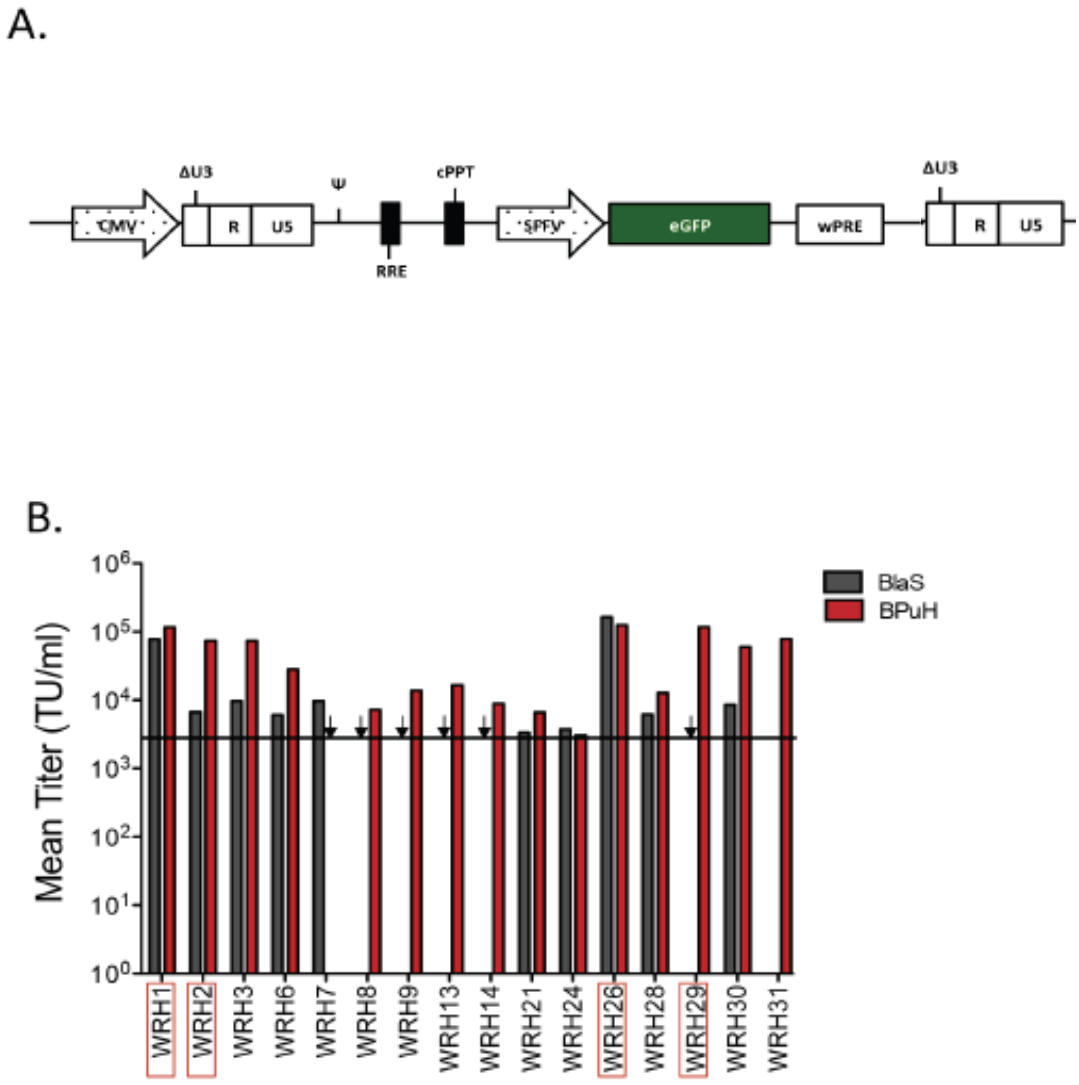

Figure 3.2. Generation of stable producer cell lines for a GFP-expressing SIN LV.
(A) Schematic representation of SIN LV expression cassette in the SIN pHV plasmid. **(B)** Screening of Blasticidin-resistant clones stably co-transfected with SIN pHV and pSELECT Blasti MCS before and after re-selection with puromycin and hygromycin. Clones WinPac-RD-HV (WRH) 1, 2, 26, and 29 were chosen for further experiments (boxed). The median titer of all screened BPuH-resistant clones was 1.66 x 10^4 293T TU/ml (range: 3.05 x 10^3 – 1.25 x 10^5). Data shown represents mean of two replicates. Black horizontal line: threshold level of detection; Downward arrows: titers below threshold.

(Figure 3.2 continued)

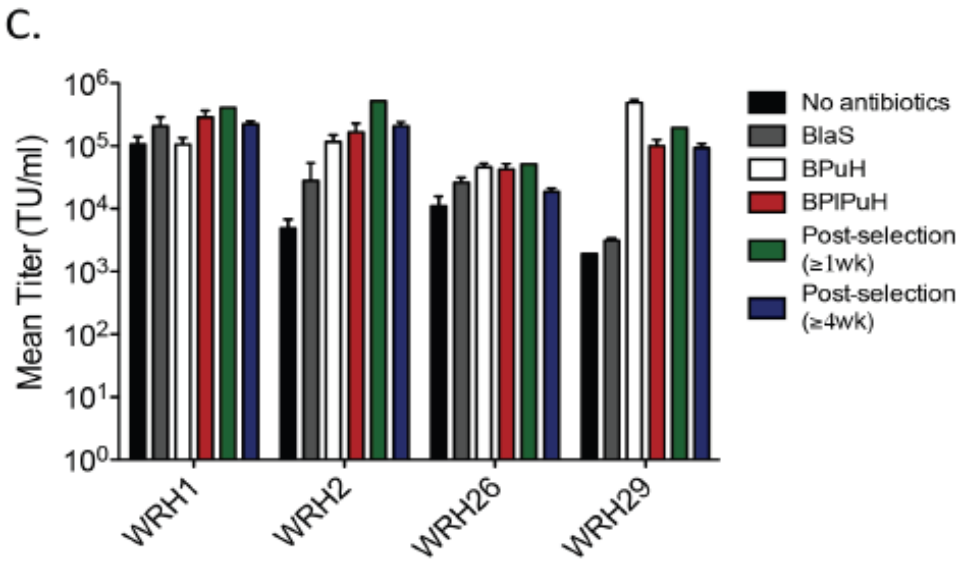

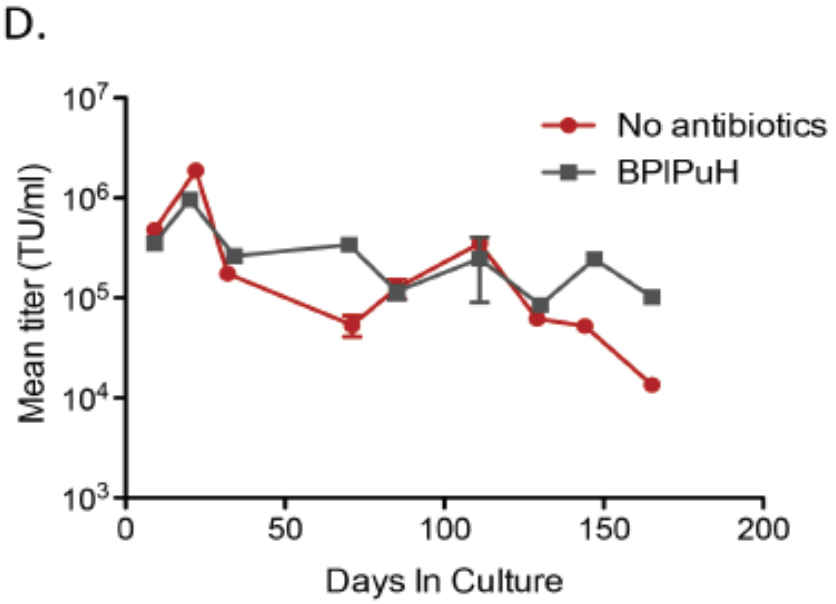

Figure 3.2 continued: (C) Titers of the four WRH clones (1, 2, 26, and 29) during step-wise drug re-selection, and after 4 weeks following the removal of antibiotics. Data shown represents the mean ± range of two replicates. **(D)** Stability of titers during long-term (>5 months) culture in the presence or absence of antibiotic selection. Data shown represents the mean ± range of two replicates. SFFV, spleen focus-forming virus, BlaS, blasticidin; BPuH, blasticidin + puromycin + hygromycin; BPlPuH, blasticidin + phleomycin + puromycin + hygromycin.

Table 3.4. Screening steps for high-titer vector producer cell lines.

Step	Number of Clones
Blasticidin-resistant clones isolated	22
BPuH/BPlPuH-resistant clones screened	17
BPuH/BPlPuH-resistant clones with detectable titers	15

3.3.4 Optimization of vector harvests

A series of experiments were then conducted to determine the optimal harvesting conditions for WRH clones. These experiments showed that higher titers were achieved when cells were confluent at the start of a 24-hour vector production period (Figure 3.3A). Moreover, lowering the volume of medium during production is a simple way of obtaining higher titers (Figure 3.3B). No positive effect on titers was observed when the incubation temperature during vector production was lowered to 32 °C, nor when the glucose in the culture medium was substituted with fructose (Merten, 2004). Likewise, various inducing agents previously shown to increase HIV-1 vector/virus production were preliminarily tested. These include caffeine, valproic acid (histone deacetylase inhibitor) and RG108 (DNA methyltransferase inhibitor), but no significant increase in titers was detected. Further extensive testing would be necessary to confirm these negative results.

Animal sera are routinely used for culturing 293-derived cell lines and for retroviral vector production. Using serum-free media can have deleterious effects on vector titers, which may be explained by alterations in the lipid composition of their membranes, which may adversely affect retroviral vector assembly and release (Ono and Freed, 2001; Pickl et al., 2001) as well as their infectivity (Rodrigues et al., 2009; Waheed and Freed, 2010). However, serum-free vector production would eliminate the risk of introducing contaminants of animal origin (Tuschong et al., 2002) and would simplify downstream processing of vectors. Therefore, vectors were harvested in media containing reduced or no serum from WRH producer clones. This revealed that harvesting in DMEM supplemented with 1% FBS (D1) is well tolerated over multiple harvests (Figure 3.3C).

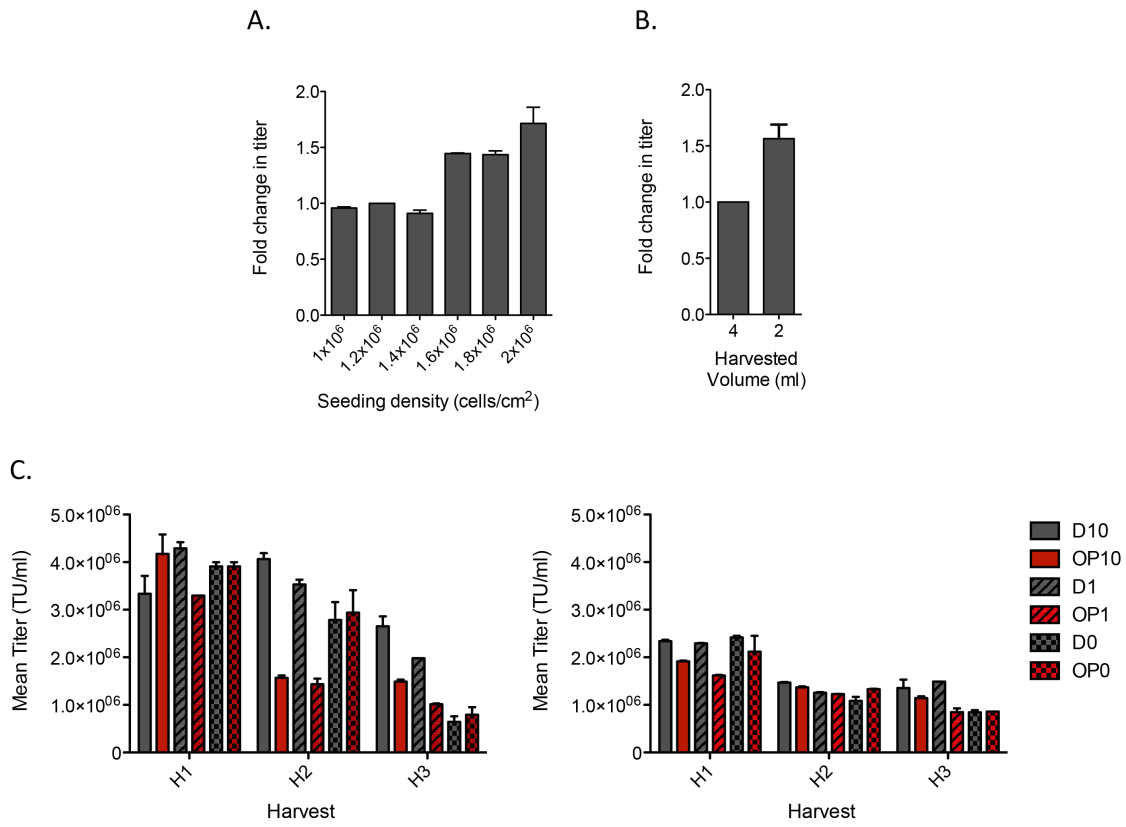

Figure 3.3. Optimization of vector harvests.

(A) Titers of WRH2 clone when seeded at increasing cell densities resulting in different levels of confluence at the start of 24 hour harvesting periods. Data represents mean and range of two replicates. **(B)** Titers of WRH1 clone after harvesting vectors from T25 flasks in 4 or 2 ml of medium. Data represents mean and range of two replicates. **(C)** Titers of WRH2 (left) and WRH26 (right) clones after harvesting vectors from 6 well plates in either one of two media with/without FBS supplementation: D10 (DMEM +10% FBS), OP10 (OptiPro + 10% FBS), D1 (DMEM +1% FBS), OP1 (OptiPro + 1% FBS), D0 (DMEM without FBS), OP0 (OptiPro without FBS) various compositions. Data represents mean and range of two experiments.

After determining the optimal conditions for obtaining high-titer vector preparations from WRH producer cells, harvests were collected beginning at 72 hours after seeding under the following conditions: seeding density = 2.1–2.3 x 10^5 cells/cm^2 and harvest volume (ml): surface area (cm^2) ratio < 0.1. These harvests had titers up to 3 x 10^6 TU/ml (Figure 3.4A, -spinoculation). It has been previously shown that spinoculation improves the efficiency of transduction of HIV-1-based vectors by depositing the vectors onto the target cells (O'Doherty et al., 2000). Accordingly, spinoculation resulted in 2–3 fold increase in titers (up to 5 x 10^6 TU/ml) (Figure 3.4A, +spinoculation). Vector production was also scaled up to allow the collection of 640 ml or 560 ml per harvest using 10-layer CellSTACKs (Corning) or HYPERFlasks (Corning) respectively. After scale up, vector titers had a mean of 7.28 x 10^6 (SD = 1.47 x 10^6) and 5.00 x 10^6 (SD = 8.02 x 10^5) TU/ml over four days, respectively (Figure 3.4B).

The mean productivity per cell was 1.75 (SD = 0.28) TU/cell/day (for cells harvested in DMEM + 10% FBS). Additionally, cells tolerated reduction of FBS concentration down to 1% in HYPERFlask and continued to produce > 5 x 10^6 TU/ml up to the 4th harvest (Figure 3.4B). HIV-1 p24 level and transduction titers were compared for vector harvests from stable WinPac- and STAR-derived vector producer cells as well as transient 293FT producers for RDpro and VSV pseudotyped vectors (Figure 3.4C). HIV-1 p24 levels and transduction rates were not significantly different between RDpro pseudotyped vectors, regardless of whether they were stably or transiently produced. In contrast VSV-G pseudotyped vectors had significantly higher transduction rate per physical particle (estimated via p24 levels measured by ELISA; Figure 3.4C). Higher transduction efficiency of VSVG LVs in comparison to RDpro-pseudotyped LVs on immortalized cell lines, such as 293T cells, have been previously reported (Bell et al., 2010; Ikeda et al., 2003a; Strang et al., 2004).

However, of note, HYPERFlask harvests of WinPac–RD supernatants had about 10-fold higher ratio of 293T transducing units /p24 level compared with small-scale routine harvests (mean ratios of 4.2 x 10^4 versus 3.0 x 10^3 293T TU/ng p24 respectively, Figure 3.4D).

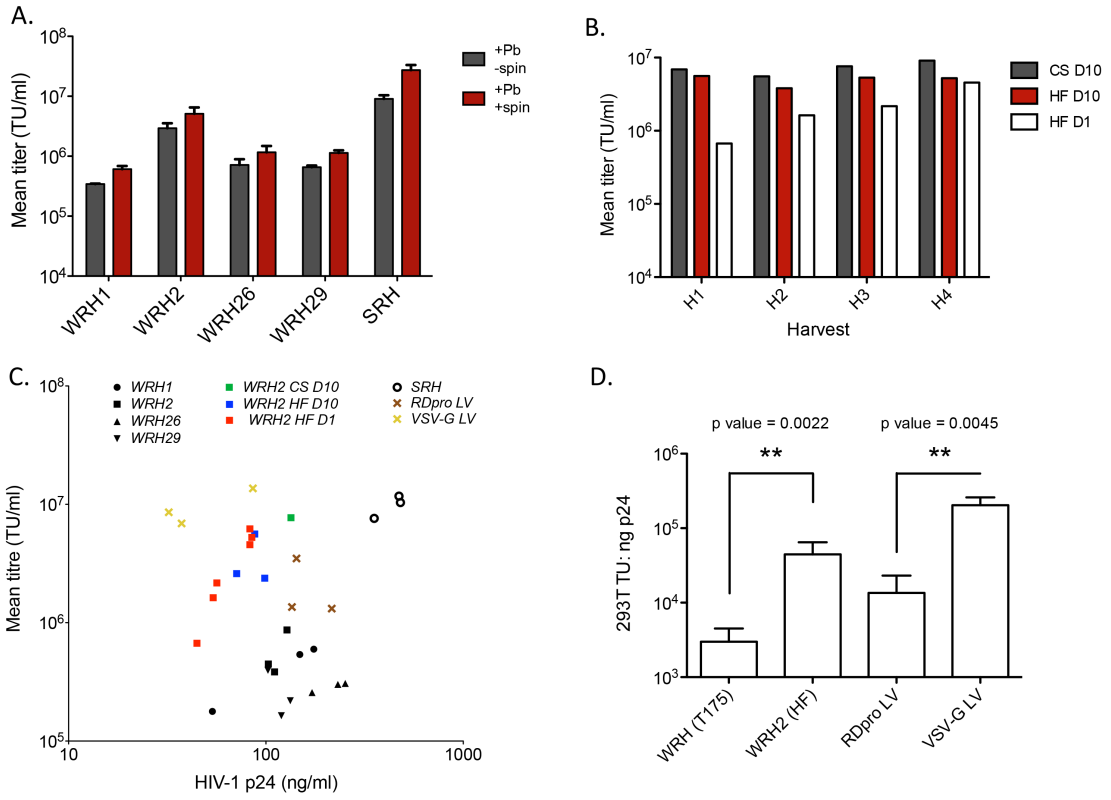

Figure 3.4. Large-scale production.

(A) Optimized GFP infectious titers of the four WinPac-RD-HV (WRH) clones cultured in 6-well plates after re-selection with blasticidin, phleomycin, puromycin, and hygromycin (BPlPuH). Vectors were titrated on 293T cells in the presence of polybrene (Pb) with/without spinoculation (spin). Data shown represents mean ± SD of three independent experiments). **(B)** Scaled up vector harvests using 10-layer CellSTACK (CS) and HYPERFlask (HF) were collected daily from 72 h (H1) to 144 h (H4) after cell seeding, and were titrated on 293T cells. Vectors were harvested in DMEM supplemented with either 10% (D10) or 1% (D1) FCS. Cells in HYPERFlasks with 1% FCS maintained vector production at titers ≥ $5x10^6$ TU/ml for two more days (data not shown). **(C)** Functional titers (293T TU/ml) and HIV-1 p24 concentration (ng/ml) of vector harvests. Data shown represents three independent harvests from each of the following: WRH1 and WRH2 (WinPac-RD-HV producer clones harvested from T175 flasks); SRH (STAR-RDpro-HV producer cells expressing non-SIN HV vector harvested from T175 flasks), RDpro LV (produced by 3 plasmid transient transfection of 293FT cells in 10 cm^2 plates using a RDpro env expressing plasmid); VSV-G LV (produced by 3 plasmid transient transfection of 293FT cells in 10 cm^2 plates using a VSV-G expressing plasmid). WRH2

HF D10 and WRH2 HF D1 samples represent multiple harvests obtained from clone WRH2 cultured in a HYPERFlask (HF) and harvested in the DMEM supplemented with 10% (D10) or 1% (D1) FBS, respectively. WRH2 CS D10 sample was obtained from clone WRH2 cultured in a 10-layer CellSTACK in DMEM supplemented with 10% FBS (D10). All vectors, except those produced by SRH cells, are SIN LVs. **(D)** Infectivity of stably and transiently produced LV preparations. Ratio of 293T transducing units: p24 level (ng/ml) determined by ELISA was used as a measure of infectivity. WRH (T175) represents the mean ratio for four different WinPac-RD-HV clones (mean ratio for each clone was determined from 3 vector preparations obtained from T175 flasks). WRH (HF) represents the mean ratio for 9 vector preparations obtained from HYPERFlasks and produced by clone WinPac-RD-HV2. For each of RDpro LV and VSV-G LV, data shown represents the mean ratio for 3 vector preparations produced by transient transfection of 293FT cells in 10cm^2 plates. Error bars represent SD. Unpaired t-test was used to compare mean ratios.

3.3.5 Vector processing

Vector processing including concentration and purification is required before any clinical application. Concentration is particularly needed because of erally necessitate the use high titer vector preparations to achieve efficient transduction as opposed to cell lines, which are more efficiently transduced. Various methods have been used to concentrate LVs.

Ultracentrifugation has been widely used to concentrate lentiviral vectors for laboratory-based applications. A maximum capacity of around 210 ml of VCM per rotor of a typical ultracentrifuge meets the requirements of most of these applications. However, concentrating large volumes of VCM needed for clinical applications by ultracentrifugation is impractical and time-consuming. In addition to that, a considerable portion of infectious vector activity is lost following each spin. This is of particular relevance to this work since LVs pseudotyped with γ-retroviral envelopes may be mechanically more fragile than VSV-G pseudotyped vectors (Strang et al., 2004).

Based on that, lentiviral vectors were initially concentrated by ultracentrifugation or low-speed centrifugation. Results from a representative experiment for each condition are shown in Figure 3.5A. Although, RDpro pseudotyped vectors could be concentrated to high titers of around 10^8 TU/ml the recovery was relatively low compared to that of VSV-G (range of 10-25% and 40-70% respectively). Additionally, less than 10% of WRH infectious vectors were detectable in the supernatant following low-speed centrifugation suggesting that the loss of infectious vectors was mostly due to inactivation rather than inefficient precipitation.

Tangential flow filtration (TFF), on the other hand, is a form of membrane filtration in which the feed stream passes parallel to a porous membrane surface allowing size-based separation of particles. Components of the feed that are smaller than the pore size can pass through the membrane pores (permeate), while the remainder (retentate) is re-circulated back to the feed reservoir (Figure 3.5B). TFF is a particularly useful means of concentrating lentiviral vectors for clinical applications (Cavazzana-Calvo et al., 2010; Segura et al., 2013). Previous reports suggest that it is well tolerated, at least by VSV-G-pseudotyped LVs (Cooper et al., 2011; Geraerts et al., 2005). It can also be scaled-up based on conditions established during small-scale pilot trials. Available TFF devices can efficiently process hundreds of liters of a product within hours. Additionally, TFF

provides a means to concentrate and diafilter vectors in a single step, which potentially reduces vector losses.

To determine whether TFF can be successfully used to concentrate RDpro LVs, I initially concentrated a relatively small volume of vector-containing medium (VCM) produced by WRH cells. 50 ml of VCM was concentrated ≈10-fold with complete recovery (100% of input vectors where recovered). For this trial, a 115 cm^2 hollow-fiber with 100 kDa molecular weight cut-off (MWCO) was used and the inlet pressure was <0.3 psi while flow rate was < 20 ml/min.

A recent report outlined the use of two consecutive rounds of TFF to achieve around 1800-fold concentration of 5.5L of VSV-G LVs with high recovery (>94%) and speed (<3 hour) (Cooper et al., 2011). In this report VSV-G LVs were produced by transient transfection of 293T cells in HYPERFlasks. They were collected in serum-free medium and diafiltered in PBS with 0.25% Fetal Calf Serum (FCS). In the first round of the TFF, 5500 ml of VCM was diafiltered in 1000 mL of PBS with 0.25% FCS and concentrated down to 50 mL using a 615 cm^2 hollow fiber module with 500 kDa MWCO (surface area (cm^2) : volume (ml) ratio (sa : v) ≈ 112). In the second round of TFF, vectors were concentrated to a volume of ≈ 3 ml using a 40 cm^2 hollow fiber module (sa : v ratio ≈ 800). Inlet pressure was maintained below 9 psi throughout the process.

Similarly, I attempted to concentrate larger volumes of RDpro LV produced by WRH cells in 10-layer CellSTACKs or HYPERFlasks. Given that minimal cell debris was noted when vectors were produced using WRH cells, neat non-clarified VCM was used in order to minimize the number of processing steps undertaken. A flowchart outlining the basic steps involved in the TFF process is shown in Figure 3.5C. Table 3.5 and Figure 3.5D summarize the main features and results in all TFF trials conducted.

In the first trial, referred to as Trial 1, I elected to concentrate vectors using two consecutive rounds of TFF. In the first round a 320 cm^2 hollow-fiber was used to reduce the volume of VCM 5-fold (1075 ml to 200 ml), followed by diafiltration in 800 ml of PBS. At this point, the second round of TFF was initiated using a 115 cm^2 hollow fiber to achieve a 135-fold final reduction in volume (down to ≈ 8 ml). This was followed by diafiltration in 40 ml of X-VIVO 10.

However, only 21% of vector input was recovered following the initial 5-fold concentration in the first round of TFF and 23% after the second round of TFF. Importantly, a progressive decline in flux rate was observed early in both rounds of TFF. The decline in flux rate was hypothesized to be due to the formation of a gel layer within the lumen of the hollow fibers leading to a reduction in its effective diameter and a blockade of the pores. Additionally vectors can get trapped in such a layer, which would explain the relatively low recovery rate obtained following TFF. This was hypothesized to be more likely than vector inactivation based on the relatively low shear throughout the run (4000) which was well-tolerated by VSV-G LVs (Cooper et al., 2011). Since high protein content and/or cell debris in the starting material are generally implicated in gel layer formation, diafiltration was initially performed in pure PBS with a 4-fold dilution. The aim was to reduce protein concentration and avoid gel layer formation in the second round of TFF. Nevertheless, a similar decline in flux rate was observed.

Based on the 'gel layer formation' hypothesis, we planned to do another trial after introducing a few modifications. In trial 1, around 80-85% of input vectors were lost following each round of TFF. Therefore, a single hollow fiber module with a surface area of 115 cm^2 was used to concentrate 1075 ml of VCM down to a volume of ≈ 10 ml (sa : v ratio ≈ 105). To reduce the risk of gel layer formation, diafiltration with PBS was started at an earlier time point (after 3x initial reduction in volume). Additionally, the flow path was washed with 10ml PBS at the end of the run in an attempt to recover any gel layer that may have formed (as well as any vectors trapped within that layer).

Trial 2 allowed recovery of 32% of input vectors in the retentate, and none were detected in the permeate. Despite earlier initiation of diafiltration with PBS, the decline in flux efficiency was observed and was not reversed or halted. The wash in 10ml PBS at the end of the run did not successfully restore the flux rates to starting levels and this was interpreted as an indication that the gel layer was incompletely recovered. Around 5% of input vectors were detected in the PBS wash which was stored and tested separately from the original retentate.

In another attempt to reduce the chances of gel layer formation (Trial 3), vectors were harvested in OptiPro (serum-free medium) supplemented with 4mM L-Glutamine from WRH2 cells growing in HYPERFlasks. This was aimed at reducing the protein content in the VCM while maintaining high initial titers (Figure 3.4B). However, the decrease in flux rate was still observed early after starting the run so diafiltration with PBS

was initiated after ≈3x reduction in volume. Despite the progressive decrease in flux rate, an initial 22x reduction in volume (1100 ml to 50 ml) was conducted before starting another diafiltration in X-VIVO 10 (50 ml to 100 ml). This was done in order to have the concentrated vectors in a medium that is favorable for transduction of human primary hematopoietic cells, and to reduce the risk of vector aggregation following excessive protein depletion (due to lack of serum in starting VCM and initial diafiltration in pure PBS). Assuming the observed decrease in flux rate was due to gel layer formation, a 30-minute recirculation step was introduced at this point in attempt to re-dissolve the gel layer. Thus the permeate outlet was closed and the retentate was allowed to recirculate in the flow path and hollow fiber for 30 minutes, but this did not restore the flux rate. Despite that, a final concentration to a volume of 12.5 ml (4-fold decrease in volume) was conducted. Then the flow path was washed with 50ml PBS, which was allowed to recirculate for 30 minutes. Although this did not rescue the flux rate either, the PBS was collected and mixed with the concentrated vectors (bringing the total volume to 62.5 ml). A final concentration step was then conducted to bring the volume to 12.5 ml (5-fold reduction in volume). Unfortunately only 15% of input vectors were recovered in the final retentate.

Since the decline in flux rate was observed in the presence and absence of serum in the initial VCM, factors other than initial protein content might be implicated in promoting the formation of the gel layer. Cell debris in the starting VCM might be one factor. Another factor is the relatively low feed flow rate (50ml/min; Table 3.5), which had been chosen to reduce the shear rate and possible damage to the vector particles.

Based on that, a fourth trial was conducted using VCM supplemented with 1% FBS and 20mM HEPES buffer and was clarified using a 0.45 μm filter. This was expected to minimize the protein concentration while maintaining the protective effect of serum on vectors. The use of HEPES buffer was aimed at stabilizing the pH of VCM in order to avoid extreme pH levels, which might influence the protein-binding characteristics of polyethersulfone (PES) (the material from which the hollow fibers were made). In this trial a higher flow rate of 140 ml/min was applied from the start of the run and a hollow fiber module with was used (sa : v ratio ≈ 630). No reduction in flux rate was observed under these conditions. This allowed rapid concentration of ≈ 515 ml VCM to a volume of 40 ml followed by diafiltration in ≈400 ml of PBS. Finally, the sample was

concentrated to a volume of 12 ml. The flow path was then washed with ≈ 20 ml PBS. The entire process was completed in ≈ 30 minutes.

Despite the fact that no evidence of gel layer formation was observed in trial 4, only 15% of input vectors were recovered in the final retentate. Only 2% of vectors were detected in the permeate. Moreover, around 5% of input vectors were detected in the PBS wash suggesting that a gel layer might still have formed leading to the trapping of vector particles in the hollow fiber module even though the flux rate did not show the rapid decrease that was seen in previous trials.

The HIV-1 p24 level was also determined in the vector preparations before and after concentration by TFF in this trial as a measure of physical vector particles. This revealed that the concentration of p24 increased by ≈ 10-fold despite a 43-fold reduction in volume. This represents a decrease of around 75% of the total input p24 content. Measurement of p24 levels in the permeate would have been helpful to explain this. If the permeate had a high p24 content then this would suggest vector particle damage possibly secondary to shear stress and subsequent loss of disassembled particles in the permeate. On the other hand, a low p24 level in the permeate would suggest trapping and loss of vector particles in a gel layer that might have formed in the hollow fiber module as explained above. Unfortunately, the p24 level in the permeate could not be determined since none of the permeate samples were available when the p24 assay was performed.

The ratio of 293T TU : p24 also decreased by around 2-2.5 fold in the final retentate when compared to the VCM before TFF. This decrease in infectivity might have resulted from vector inactivation due to the higher flow rate used in this trial even the shear rate was maintained below $3200s^{-1}$. Another possible cause for the loss infectivity could be vector aggregation as a consequence of decreased protein content especially following diafiltration with pure PBS (Cooper et al., 2011).

Therefore, plans are underway to optimize the flow rate in order to minimize vector inactivation while avoiding the formation of a gel layer. This will be done by directly comparing running the VCM at a high flow rate (up to 500ml/min) and at a lower flow rate of around 100 ml/min, and the diafiltration step will be omitted. This will be conducted using clarified VCM supplemented with 1% FBS and 20mM HEPES buffer. A final step of diafiltration in a serum-free medium like X-VIVO 10 will also be re-introduced (Figure 3.5C).

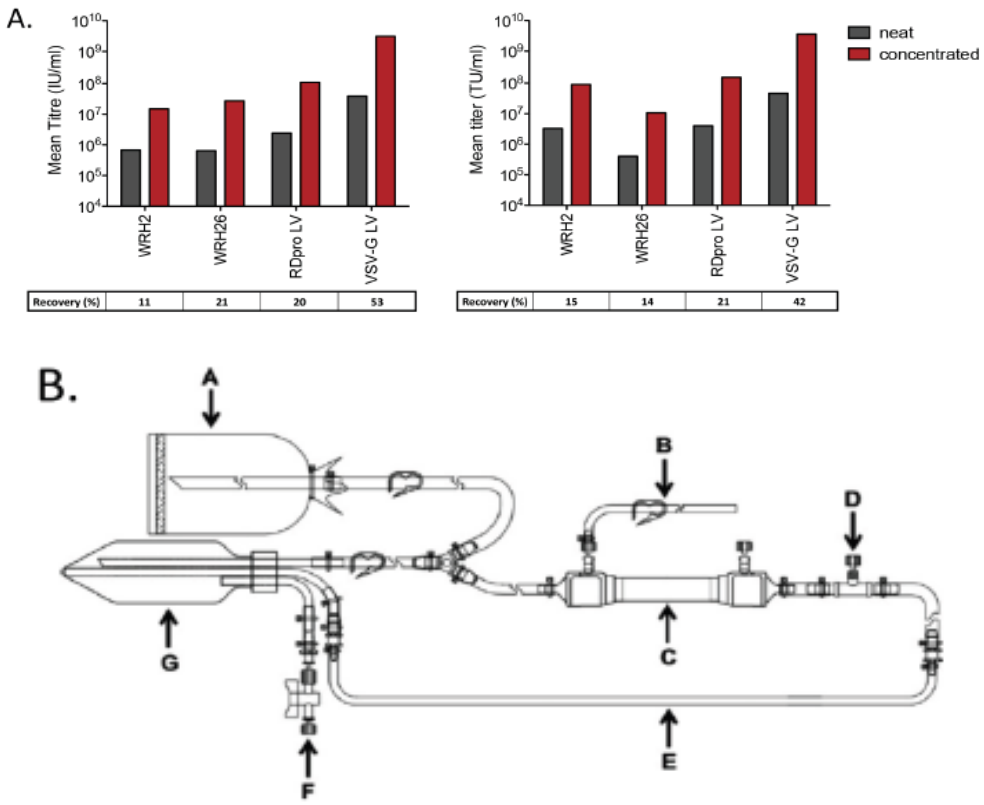

Figure 3.5 Concentration of RDpro-pseudotyped vectors.

(A) Concentration of stably (WRH2 and WRH26) and transiently (RDpro LV and VSV-G LV) produced vectors by ultrancentrifugation (performed left panel) or centrifugation (performed right panel). Ultracentrifugation was performed under the following conditions: for RDpro psuedotypes 37 000 x g for 2 hours at 4 °C; for VSV-G psedudotypes 37 000 x g for 2 hours at 4 °C. Centrifugation was performed under the following conditions: 4000*g* for18 hours at 4 °C. The percentage of recovered vectors (recovery %) was calculated using the following formula: [(concentrated titer x recovered volume) / (neat titer x volume concentrated)] x 100%. "Neat" refers to titers before concentration. Mean titers obtained from duplicate titrations are shown. **(B)** Schematic representation of tangential flow filtration (TFF) flow path. A: inlet; B: Permeate; C: hollow fiber; D: pressure transducer; E: tubing loop for peristaltic pump; F: pressure release port; G: Reservoir.

(Figure 3.5 continued)

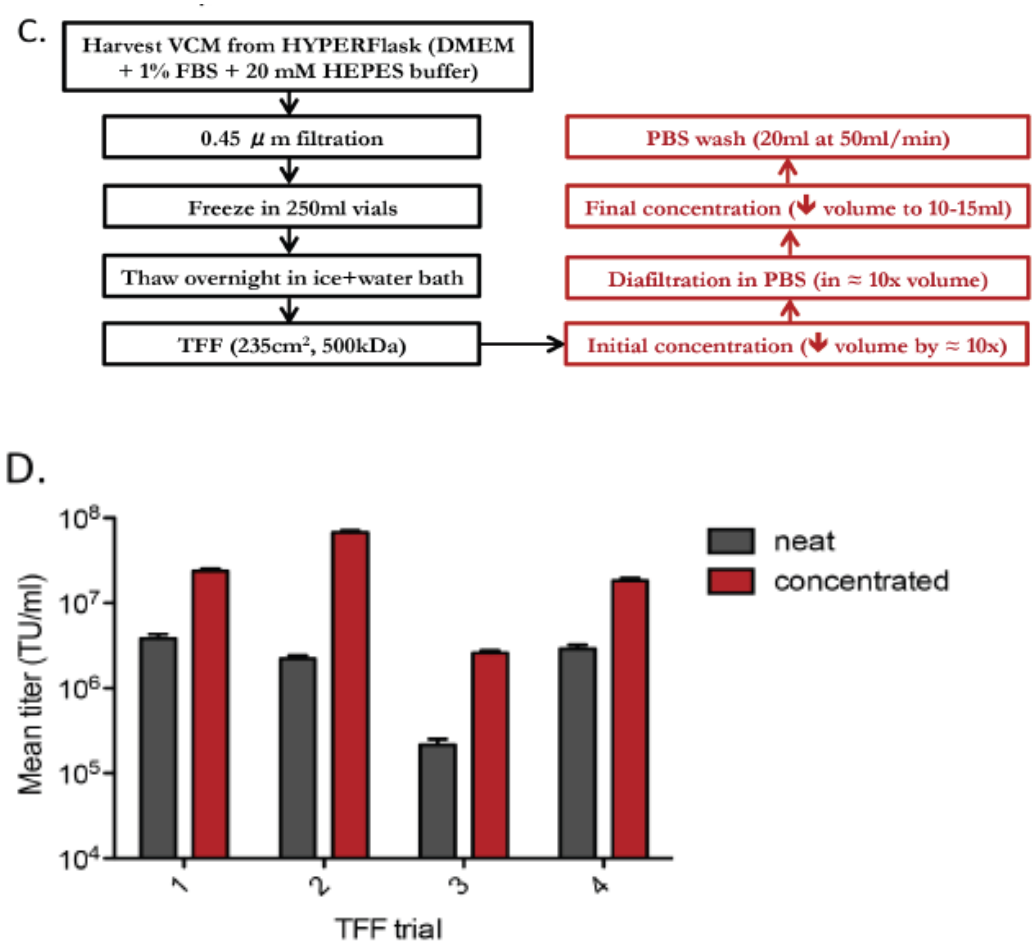

Figure 3.5 continued: (C) Flow chart outlining the general steps involved in a typical TFF process. **(D)** Titers of WRH2-produced vectors before and after concentration by TFF in the four trials undertaken (see Table 3.5 for more details). Vectors used in these experiments were produced in either HYPERflasks or 10-layer cellSTACKs. Data shown represents mean titer and range of duplicate titrations.

Table 3.5. Summary of TFF trials.

	Trial 1	**Trial 2**	**Trial 3**	**Trial 4**
Harvesting medium	D10	D10	OP0	D1 + 20 mM HEPES
Clarification	-	-	-	+
Diafiltration medium	PBS	PBS	PBS	PBS
Fold ↓ V before start of diafiltration	5	3	3	13
Hollow fiber:				
Material	PES	PES	PES	PES
MWCO (kDa)	500	500	500	500
SA (cm^2)	a. 325, b. 115	115	115	235
Flow rate (ml/min)	a. 100, b. 80	50	50	140
P_i (psi)	a. < 12, b. < 7.5	< 3	< 7.5	< 9
Shear (s^{-1})	a.< 4000, b.< 3000	< 3000	< 2000	< 3200
PBS wash at end of run	-	+	+	+
% vectors detected in PBS wash	N/A	≈ 5%	≈ 6%	≈ 5%
Initial V	1075	1075	1100	515
Final V	7.8	11.5	12.3	12
Fold ↓ in V	≈138	≈ 93	≈ 88	≈ 43
Initial titer (TU/ml)	3.9×10^6	2.2×10^6	2.2×10^5	2.9×10^6
Final titer (TU/ml)	2.4×10^7	6.8×10^7	2.6×10^6	1.9×10^7
% Recovery	a. 23%, b. 21% overall: 4%	32%	15	15

V: Volume, PES: Polyethersulfone (a polymer with low protein binding properties), MWCO: Molecular Weight Cut-off, SA: Surface Area, P_i: Inlet pressure, PBS: Phosphate-buffered saline, FBS: Fetal bovine serum.

3.3.6 Transduction of primary cells by stably-produced RDpro-pseudotyped LVs

CD34+ cells and T cells are important targets in human gene therapy (Aiuti et al., 2013; Biffi et al., 2013; Cavazzana-Calvo et al., 2010; Grupp et al., 2013). We therefore tested the transduction efficiency of our stably produced RDpro-pseudotyped LVs and compared it to that of transiently produced LVs (concentrated by ultracentrifugation). Equal number of 293T TU were used to transduce either human CD34+ cells isolated from G-CSF mobilized peripheral blood of a healthy donor or human T cells by pre-loading retronectin-coated plates. For both cell types, stably produced RDpro pseudotypes outperformed VSV-G pseudotypes especially at lower MOIs (Fig. 3.6A). Transduction of CD34+ cells was done with Giorgia Santilli's help at Adrian Thrasher's lab at the Institute of Child Health (ICH, UCL).

For T cells, it was noted that the percentage of GFP positive T cells following transduction with WRH2 vectors (concentrated by TFF using a hollow fiber with 100KDa cut-off) at MOI 25 was lower than that at MOI 5 (Figure 3.6B). Therefore, we examined the SSC vs. FSC FACS plots to look for evidence of cell death at high MOI that might account for this observation. However, no discernible differences were seen between the cells transduced at the different MOIs (Figure 3.6C).

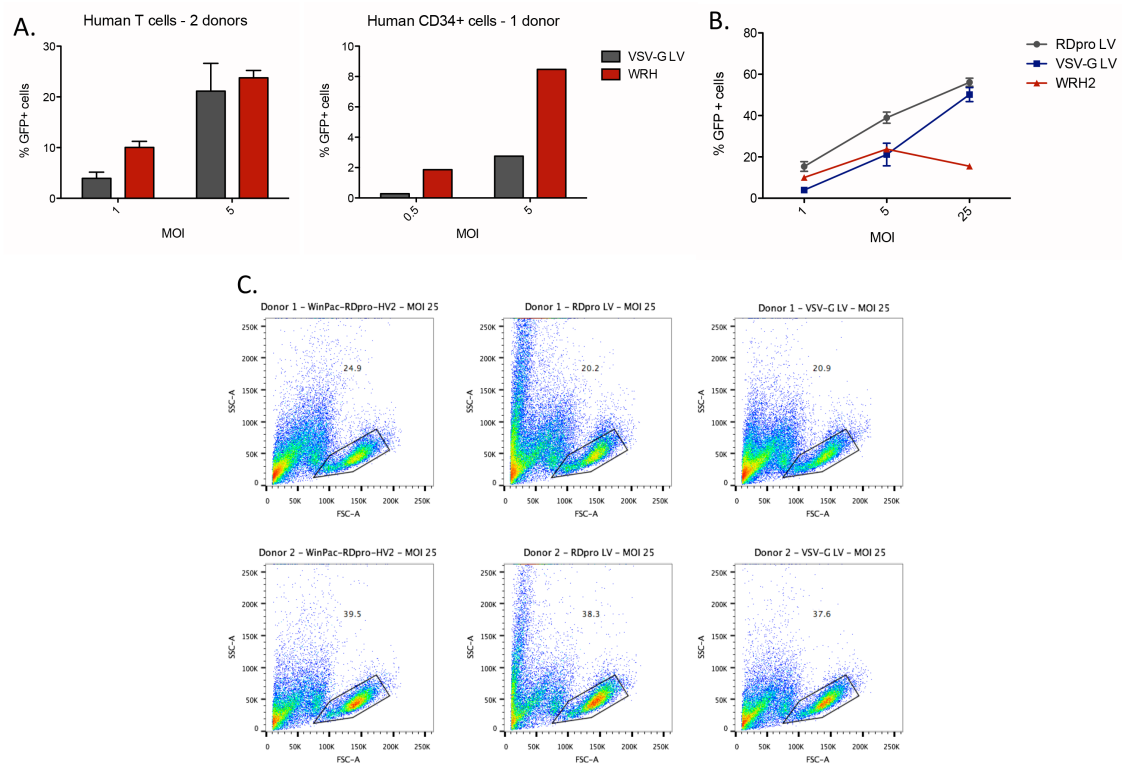

Figure 3.6. Transduction of human T cells and CD34+ cells.

(A) Activated T cells from peripheral blood of two donors and CD34+ cells from one donor were challenged with GFP-expressing SIN LV either stably produced by WinPac-RD-HV cells (WRH; RDpro pseudotyped) or transiently produced by 293FT cells (VSV-G pseudotyped) at two different vector doses: multiplicity of infection (MOI) was based on infectious titers on 293T cells. For T cells, data shown represents mean ± range for two donors. The experiment was performed in triplicates for each donor. **(B)** Percentage of GFP positive (%GFP +) cells obtained after challenging human T cells with GFP-expressing SIN LV either stably produced by WinPac-RD-HV cells and concentrated by TFF, or transiently produced by 293FT cells (either RDpro-pseudotyped (RDpro LV) or VSV-G-pseudotyped (VSV-G LV)) and concentrated by centrifugation. T cells were challenged at an MOI of 1, 5 or 25 with each vector preparation. Data shown represents mean ± range for two donors. The experiment was performed in triplicates for each donor. **(C)** FACS plots of SSC vs. FSC for the T cells from two donors challenged at MOI 25 with each of the three vector preparations described in '(B)'.

3.3.7 DNA copy numbers of vector components and their RNA expression levels

In order to examine the stability of the integrated expression cassettes of the various vector components and their expression levels, DNA (Figure 3.7) and RNA (Figure 3.8) levels were determined in a number of vector producer clones at two time points during continuous culture approximately 10 weeks apart (early and late). Vector titers of corresponding harvests were also measured at the same two time points. The DNA copy number for Gag-Pol, at the LoxP tagged locus, was stable in WinPac derived cell lines (Figure 3.7A). Consistent with our lab's previous report (Ikeda et al., 2003a), STAR-derived cells contained multiple Gag-Pol copies. Notably, the stable DNA copy numbers of the SIN-HV genome DNA in the tested clones (Figure 3.7D) suggest the absence of significant autotransduction likely due to the interference phenomenon (Coffin et al., 1997a). Gag-Pol RNA levels were relatively stable, suggesting that the LoxP tagged locus can support high expression levels long-term (Figure 3.7E). RDpro env and Rev RNA levels decreased with time in some of the clones tested.

Vector titers were then compared with component RNA levels to examine which RNA might be limiting for vector titer in a variety of WRH and SRH clones. Figure 3.7 shows that RNA levels for Gag-Pol, Rev and SIN-HV genome, but not that for RDpro env, positively correlated with transduction titers (Figure 3.8). This suggests that particular attention should be paid to expression levels of Gag-Pol, Rev and vector genome. Analysis of data from individual clones suggested that any of these could limit vector titer (WRH1 (early, BPlPuH): vector genome; WRH2 (early, no antibiotics): Gag-Pol/Rev; WRH26 (early, no antibiotics): Rev; Figure 3.8).

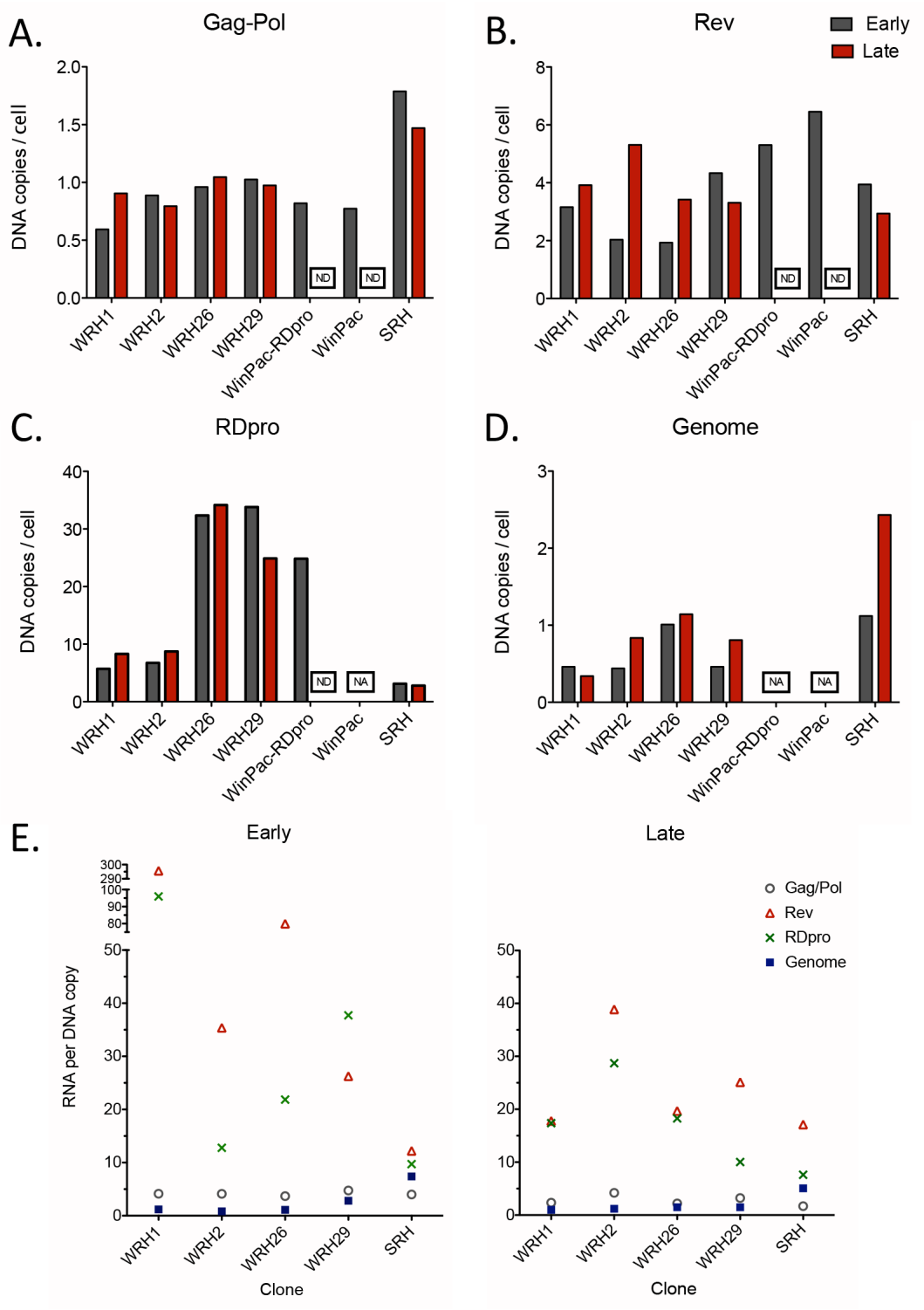

Figure 3.7. DNA copy numbers and mRNA expression levels of the vector components in packaging and producer cell lines.

DNA copy numbers per cell for Gag-Pol **(A)**, Rev **(B)**, RDpro **(C)** and vector genome **(D)** expression cassettes, measured by Q-PCR. Cell number per reaction was estimated by performing Q-PCR for β-actin in parallel. Data shown represents mean of two replicates. **(E)** RNA expression levels per DNA copy number of each vector component are shown.

RNA expression levels were measured by q-RT-PCR and normalized to the b-actin RNA expression levels in each sample and divided by the corresponding DNA copy number. Early (after <2–4 weeks in culture) and late (after <12–14 weeks in culture) time points were around 8–10 weeks apart. NA, not applicable; ND, not done.

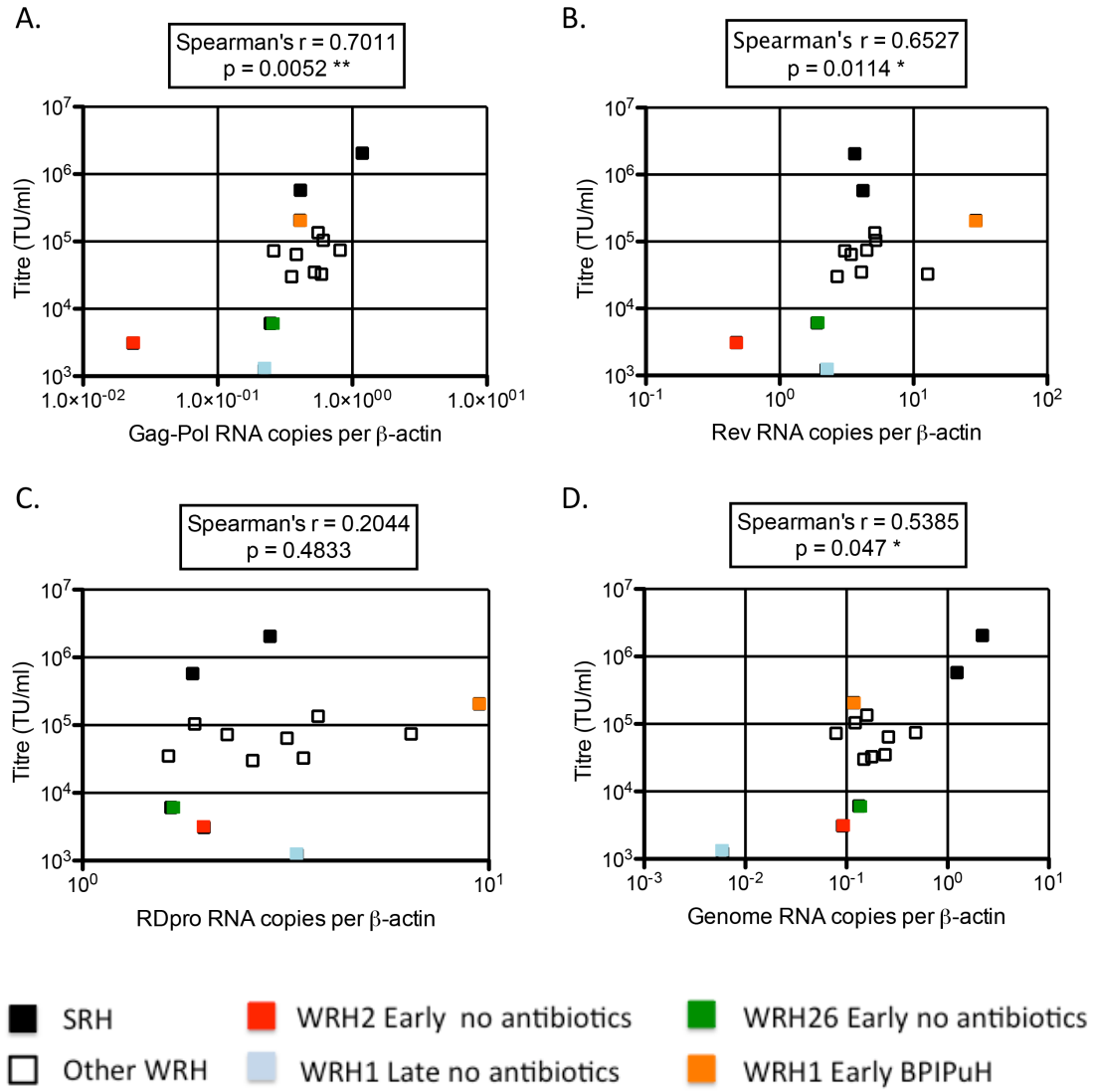

Figure 3.8. Correlation between RNA expression levels of vector components and functional titers.

RNA expression levels for Gag-Pol **(A)**, Rev **(B)**, RDpro **(C)** and vector genome **(D)**. Points in each graph represent the RNA expression levels (normalized to β-actin RNA expression levels) of the various vector components at the Early and Late time points for the four WinPac-RD-HV (WRH) producer clones (while growing in the presence or absence of selection antibiotics) and STAR-RDpro-HV (SRH) cells plotted against the titers determined at the time of RNA extraction. The data represents the mean of two replicates. Black: SRH, Orange: WRH1 Early BPlPuH, Red: WRH2 Early no antibiotics, Blue: WRH1 Late no antibiotics, Green: WRH26 Early no antibiotics, White: remaining WRH.

3.3.8 Safety characteristics.

APOBEC3G (A3G) belongs to the apolipoproteinB mRNA editing enzyme catalytic polypeptide-like (APOBEC) family of proteins (reviewed in (Malim, 2009)) and was initially identified as a potent restriction factor against HIV-1 infection in human CD4+ T cells (Sheehy et al., 2002) . APOBEC3G-mediated G to A hypermutation in integrated proviral copies of γ-retroviral vectors produced by the HT1080-derived FLYA13 packaging cell lines has been previously demonstrated (Miller and Metzger, 2011). These mutations can have important consequences if they occur in the region coding for the therapeutic gene of interest, as they may lead to decreased levels of production, or the production of an inactive or immunogenic variant of the therapeutic protein. However, no hypermutation of vectors produced by 293 cells was detectable in that report. This was consistent with a previous report demonstrating that A3G RNA was undetectable in 293T cells (Kinomoto et al., 2007). Thus, we tested whether WinPac cells express A3G or not at various stages of their development. As expected, APOBEC3G protein was not detected by western blot in WinPac, WinPac-RD, and WinPac-RD-HV1 cells (Figure 3.9A).

We hypothesized that stable LV production yields preparations containing less plasmid DNA and cell-derived contaminants, compared to transient production methods. Importantly, plasmid DNA contaminants in clinical vector preparations can potentially induce immune responses via Toll-Like Receptors (Pichlmair et al., 2007). To compare the relative amounts of such contaminants in untreated stably- and transiently produced vector preparations, Q-PCR-based assays were used to detect cell-derived DNA encoding SV40T Ag and plasmid DNA (Figure 3.9B). Although there were similar levels of cell-derived DNA in all preparations tested, there were higher levels of plasmid DNA in transiently produced vector preparations.

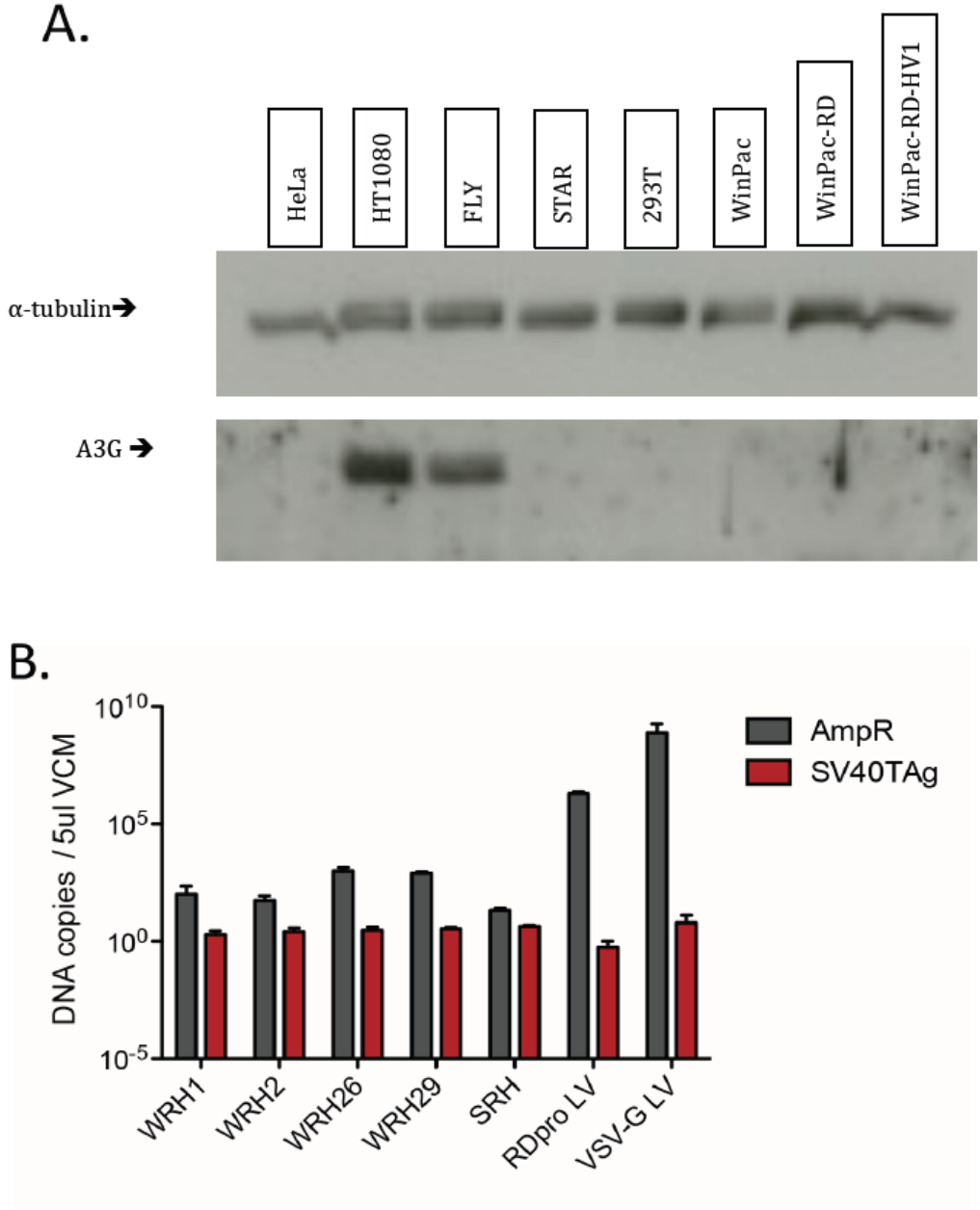

Figure 3.9. Safety assays.

(A) Western blot for APOBEC3G on lysates derived from 293FT, WinPac, WinPac-RD and WinPac-RD-HV cells. HeLa cells were used as a negative control, while HT1080 and FLY cells (HT1080-derived γ-retroviral packaging cell line) were used as positive controls. **(B)** Detection of plasmid and cell-derived DNA in stably- and transiently-produced vectors. Equal volume of untreated culture supernatant for each vector was used in the Q-PCR assays. Primers that amplify a segment of the ampicillin resistance gene (AmpR) were used to detect DNA, mainly derived from transiently transfected plasmids. Primers

that amplify a segment of the gene encoding SV40TAg were used to detect cell-derived DNA. Data shown represents mean titer ± SD (n=3). Q-PCR assay was performed in triplicates.

3.4 Discussion

The construction of WinPac cells and the derivation of stable producer cells is an important milestone. This work has demonstrated that it is possible to express HIV-1 Gag-Pol constitutively, at a high level, from a single copy cassette inserted into the producer cell genome by Cre-mediated cassette exchange. The target LoxP sites were introduced using a GRV vector since our lab previously demonstrated that GRV insertion sites would support HIV-1 Gag-Pol expression (Ikeda et al., 2003a). This method could be adapted to use the CRISPR-Cas9 technology to insert LoxP sites into known loci. It will also be possible to modify the Gag-Pol expression cassette to test other enhancer/promoters. The CMV immediate early promoter was chosen because since it worked well in STAR cells.

Furthermore, it was shown that linking expression of the various vector components with that of selectable markers ensures high titers are achieved. This is particularly important for Gag-Pol, Rev and the vector genome since it was shown that their expression levels correlate positively with LV titer. Practically, re-selection with antibiotics would be recommended before and after the expression of new vector component in packaging cells as well as after thawing out producer cells. Subsequently, cell culture can be scaled up and vector batch production can be reliably undertaken in the absence of antibiotics.

The RDpro envelope protein was chosen to exemplify the method since it allowed efficient transduction of human primary cells. Other non-cytotoxic viral envelopes could be substituted, such as those from amphotropic murine leukemia virus or Gibbon ape leukemia virus, which have been used in clinical gene therapy trials with GRV (Mukherjee and Thrasher, 2013). It would also be possible to use an inducible construct for a cytotoxic envelope such as VSV-G, in cells containing all the other LV components. This induction in the presence of optimal expression of Gag-Pol, Rev and SIN vector, should be more efficient than simultaneous induction of multiple components.

Our novel, clinical-grade WinPac cells with the RD114-derived envelope, RDpro, can continuously produce third generation SIN LV at titers in the order of 10^6 TU/ml. In current successful, gene therapy trials, roughly 1–40 x 10^9 transducing units of vectors per patient are required (Aiuti et al., 2013; Biffi et al., 2013; Cartier et al., 2009; Cavazzana-Calvo et al., 2010). It is certainly feasible to produce clinically useful batches of

therapeutic LV by optimized scaling-up of cell culture, vector harvest and processing using WinPac-RD packaging cells. Such continuous LV production methods will have considerable advantages over current transient vector production methods, being cheaper, more reproducible and lower in contaminants.

Compared to currently available PCLs, WinPac cells can support the production of SIN LV at superior titers compared to the other constitutive LV PCL reported to date (Stornaiuolo et al., 2013). In contrast to inducible PCLs proposed for clinical LV production, like the GPRG cell line (Throm et al., 2009) continuous production using WinPac cells is easier to scale up and avoids the rapid decline in titers following induction. Interestingly, WinPac-derived producers had titers similar to GPRG-derived producers obtained following plasmid transfection as opposed to concatemeric array transfection, which is difficult to reproduce and is less stable.

Notably, the expression level of the SIN vector genome in our model producer cells is suboptimal and limits titers. The highest titer producer cell lines from STAR-RDpro contained a transfer vector carrying a full length LTR in the presence of HIV-1 tat. This might account for the higher expression of the vector genome RNA. Therefore, work has been done to optimize its expression level for SIN LV production in WinPac cells using alternative techniques including RMCE at a pre-defined locus (see Chapter 4 for details). This strategy would facilitate the reproducible construction of various producer cell lines from a master packaging cell line.

To facilitate the use of these cell lines, optimization of the downstream processing protocols for RDpro-pseudotyped LVs is warranted. Tangential flow filtration is a scalable and efficient method that allows concentration and diafiltration of vectors in a single step. Significant progress has been made by overcoming the problem of gel layer formation when a large volume (> 0.5 L) of VCM was processed by tangential flow filtration using hollow fibers with 500 kDa MWCO. However, there is still a need to improve vector recovery by determining the optimal flow rate, which would allow efficient processing of VCM while minimizing vector inactivation.

Optimization of this process would allow us to further investigate the inhibition of infection observed with WRH vectors concentrated by TFF hollow fibers with 100 kDa MWCO. One possible explanation for this phenomenon is the presence of an inhibitor that can be diluted away when low volumes of TFF-concentrated VCM were used to

transduce target cells. This inhibitor might represent shed RDpro envelope glycoprotein (Cook and Lee, 2013) or empty virus-like particles. Although the RD114 envelope is normally a 70KDa glycoprotein (Dunn 1993), it might not be efficiently filtered out by hollow fibers with 100 kDa MWCO. If present, either one of these 'contaminants' can potentially bind to the target cell receptors of the RD114-derived envelope glycoproteins, previously identified as human sodium-dependent neutral-amino-acid transporter B^0 (Rasko et al., 1999; Tailor et al., 1999). This would result in an envelope-dependent inhibition of infection by RDpro-pseudotyped LVs but not by other pseudotypes that target different receptors.

If free envelope is the culprit, then processing VCM using TFF hollow fibers with 500 kDa MWCO might rescue infectivity of the concentrated vectors at high MOIs. To elucidate this, the infection assay on human T cells will be repeated when a batch of TFF-concentrated vectors is obtained under optimized conditions. If the inhibition phenomenon persists, the plan is to determine whether the observed inhibition is envelope-specific or not. To this end, an mCherry-expressing LV plasmid (SIN pHVC) was constructed by replacing the GFP gene in SIN pHV with that of mCherry. I am planning to use this plasmid to produce mCherry-expressing VSV-G- or RDpro-pseudotyped LVs. Each of these vectors will then be used to co-infect 293T cells in the presence of the TFF-concentrated vectors. If mCherry positive cells are discerned with VSV-G pseudotypes but not with RDpro pseudotypes, this would confirm the presence of an envelope-dependent inhibitor.

Another possible cause of the inhibition seen at MOI 25 is the triggering of innate sensors leading to type I IFN production and the induction of an antiviral state by upregulating the expression of IFN-inducible restriction factors. The *CA* encoded by *Gag* in WinPac harbors the naturally occurring H87Q mutation, which impairs binding to CypA (Chatterji et al., 2005; Ikeda et al., 2004; Kootstra et al., 2007). Another CypA-independent *CA* mutant (P90A) has been shown to trigger such an innate immune response in primary human monocyte-derived macrophages (Rasaiyaah et al., 2013). Thus, it would be interesting to measure type I IFN levels in the supernatant after infection of cells at the different MOIs. Moreover, including vectors produced by STAR-RDpro-HV cells as an additional control might be informative since these cells express the wild-type *CA*.

CHAPTER

4

Generation of Producer Cell lines Using Recombinase-mediated Cassette Exchange

4 Generation of producer cell lines using recombinase-mediated cassette exchange (RMCE)

4.1 Introduction

SIN lentiviral vectors have been developed by deleting a significant part of the U3 region (including the TATA box) in the 3' LTR of the DNA plasmid encoding the lentiviral vector (Miyoshi et al., 1998; Zufferey et al., 1998). During reverse transcription of the vector RNA in transduced cells, this deletion is copied to the 5' LTR of proviral DNA. Since the deletion includes the viral promoter sequences, this almost abolishes the viral LTR transcriptional activity and consequently the expression of the full-length, packable vector gRNA in the transduced cells. Consequently, the SIN LV genome cannot be expressed in packaging cells by transducing them with the vectors, which is the method previously used for the generation of producer cells for vectors with an intact *Tat*-dependent LTR (Table 3.1; (Ikeda et al., 2003a; Stornaiuolo et al., 2013)). Instead, the DNA plasmid is simply transfected into producer cells allowing vector genome expression driven by a heterologous promoter that replaces the U3 region of the 5' LTR (Dull et al., 1998; Miyoshi et al., 1998) (Figure 4.1).

The chromatin structure of the chromosomal locus at which integration occurs is an important determinant of the expression level and its stability. Since the integration of a transfected DNA expression cassette occurs randomly, this process results in highly variable expression levels. This variability complicates the generation of high-titer producer cell lines and necessitates the screening of a large number of clones. Indeed, the co-transfection of the vector genome with another plasmid encoding a selectable antibiotic resistance gene into PCLs resulted in low titers that diminish relatively rapidly with time in culture (after 1 month). In contrast, the transduction of PCLs with a non-SIN LV and subsequent expression of the vector genome resulted in high titer vector production for more than 3 months (Ikeda et al., 2003a, b).

The detailed analysis of WinPac-derived producer cell lines (see Chapter 3 for details) revealed that they expressed similar levels of Gag-Pol, Rev and the envelope glycoprotein compared to STAR-derived cells. However, they expressed lower levels of the vector genome even after selection with blasticidin resulting in relatively low titers (Figure 3.8).

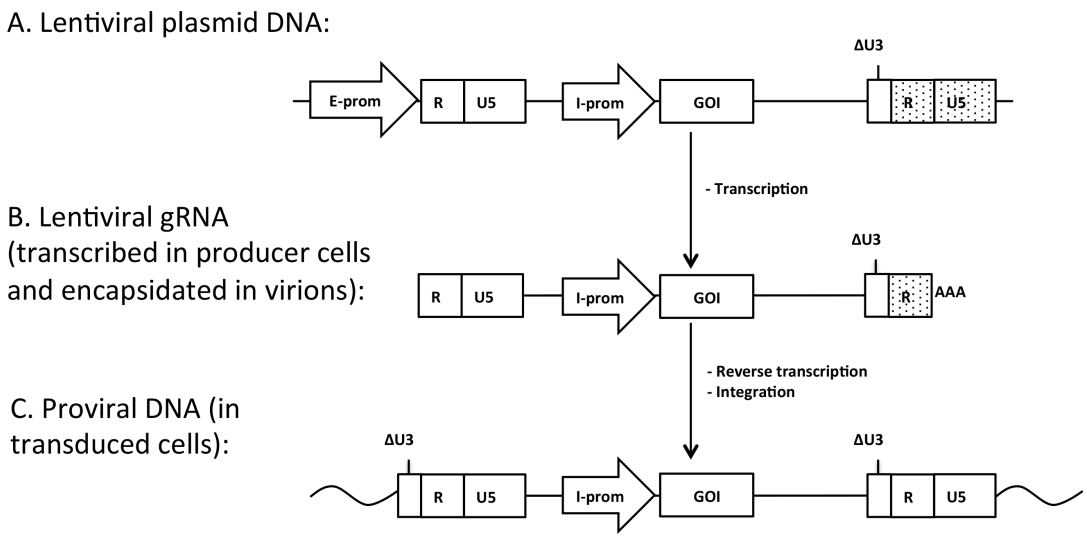

Figure 4.1. Schematic representation of a third generation SIN LV.

(A) Plasmid DNA in which an external promoter (E-prom) upstream from the 5'LTR of the LV drives the transcription of the full-length genomic RNA (gRNA) in producer cells. The 3' LTR of the LV carries has a deletion that eliminates the promoter and enhancer sequences mainly in its U3 region (ΔU3). The internal promoter (I-prom) drives the expression of the gene of interest (GOI). **(B)** Genomic RNA (gRNA) that is transcribed from the plasmid DNA in producer cells and then encapsidated within LV particles (the Gag-Pol, Rev and Env functions that are required are provided by separate plasmids that are co-transfected with the SIN LV encoding plasmid (A)). The gRNA carries the partially-deleted 3' LTR. **(C)** Proviral DNA following integration into the genome of transduced cells. The gRNA of the vectors is released into the target cell cytosol following vector entry (exact mechanism depends on pseudotyping envelope glycoprotein) and uncoating. During transport to the nucleus, the gRNA is reverse transcribed by the viral reverse transcriptase activity. This results in copying of the ΔU3 to the 5' end while the U5 region of the 5' LTR is copied to the 3' end. A complementary DNA strand is synthesized forming a double-stranded DNA that integrates into the target cell genome. The proviral DNA has the ΔU3 in its 5' and 3' LTRs, which therefore have no promoter/enhancer activity. Consequently the provirus cannot express its own full-length gRNA from its 5'LTR. Moreover, this reduces the risk of insertional mutagenesis, as there is no retroviral promoter/enhancer activity in both LTRs that could have otherwise altered expression of nearby cellular genes. Careful choice of the internal promoter (I-prom) can further reduce such a risk.

This prompted me to seek alternative methods to stably express a third generation, SIN LV genome in producer cells. One attractive solution is to adopt a two-step process whereby site specific recombinases exchange a SIN LV expression cassette at a pre-characterized locus flanked by recombinase recognition targets (RTs) (reviewed in (Turan and Bode, 2011)). This strategy had been originally employed to establish master GRV PCLs that can be used to predictably express various vectors at a pre-characterized locus and facilitate the rapid generation of higher titer producer cell lines (Coroadinha et al., 2006; Karreman et al., 1996; Schucht et al., 2006). It was more recently used to establish SIN GRV producer cell lines (Loew et al., 2010).

To achieve this, packaging cells are initially transduced at a low MOI with a gamma-retroviral vector carrying twin heterospecific FLP recognition target (FRT) sites in the U3 region of its 3'LTR. The chosen heterospecific sites, usually spacer mutants carrying a mutation(s) in the 8bp spacer sequence of the FRT sites, should ideally exhibit maximal self-interaction (FxF or F'xF') with minimal cross-interaction (FxF') (Turan et al., 2010). Since the twin FRT sites (FF') are copied to the 5'LTR during reverse transcription, the integrated provirus can serve as a target cassette expressing a reporter gene flanked by two sets of twin sites (FF'-reporter-FF'). After transduction, single clones are isolated and the expression of the reporter gene is measured to determine the intrinsic expression characteristics of the tagged loci. Clones with favorable expression characteristics are then selected and single copy integration is confirmed. Once a clone is selected, a master cell bank can be established. In a second step, donor cassette expressing a SIN LV genome and flanked by single heterospecific FRTs (F-SIN LV-F') can be exchanged for the target cassette using Flpe recombinase. Since the remaining single heterospecific sites exhibit minimal cross-interaction the donor cassette becomes stably integrated in producer cells (Figure 4.2) (Wirth et al., 2007).

Another strategy that allows the selection of producer clones in which the SIN LV genome expression cassette is integrated at an actively transcribed site is via the use of a promoterless selectable marker arranged *in cis* with the genome expression cassette. Thus following transfection of the DNA plasmid, the selectable marker should be stably expressed only if the plasmid integrates in the proximity of an active cellular promoter.

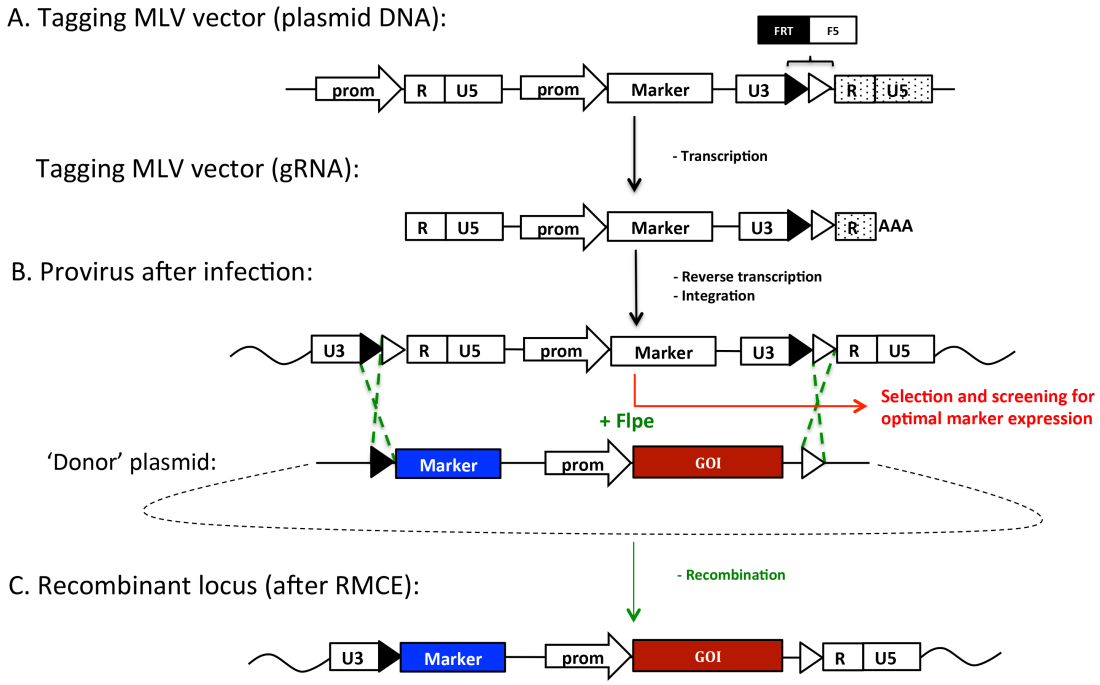

Figure 4.2. Schematic representation of Flp recombinase-mediated cassette exchange (Flp RMCE).

(A) Top: DNA plasmid encoding MLV-based gamma-retroviral vector (GRV) that carries the FRT and F5 sites in the U3 region of its 3' LTR. This plasmid is co-transfected into 293T cells with a packaging plasmid and an envelope plasmid. Bottom: Genomic RNA (gRNA) of the tagging MLV vector is transcribed in 293T cells and encapsidated in the vector particles. The gRNA carries the FRT and F5 sites in in the U3 region of its 3' LTR. **(B)** Top: proviral DNA following integration into the genome of transduced cells. The gRNA of the vectors is released into the target cell cytosol following vector entry and uncoating. The gRNA is then imported into the nucleus and reverse transcribed by the viral reverse transcriptase activity. This results in copying of the U3 region (including the FRT and F5 sites) from the 3' LTR to the 5' end while the U5 region of the 5' LTR is copied to the 3' end. A complementary DNA strand is synthesized forming a double-stranded DNA that integrates into the target cell genome. Most of the proviral DNA becomes flanked by the FRT and F5 sites in its 5' and 3' LTRs (except for the 3' U3 region and the 5' R and U5 regions). Selectable marker expression driven by an internal promoter allows selection and screening of clones for loci with favorable expression profiles. Bottom: A donor plasmid encodes a promoterless selectable marker gene and a gene of interest (GOI) expression cassette is flanked by an upstream FRT site and a downstream F5 site. The donor plasmid is co-transfected with a plasmid encoding the

Flpe recombinase into a clonal cell population that was tagged with the MLV vector. Flpe recombinase mediates the exchange of the cassettes flanked by FRT and F5 sites. **(C)** The recombinant locus following successful RMCE reaction. The marker gene in the tagging provirus (white) is lost and the marker gene in the donor cassette (blue) is expressed by the U3 promoter activity of the tagging MLV vector allowing selection of successful recombination events. Predictable and optimal GOI expression would be expected as the donor cassette becomes stably integrated at the pre-selected tagged locus in the target cells.

4.2 Aims

The work presented in this chapter was aimed at establishing a master packaging cell line in which SIN LV vector genomes can be reproducibly expressed at a predefined locus through the use of Flp-RMCE. Further work was done to test and optimise the process of recombination and producer cell derivation with the goal of rapidly generating producer cell lines with predictable titers. Additionally, other methods were to be tested to determine if they can achieve reproducibly high and stable expression of a SIN LV genome in producer cell lines.

4.3 Results

4.3.1 Marking chromosomal loci in WinPac-RDpro cells and establishment of the targetable WinRD-F1 cell line (Sean knight)

The overall scheme for the Flp-RMCE strategy is shown in Figure 4.3. Initially, plasmid pCFG was constructed to encode a GFP-expressing MLV-based vector that has the wild-type FRT and F5 (a FRT variant with a single nucleotide mutation in the spacer region) (Turan et al., 2010) sites cloned into the U3 region of its 3'LTR (Figure 4.3A: top panel). This plasmid was then used to produce VSV-G-pseudotyped MLV vectors by three-plasmid transient transfection of 293T cells. Infectious titers were determined using 293T cells as targets. These vectors were then used to transduce WinPac-RDpro cells at an MOI of 0.1 or 0.01 to ensure single copy integration of provirus DNA per cell, thereby establishing one chromosomal targetable cassette in each infected cell (Figure 4.3A: middle panel). Single clones were then isolated by limiting dilution in 96-well plates and screened for GFP expression; initially by fluorescence microscopy, and then by flowcytometry to determine mean fluorescence intensity (MFI) as a measure of GFP expression levels (Figure 4.3B). The number of copies of integrated GRV vectors was also determined by Q-PCR (Fig 4.3B). Clone WinRD-F1 was selected for further experiments based on its relatively high MFI as well as having a single integrated GRV vector copy per cell. It was also one of two clones that could produce detectable titer following the transient transfection of SIN pHV (mean titer = $7.2x10^4$ TU/ml).

Unfortunately, attempts made to sequence the integration site using linker-mediated RCR (LM-PCR) or inverse-PCR (I-PCR) failed despite the use of multiple restriction enzymes (Bartholomae et al., 2012). It is known that restriction enzyme-dependent methods may miss integration sites that lack a suitable restriction sites in their proximity.

Alternative methods are available that can overcome such an obstacle (Paruzynski et al., 2010), but non-restriction enzyme-related factors may also bias integration site mapping (Wu et al., 2013).

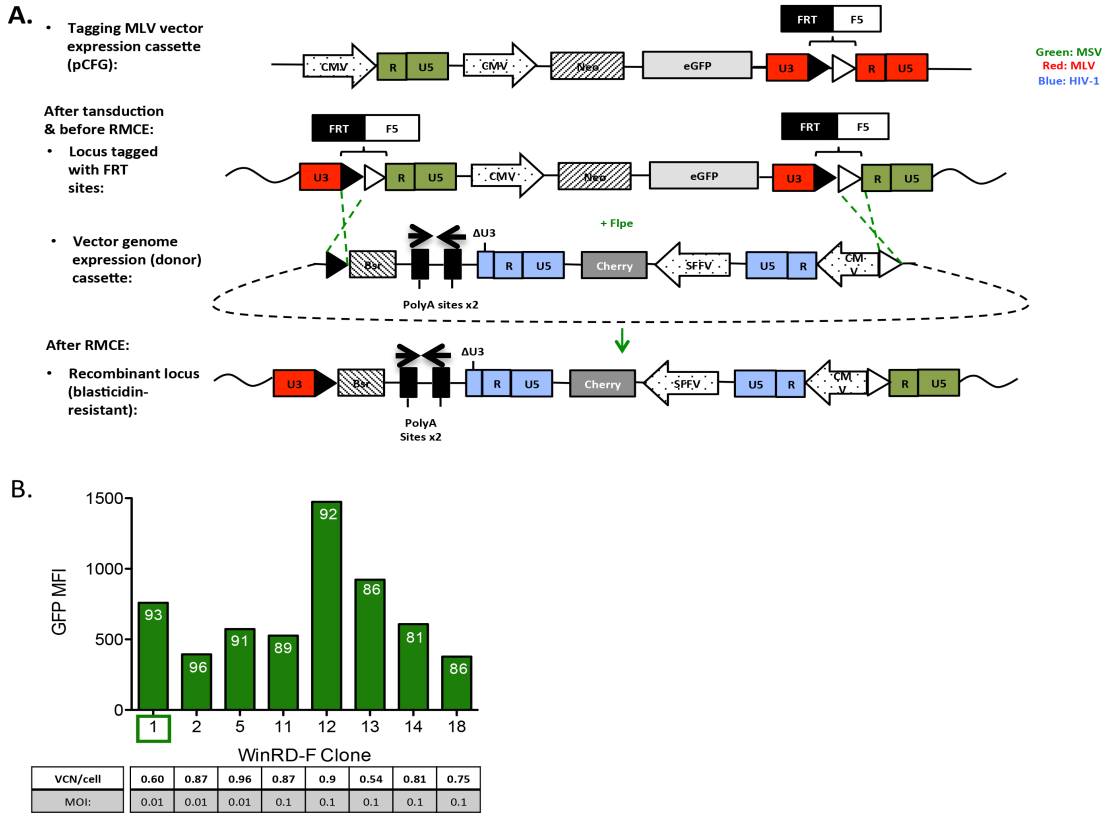

Figure 4.3. Overview of recombinase-mediated cassette exchange (RMCE) strategy and Tagging of WinPac-RDpro cells with FRT/F5 sites.

(A) Scheme of the Flpe recombinase-mediated cassette exchange (RMCE) strategy employed to generate SIN LV producer cell lines. Top panel: DNA plasmid of MLV vector used to tag a locus with FRT and F5 sites in WinPac-RDpro cells. Second from top panel: Scheme of integrated provirus in WinRD-F1 cells. Second from bottom panel: donor DNA plasmid encoding the SIN LV expression cassette. The LV cassette is placed in the opposite direction to the Bsr marker-poly A site cassette, hence two two poly A sites are in the opposite direction each other. Bottom panel: recombinant locus following successful Flpe-mediated recombination reaction resulting in replacement of the tagging GFP expression cassette with the donor SIN LV expression cassette. (B) Screening of WinRD-F clones. Mean fluorescence intensity (MFI) of GFP expressing clones isolated by limiting dilution following the transduction of WinPac-RDpro cells by the tagging MLV vectors. Numbers at the top of each bar represents % of GFP positive cells for each clone. The table shows vector copy number (VCN) per cell and the MOI at which the parental population (WinPac-RDpro) was transduced (for MOI 0.1: 5/94 clones were GFP positive; for MOI 0.01: 3/223 clones were GFP positive). Clone WinRD-F1 (enclosed in green square) was selected for further experiments.

4.3.2 Expression of vector genome and screening titers

A donor plasmid (pFBCF) encoding a mCherry-expressing SIN LV was constructed. Downstream from the SIN-LV expression cassette two polyA signals were inserted, and further downstream from those, a promoterless Bsr (blasticidin resistance) gene was placed with its ORF in reverse orientation to that of the SIN LV expression cassette. All these elements were flanked by an F5 site (upstream to the LV expression cassette) and a FRT site (downstream to the promoterless Bsr gene). The pCflpe plasmid (a kind gift from Dr. Dagmar Wirth) was used to express flpe (an engineered Flp recombinase enzyme with improved activity at 37 °C) (Buchholz et al., 1998).

Initial attempts to isolate blasticidin-resistant clones following the co-transfection of pCflpe and pFBCF failed. Given the evidence indicating the functionality of the target FRT sites and pCflpe plasmid, I hypothesized that the concentration of Blasticidin used might have been too high. I initially used Blasticidin at a concentration of 10μg/ml which was previously used to select for cells transfected with pSELECT-blasti-MCS in which Bsr (Blasticidin resistance gene) was driven by a human cytomegalovirus immediate-early gene 1 promoter/enhancer. In cells where recombination successfully occurs, the Bsr gene would be driven by the MLV enhancer/promoter of the MLV U3 region. This may result in lower levels of expression that would necessitate the use of a lower concentration of blasticidin to allow selection of resistant clones. Therefore, a range of blasticidin concentrations (3-10 μg/ml) was tested on WinRD-F1 cells co-transfected with pCflpe and pFBCF. A concentration of 5 μg/ml was found to allow reproducible and efficient selection of resistant cells. The ability of blasticidin at the above concentrations was sufficient to kill WinRD-F1 cells.

In addition to that, I co-tranfected a molar excess of pCflpe compared to pFBCF (molar ratio 4:1). This was done in an attempt to minimize the occurrence of random integration of the pFBCF plasmid, by reducing the chances of that plasmid successfully transfecting a cell in the absence of pCflpe.

In the final protocol (see Section 2.4), WinRD-F1 cells were initially selected with puromycin, hygromycin and phleomycin for around 10 days. The cells were then transfected with either 9 μg pCflpe + 3 μg pFBCF or 3 μg pFBCF. The latter resulted in random integration only and served two purposes: Firstly, the determination of background gain of blasticidin-resistance in the absence of recombination events;

secondly, the utility of using a promoterless selectable marker gene as a means to express SIN LV genomes in packaging cells. 72 hours after transfection, the cells were harvested and seeded in 10 cm^2 plates at six ten-fold dilution and selection with Blasticidin was initiated. After 2-3 weeks of selection, the surviving mono-/ -clonal populations were isolated. These clones were then re-selected with puromycin, hygromycin and phleomycin. Clones that underwent successful recombination should become GFP negative and mCherry positive. Thus, an initial flowcytometry-based screening was conducted to identify such clones. Vector-containing medium was also collected and titrated on 293T cells to identify the best-performing populations. It was hypothesized that subsequently subcloning the best performing populations would increase the chances of isolating clones that were capable of stably producing SIN LVs at high-titer (Cockrell et al., 2006).

For cells co-transfected with pCflpe + pFBCF, a total of 26 oligoclonal populations were isolated and screened. Most of these populations (16/26, ≈ 60%) were GFP negative and mCherry positive (Figure 4.4A; Table 4.1). None of the populations isolated were mCherry+/GFP+ (double positive) suggesting that pCflpe was efficiently mediating the excision of the target locus and that the probability of transfecting a cell with pFBCF in the absence of pCflpe was successfully minimized. However, it is still possible that pFBCF insertion might occur independently from Flpe-mediated GFP excision in any single cell resulting in its random integration into the cell's genome.

Of the populations screened, 11/26 produced mCherry expressing vectors at detectable titers (mean=$2.1x10^5$ TU/ml and range: $3.2x10^4$ – $5.4x10^5$ TU/ml; Figure 4.4B). All of these populations were either mCherry+/GFP- or a mix of mCherry+/GFP- and mCherry-/GFP+ cells. An estimate of the productivity per cell per 24hr was calculated based on the number of cells at the end of the 24-hour harvest (mean= 0.041 TU/cell/day, range= 0.003-0.094 TU/cell/day; Figure 4.4C).

As expected, cells transfected with pFBCF alone (without pCflpe) were doubly GFP and mCherry positive (Figure 4.4A, Row 1-Column 3). Five oligoclonal populations isolated from this population of cells yielded relatively high titers (mean= $3.6x10^6$ TU/ml, range = $1.1x10^5$ - $1.3x10^7$ TU/ml; Figure 4.4D). This suggests that a promoterless selectable marker gene can be used as a simple and efficient method to express SIN LV genomes in packaging cells. Moreover, loci with better transcriptional profiles compared to the FRT-tagged locus in WinRD-F1 cells likely exist and could be exploited to achieve higher expression levels (see Chapter 6 for more details).

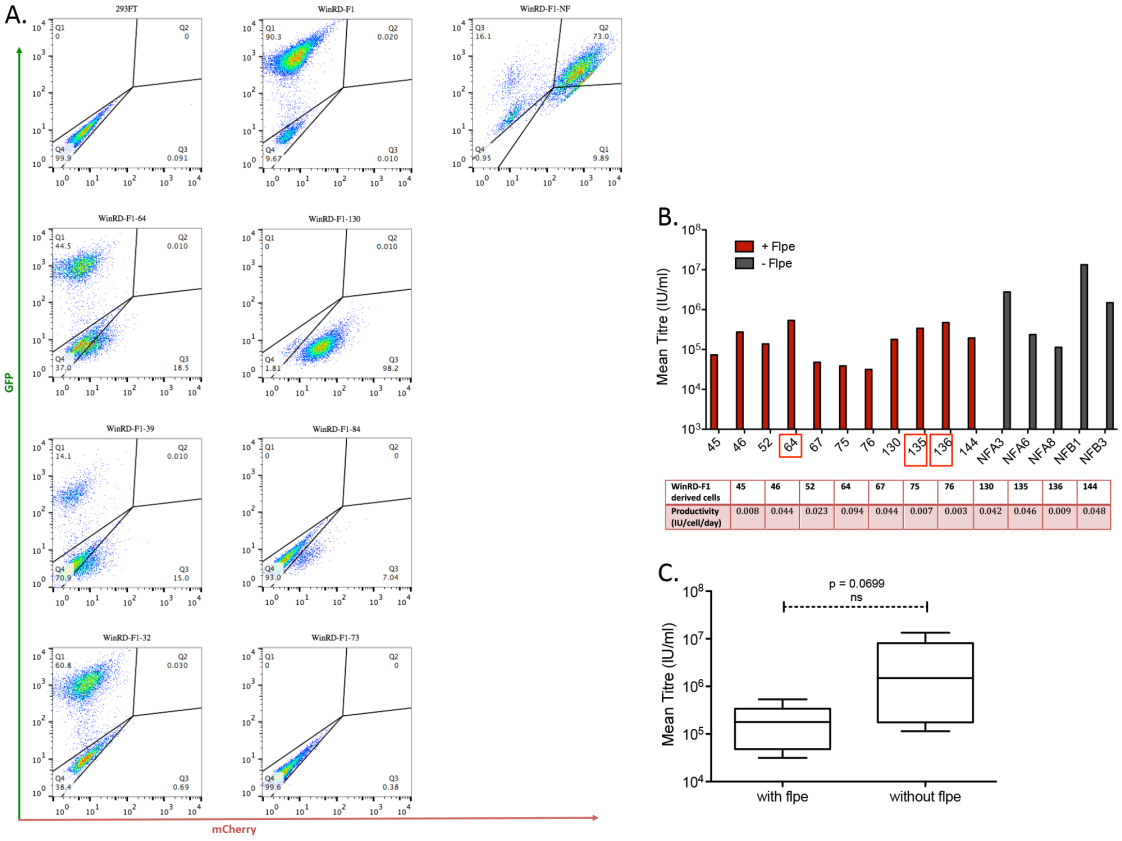

Figure 4.4. Generation of oligoclonal producer populations from WinRD-F1 cells.

(A) FACS plots of GFP (y-axis) against mCherry (x-axis) expression following co-transfection of WinRD-F1 cells with pCflpe and pFBCF. Top 3 panels: double negative 293FT cells, GFP+ parental WinRD-F1 cells and WinRD-F1-NF5 cells (following transfection with pFBCF alone). Middle 4 panels: representative FACS plots of the phenotype of cells that produced vectors at detectable titers following co-transfection with pCflpe and pFBCF (mixture of GFP+ or mCherry+ cells; mCherry + cells). Bottom 2 panels: representative FACS plots of the phenotype of cells that did not produce vectors at detectable titers following co-transfection with pCflpe and pFBCF (mixture of GFP+ or mCherry+ cells; mCherry + cells; GFP+ cells; double negative cells). **(B)** Mean titers of oligoclonal producer cell populations from WinRD-F1 cells. Red bars represent titers of populations obtained following co-transfection with pCflpe and pFBCF. Grey bars represent titers of populations obtained following transfection with pFBCF alone. Mean titers were calculated from duplicates. The populations chosen for further experiments are enclosed in red squares. **(C)** The mean of titers obtained from the 11 oligoclonal populations that produced vectors at detectable titers following co-transfection with pCflpe and pFBCF was compared to the mean of titers obtained from the 5 oligoclonal populations tested following transfection with pFBCF alone. The horizontal solid lines represent mean titers and the whiskers represent the range of titers.

Table 4.1. Fluorescence phenotype of cell populations isolated following co-transfection of WinRD-F1 cells with pCflpe and pFBCF.

Fluorescence phenotype	Number of oligoclonal populations
mCherry+/GFP-	5
mCherry+/GFP- and mCherry-/GFP+	16
mCherry-/GFP+	1
mCherry-/GFP-	4
mCherry+/GFP+	0

For cells co-transfected with pCflpe + pFBCF, monoclonal populations where derived by limiting dilution (in 96-well plates) from each of three oligoclonal populations that had the highest titers and productivities (WinRD-F1-64/135/136). These clones were then analyzed by flowcytometry to confirm that they were mCherry+ and GFP- (Figure 4.5A). Vector-containing medium was also collected and titrated on 293T cells. The mean and range of titers were $4.5x10^5$ TU/ml and $1.4x10^4$ – $2.8x10^6$ TU/ml, respectively (Figure 4.5B). For monoclonal cell lines derived from the best performing population, WinRD-F1-64, the mean and range of the titers were $1.1x10^6$ TU/ml and $2.5x10^5$ – $2.8x10^6$ TU/ml, respectively.

A.

WinRD-F1R subclone	% GFP+	% mCherry+
C-G5E	0.91	69.4
B-G9C	0.49	87.7
A-D4C	1.44	86.0
A-C4G	1.08	87.2
A-B8B	0.58	77.5
293FT	0.15	3.28

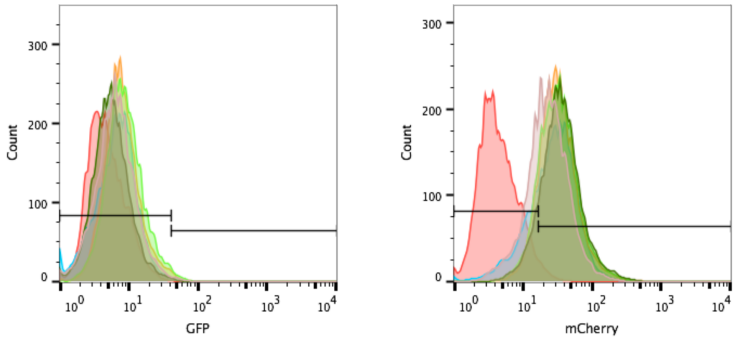

B.

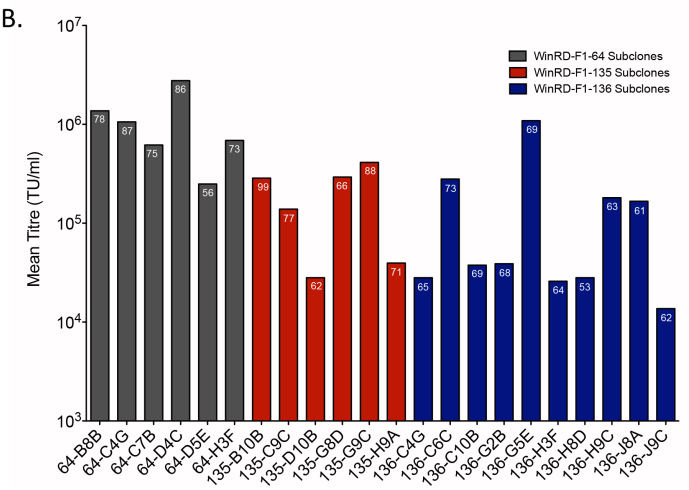

Figure 4.5. Isolation of high-titer monoclonal producer cell lines.

(A) Representative fluorescence phenotype of monoclonal cell lines derived from three oligoclonal populations (WinRD-F1-64/135/136). **(B)** Mean titers of monoclonal cell lines derived from three oligoclonal populations (WinRD-F1-64, 135 and 136). Data shown reperesents mean titers were calculated from duplicates.

Undiluted as well as two five-fold dilutions were used in the titration experiments. It was noted that when 250µl of undiluted VCM was used to transduce target cells in a total volume of 500µl only a small increase in percentage of transduced cells was seen (Figure 4.6A). This was unexpected since it wasn't seen when transiently produced VSV-G or RDpro pseudotyped vectors (VSV-G LV or RDpro LV) nor when vectors produced stably by WinPac-RD-HV cells (see Chapter 3) were titrated on 293T cells (Figure 4.6A).

Analysis of SSC vs. FSC flowcytometry data analysis showed a similar profile for cells transduced with diluted and undiluted VCM, which was also similar to that for untransduced control 293T cells (Figure 4.6B). This suggests that this phenomenon is unlikely to be due to cytotoxicity when cells were transduced using the undiluted VCM. Another possible explanation is the presence of an inhibitor in the VCM. Such an inhibitor could represent either free RDpro envelope or enveloped but empty vector particles (Figure 4.6A). This phenomenon was noted in all populations derived from WinRD-F1 cells and might be due to a suboptimal ratio of the various vector components in this clone. To test this hypothesis, I plan to initially determine whether this inhibition is RDpro env-dependent or not. This will be done by transducing 293T cells with undiluted VCM from WinRD-F1-derived clones in the presence of GFP-expressing VSV-G- or RDpro-pseudotyped vectors. Transduction of the cells with VSV-G but not RDpro pseudotypes would suggest the presence of an envelope-dependent inhibitor in WinRD-F1-derived VCM. In that case, size-exclusion chromatography will be used to determine whether it is free RDpro env or empty particles. If free RDpro env is the inhibitor then the infectivity of the vectors should be restored following this purification step.

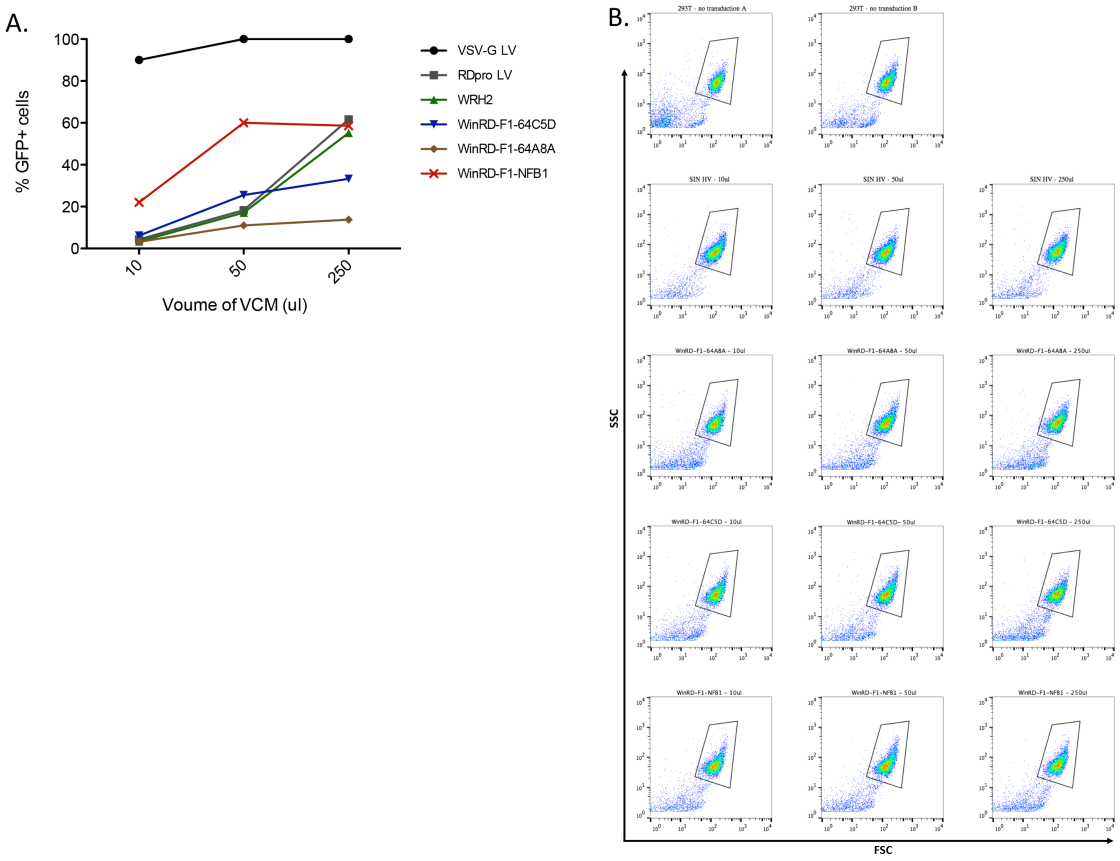

Figure 4.6. Inhibition of transduction with undiluted vector-containing medium (VCM).

(A) Percentage GFP+ (% GFP+) cells following transduction of 293T cells with equal volumes of each of the following vector preparations: VSV-G LV: transiently produced VSV-G-pseudotyped LV; RDpro LV: transiently produced RDpro-pseudotyped LV; WRH2: RDpro-pseudotyped LV stably produced by WinPac-RDpro-HV2 cells (Chapter 3); WinRD-F1-64C5D: RDpro-pseudotyped LV stably produced by WinRD-F1-64C5D cells; WinRD-F1-64A8A: RDpro-pseudotyped LV stably produced by WinRD-F1-64A8A cells; WinRD-F1-NFB1:RDpro-pseudotyped LV stably produced by WinRD-F1-NFB1 cells. $6x10^5$ cells were transduced with a total volume of 500ul at transduction. **(B)** FACS plots of SSC (y-axis) against FSC (x-axis) for cells transduced with various dilutions of VCM of the viral preparations.

4.3.3 Analysing RMCE and random integration events: Nested PCR

In cells co-transfected with pCflpe + pFBCF, loss of GFP expression coupled with the gain of mCherry expression could represent any of three possible outcomes:

1. Excision of the GFP cassette and random integration of the donor plasmid.
2. Successful recombination reaction involving excision of the GFP cassette and insertion of the donor cassette at the tagged locus.
3. Successful recombination reaction as well as random integration of the donor plasmid.

Therefore, nested PCR assays were designed to detect excision/recombination events as well as random integration events in the high-titer monoclonal populations (Table 4.2; Figure 4.7A). These PCRs have been optimized and are currently being performed on the best-preforming clones. The nested PCR assay amplifying eGFP is shown in Figure 4.7B confirming the presence of the eGFP gene in WinRD-F1 and WinRD-F1-NF consistent with the flowcytometry data (Figure 4.5A and 4.6A).

Table 4.2. Interpretation of possible results of PCR assays.

Target	RMCE	Random Integration	RMCE + Random Integration
GFP	-	+/-	-
mCherry	+	+	+
US recombinant	+	-	+
DS recombinant	+	-	+
US backbone	-	+	+
DS backbone	-	+	+

US, upstream; DS, downstream; RMCE, recombination mediated cassette exchange

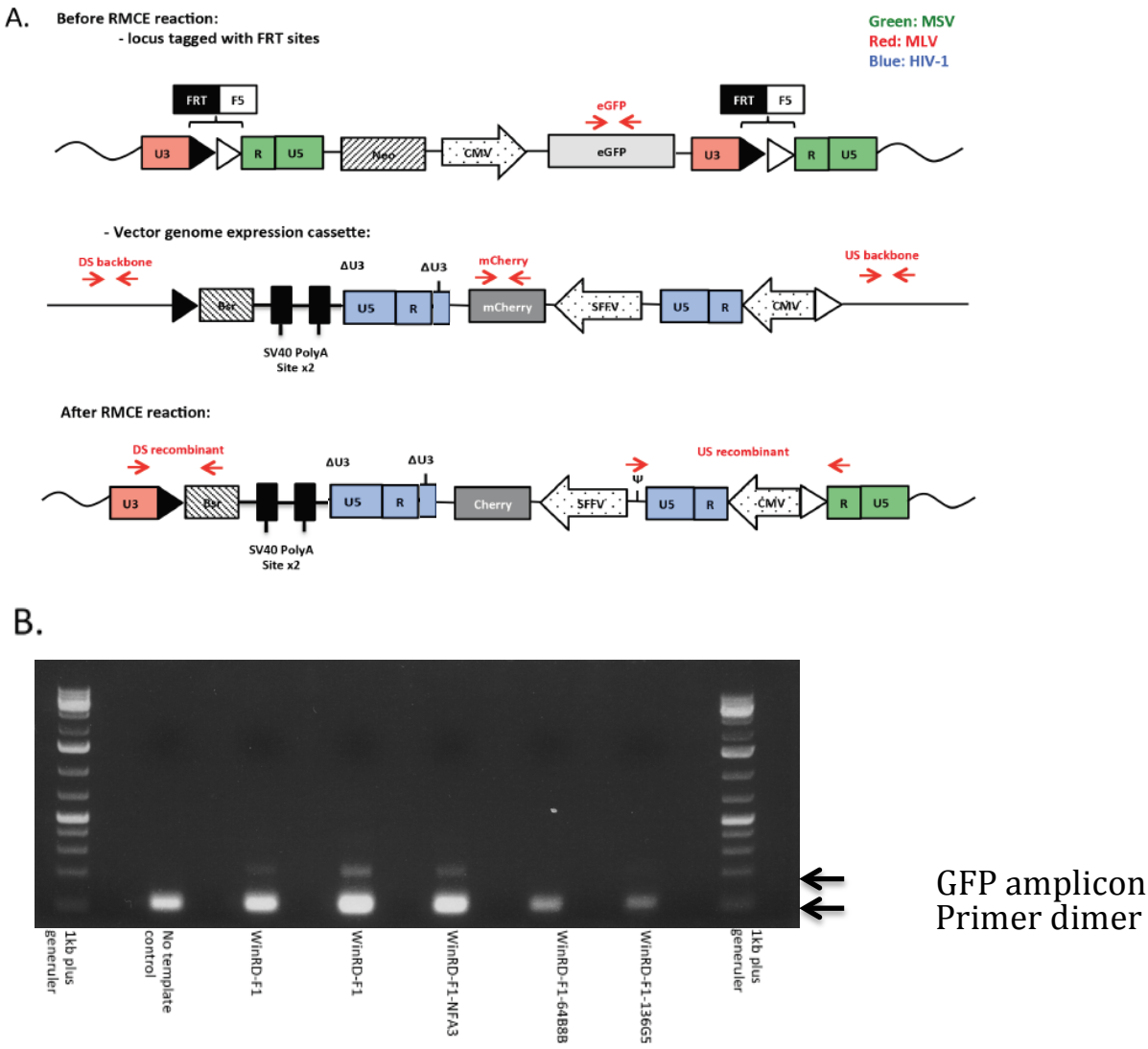

Figure 4.7. PCR assays to detect successful recombination events and random integration events.

(A) Schematic representation of the primer pairs used for the PCR assays for various targets in the tagged locus and donor plasmid. **(B)** Initial PCR assay for the detection of the GFP marker gene.

4.4 Discussion

In this chapter a master PCL with a FRT/F5 tagged locus (WinRD-F1) was generated. This locus can be targeted to allow the expression of SIN LV genomes at levels sufficient for high titer vector production. This was exemplified by the generation of producer cells for a model mCherry-expressing SIN LV. The use of retroviral tagging followed by Flpe-RMCE facilitated the attainment of two desirable goals:

1. Efficient marking of a transcriptionally active site: this is achieved by exploiting the intrinsic ability of GRVs to preferentially integrate at such sites (Bushman et al., 2005).

2. Minimizing foreign GRV-derived sequences: only partial LTR sequences remain in our producer cell lines (Figure 4.3A)

Our RMCE strategy was originally designed to allow efficient exchange and stable donor cassette integration. This was done by using heterospecific twin FRT sites (FRT and F5 sites) cloned in tandem in the U3 region of the 3'LTR of the gammaretroviral vector. During reverse transcription the twin sites are copied to 5' LTR resulting in an integrated proviral DNA with the following configuration: FRT/F5-reporter-FRT/F5. The heterospecific sites can efficiently recombine with self (FRTxFRT and F5xF5) but have minimal cross-interaction (FRTxF5). Thus, after successful recombination, the donor cassette at the tagged locus (FRT-donor cassette-F5 sites) becomes stably integrated and inefficiently excised by Flpe recombinase (Figure 4.2 and Figure 4.3A). This drives the reversible recombination reaction in the direction of exchanging the donor cassette for the tagging cassette.

However, this needs further confirmation to ensure that the excision and insertion reactions were efficiently coupled resulting in insertion of the SIN LV expression cassette at the FRT/F5 tagged locus. The PCR analysis described in Section 4.3.3 was designed to test that. This is currently being finalized although this cell line will not be used for further generation of producer cell lines. This is because the work presented in this chapter highlighted two important issues that need to be addressed in order to improve the practicality and efficiency of the RMCE-based strategy used:

1. Extensive testing and characterization of the target locus in the master packaging cell line to ensure favorable transcriptional characteristics:

Although the tagged site in WinRD-F1 cells allowed us to generate high-titer producer cell lines, our data suggests that alternative loci might offer a more favorable transcriptional activity since cells transfected with pFCBF alone supported vector production at similar or higher titers (Figure 4.4D). One way to overcome this issue is by targeting pre-characterized sites that have been shown to possess an open chromatin configuration using state of the art gene editing technologies like CRISPR/Cas9 and/or TALENs (see Section 6.4.1). This would also allow us to avoid introducing exogenous retroviral sequences into our producer cell lines.

2. Efficient selection for successful recombination events:

   Transfection of the donor plasmid (pFBCF) alone into WinRD-F1 cells gave rise to Blasticidin-resistant cells likely through expression of the Bsr gene from a cellular promoter in the proximity of the plasmid integration site. Therefore, a more stringent way to select successful recombination events is needed in order to reduce the background gain of resistance in the absence of the recombinase enzyme and make the screening for high-titer producers more practical. This could be further simplified by eliminating cells with unwanted random integration of the donor plasmid which might occur even in cells undergoing successful recombination. This requires modifications to be made to the design of the tagging and donor constructs (see Section 6.2).

Additionally, we are attempting to exploit the design of pFBCF; wherein a promoterless selectable marker (such as the Bsr gene) is placed *in cis* with the SIN LV expression cassette. This configuration offers a simple means of deriving high-titer producer cell lines by stable transfection of a single plasmid. We are currently using this strategy to generate producer cell lines for therapeutic vectors designed to treat patients suffering from X-linked Severe Combined Immunodeficiency (SCID-X1) caused by mutations affecting the common cytokine receptor gamma chain (also known as the interleukin-2 receptor subunit gamma or IL-2RG). This is a particularly promising target for SIN LV-mediated gene therapy since previous clinical trials using GRVs with full-length LTRs showed clinical efficacy but were complicated by a high incidence of malignant transformation of transduced cells (Gaspar et al., 2011a; Hacein-Bey-Abina et al., 2010). The design and construction of the plasmids used are detailed in Sections 2.1.11.3 and 2.1.11.4.

Plans to further characterize the producer cell lines generated in this chapter included cloning the integration site of the tagging vectors in WinRD-F1 cells and performing Q-PCR and RT-Q-PCR assays to examine DNA copy numbers and RNA expression levels of the various components. However, these plans have been postponed since we believe this work has elucidated important issues that need to be addressed in order to develop a reliable method that allows quick and reproducible generation of high-titer producer cell lines from WinPac-derived master packaging cell lines.

CHAPTER

5

Generation of a Packaging Cell Line with an Alternative Pseudotyping Envelope Glycoprotein

5 Generation of a packaging cell line with an alternative pseudotyping envelope glycoprotein

5.1 Introduction

5.1.1 Rhabdoviral G-proteins for pseudotyping lentiviral vectors

Pseudotyping refers to the incorporation of the surface glycoproteins of one virus into the envelope membrane of another. This phenomenon was initially described in cells simultaneously infected with two viruses resulting in the formation of phenotypically mixed particles or pseudotypes (Weiss et al., 1977; Zavada, 1982). Pseudotyping has been exploited for a variety of applications including modifying the tropism of LVs (reviewed in (Cronin et al., 2005)). The choice of envelope glycoprotein utilized would determine important characteristics of a particular LV pseudotype including its tropism, physical stability and sensitivity to serum complement proteins. The glycoprotein (G) of vesicular stomatitis virus (VSV-G)* is the glycoprotein most commonly used to pseudotype LVs for experimental and clinical applications (Naldini et al., 1996; Reiser et al., 1996). VSV-G-pseudotyped LVs can be produced at high-titers and their physical stability allows for their concentration by ultracentrifugation. They can also transduce a wide range of cell types including important gene therapy targets like hematopeitic stem cells and T cells. However, VSV-G LVs are sensitive to human serum which precludes their use for *in vivo* applications (DePolo et al., 2000). In addition to that, VSV-G is cytotoxic (Hoffmann et al., 2010) and cannot be constitutively expressed in packaging cell lines (Yee et al., 1994). This led some investigators to use inducible promoters to drive the expression of this envelope glycoprotein (Stewart et al., 2011; Throm et al., 2009; Yang et al., 1995).

Since we aimed to develop a PCL that can support the continuous production of LVs, we initially adopted an RD114-derived envelope glycoprotein (RDpro) that can be

---

** It should be noted that the VSV-G used in most gene therapy applications is the G protein of the Indiana serotype (VSIV-G), but it has been conventionally referred to simply as VSV-G. This convention has been followed in this chapter but the distinction between the G protein of the Indiana (VSIV-G) (Rose and Gallione, 1981) and New Jersey (VSNJV-G) (Rose and Gallione, 1983) serotypes will be made clear when needed.*

constitutively expressed in PCLs (Ikeda et al., 2003a). These efforts lead to the generation of the WinPac-RDpro cell line (see Chapter 3 for details). Although RDpro-pseudotyped LVs could efficiently transduce important gene therapy target cell types, they were difficult to concentrate and purify likely due to reduced physical stability compared to VSV-G LVs. To overcome this obstacle, we attempted to optimize scalable concentration and purification protocols to achieve high recovery of input vectors (see Section 3.3.5 for details). An alternative approach involved investigating the use of other surface glycoproteins that would impart favorable characteristics to LV pseudotypes while allowing continuous, high-titer production using PCLs. Among a panel of glycoproteins tested in our lab, the glycoprotein (G) of Cocal Virus (COCV-G) was particularly promising (Ferraresso, 2014).

Similar to VSV, Cocal virus (COCV) is a rhabdovirus that belongs to the genus Vesiculovirus. Vesiculoviruses have been divided into two major serotypes: New Jersey (VSNJV) and Indiana (VSIV), which are further divided into subtypes. COCV is the prototype virus of the VSIV 2 subtype and was originally isolated from mites collected from rice rats in Trinidad. It was later isolated from cattle, horses, and insects in Trinidad, Brazil and Argentina. Infection with COCV can cause vesicular stomatitis in cattle and a flu-like illness in humans (Pauszek et al., 2008). Like other vesiculoviruses its (-)ssRNA genome encodes 5 proteins: nucleoprotein (N), phosphoprotein (P), matrix protein (M), glycoprotein (G) and polymerase (L). The G protein is on the surface of the particle and mediates pH-dependent cell entry via receptor binding and membrane fusion (Albertini et al., 2012a).

In a transient production system, the G protein of COCV (COCV-G) could efficiently pseudotype LVs resulting in high titer vector production (in the order of 10^7 TU/ml). These pseudotypes could be concentrated via low speed ultracentrifugation with recoveries exceeding 50%, which was comparable to that obtained with VSV-G LVs. COCV-G LVs had a broad tropism as they could efficiently transduce a panel of cell lines of various origins as well as human, primate and dog hematopoietic progenitor cells. Compared to VSV-G LVs, these pseudotypes were found to be relatively more resistant to human and dog serum, which is important for *in vivo* applications (Trobridge et al., 2010). The generation of a PCL that is capable of continuously producing LV pseudotypes with these favorable characteristics would facilitate affordable large-scale vector production. This would greatly improve the clinical applicability of LVs and would

help propel the field of LV-mediated gene therapy forward (Matrai et al., 2010; Thrasher, 2013).

Since COCV-G is closely related to VSV-G with a high degree of amino acid sequence homology (Bhella et al., 1998), it likely posses a pH-dependent fusogenic activity that is mediates rhabdoviral entry into target cells following endocytosis (Albertini et al., 2012a). Since the fusogenic activity of VSV-G, is hypothesized to be the major contributor to its cytotoxicity (Hoffmann et al., 2010), it is possible that COCV-G might be similarly cytotoxic precluding its preclude its constitutive expression at levels sufficient for high-titer vector production.

However, it has been shown that single amino acid substitutions in VSV-G can affect its pH-dependent activity (summarized in (Roche et al., 2008) and (Sun et al., 2008)). Also, the G proteins of various rhabdoviruses show phenotypic differences in pH-dependent fusogenicity and infectivity (Martinez and Wertz, 2005; Steffen et al., 2013). Thus, it is plausible that COCV-G might have a different pH threshold and optimal pH levels compared to VSV-G. A G protein whose fusogenic activity is triggered at a sufficiently low pH threshold might be expected to be amenable to constitutive expression in mammalian cell lines since the pH under normal cell culture conditions is usually maintained above 6.3 (Naciri et al., 2008). Although the pH threshold for the induction of fusion by VSV-G is around 6.3, residual activity could be detected at higher pH levels up to 6.6 in cell-to-cell fusion assays (Ferlin et al., 2014; Sun et al., 2008) and up to 6.5 in virus-to-liposome fusion assay (Libersou et al., 2010). This might explain why it has been challenging to constitutively express VSV-G in PCLs at levels sufficient for high titer vector production without incurring deleterious cytotoxic effects (Ikeda et al., 2003a; Yee et al., 1994).

A review of the literature did not reveal a detailed analysis of the COCV-G pH-dependent fusogenic activity. However, it has been reported that cell-to-cell fusion could be readily detected when COS cells expressing COCV-G were exposed to a buffer at pH 5.6, whereas no significant cell fusion was reported in the absence of acid exposure (Bhella et al., 1998).

In light of the above considerations, the remainder of the introduction of this chapter will address the current knowledge of the structure and properties of rhabdoviral G proteins with an emphasis on their pH-dependent fusogenic activity.

5.1.2 Rhabdoviruses

5.1.2.1 Introduction: Classification, genome organization and viral proteins

VSV and COCV both belong to the genus Vesiculovirus. The Vesiculovirus genus along with 5 other genera (including Lyssavirus genus) make up the family Rhabdoviridae family, which is classified in the order Mononegavirales (Albertini et al., 2012a).

Vesiculoviruses are enveloped ssRNA viruses with bullet shaped virions that are 100–430 nm long and 45–100 nm in diameter. They have a linear, single-stranded, negative-sense RNA genome encoding five structural genes in the following order (3' to 5'): Nucleoprotein (N)- Phosphoprotein (P)- Matrix protein (M)- Glycoprotein (G)- Large protein or RNA-dependent RNA polymerase (L).

The proteins N, P and L are associated with the RNA genome forming the ribonucleoprotein core (RNP), which, in turn, associates with the M protein into a helical structure (M-RNP) (Kuzmin et al., 2009). G protein is thought to contribute to the initiation of virus budding by organising in to G protein-enriched microdomains at the infected cell surface and inducing significant, localized curvature in the plasma membrane, which facilitates M–RNP interactions and the pulling of the plasma membrane around the budding virion (Jayakar et al., 2004).

Following viral budding and release, the G protein forms the spikes that protrude from the envelope of the bullet-shaped viral particles, and play a critical role during the early stages of infection by mediating pH-dependent cell entry (Kuzmin et al., 2009). It binds a specific receptor on target cells resulting in endocytosis. The decrease in pH in the early endosomal compartment induces conformational changes in the glycoprotein G that lead to fusion of the viral envelope with that of the target cells (Libersou et al., 2010; Mire et al., 2010; Sieczkarski and Whittaker, 2003).

5.1.2.2 Rhabdoviral G proteins

The G proteins of VSV (prototype of vesiculoviruses) and Rabies Virus (RABV, prototype of lyssa viruses) have been extensively studied. These two G proteins bear a high degree of structural and functional similarity that is likely to be shared with other rhabdoviral G proteins (Albertini et al., 2012a; Sun et al., 2010). In accordance with that, a recent study that examined the structure and fusion function of Chandipura Virus G

protein (CHAV-G) has shown significant similarity between CHAV-G and VSV-G (Baquero et al., 2015).

5.1.2.2.1 Basic biochemical properties

The G protein is a type I membrane glycoprotein made up of around 500 amino acids†, and is divided into three major parts: the ectodomain, transmembrane domain and endodomain. It is synthesized in the endoplasmic reticulum (ER) where it undergoes N-linked glycosylation and folding. The G protein monomers assemble into trimers, which are transported to the cell membrane via the secretory exocytic pathway (Chen et al., 1998; Doms et al., 1987; Hirschberg et al., 1998). The trimeric structure is unstable at high pH and a dynamic equilibrium is thought to exist *in vitro* when in solution as well as *in vivo* in the ER (Zagouras et al., 1991).

5.1.2.2.2 G protein conformational states

Based on analysis of the fusion kinetics of VSV-G and RABV-G (studied using spectrophotometric assays that detect dequenching of fluorophores after fusion of viral particles with target membranes/ liposomes), a model was proposed whereby the G protein exists in 3 distinct conformations: the native (N), pre-fusion or high-pH conformation; the active (A) conformation; and inactive (I), post-fusion or low-pH conformation (Figure 5.1).

---

† It should be noted that the amino acid sequence of the full-length G proteins (including the signal peptide) were referred to in this chapter. Accordingly, reference to specific residue numbers is made in the context of these full-length sequences.

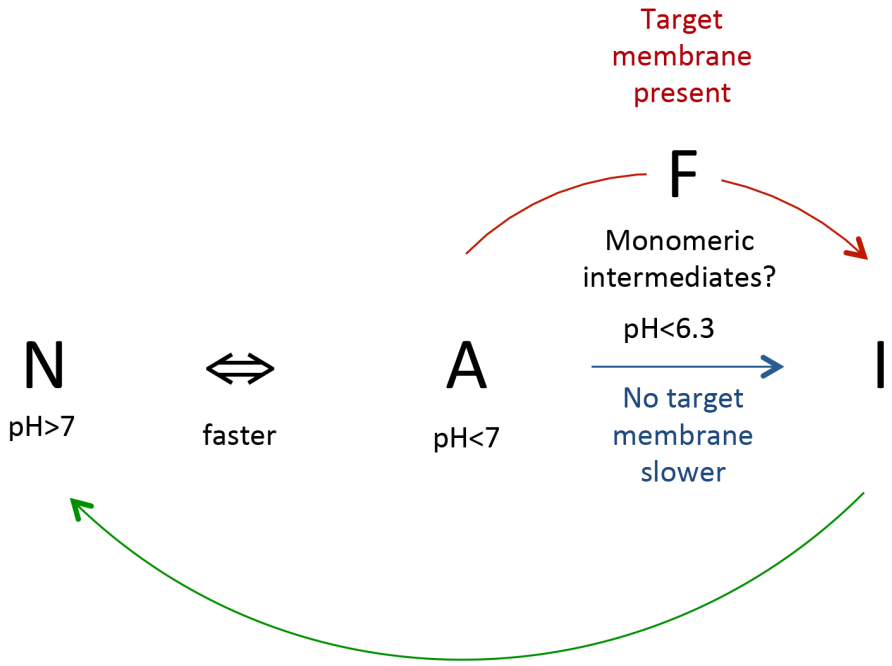

Figure 5.1. Proposed model for equilibrium between the conformational states of VSV-G.

pH values shown indicate the pH at which the different states are most prevalent. The transition between different states likely involves multiple intermediate conformations. The fusion complex (F) is thought to consist of multiple co-operating VSV-G units. N: Native (pre-fusion/high pH), A: Active, F : Fusion complex, I: Inactive (post-fusion/low pH).

These states are hypothesized to exist in a pH-dependent equilibrium (Figure 5.1) that shifts toward the I conformation at low pH (for VSV-G: (Clague et al., 1990; Pak et al., 1997); for RABV-G: (Roche and Gaudin, 2002)). The N conformation is detected at infected cell and viral surfaces at pH above 7 and is thought to mediate target receptor recognition (Libersou et al., 2010). At more acidic pH, the A conformation is hypothesized to mediate the early stages of membrane fusion as it exposes the hydrophobic bipartite fusion loops to the target membrane (for VSV-G and RABV-G: (Pak et al., 1997), for RABV-G: (Durrer et al., 1995)). Under longer incubation periods in

acidic pH and in the absence of a target membrane, the G protein assumes the I state and is unable to mediate fusion. However, this inactivation is completely reversible if pH is raised back to a pH higher than 7 (VSV-G and RABV-G: (Clague et al., 1990), RABV-G: (Roche and Gaudin, 2002)). The I conformation is thought to be the state in which the newly synthesized G protein is transported to the cell membrane through the acidic environment of the golgi network to avoid undesirable fusion (Gaudin et al., 1995). This state is biochemically (more sensitive to proteases) and morphologically (under electron microscopy) distinct from the N state (Gaudin et al., 1995; Libersou et al., 2010). It is also antigenically distinct, at least for RABV-G (Gaudin et al., 1993). Moreover, the kinetics of the conformational transitions from N to A and from N to I seem to be distinct (Gaudin et al., 1995).

For VSV-G, hydrophobic photolabeling experiments have estimated the pH threshold for fusion induction to be around 6.2-6.3 and no fusion was detected at pH 6.6 (Durrer et al., 1995; Pak et al., 1997). In cell-to-cell fusion assays, a similar threshold was reported but minimal fusogenic activity was detectable at pH 6.6 (293T cell-based assay (Sun et al., 2008), BSR cell-based assay (Ferlin et al., 2014)).

It has been hypothesized that multiple VSV-G units would be needed for fusion to occur since the energy barrier for the fusion reaction likely exceeds the energy released by the reversible conformational transition of the G protein (Roche et al., 2008). Consistent with this, around 15 VSV-G monomers (or 5 trimers) have been estimated to make up a VSV functional fusion unit based on its size (Bundo-Morita et al., 1988).

5.1.2.2.3 G protein structure

Recently, the trimeric crystal structures of the majority of the ectodomain of Vesicular Stomatitis Indiana Virus (VSIV)-G in the N and I states have been elucidated by x-ray crystallography (Roche et al., 2006; Roche et al., 2007), whereas that of the A state remains elusive. Although VSV-G shared some features with class I and class II fusion proteins, it has been classified in a novel class of fusion proteins (class III; reviewed in (Backovic and Jardetzky, 2009)) on the basis of their structural architecture and the reversibility of their conformational changes (Roche et al., 2008; Steven and Spear, 2006).

5.1.2.2.3.1 Crystal structure of the G protein ectodomain

In both structures (N and I), four distinct domains were identified within the ectodomain (Figure 5.2, Table 5.1) (Roche et al., 2006; Roche et al., 2007). Domain IV is the only domain made of a single continuous segment, and is inserted into domain III, which is, in turn, inserted into domain II. A brief description of each of these domains follows:

- Domain I (DI) or lateral domain:

It is made up of around 90 amino acid residues in two discontinuous segments and is organized into multiple β-sheets. An epitope has been reported in this domain (Vandepol et al., 1986).

- Domain II (DII) or trimerization domain:

It is made up of around 90 amino acids in three discontinuous segments that are organized into four α-helices. It is involved in forming the so-called central 'six-helix bundle' in the trimeric N conformation.

- Domain III (DIII) or pleckstrin homology (PH) domain:

It is made up of around 90 amino acids that are located in two discontinuous segments (Figure 5.2C). It is organized into two β-sheets and two α-helices, and contains the fold of a pleckstrin homology (PH) domain. Multiple epitopes have been reported in this domain (Vandepol et al., 1986), which is thought to be the major target of neutralizing antibodies. This is consistent with the fact that it is most exposed domain in the N conformation (Figure 5.2B). It is also the most divergent domain among vesiculoviruses, which might reflect the effect of host-pathogen interactions (Baquero et al., 2015). Moreover, since it is situated at the top of the N conformation, it might be involved in receptor recognition.

- Domain IV (DIV) or fusion domain:

It is made up of around 130 amino acids, and has two hydrophobic fusion loops that are able to interact with target membranes. The two loops lie next to each other at one end of an elongated structure formed by extended β-strands. At the other end, of this structure is a so-called 'β-barrel' made up of six β-strands with a

highly conserved amino acid sequence. Multiple disulfide bonds help stabilize the complex structure of this domain.

- C-terminal region (C-ter):

Only part of the C-terminal region of the ectodomain (i.e the membrane proximal region) was included in these crystal structures and it's exact structural organization remains unknown.

The trimeric N conformation resembles a tripod. Each leg consists of the fusion domain whose fusion loops are pointing towards the viral membrane (Figure 5.2A). The trimeric I conformation, on the other hand, resembles a hairpin with the fusion loops pointing towards the viral membrane and a central six helix bundle stabilizing the trimer (Figure 5.2B). The transition from the N to the I state is thought to occur around a rigid block consisting of the lateral domain and a part of the trimerization domain (RbI-II). During this transition, the fusion domain is thought to move away from the viral membrane and towards the target membrane resulting in a postulated extended intermediate (Roche et al., 2008; Roche et al., 2006; Roche et al., 2007). There is evidence for the involvement of monomeric forms in this transition (Albertini et al., 2012b; Baquero et al., 2013).

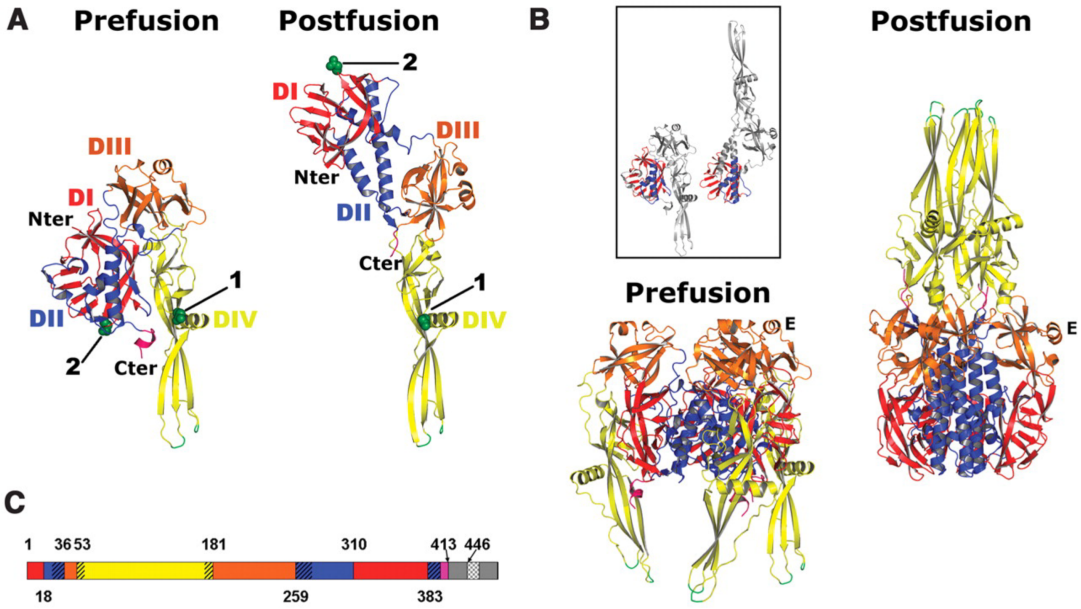

Figure 5.2. Overall structure of VSV-G in pre- (N) and post-fusion (I) conformations.

(A) View of the VSV-G protomers (consisting of residues 1 to 422 generated by limited proteolysis of virions with thermolysin) superimposed on their fusion domains (DIV) and colored by domain (I: red; II: blue; III: orange; IV: yellow) with the fusion loops in green. The two glycosylated asparagines (N163 (labeled "1") and N320 (labeled "2")) are displayed as dark green spheres. The fusion domains (yellow in figure) point towards the viral membrane in the pre- and post-fusion conformations. **(B)** View of the VSV-G trimers, colored by domains as in (A). The trimers were superimposed on the rigid blocks made of DI and the invariant part of DII (RbI-II; highlighted in the boxed inset for one protomer of each conformation). **(C)** Domain architecture of VSV G plotted on a linear diagram, color-coded as in (A) with domain boundaries numbered. The unobserved C-terminal segment is in gray, with a checkerboard pattern for the TM domain. The regions that refold in the transition are hatched. All structural figures were generated with PyMOL. Nter, N-terminus; Cter, C-terminus.

From (Roche S, Rey FA, Gaudin Y, Bressanelli S. 2007. Structure of the prefusion form of the vesicular stomatitis virus glycoprotein G. Science 315:843-848). Reprinted with permission from AAAS.

5.1.2.2.3.2 pH sensing mechanism: insights from crystal structure

A group of conserved histidine residues located in the fusion domain and membrane proximal region (H76, H178, H423) cluster together in the N conformation of VSV-G and is thought to act as a 'pH-sensing molecular switch'. At high pH, hydrogen bonds between these residues may help stabilize the pre-fusion conformation. When these residues are protonated at acidic pH levels, the repulsive forces that arise are thought to destabilize the interaction between the fusion domain and the membrane proximal region. This would then trigger the movement of the fusion domain away from the viral membrane and towards the target membrane (A conformation).

In the I conformation, a group of acidic amino acids (D274, D290, E292, D409, D411) are thought to cluster together at the 'six-helix bundle'. Under acidic conditions the hydrogen bonds that form between these residues help stabilize the I conformation. However, when they get deprotonated at higher pH levels, the resulting repulsive forces destabilize the structure and trigger the conformational transition into the N state (Roche et al., 2006).

5.1.2.2.3.3 Comparison to CHAV-G: functional and structural similarities

Chandipura Virus (CHAV) is a vesiculovirus whose G protein shares 40% amino acid sequence identity (65% similarity) with VSV-G. A recent report investigated the fusion activity of CHAV-G and revealed its crystal structure in the trimeric I conformation (Baquero et al., 2015). CHAV-G showed a pH-dependent fusion activity that was induced at a lower pH threshold compared to VSV-G in a cell-cell fusion assay. A liposome floatation assay also showed that CHAV-G reversibly interacted with the liposomal membranes at low pH.

Importantly, the crystal structure of Chandipura Virus G protein (CHAV-G) in the I conformation showed similar domain orientation as that seen in VSV-G. Moreover, a group of acidic residues clustered together in the I conformation of CHAV-G and are thought to act as the putative pH-sensing molecular switch similar to that in found in VSV-G. However, some of the residues implicated in this pH sensor where located at different positions in the two G proteins. All these structural and functional similarities between the two G proteins suggest key features of G proteins are highly conserved at least among vesiculoviruses.

5.1.2.2.4 Effects of mutations on fusogenic activity of the G protein

Before the crystal structure of VSV-G was discovered, early studies employed mutational analyses to identify the sequences important for its fusogenic activity. An early study showed that 3 amino acid insertions positioned in two highly conserved regions of the ectodomain significantly impaired fusion: one in a putative fusion peptide (residues 117-137) and another in the membrane proximal region (residues: 395-418) (Li et al., 1993). A region encompassing the putative fusion peptide was later implicated in mediating fusion in hydrophobic labeling experiments (Durrer et al., 1995; Pak et al., 1997). The importance of both regions for membrane fusion was further confirmed by analyzing the fusogenic activity of mutants with a single amino acid substitution in the fusion domain (Fredericksen and Whitt, 1995; Zhang and Ghosh, 1994) or membrane proximal region: (Jeetendra et al., 2003; Shokralla et al., 1998) as well as (Shokralla et al., 1999) amino acid substitutions.

When tested in cell-to-cell fusion assays, several of these mutants exhibited lower pH thresholds and optimum pH levels for fusion compared to wild-type VSV-G. However, compared to wild-type VSV-G, they exhibited reduced fusogenicity in cell-to-cell fusion assays even at optimal pH levels despite having similar surface expression levels (Jeetendra et al., 2003; Shokralla et al., 1998; Zhang and Ghosh, 1994). In infection assays, the mutants tested had reduced infectivity despite similar levels of incorporation into virions (Fredericksen and Whitt, 1996; Jeetendra et al., 2003). When two of these mutants (D137L and E139L) were compared to wild-type VSV-G in *in vitro* growth assays using recombinant VSV, they also exhibited lower titers despite similar efficiencies of incorporation into virions. This was hypothesized to be due to reduced infectivity secondary to reduced fusogenic activity (measured using a fluorophore dequenching assay at a pH range of 5.8-6.3) since the their ability to bind to target cells at a near-physiologic pH 7.0 was similar to that of wild-type VSV-G. The reduction in infectivity was also confirmed by a similar reduction in viral RNA synthesis in target cells (measured by the level of radioactive uridine incorporated into viral RNA). Additionally, these mutants were more sensitive to chloroquine, which can raise the pH of endosomal compartments in a concentration-dependent manner. This may reflect a need for lower endosomal pH levels to induce fusion by the mutant G proteins. Additional adverse effects on VSV uncoating and/or RNA synthesis due to fusion and release at an abnormal endosomal comportments, which might have contributed to the observed decrease in infectivity, could not be excluded in this study (Fredericksen and Whitt, 1998).

5.2 Aims

The aims of the work presented in this chapter were to:

1. Analyze the amino acid sequence of COCV-G in relation to that of other rhabdoviral G proteins that have characterized more thoroughly.

2. Generate monoclonal populations of WinPac-derived PCLs expressing COCV-G to test their potential to support continuous and stable vector production at high titers.

5.3 Results

5.3.1 Sequence and phylogenetic analysis of COCV-G

Phylogenetic analysis of the amino acid sequences of the G protein of COCV and other Rhabdoviruses showed that it is closely related to VSIV-G (Figure 5.3) as previously reported (Bhella et al., 1998; Pauszek et al., 2008; Pauszek et al., 2011).

A multiple-sequence alignment for the amino acid sequence of COCV-G and G proteins of other rhabdoviruses is shown in Figure 5.4. This highlighted the structural similarities between these viral glycoproteins that were more pronounced among vesiculoviruses. These include the N-terminal signal peptide (Kotwal et al., 1983), two bipartite fusion loop motifs (WY: 89/90 and YA:133/134) and two consensus sites for N-linked glycosylation (positions: 180 and 337) (Bhella et al., 1998). The four domains and membrane proximal region making up the ectodomain (Roche et al., 2006; Roche et al., 2007) were also arbitrarily identified (Table 5.1).

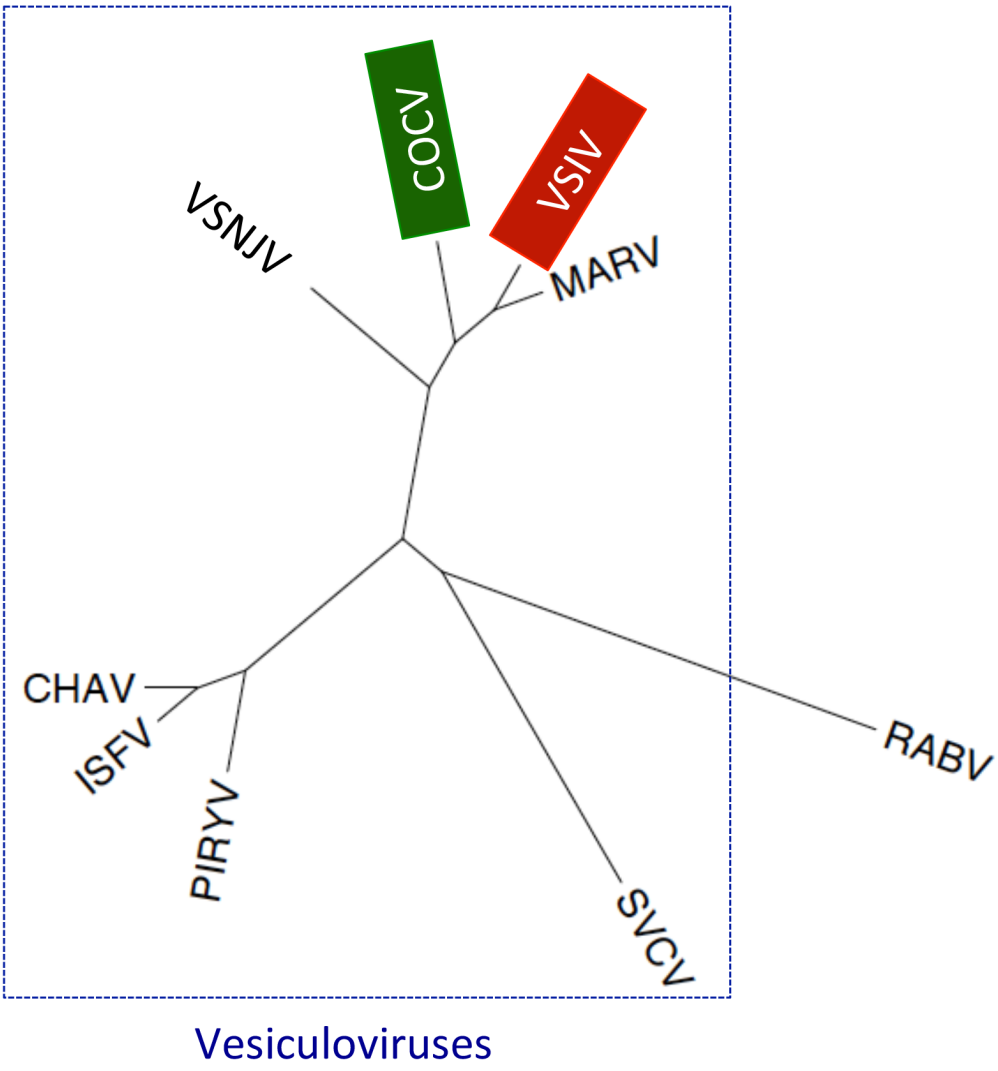

Figure 5.3. Phylogenetic relationship of vesiculoviruses and rabies virus based on G protein amino acid sequences.

G proteins of vesiculoviruses listed in Table 2.15 as well as the G protein of the Rabies Virus were included in the analysis. The BEAST v1.8.1 software (Drummond and Rambaut, 2007) was used to perform bayesian analysis of the amino acid sequences. The tree was visualized with FigTree v1.4.2. COCV, Cocal Virus, VSIV, Vesicular Stomatitis Indiana Virus; VSNJV, Vesicular Stomatitis New Jersey Virus; MARV, Maraba Virus; CHAV, Chandipura Virus; ISFV, Isfahan Virus; PIRYV, Piry Virus.

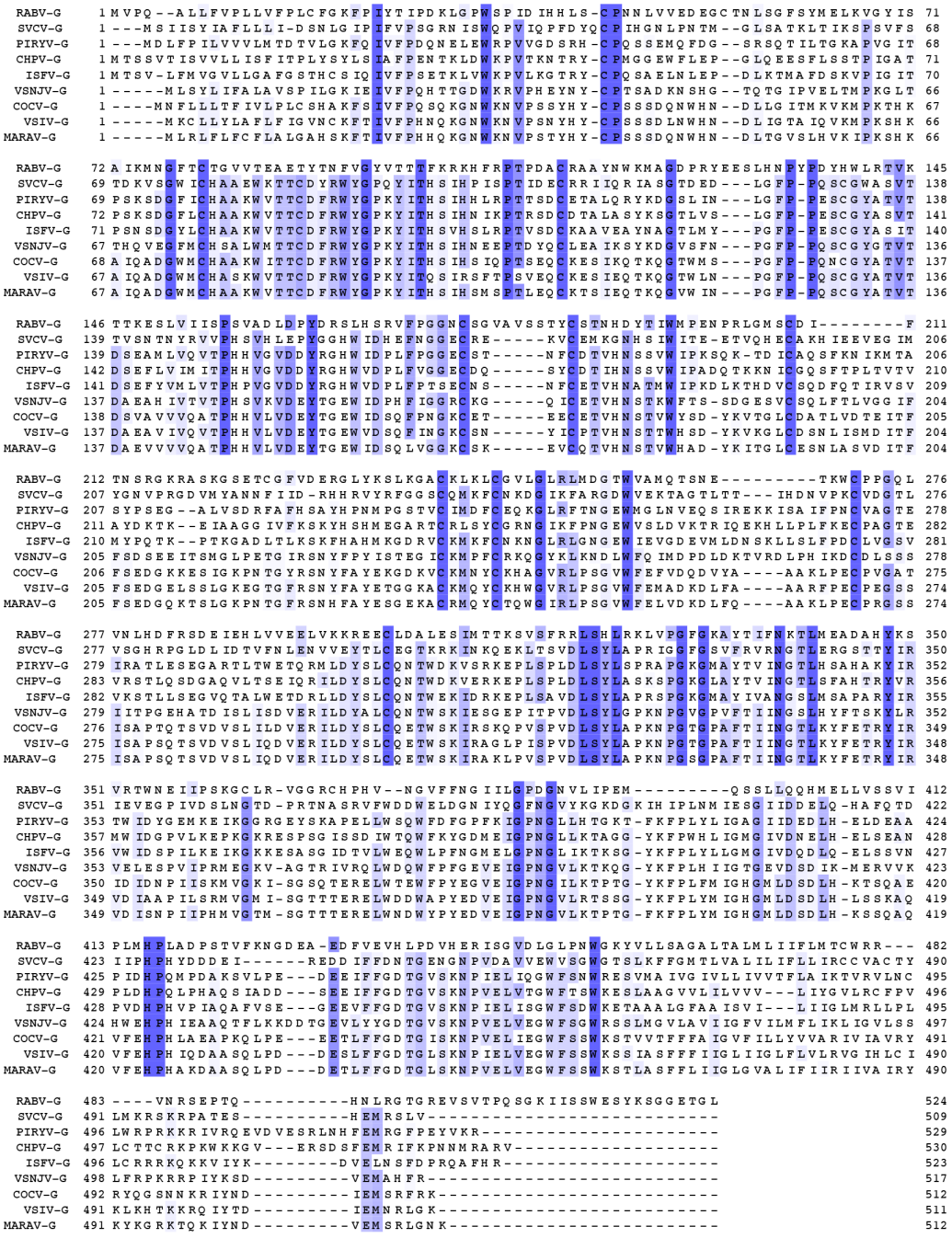

Figure 5.4. Multiple amino acid sequence alignment of the G protein of Cocal Virus with that of other vesiculoviruses and Rabies virus.

Blue shading indicates percent identity; dark blue: 80-100%, medium blue: 60-80%, light blue: 40-60%, and no color indicating <40% identity. Alignment was done using ClustalOmega online multiple sequence alignment tool (EMBL-EPI) and visualised using JalView (Waterhouse et al., 2009).

Table 5.1. Comparison of structural domains of COCV-G and VSIV-G

Domain/segment/peptide	aa residues in COCV-G	aa residues in VSIV-G (San Juan)	% aa sequence identity
Full length	1-512	1-511	71.62
Signal peptide	1-17	1-16	
Ectodomain	18-463	17-462	76.91
Domain I (Lateral)	18-34/ 327-399	17-33/ 326-398	78.89
Domain II (Trimerization)	35-52/ 276-326/ 400-422	34-51/ 275-325/ 399-421	85.87
Domain III (Pleckstrin Homology - PH)	53-63/ 198-275	52-62/ 197-274	65.71
Domain IV (fusion)	70-189	69-188	79.17
Membrane proximal segment	422-463	421-462	73.81
Transmembrane domain	464-483	463-482	45
Endodomain/cytoplasmic tail (C-terminus)	484-512	483-511	34.48

aa, amino acid

The sequences of these domains in COCV-G and VSIV-G (San Juan strain) were examined more closely and the degree of sequence homology between individual domains was determined. The fusion domain and C-terminal membrane-proximal region were of particular interest since they have been shown to be important for G-protein fusogenic activity, and single amino acid substitutions in these domains affected the fusogenic activity of G proteins and the pH at which it is induced (Fredericksen and Whitt, 1995; Roche et al., 2008; Zhang and Ghosh, 1994). Moreover, these domain contain the putative pH-sensing molecular switch consisting of a group of conserved histidine residues (H^{76}, H^{178}, H^{423}) that cluster together in the pre-fusion conformation of VSV-G ((Roche et al., 2007); Section: 5.1.2.2.3.2).

The percentage of sequence homology between VSV-G and COCV-G fusion domains and membrane proximal regions were 79.17% and 73.81%. Moreover, most of the mismatches were between amino acids with highly conserved properties. However, compared to VSV-G, the COCV-G fusion domain contains an extra Histidine residue (H97 replacing Q98 in VSV-G) and Lysine residue (K114 replacing E113 in VSV-G), which might contribute to the cluster of other conserved Histidine residues in the postulated pH-sensing mechanism. Unconserved mismatches in the fusion domain include Q103 and S106 (replacing T102 and V105 respectively in VSV-G). Both Q and S can form hydrogen bonds that might help stabilize the pre-fusion conformation unlike the hydrophobic T and V residues, which can only form weaker Van Der Waals interactions.

5.3.2 Stable expression of COCV-G in WinPac cells

To ensure optimal expression of the COCV-G, a codon-optimized COCV-G gene ((Trobridge et al., 2010); a kind gift from Dr. Hans-Peter Kiem) was chosen for stable expression in WinPac cells. Alignment of the wild-type ((Bhella et al., 1998); GenBank accession no. AF045556) and codon-optimized COCV-G nucleotide sequences is shown in Figure 5.5, and their codon adaptation indices (Carbone et al., 2003; Sharp and Li, 1987) were determined using CAIcal (Puigbo et al., 2008): 0.77 and 0.81 respectively.

```
COCVG           ATGAATTTTCTTCTCTTGACCTTTATCGTCCTTCCGCTCTGCAGTCACGCTAAATTTTCG
WTCVG           ATGAATTTCCTACTCTTGACATTTATTGTGTTGCCGTTGTGCAGCCACGCCAAGTTCTCC
                ******** ** ******** ***** **  * *** * ***** ***** ** ** **

COCVG           ATCGTCTTCCCACAGAGTCAGAAGGGCAATTGGAAGAATGTACCGAGTTCATATCATTAT
WTCVG           ATTGTATTCCCTCAAAGCCAAAAAGGCAATTGGAAGAATGTACCATCATCTTACCATTAC
                ** ** ***** ** ** ** ** ********************    ** ** *****

COCVG           TGTCCAAGCAGCTCTGATCAAAACTGGCATAACGACCTGCTGGGCATTACCATGAAGGTG
WTCVG           TGCCCTTCAAGTTCGGATCAAAACTGGCACAATGATTTGCTTGGAATCACAATGAAAGTC
                ** **    ** ** ************** ** **  **** ** ** ** ***** **

COCVG           AAAATGCCTAAGACACATAAGGCGATTCAGGCAGACGGGTGGATGTGCCACGCAGCCAAG
WTCVG           AAAATGCCCAAAACACACAAAGCTATTCAAGCAGACGGGTGGATGTGTCATGCTGCCAAA
                ******** ** ***** ** ** ***** ***************** ** ** *****

COCVG           TGGATTACAACTTGTGACTTCCGATGGTACGGTCCTAAGTATATTACTCACTCCATACAC
WTCVG           TGGATCACTACCTGTGACTTTCGCTGGTACGGACCCAAATACATCACTCACTCCATTCAT
                ***** ** ** ******** ** ******** ** ** ** ** *********** **

COCVG           AGCATCCAGCCCACCAGTGAGCAGTGCAAAGAGAGTATCAAGCAGACCAAGCAGGGAACC
WTCVG           TCCATCCAGCCTACTTCAGAGCAGTGTAAAGAAAGCATCAAGCAAACAAAACAAGGTACT
                  ********* **    ******** ***** ** ******** ** ** ** ** **

COCVG           TGGATGTCACCTGGCTTTCCACCTCAGAATTGTGGCTATGCAACAGTGACAGACTCAGTG
WTCVG           TGGATGAGTCCTGGCTTCCCTCCACAGAACTGCGGGTATGCAACAGTAACAGACTCTGTC
                ******   ******** ** ** ***** ** ** *********** ******** **

COCVG           GCTGTTGTGGTGCAGGCAACCCCCCACCACGTACTCGTTGACGAATATACAGGCGAATGG
WTCVG           GCTGTTGTCGTCCAAGCCACTCCTCATCATGTCTTGGTTGATGAATATACTGGAGAATGG
                ******** ** ** ** ** ** ** ** **  * ***** ******** ** ******

COCVG           ATTGACTCCCAGTTTCCCAACGGTAAATGCGAGACAGAAGAGTGCGAGACTGTGCACAAT
WTCVG           ATCGACTCTCAATTCCCCAACGGGAAATGTGAAACCGAAGAGTGCGAGACCGTCCACAAC
                ** ***** ** ** ******** ***** ** ** ************** ** *****

COCVG           TCAACAGTGTGGTACTCCGATTATAAGGTTACCGGGCTTTGCGACGCCACACTGGTGGAC
WTCVG           TCTACCGTATGGTACTCTGACTACAAAGTAACTGGATTATGTGACGCAACTCTGGTAGAC
                ** ** ** ******** ** ** ** ** ** **  * ** ***** ** ***** ***

COCVG           ACAGAGATAACGTTTTTTTCCGAAGACGGAAAAAAGGAAAGTATCGGGAAACCCAACACT
WTCVG           ACAGAGATCACCTTCTTCTCTGAAGATGGCAAAAAAGAATCTATCGGGAAGCCCAACACA
                ******** ** ** ** ** ***** ** ***** ***  ********* ********

COCVG           GGATACCGGAGCAATTACTTCGCGTATGAGAAAGGAGATAAGGTCTGCAAAATGAATTAT
WTCVG           GGCTATAGGAGCAACTACTTCGCTTATGAGAAAGGGGACAAAGTATGTAAAATGAACTAC
                ** **  ******* ******** *********** ** ** ** ** ******** **

COCVG           TGCAAACACGCCGGGGTAAGGCTGCCCTCCGGCGTGTGGTTTGAGTTCGTGGACCAGGAC
WTCVG           TGCAAGCATGCGGGTGTGAGGTTGCCTTCCGGGGTTTGGTTTGAGTTTGTGGATCAGGAT
                ***** ** ** ** ** *** **** ***** ** *********** ***** *****

COCVG           GTCTACGCAGCCGCCAAATTGCCCGAGTGTCCAGTGGGAGCTACAATTTCCGCACCGACA
WTCVG           GTCTACGCCGCCGCCAAACTTCCAGAATGCCCCGTTGGTGCCACTATCTCCGCTCCGACA
                ******** ********* * ** ** ** ** ** ** ** ** ** ***** ******

COCVG           CAAACCTCAGTGGATGTGTCTCTGATTCTGGACGTAGAGAGGATCCTCGACTACTCTTTG
WTCVG           CAGACCTCTGTTGACGTAAGTCTCATTCTAGATGTAGAGAGAATTTTAGATTACTCTCTG
                ** ***** ** ** **   *** ***** ** ******** **  * ** ****** **
```

(Figure 5.5. Nucleotide sequence alignment, continued)

```
COCVG           TGTCAGGAGACGTGGAGCAAGATACGGTCTAAGCAACCAGTCTCACCCGTAGATTTGAGC
WTCVG           TGTCAAGAGACATGGAGCAAGATCCGGTCCAAACAGCCAGTATCCCCTGTTGACCTTAGT
                ***** ***** *********** ***** ** ** ***** ** ** ** **  * **

COCVG           TACCTCGCCCCGAAAAACCCAGGCACGGGCCCAGCGTTCACGATCATCAACGGCACGCTT
WTCVG           TACTTGGCCCCCAAGAATCCTGGGACCGGACCGGCATTCACAATCATCAATGGCACTCTG
                *** * ***** ** ** ** ** ** ** ** ** ***** ******** ***** **

COCVG           AAATATTTCGAGACTCGCTATATCCGCATCGACATCGACAATCCTATCATCTCTAAGATG
WTCVG           AAGTACTTTGAGACCAGATACATTCGGATTGATATAGACAATCCAATCATCTCCAAGATG
                ** ** ** *****  * ** ** ** ** ** ** ******** ******** ******

COCVG           GTGGGTAAGATCTCTGGATCCCAGACTGAACGAGAACTGTGGACAGAATGGTTCCCCTAC
WTCVG           GTGGGGAAAATAAGTGGCAGTCAAACAGAACGAGAATTGTGGACAGAGTGGTTCCCCTAC
                ***** ** **   ***    ** ** ********* ********** ************

COCVG           GAGGGCGTCGAGATTGGCCCTAACGGAATACTGAAGACCCCTACCGGCTATAAGTTCCCT
WTCVG           GAGGGTGTCGAGATAGGGCCAAATGGGATTCTCAAAACCCCTACAGGATACAAATTCCCA
                ***** ******** ** ** ** ** ** ** ** ******** ** ** ** *****

COCVG           CTGTTTATGATCGGCCACGGAATGCTGGATTCTGATTTGCATAAGACTTCACAAGCAGAA
WTCVG           CTCTTCATGATAGGACACGGGATGCTAGATTCCGACTTGCACAAGACGTCCCAAGCAGAG
                ** ** ***** ** ***** ***** ***** ** ***** ***** ** ********

COCVG           GTCTTTGAACATCCTCACCTCGCCGAAGCACCTAAACAGTTGCCTGAGGAAGAGACCCTG
WTCVG           GTCTTTGAACATCCTCACCTTGCAGAAGCACCAAAGCAGTTGCCGGAGGAGGAGACTTTA
                ******************** ** ******** ** ******** ***** *****  *

COCVG           TTCTTCGGCGATACAGGTATATCCAAAAACCCGGTGGAGCTTATCGAAGGTTGGTTTAGC
WTCVG           TTTTTTGGTGACACAGGAATCTCCAAAAATCCGGTCGAACTGATTGAAGGGTGGTTTAGT
                ** ** ** ** ***** ** ******** ***** ** ** ** ***** ********

COCVG           AGCTGGAAGTCAACAGTGGTAACTTTCTTCTTCGCCATCGGCGTGTTTATACTTCTGTAC
WTCVG           AGTTGGAAGAGCACTGTAGTCACCTTTTTCTTTGCCATAGGAGTATTTATACTACTGTAT
                ** ******   ** ** ** ** ** ***** ***** ** ** ******** *****

COCVG           GTAGTGGCCCGCATCGTGATCGCAGTGCGCTACAGATACCAAGGAAGCAACAACAAAAGA
WTCVG           GTAGTGGCCAGAATTGTGATCGCAGTGAGATACAGATATCAAGGCTCAAATAACAAAAGA
                ********* * ** ************ * ******** *****    ** *********

COCVG           ATCTACAACGACATAGAGATGAGCCGCTTCAGGAAGTGA
WTCVG           ATTTACAATGATATTGAGATGAGCAGATTTAGAAAATGA
                ** ***** ** ** ********* * ** ** ** ***
```

Figure 5.5. Nucleotide sequence alignment of codon-optimized (COCVG) and wild-type (WTCVG) Cocal virus G protein genes.

Alignment was done using ClustalX multiple sequence alignment programme: * indicates identical nucleotide shared by two sequences.

The RDpro gene in pRDproLF was initially replaced with the codon-optimized COCV-G gene to create pCVGLFA. In this construct two separate MLV LTRs drive COCV-G and *ble* (a phleomycin resistance gene) expression (Figure 5.6A). This allowed the use of phleomycin to select cells expressing COCV-G. To test our new COCV-G expression construct, pCVGLFA, we attempted to produce pseudotyped LVs by transient transfection of 293T or WinPac cells. VSV-G and RDpro pseudotypes were produced in parallel for comparison (Figure 5.6B). Titers of COCV-G (293T mean= $9.3x10^7$ TU/ml, WinPac mean= $1.4x10^7$ TU/ml) and VSV-G (293T mean= $9.6x10^7$ TU/ml, WinPac mean= $1.9x10^7$ TU/ml) pseudotypes were similar and around 2 logs higher on average compared to that of RDpro pseudotypes (293T mean= $5.2x10^6$ TU/ml, WinPac mean= $1.4x10^5$ TU/ml). The 6-7 fold difference in titers between 293T and WinPac cell lines could be partly accounted for by the difference in transfection efficiency in the two cell lines.

After confirming efficient expression and pseudotyping in a transient production system, WinPac cells were thawed and re-selected with puromycin and hygromycin for 10 days to ensure high-expression of gag-pol and rev respectively. The cells were then transfected with pCVGLFA and selected with phleomycin followed by re-selection with puromycin and hygromycin selection. A bulk population of phleomycin-resistant cells was obtained (WinPac-CVG bulk), and nineteen phleomycin-resistant clones were isolated by limiting dilution. Frozen stocks of all cells were prepared.

A functional screening test was used to determine the cells' potential to produce LVs (Table 2.13). This entailed seeding $2.0x10^6$ cells/well in 6-well plates and then transiently transfecting the cells with SIN pHV (a GFP-expressing SIN LV; Figure 3.2A) at 48 hours post-seeding. VCM was then collected over three consecutive 24-hour periods and infectious titers were determined. An extra well was used to harvest and analyze cells for GFP expression by flowcytometry at 24 hours post-transfection as a measure of the transfection efficiency. The WinPac-CVG bulk population was initially tested in parallel with a similarly derived WinPac-RDpro bulk population (except pRDproLF was transfected instead of pCVGLFA) and the WinPac-RDpro clone previously isolated by Sean Knight (WinPac-RDpro clone; see Chapter 3 for details). WinPac-CVG bulk population and WinPac-RDpro clone were kept in culture for a period of three weeks during which the transfection of SIN pHV and subsequent titer determination were performed three times. The WinPac-CVG bulk population and WinPac-RDpro clone

performed similarly in these experiments with titers of around 10^6 TU/ml maintained over a period of around 3 weeks (mean = 9.2 x10^5 TU/ml, SEM= 4.6 x10^5; mean= 1.5 x10^6 TU/ml, SEM= 9.9 x10^5 respectively; Figure 5.6C). These results were encouraging since a clone with favorable expression profile isolated from the bulk population (with heterogeneous expression levels) would be expected to perform better. In addition to that, the mean transfection efficiency was 15.3% (SD = 3.8%) for WinPac-CVG bulk and 21.9% (SD = 4.0%) for WinPac-RDpro clone. Therefore, ensuring efficient selection following the stable expression of a vector genome in WinPac-CVG cells can potentially yield higher titers especially after optimization of harvesting conditions. The WinPac-RDpro bulk population initially had a titer of around 10^4 TU/ml, which dropped below the threshold of detection on subsequent testing during the 2nd and 3rd weeks in culture (transfection efficiency mean = 15%, SD = 3.5%).

Subsequently, WinPac-CVG clones were tested in a similar manner. Titers from 17 out of 19 clones were tested (mean= 3.1x10^5 TU/ml, range: 3.3x10^3 – 1.7x10^6 TU/ml) (Figure 5.6D). Clone H4 and E25 have been chosen for further testing since they had the highest titers (mean= 1.7x10^6 and 6.0x10^5 TU/ml respectively). Titration of VCM harvested from the remaining 2 clones (out of 19) as well as that harvested from experiments conducted in week 2 and 3 for all clones as well as the WinPac and 293T cells is in progress. Initial results seem to confirm titer stability for the tested clones (Figure 5.6E). gDNA and RNA samples have been collected at the time of transfection in order to determine DNA and RNA copy numbers of the packaging components in the clones over a period of three weeks. This would help ensure the best clones are selected for the generation of producer cells

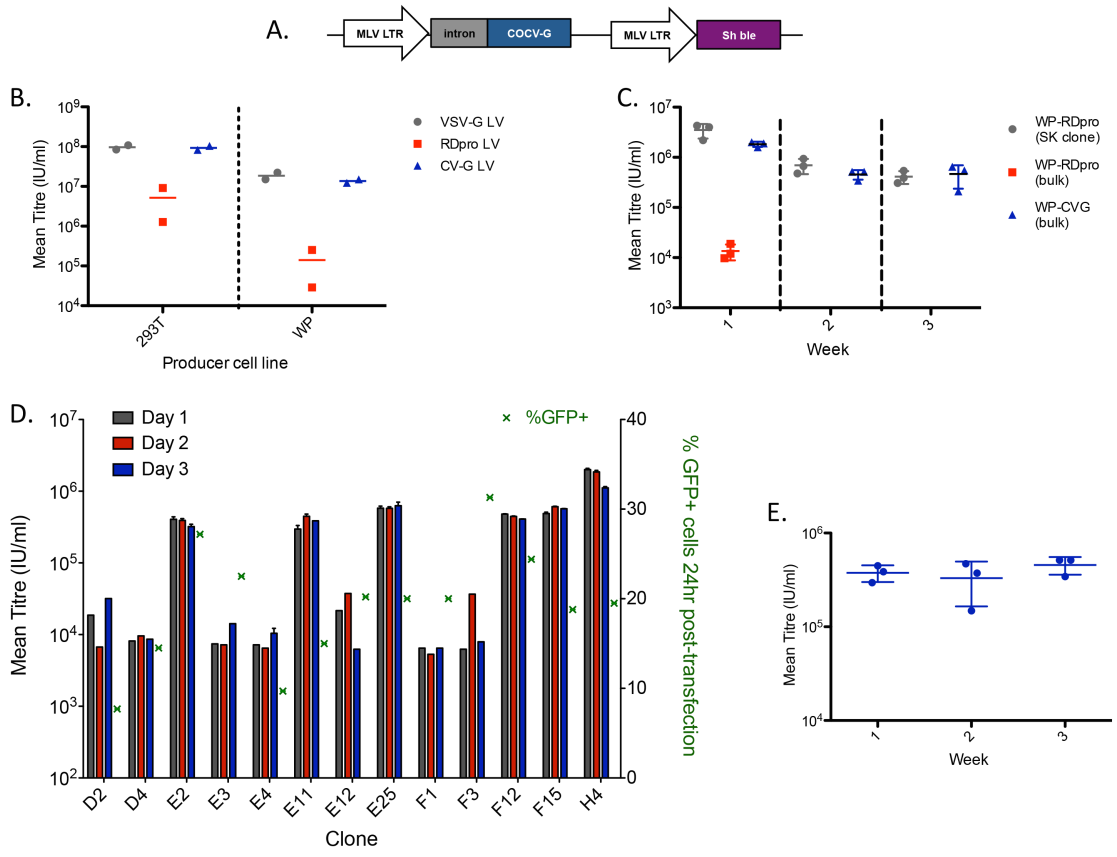

Figure 5.6. Expression of COCV-G in stable PCLs.

(A) Schematic representation of pCVGLFA (COCV-G expression plasmid). **(B)** Titers of COCV-G/VSV-G/RDpro-pseudotyped LVs produced by 3-plasmid transient transfection of 293T cells. Data shown represents mean titers of two 24-hour harvests collected on two consecutive days. The horizontal lines represent the average of the two harvests. **(C)** Titers of COCV-G/VSV-G/RDpro-pseudotyped LVs produced by transient transfection of WinPac cells with 2 plasmids (Env-expressing plasmid and SIN pHV). Data shown represents mean titers of three 24-hour harvests collected on three consecutive days. The horizontal lines represent the average of the three harvests and the error bars represent SD. Experiments were done in duplicates. **(D)** Titers of COCV-G-pseudotyped LVs produced by transient transfection of WinPac-CVG cells with SIN pHV. Harvests were collected over 24-hour periods on three consecutive days. Data shown represents mean titers +/- range calculated from duplicates. %GFP+ cells shown represent is shown as a measure of relative transfection efficiency. **(E)** Titers of COCV-G-pseudotyped LVs produced by transient transfection of WinPac-CVG E11 cells with SIN pHV. Data shown represents mean titers calculated for three 24-hour harvests collected on three consecutive days. The horizontal lines represent the average of the three harvests and the error bars represent SD. Experiments were done in duplicates.

5.3.3 Is the LDL-R involved in COCV-G pseudotyped LV entry?

Given that COCV-G and VSV-G pseudotyped LVs share a broad tropism and that they are phylogenetically and serologically closely related with more than 70% sequence identity on the amino acid level, we hypothesized that they might have similar cell entry mechanisms. Since the LDL-R family of proteins have been suggested to act as the target receptors for VSV-G (Finkelshtein et al., 2013), we set out to determine whether the soluble LDL-R (sLDL-R) can block infection of 293T cells by COCV-G pseudotypes.

A maximum of 4-fold decrease in the percentage of GFP^+ cells was observed for COCV-G pseudotypes (Figure 5.7A), whereas a maximum of 10-fold decrease was seen for VSV-G pseudotypes (Figure 5.7B) in the presence of 3 μg/ml sLDL-R. No change in the percentage of GFP^+ cells was seen for RDpro pseudotypes in the presence or absence of sLDL-R (Figure 5.7C).

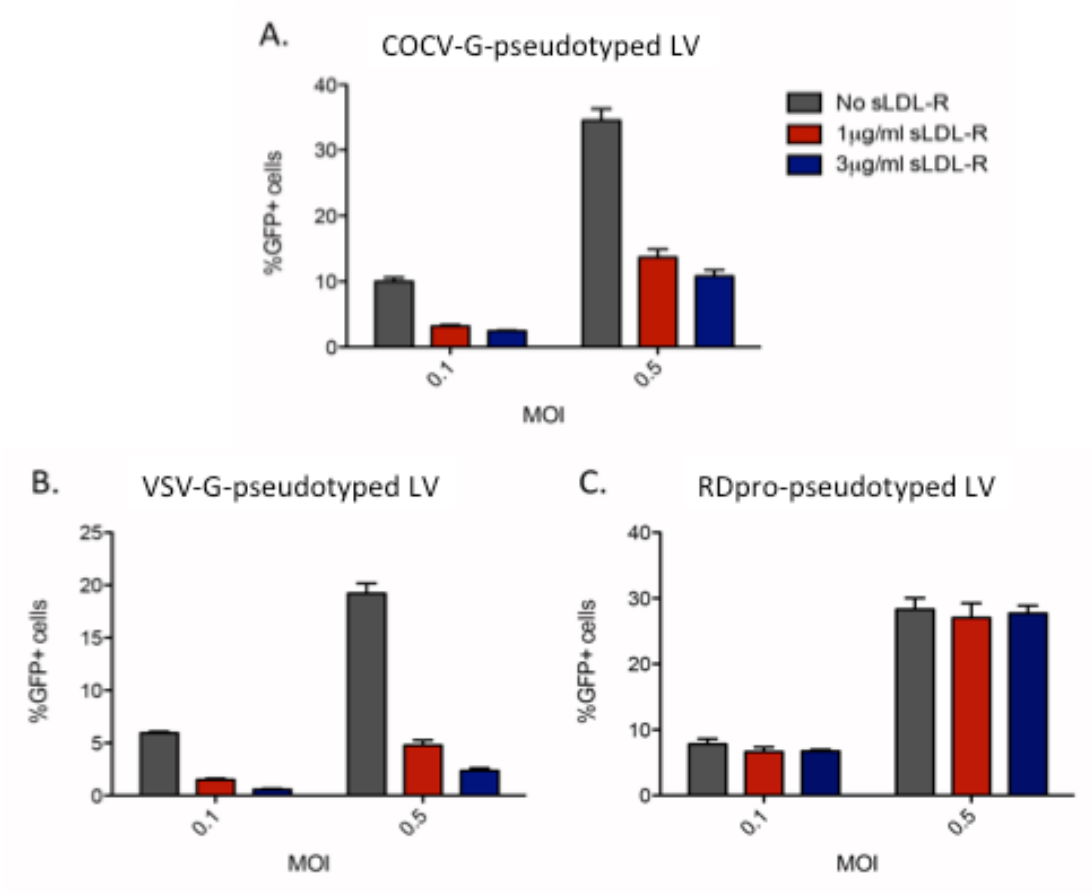

Figure 5.7. LDL-R plays a role in the transduction by COCV-G and VSV-G pseudotyped LVs.

Transduction efficiency of 293T cells in the presence of 1 µg/ml, 3 µg/ml or no sLDL-R by GFP-expressing LV pseudotyped with **(A)** COCV-G, **(B)** VSV-G, or **(C)** RDpro envelope glycoprotein at MOI of 0.1 or 0.5. LV pseudotypes were produced by 3-plasmid transient transfection of 293T cells and titrated on 293T in order to normalize the amount of LV used by MOI. Percentage of GFP^+ cells was determined by flowcytometry 48-hrs after transduction. Data shown represents percentage of GFP^+ cells +/- SD for three experiments.

5.4 Discussion

VSV-G is most commonly used envelope glycoprotein to pseudotype LVs for experimental and clinical applications. VSV-G LVs can be produced at high titers and are highly stable allowing efficient concentration by ultracentrifugation. They can also infect a wide range of target cells (Naldini et al., 1996). COCV-G has been shown to allow production of LV pseudotypes that share all these characteristics including the ability to efficiently transduce human hematopoietic progenitor cells. These pseudotypes are also less sensitive to inactivation with human serum (Trobridge et al., 2010).

A PCL, named WinPac-CVG, that is capable of continuously producing COCV-G-pseudotyped LVs was generated. This cell line was able to support transient vector production at stable levels of around 10^6 TU/ml for at least three weeks (Figure 5.5E). Current work is aimed at stably expressing therapeutic SIN LV genomes in WinPac-CVG clones at high levels using the methods that have been tested and optimized as detailed in Chapter 4. This would facilitate testing the physical stability of the COCV-G pseudotypes in the context of large-scale production and concentration using TFF and other scalable concentration and purification technologies.

Once it is fully characterized, the WinPac-CVG cell line would be expected to facilitate affordable large-scale production of potent LVs to meet the needs of larger clinical trials and patient populations. This would help propel the field of LV-mediated gene therapy forward (Thrasher, 2013).

5.4.1 Constitutive expression of COCV-G: a working hypothesis

COCV-G shares considerable sequence homology and structural organization with other G proteins especially VSIV-G, which has been extensively studied. Indeed, data from experiments performed on VSV-G and RABV-G independently lead to similar conclusions that are thought to apply to rhabdoviral G proteins in general (Albertini et al., 2012a; Sun et al., 2010). Based on available data, the fact that COCV-G could be constitutively expressed in WinPac cells allowing efficient vector production likely relates to its pH-dependent fusion profile and can be best explained by considering factors that can affect this profile:

1. Variations in the amino acid sequences:

   Single amino acid substitutions can have significant effects on pH-dependent fusogenicity (Fredericksen and Whitt, 1995; Roche et al., 2008; Zhang and Ghosh, 1994) and infectivity (Fredericksen and Whitt, 1996, 1998). Thus the amino acid sequence of G proteins would be expected to affect the dynamics of their pH-dependent equilibrium (Baquero et al., 2015; Steffen et al., 2013).

   We have identified differences in the amino acid sequences of COCV-G and VSIV-G that might impart greater stability to the N conformation, which is the major conformational state for G proteins at the cell surface. This can shift the equilibrium towards the N state and result in a pH threshold for fusion activation that is usually not reached under normal mammalian cell culture conditions where the pH is usually ≥ 6.5 (Naciri et al., 2008). It should be noted here that in the absence of the crystal structure of COCV-G, the exact impact of individual amino acid variations is difficult to predict.

2. Variations in cell lines:

   It has been proposed that the post-fusion conformation is the state in which the newly synthesized G proteins are transported from the ER and through the acidic environment of the exocytic pathway in order to avoid undesirable fusogenic activity (Gaudin et al., 1995). However, different cell lines have slightly different pH levels in their intracellular compartments (including the trans-golgi network) possibly due to variation in the number of proton pumps and ion exchangers in their membranes (Anderson and Orci, 1988). This may, in turn, affect the state in which G proteins are transported through the acidic environment of the exocytic pathway.

   In HEK-293 cells (the parental cell line from which 293T and 293FT cells are derived), the pH of the trans-golgi network has been estimated to be around 6.36 (Machen et al., 2003). Although this is slightly greater than the reported threshold pH level for VSV-G-mediated fusion, some fusogenic activity has been detected at pH levels ≥6.3 (Ferlin et al., 2014; Pak et al., 1997). This might explain the problems faced by investigators attempting to constitutively express VSV-G in 293T cells (Burns et al., 1993; Yee et al., 1994). Additionally, VSV-G expressed in an endometrial cell line was found to induce extensive syncytia formation without

an exogenous pH trigger. Since this fusogenic activity could be inhibited by neutralization of the pH of the vesicular transport compartment, it was proposed that fusion was activated during transport to the cell membrane (Roberts et al., 1999).

A shift in equilibrium towards the I conformation might minimize the proportion of G proteins that are transported in the A conformation. This would allow G proteins to be expressed and transported in 293-derived cell lines without overt fusogenic effects until they reach the cell membrane and transition into the pre-fusion conformation under neutral pH conditions.

3. Temperature:

   When fusion at a given pH was monitored at different temperatures, lower temperatures reduced the rate of conformational transition and the rate of fusion (Clague et al., 1990). Therefore, it would be interesting to test whether the titer/productivity per cell changes when producer cells are incubated at different temperatures (for example 32 °C). Notably, VSV-G has been constitutively expressed in TE671-derived in the γ-RV FLY cells allowing high-titer vector production at low temperature (32 °C) (Collins et al., 2000).

4. Level of expression:

   It has been estimated that multiple (around 15 monomers or 5 trimers) fusion-active VSV-G units are needed for fusion to occur since the energy barrier for the fusion reaction likely exceeds the energy released by the reversible conformational transition of the G protein (Bundo-Morita et al., 1988; Roche et al., 2008). Given that at any pH only a certain percentage of G proteins are in the fusion-active state, the absolute number of such proteins will depend on the total number of proteins available. Thus, a higher expression level of G proteins on cellular membranes will make it more likely that enough fusion-active units are available to drive the fusion reaction.

Overall the amino acid composition of COCV-G might allow for favorable equilibrium dynamics between the three G protein conformations and a low threshold for pH-induced fusion activity. Thus, under the acidic environment of the exocytic transport pathway, COCV-G would be transported mainly in the post-fusion state (at least in 293-

derived cell lines). On the other hand, the pre-fusion conformation would be prevalent on the cell membrane under the typical mammalian cell culture pH conditions. This might account for the fact that it was possible to express COCV-G in our 293FT-based WinPac cells.

5.4.2 Derivation of VSV-G mutants that can be constitutively expressed in PCLs

VSV-G mutants, whose fusogenic activity is triggered at lower pH levels compared to wild-type VSV-G, might be expected to have more stable N conformation. This would theoretically be advantageous when attempting to express these mutants in PCLs, since it would reduce the chances of fusion activation during transport through the acidic exocytic pathway (Gaudin et al., 1995; Roberts et al., 1999) and after expression at the cell surface.

However, single amino acid substitutions in the fusion domain or membrane proximal region that gave rise to such mutants also resulted in suboptimal fusogenic activity and impaired infectivity of recombinant VSV (See Section 5.1.2.2.3). The negative impact of fusion domain mutations on VSV-G fusogenicity may be partly explained by the disruption of the highly organized structure of this domain (Figure 5.2; (Roche et al., 2008)).Therefore, using such mutants to pseudotype lentiviral vectors may result in the production of less infectious vector particles even if these mutants can be constitutively expressed in stable PCLs without significant cytotoxic effects.

In a particularly interesting study (Martinez and Wertz, 2005), a recombinant VSIV (strain: San Juan) carrying the gene encoding the G protein of the New Jersey serotype (G^{NJ}) was able to replicate efficiently in acidic pH. This phenotype was conferred by G^{NJ} since the G protein of the Indiana serotype (Strain: Orsay; G^{I}) tested in the same genomic background (that is VSIV - San Juan) was unable to mediate efficient replication at pH 6.8. This recombinant virus (designated here as VSIV(G^{I})) also exhibited a reversible reduction in infectivity at that pH. This was postulated to be the result of an increased stability of the pre-fusion (N) conformation of G^{NJ} compared to that of G^{I}. Thus, G^{I} is hypothesized to undergo transition to the post-fusion (I) conformation under mildly acidic conditions (pH 6.8) resulting in a reversible reduction in infectivity (Roche et al., 2008).

VSIV(G^{I}) was subsequently adapted to grow under increasingly acidic conditions (pH 6.8 to 6.6 to 6.4) and the glycoprotein (G) gene of the virus emerging at each stage

was sequenced. In the end, a total of 4 single nucleotide changes that lead to 4 amino acid substitutions were detected in the G protein of the final viral isolate (which was able to replicate at pH 6.4). Further analysis of the individual mutations revealed that two of them, namely F18L and Q301R, seemed to have the greatest impact on the phenotype of reduced pH sensitivity, and were located in domains I and II respectively. Interestingly, these mutations allowed the conservation of the replicative potential of the recombinant viruses while altering the profile of pH-dependent conformational changes of G^I, possibly by increasing the stability of the N state such that more acidic conditions would be required to induce the conformational transition into the A or I states. Thus, it might be possible to constitutively express VSIV-G mutants carrying one or more of these mutations in stable PCLs in order to stably produce infectious LV pseudotypes.

5.4.3 Investigation of host factors involved in COCV-G-pseudotyped LV entry

The VSV-G envelope is necessary for infection by VSV (Bishop et al., 1975) and mediates attachment to target cells by binding a surface receptor followed by entry via clathrin-mediated endocytosis (Johannsdottir et al., 2009). Although early studies suggested phosphatidylserine (PS) as the target receptor for VSV-G (Schlegel et al., 1983), this was disputed by more recent studies that showed a lack of correlation between VSV infectivity and PS levels in target cell membranes, and that infection with VSV-G-pseudotyped GRVs was not inhibited in the presence of saturating levels of Annexin V which specifically binds PS (Coil and Miller, 2004).

More recently the low-density lipoprotein receptor (LDL-R) and its family of proteins have been proposed to be the VSV-G receptor (Finkelshtein et al., 2013). This was based on a series of experiments were infection by VSV or a GFP-expressing VSV-G-pseudotyped LVs was significantly reduced using a monoclonal antibody against the LDL-R (specifically, the class A cysteine-rich repeat 3) in the presence of the receptor-associated protein (RAP) which blocks other members of the LDL-R family of proteins.

Data from infection assays were represented in the form of relative expression level of eGFP, without indicating the percentage of GFP^+ cells. GFP expression could still be detected in target cells in the presence of the antibody and RAP, suggesting the involvement of other host cell factors in mediating VSV-G LV entry and infection. Notably, knockdown of LDL-R expression via siRNA in a human fibroblast cell line (FS-11) moderately lowered LDL-R expression, resulting in moderate 2-2.5 fold decrease in

relative expression of eGFP. Moreover, expression of LDL-R in a different LDL-$R^{-/-}$ GM701 cell line resulted in a 6-fold increase in eGFP expression.

In support of the claim that LDL-R plays an important role in entry of VSV-G LV, it was shown that unstimulated T cells, B cells and HSCs express low levels of LDL-R at their surfaces. Following stimulation with a cytokine cocktail, LDL-R surface expression increased in T cell and HSCs and this correlated with an increased transduction efficiency with VSV-G LV (Amirache et al., 2014).

We are attempting to identify the target cell receptor and other host cell factors that mediate entry of COCV-G LVs. As part of this work we aim to further characterize the role of LDL-R in VSV-G/COCV-G LV entry. In particular, infection assays with be performed in the presence or absence of blocking anti-apoE and/or anti-apoB antibodies to exclude interactions between LDL-R and its classical ligands (apoE and apoB), which might be present on the envelope of VSV-G/COCV-G LV. Other infection assays and co-immunoprecipitation assays are also planned.

CHAPTER

6

CONCLUSIONS AND FUTURE DIRECTIONS

6 Summary, conclusions and future directions

6.1 Summary and conclusions

The construction of WinPac-RD cells in our lab represents an important step forward towards achieving affordable large scale SIN LV production. It comes at an exciting time in the field of gene therapy during which the use of these vectors in clinical trials is yielding remarkable efficacy without serious adverse events, although long-term follow-up is warranted. These cells have been based on a traceable 293FT cell line and handled under Good Laboratory Practice (GLP) guidelines in order to facilitate their approval for use in manufacturing clinical-grade vectors.

The work presented in Chapter 3 provides a proof-of-principle that WinPac-based cells have the potential to support vector production at titers that are well within the range needed for use in clinical trials. They are uniquely able to continuously produce SIN LVs for prolonged periods, which facilitated scaling up of cultures to yield relatively large batches of vectors with titers exceeding 10^6 TU/ml. This is partly due to the stable constitutive expression of HIV-1 Gag-Pol through RMCE-based targeted integration at a locus pre-selected using a gamma-retroviral vector. Another important feature is the constitutive expression of the RD114-derived envelope glycoprotein. Efficient antibiotic-based selection also was a practically important feature to ensure long-term vector production.

As described in Chapter 4, establishing reliable protocols that allow the rapid generation of SIN LV producer cell lines from a master cell bank of packaging cells is highly desirable. Introduction of SIN LV expression cassettes at pre-selected loci mediated via recombinase enzymes is an attractive option. Additionally, the use of stringent selection methods and promoterless selectable markers offer a simple means to ensure high expression levels. Flanking expression cassettes with cis-acting elements that are thought to help maintain a favorable chromatin environment such as matrix attachment regions (MARs) (Dijkwel and Hamlin, 1988) might also help establish and maintain high expression levels of the GOI.

The generation of WinPac-CVG cells is another important milestone that might facilitate the production of physically stable LV pseudotypes at high titers. However,

further characterization of this packaging cell line as well as the COCV-G-pseudotyped LVs is warranted.

WinPac-derived producer cells are expected to facilitate the reproducible production of large vector batches that are suitable for use in early phase 1 clinical trials. Therefore, adaptation to growth in suspension and possibly in serum free medium would be desirable. The use of bioreactors to scale up cell culture and vector production as well as optimization of downstream concentration and purification protocols are needed.

6.2 Refining the RMCE strategy

6.2.1 Tagging pre-characterized loci

As an alternative to tagging transcriptionally active sites using GRVs, gene editing techniques using TALENS or the CRISPR/Cas9 system to tag pre-characterized sites. The AAVS1 site has been shown to possess a transcriptionally favorable chromatin configuration in both iPSCs and HSCs (Lombardo et al., 2011; van Rensburg et al., 2013), and might also be a transcriptionally active locus in transformed cell lines such as the 293FT-derived WinPac cells. The utilization of the AAVS1 locus by flanking it with FRT/F5 sites using homologous recombination mechanisms might be simpler and more reliable than screening retrovirally tagged sites and would avoid introducing unnecessary retroviral sequences in PCLs.

6.2.2 Efficient selection of successful recombination events

The cassettes used in Chapter 4 did not eliminate background random integration and expression of Bsr gene under the control of a cellular promoter since transfection of pFBCF alone into WinRD-F1 cells gave rise to Blasticidin-resistant cells (Figure 4-4).

One way to overcome this is to use a promoter-less and ATG-less marker gene in the donor cassette (pFBCF). An ATG must also be introduced in the tagging cassette between the FRT and F5 sites (pCFG). Thus, the marker gene would be complemented with the U3 promoter and ATG sequence necessary for its expression only when successful recombination occurs. However, functionality of the marker gene (such as Bsr) has to be confirmed despite the presence of the F5 site downstream from the ATG sequence.

Another way to address this issue is by using a donor plasmid that has the human herpes simplex virus thymidine kinase type 1 gene (HSVtk) outside the expression cassette flanked by the FRT sites. Applying ganciclovir after the RMCE reaction should eliminate randomly integrated donor plasmids. Both strategies can be employed simultaneously to further improve efficiency.

6.3 Construction of packaging cell lines with alternative envelopes

It would also be interesting to test other promising envelope glycoproteins like the baboon endogenous retrovirus-derived envelope, which has been recently reported to efficiently transduce quiescent human hematopoietic stem cells (Girard-Gagnepain et al., 2014). This is thought to be due to the basal expression of their receptors (the neutral amino acid transporters ASCT-1 and ASCT-2) on these cells obviating the need for stimulation. This is useful as it may help preserve the 'stemness' and engraftment potential of the cells.

6.4 The growing field of gene therapy: a peek into the future

6.4.1 Genome editing

Although most gene therapy clinical trials to date have utilized gene addition techniques, the possibility of gene editing or deletion opens up a great number of possibilities. Targeted genome editing refers to the use of engineered endonucleases to introduce gene deletions or substitutions at a pre-determined locus (Lombardo and Naldini, 2014). In this approach an endonuclease is used to introduce a double-stranded break (DSB) in a target genomic locus. The DSB is then repaired either by non-homologous end joining (NHEJ) or homologous recombination (HR). The former usually introduces random nucleotide additions or deletions at the break site, which can disrupt the reading frame of a target gene and prevent its expression thereby effectively achieving gene deletion. Homologous recombination on the other hand, can introduce a tailored DNA template at the site of the DSB by flanking that template with sequences that are homologous to the targeted genomic locus. This can be used to repair a mutated sequence (gene repair) or introduce the expression cassette of a gene of interest at a predetermined locus.

IL2RG gene repair was also achieved in HSCs obtained from a patient with SCID-X1 by introducing the template DNA using an integration-deficient LV (IDLV) followed

by mRNA electroporation to transiently express engineered ZFNs targeting the IL2RG gene locus (Genovese et al., 2014).

A pioneering clinical trial that employed gene deletion in T cells for the treatment of patients with HIV-1 infection was recently reported (Tebas et al., 2014). In this study the investigators used an adenoviral vector to transiently express an engineered zinc finger nuclease (ZFN) that induces a double-stranded break (DSB) in the coding region of the CCR5 gene encoding an HIV-1 accessory receptor. Repair by NHEJ then disrupted the coding sequence of the CCR5 gene in order to create $CCR5^-$ HIV-1-resistant T cells. This resulted in a reduction in HIV RNA in all four patients treated following HAART interruption with the levels falling to undetectable levels in one of the patients.

However, for these strategies to become widely applicable more efficient delivery and expression of nucleases in target cells are needed. Off-target DSBs also need to be minimized to ensure safety and avoid possible mutagenic events. Newer artificial nuclease platforms such as Transcription activator-like effector nucleases (TALENs) and the RNA-guided CRISPR-associated protein-9 (Cas9) system are being constantly improved in order to achieve these goals (Kim and Kim, 2014).

6.4.2 Integration-deficient lentiviral vectors

Integration deficient lentiviral vectors (IDLVs) are also attractive gene delivery tools that can harness the natural capacity of lentiviruses to efficiently infect cells while reducing, but not eliminating, the risk of insertional mutagenesis since they have 3-4 fold lower integration potential than integration proficient LVs (reviewed in (Wanisch and Yanez-Munoz, 2009)). IDLVs are developed by mutating the viral integrase (*IN*; most commonly D64V) with or without mutations in the integrase attachment sites (*att*).

They are especially useful for targeting terminally-differentiated non-dividing cells such as antigen presenting cells (APCs) or muscle cells, as well as for transient delivery of transgenes into dividing cells which can be useful for genome editing applications as described in Section 6.4.1.

However, low-titer production as well as low transgene expression (compared to the integration proficient LVs) limits their widespread use and applicability. Therefore, it would be interesting to generate an IDLV producer cell line derived from WinPac-CVG cells using the refined RMCE strategy described in Section 6.2.

6.4.3 LV targeting

Targeting of LVs is an important aim for the field of gene therapy and especially for its *in vivo* applications in order to avoid off-target adverse events. This can be achieved through targeted transduction and/or targeted expression.

6.4.3.1 Targeted transduction

Pseudotyping LVs with heterologous envelope glycoproteins that specifically target surface receptor is an attractive way to achieve efficient delivery to a specific cell type (Cronin et al., 2005). Moreover, measles virus glycoproteins (hemagglutinin (H) and fusion (F)) can be used to retarget pseudotyped LVs by fusing a mutated H glycoprotein with a single-chain antibody (scFv) targeting a specific receptor (Anliker et al., 2010). As an alternative to that, the H glycoprotein can be fused with designed ankyrin repeat proteins (DARPins), which can be selected to become high-affinity binders to any kind of target molecule (Munch et al., 2011).

6.4.3.2 Targeted expression

Targeted expression is also a useful strategy to avoid off-target effects of gene therapy. Targeted expression can be achieved on two levels. The first involves the use of tissue/lineage-specific promoters to ensure expression only in cells of desired lineage. The second employs microRNA binding sites that allow restriction of transgene expression in specific cell types (Brown and Naldini, 2009).

These strategies have important applications for both *in vivo* and *ex vivo* gene therapy strategies. For example, It can be used to de-target antigen presenting cells during *in vivo* delivery in order to avoid an immune response against the therapeutic transgene (Lopes et al., 2008). Whereas, in *ex vivo* HSC gene therapy, the non-physiologic expression of therapeutic transgenes can adversely affect the engraftment and differentiation potential of transduced stem cells. Thus, targeted expression lineage-specific promoters as well as the inclusion of HSC-specific miRNA target sites in LV cassettes can restrict transgene expression to more differentiated cell lineages (Chiriaco et al., 2014).

REFERENCES

Agarwal, K.L., Buchi, H., Caruthers, M.H., Gupta, N., Khorana, H.G., Kleppe, K., Kumar, A., Ohtsuka, E., Rajbhandary, U.L., Van de Sande, J.H.*, et al.* (1970). Total synthesis of the gene for an alanine transfer ribonucleic acid from yeast. Nature *227*, 27-34.

Ahn, J., Hao, C., Yan, J., DeLucia, M., Mehrens, J., Wang, C., Gronenborn, A.M., and Skowronski, J. (2012). HIV/simian immunodeficiency virus (SIV) accessory virulence factor Vpx loads the host cell restriction factor SAMHD1 onto the E3 ubiquitin ligase complex CRL4DCAF1. J Biol Chem *287*, 12550-12558.

Ailles, L., Schmidt, M., Santoni de Sio, F.R., Glimm, H., Cavalieri, S., Bruno, S., Piacibello, W., Von Kalle, C., and Naldini, L. (2002). Molecular evidence of lentiviral vector-mediated gene transfer into human self-renewing, multi-potent, long-term NOD/SCID repopulating hematopoietic cells. Mol Ther *6*, 615-626.

Aiuti, A., Biasco, L., Scaramuzza, S., Ferrua, F., Cicalese, M.P., Baricordi, C., Dionisio, F., Calabria, A., Giannelli, S., Castiello, M.C.*, et al.* (2013). Lentiviral Hematopoietic Stem Cell Gene Therapy in Patients with Wiskott-Aldrich Syndrome. Science.

Aiuti, A., Cassani, B., Andolfi, G., Mirolo, M., Biasco, L., Recchia, A., Urbinati, F., Valacca, C., Scaramuzza, S., Aker, M.*, et al.* (2007). Multilineage hematopoietic reconstitution without clonal selection in ADA-SCID patients treated with stem cell gene therapy. J Clin Invest *117*, 2233-2240.

Aiuti, A., Cattaneo, F., Galimberti, S., Benninghoff, U., Cassani, B., Callegaro, L., Scaramuzza, S., Andolfi, G., Mirolo, M., Brigida, I.*, et al.* (2009). Gene therapy for immunodeficiency due to adenosine deaminase deficiency. N Engl J Med *360*, 447-458.

Aiuti, A., Vai, S., Mortellaro, A., Casorati, G., Ficara, F., Andolfi, G., Ferrari, G., Tabucchi, A., Carlucci, F., Ochs, H.D.*, et al.* (2002). Immune reconstitution in ADA-SCID after PBL gene therapy and discontinuation of enzyme replacement. Nat Med *8*, 423-425.

Al-Herz, W., Bousfiha, A., Casanova, J.L., Chapel, H., Conley, M.E., Cunningham-Rundles, C., Etzioni, A., Fischer, A., Franco, J.L., Geha, R.S.*, et al.* (2011). Primary immunodeficiency diseases: an update on the classification from the international union of immunological societies expert committee for primary immunodeficiency. Front Immunol *2*, 54.

Al-Herz, W., Bousfiha, A., Casanova, J.L., Chatila, T., Conley, M.E., Cunningham-Rundles, C., Etzioni, A., Franco, J.L., Gaspar, H.B., Holland, S.M.*, et al.* (2014). Primary immunodeficiency diseases: an update on the classification from the international union of immunological societies expert committee for primary immunodeficiency. Front Immunol *5*, 162.

Albertini, A.A., Baquero, E., Ferlin, A., and Gaudin, Y. (2012a). Molecular and cellular aspects of rhabdovirus entry. Viruses *4*, 117-139.

Albertini, A.A., Merigoux, C., Libersou, S., Madiona, K., Bressanelli, S., Roche, S., Lepault, J., Melki, R., Vachette, P., and Gaudin, Y. (2012b). Characterization of monomeric intermediates during VSV glycoprotein structural transition. PLoS Pathog *8*, e1002556.

Amarasinghe, G.K., De Guzman, R.N., Turner, R.B., Chancellor, K.J., Wu, Z.R., and Summers, M.F. (2000). NMR structure of the HIV-1 nucleocapsid protein bound to stem-loop SL2 of the psi-RNA packaging signal. Implications for genome recognition. Journal of molecular biology *301*, 491-511.

Amirache, F., Levy, C., Costa, C., Mangeot, P.E., Torbett, B.E., Wang, C.X., Negre, D., Cosset, F.L., and Verhoeyen, E. (2014). Mystery solved: VSV-G-LVs do not allow efficient gene transfer into unstimulated T cells, B cells, and HSCs because they lack the LDL receptor. Blood *123*, 1422-1424.
Anderson, J.L., Campbell, E.M., Wu, X., Vandegraaff, N., Engelman, A., and Hope, T.J. (2006). Proteasome inhibition reveals that a functional preintegration complex intermediate can be generated during restriction by diverse TRIM5 proteins. Journal of virology *80*, 9754-9760.
Anderson, R.G., and Orci, L. (1988). A view of acidic intracellular compartments. J Cell Biol *106*, 539-543.
Anliker, B., Abel, T., Kneissl, S., Hlavaty, J., Caputi, A., Brynza, J., Schneider, I.C., Munch, R.C., Petznek, H., Kontermann, R.E.*, et al.* (2010). Specific gene transfer to neurons, endothelial cells and hematopoietic progenitors with lentiviral vectors. Nat Methods *7*, 929-935.
Ara, A., Love, R.P., and Chelico, L. (2014). Different mutagenic potential of HIV-1 restriction factors APOBEC3G and APOBEC3F is determined by distinct single-stranded DNA scanning mechanisms. PLoS pathogens *10*, e1004024.
Araki, K., Araki, M., and Yamamura, K. (1997). Targeted integration of DNA using mutant lox sites in embryonic stem cells. Nucleic Acids Res *25*, 868-872.
Ashkenazi, A., and Shai, Y. (2011). Insights into the mechanism of HIV-1 envelope induced membrane fusion as revealed by its inhibitory peptides. European biophysics journal : EBJ *40*, 349-357.
Backovic, M., and Jardetzky, T.S. (2009). Class III viral membrane fusion proteins. Curr Opin Struct Biol *19*, 189-196.
Baldauf, H.M., Pan, X., Erikson, E., Schmidt, S., Daddacha, W., Burggraf, M., Schenkova, K., Ambiel, I., Wabnitz, G., Gramberg, T.*, et al.* (2012). SAMHD1 restricts HIV-1 infection in resting CD4(+) T cells. Nat Med *18*, 1682-1687.
Baquero, E., Albertini, A.A., Raux, H., Buonocore, L., Rose, J.K., Bressanelli, S., and Gaudin, Y. (2015). Structure of the Low pH Conformation of Chandipura Virus G Reveals Important Features in the Evolution of the Vesiculovirus Glycoprotein. PLoS Pathog *11*, e1004756.
Baquero, E., Albertini, A.A., Vachette, P., Lepault, J., Bressanelli, S., and Gaudin, Y. (2013). Intermediate conformations during viral fusion glycoprotein structural transition. Curr Opin Virol *3*, 143-150.
Bartholomae, C.C., Glimm, H., von Kalle, C., and Schmidt, M. (2012). Insertion site pattern: global approach by linear amplification-mediated PCR and mass sequencing. Methods Mol Biol *859*, 255-265.
Beignon, A.S., Mollier, K., Liard, C., Coutant, F., Munier, S., Riviere, J., Souque, P., and Charneau, P. (2009). Lentiviral vector-based prime/boost vaccination against AIDS: pilot study shows protection against Simian immunodeficiency virus SIVmac251 challenge in macaques. Journal of virology *83*, 10963-10974.
Bell, A.J., Jr., Fegen, D., Ward, M., and Bank, A. (2010). RD114 envelope proteins provide an effective and versatile approach to pseudotype lentiviral vectors. Exp Biol Med (Maywood) *235*, 1269-1276.
Berthoux, L., Sebastian, S., Sokolskaja, E., and Luban, J. (2005). Cyclophilin A is required for TRIM5{alpha}-mediated resistance to HIV-1 in Old World monkey cells. Proc Natl Acad Sci U S A *102*, 14849-14853.
Bhella, R.S., Nichol, S.T., Wanas, E., and Ghosh, H.P. (1998). Structure, expression and phylogenetic analysis of the glycoprotein gene of Cocal virus. Virus Res *54*, 197-205.

Bianchi, M., Hakkim, A., Brinkmann, V., Siler, U., Seger, R.A., Zychlinsky, A., and Reichenbach, J. (2009). Restoration of NET formation by gene therapy in CGD controls aspergillosis. Blood *114*, 2619-2622.
Biasco, L., Scala, S., Basso Ricci, L., Dionisio, F., Baricordi, C., Calabria, A., Giannelli, S., Cieri, N., Barzaghi, F., Pajno, R.*, et al.* (2015). In vivo tracking of T cells in humans unveils decade-long survival and activity of genetically modified T memory stem cells. Sci Transl Med *7*, 273ra213.
Bieniasz, P.D. (2009). The cell biology of HIV-1 virion genesis. In Cell Host Microbe (United States), pp. 550-558.
Biffi, A., Aubourg, P., and Cartier, N. (2011a). Gene therapy for leukodystrophies. Hum Mol Genet *20*, R42-53.
Biffi, A., Bartolomae, C.C., Cesana, D., Cartier, N., Aubourg, P., Ranzani, M., Cesani, M., Benedicenti, F., Plati, T., Rubagotti, E.*, et al.* (2011b). Lentiviral vector common integration sites in preclinical models and a clinical trial reflect a benign integration bias and not oncogenic selection. Blood *117*, 5332-5339.
Biffi, A., Lucchini, G., Rovelli, A., and Sessa, M. (2008). Metachromatic leukodystrophy: an overview of current and prospective treatments. Bone Marrow Transplant *42 Suppl 2*, S2-6.
Biffi, A., Montini, E., Lorioli, L., Cesani, M., Fumagalli, F., Plati, T., Baldoli, C., Martino, S., Calabria, A., Canale, S.*, et al.* (2013). Lentiviral Hematopoietic Stem Cell Gene Therapy Benefits Metachromatic Leukodystrophy. Science.
Bishop, D.H., Repik, P., Obijeski, J.F., Moore, N.F., and Wagner, R.R. (1975). Restitution of infectivity to spikeless vesicular stomatitis virus by solubilized viral components. Journal of virology *16*, 75-84.
Bishop, K.N., Verma, M., Kim, E.Y., Wolinsky, S.M., and Malim, M.H. (2008). APOBEC3G inhibits elongation of HIV-1 reverse transcripts. PLoS Pathog *4*, e1000231.
Black, L.R., and Aiken, C. (2010). TRIM5alpha disrupts the structure of assembled HIV-1 capsid complexes in vitro. Journal of virology *84*, 6564-6569.
Blaese, R.M., Culver, K.W., Miller, A.D., Carter, C.S., Fleisher, T., Clerici, M., Shearer, G., Chang, L., Chiang, Y., Tolstoshev, P.*, et al.* (1995). T lymphocyte-directed gene therapy for ADA- SCID: initial trial results after 4 years. Science *270*, 475-480.
Bogerd, H.P., and Cullen, B.R. (2008). Single-stranded RNA facilitates nucleocapsid: APOBEC3G complex formation. RNA *14*, 1228-1236.
Bordignon, C., Notarangelo, L.D., Nobili, N., Ferrari, G., Casorati, G., Panina, P., Mazzolari, E., Maggioni, D., Rossi, C., Servida, P.*, et al.* (1995). Gene therapy in peripheral blood lymphocytes and bone marrow for ADA- immunodeficient patients. Science *270*, 470-475.
Borovinskaya, M.A., Shoji, S., Fredrick, K., and Cate, J.H. (2008). Structural basis for hygromycin B inhibition of protein biosynthesis. RNA *14*, 1590-1599.
Boztug, K., Schmidt, M., Schwarzer, A., Banerjee, P.P., Diez, I.A., Dewey, R.A., Bohm, M., Nowrouzi, A., Ball, C.R., Glimm, H.*, et al.* (2010). Stem-cell gene therapy for the Wiskott-Aldrich syndrome. N Engl J Med *363*, 1918-1927.
Braun, C.J., Boztug, K., Paruzynski, A., Witzel, M., Schwarzer, A., Rothe, M., Modlich, U., Beier, R., Gohring, G., Steinemann, D.*, et al.* (2014). Gene therapy for Wiskott-Aldrich syndrome--long-term efficacy and genotoxicity. Sci Transl Med *6*, 227ra233.
Bread, N.S., Jr., Armentrout, S.A., and Weisberger, A.S. (1969). Inhibition of mammalian protein synthesis by antibiotics. Pharmacol Rev *21*, 213-245.
Breckpot, K., Escors, D., Arce, F., Lopes, L., Karwacz, K., Van Lint, S., Keyaerts, M., and Collins, M. (2010). HIV-1 lentiviral vector immunogenicity is mediated by Toll-like receptor 3 (TLR3) and TLR7. Journal of virology *84*, 5627-5636.

Brenner, S., Whiting-Theobald, N.L., Linton, G.F., Holmes, K.L., Anderson-Cohen, M., Kelly, P.F., Vanin, E.F., Pilon, A.M., Bodine, D.M., Horwitz, M.E., *et al.* (2003). Concentrated RD114-pseudotyped MFGS-gp91phox vector achieves high levels of functional correction of the chronic granulomatous disease oxidase defect in NOD/SCID/beta -microglobulin-/- repopulating mobilized human peripheral blood CD34+ cells. Blood *102*, 2789-2797.
Brentjens, R.J., Davila, M.L., Riviere, I., Park, J., Wang, X., Cowell, L.G., Bartido, S., Stefanski, J., Taylor, C., Olszewska, M., *et al.* (2013). CD19-targeted T cells rapidly induce molecular remissions in adults with chemotherapy-refractory acute lymphoblastic leukemia. Sci Transl Med *5*, 177ra138.
Brentjens, R.J., Riviere, I., Park, J.H., Davila, M.L., Wang, X., Stefanski, J., Taylor, C., Yeh, R., Bartido, S., Borquez-Ojeda, O., *et al.* (2011). Safety and persistence of adoptively transferred autologous CD19-targeted T cells in patients with relapsed or chemotherapy refractory B-cell leukemias. Blood *118*, 4817-4828.
Broussau, S., Jabbour, N., Lachapelle, G., Durocher, Y., Tom, R., Transfiguracion, J., Gilbert, R., and Massie, B. (2008). Inducible packaging cells for large-scale production of lentiviral vectors in serum-free suspension culture. Mol Ther *16*, 500-507.
Brown, B.D., and Naldini, L. (2009). Exploiting and antagonizing microRNA regulation for therapeutic and experimental applications. Nat Rev Genet *10*, 578-585.
Bryant, M., and Ratner, L. (1990). Myristoylation-dependent replication and assembly of human immunodeficiency virus 1. Proceedings of the National Academy of Sciences of the United States of America *87*, 523-527.
Buchholz, F., Angrand, P.O., and Stewart, A.F. (1998). Improved properties of FLP recombinase evolved by cycling mutagenesis. Nat Biotechnol *16*, 657-662.
Bundo-Morita, K., Gibson, S., and Lenard, J. (1988). Radiation inactivation analysis of fusion and hemolysis by vesicular stomatitis virus. Virology *163*, 622-624.
Burns, J.C., Friedmann, T., Driever, W., Burrascano, M., and Yee, J.K. (1993). Vesicular stomatitis virus G glycoprotein pseudotyped retroviral vectors: concentration to very high titer and efficient gene transfer into mammalian and nonmammalian cells. Proc Natl Acad Sci U S A *90*, 8033-8037.
Bushman, F., Lewinski, M., Ciuffi, A., Barr, S., Leipzig, J., Hannenhalli, S., and Hoffmann, C. (2005). Genome-wide analysis of retroviral DNA integration. Nat Rev Microbiol *3*, 848-858.
Candotti, F., Shaw, K.L., Muul, L., Carbonaro, D., Sokolic, R., Choi, C., Schurman, S.H., Garabedian, E., Kesserwan, C., Jagadeesh, G.J., *et al.* (2012). Gene therapy for adenosine deaminase-deficient severe combined immune deficiency: clinical comparison of retroviral vectors and treatment plans. Blood *120*, 3635-3646.
Cantore, A., Ranzani, M., Bartholomae, C.C., Volpin, M., Valle, P.D., Sanvito, F., Sergi, L.S., Gallina, P., Benedicenti, F., Bellinger, D., *et al.* (2015). Liver-directed lentiviral gene therapy in a dog model of hemophilia B. Sci Transl Med *7*, 277ra228.
Carbonaro, D.A., Zhang, L., Jin, X., Montiel-Equihua, C., Geiger, S., Carmo, M., Cooper, A., Fairbanks, L., Kaufman, M.L., Sebire, N.J., *et al.* (2014). Preclinical demonstration of lentiviral vector-mediated correction of immunological and metabolic abnormalities in models of adenosine deaminase deficiency. Mol Ther *22*, 607-622.
Carbone, A., Zinovyev, A., and Kepes, F. (2003). Codon adaptation index as a measure of dominating codon bias. Bioinformatics *19*, 2005-2015.
Cartier, N., Hacein-Bey-Abina, S., Bartholomae, C.C., Veres, G., Schmidt, M., Kutschera, I., Vidaud, M., Abel, U., Dal-Cortivo, L., Caccavelli, L., *et al.* (2009). Hematopoietic stem cell gene therapy with a lentiviral vector in X-linked adrenoleukodystrophy. Science *326*, 818-823.

Case, S.S., Price, M.A., Jordan, C.T., Yu, X.J., Wang, L., Bauer, G., Haas, D.L., Xu, D., Stripecke, R., Naldini, L.*, et al.* (1999). Stable transduction of quiescent CD34(+)CD38(-) human hematopoietic cells by HIV-1-based lentiviral vectors. Proc Natl Acad Sci U S A *96*, 2988-2993.
Cattoglio, C., Facchini, G., Sartori, D., Antonelli, A., Miccio, A., Cassani, B., Schmidt, M., von Kalle, C., Howe, S., Thrasher, A.J.*, et al.* (2007). Hot spots of retroviral integration in human CD34+ hematopoietic cells. Blood *110*, 1770-1778.
Cavalieri, S., Cazzaniga, S., Geuna, M., Magnani, Z., Bordignon, C., Naldini, L., and Bonini, C. (2003). Human T lymphocytes transduced by lentiviral vectors in the absence of TCR activation maintain an intact immune competence. Blood *102*, 497-505.
Cavazzana-Calvo, M., Payen, E., Negre, O., Wang, G., Hehir, K., Fusil, F., Down, J., Denaro, M., Brady, T., Westerman, K.*, et al.* (2010). Transfusion independence and HMGA2 activation after gene therapy of human beta-thalassaemia. Nature *467*, 318-322.
Cesana, D., Sgualdino, J., Rudilosso, L., Merella, S., Naldini, L., and Montini, E. (2012). Whole transcriptome characterization of aberrant splicing events induced by lentiviral vector integrations. J Clin Invest *122*, 1667-1676.
Chan, E., Schaller, T., Eddaoudi, A., Zhan, H., Tan, C.P., Jacobsen, M., Thrasher, A.J., Towers, G.J., and Qasim, W. (2012). Lentiviral gene therapy against human immunodeficiency virus type 1, using a novel human TRIM21-cyclophilin A restriction factor. Hum Gene Ther *23*, 1176-1185.
Chandrakasan, S., and Malik, P. (2014). Gene therapy for hemoglobinopathies: the state of the field and the future. Hematol Oncol Clin North Am *28*, 199-216.
Chatterji, U., Bobardt, M.D., Stanfield, R., Ptak, R.G., Pallansch, L.A., Ward, P.A., Jones, M.J., Stoddart, C.A., Scalfaro, P., Dumont, J.M.*, et al.* (2005). Naturally occurring capsid substitutions render HIV-1 cyclophilin A independent in human cells and TRIM-cyclophilin-resistant in Owl monkey cells. J Biol Chem *280*, 40293-40300.
Chen, W., Feng, Y., Chen, D., and Wandinger-Ness, A. (1998). Rab11 is required for trans-golgi network-to-plasma membrane transport and a preferential target for GDP dissociation inhibitor. Mol Biol Cell *9*, 3241-3257.
Chinen, J., Davis, J., De Ravin, S.S., Hay, B.N., Hsu, A.P., Linton, G.F., Naumann, N., Nomicos, E.Y., Silvin, C., Ulrick, J.*, et al.* (2007). Gene therapy improves immune function in preadolescents with X-linked severe combined immunodeficiency. Blood *110*, 67-73.
Chiriaco, M., Farinelli, G., Capo, V., Zonari, E., Scaramuzza, S., Di Matteo, G., Sergi, L.S., Migliavacca, M., Hernandez, R.J., Bombelli, F.*, et al.* (2014). Dual-regulated lentiviral vector for gene therapy of X-linked chronic granulomatosis. Mol Ther *22*, 1472-1483.
Cicalese, M.P., and Aiuti, A. (2015). Clinical applications of gene therapy for primary immunodeficiencies. Hum Gene Ther *26*, 210-219.
Clague, M.J., Schoch, C., Zech, L., and Blumenthal, R. (1990). Gating kinetics of pH-activated membrane fusion of vesicular stomatitis virus with cells: stopped-flow measurements by dequenching of octadecylrhodamine fluorescence. Biochemistry *29*, 1303-1308.
Cleynen, I., and Van de Ven, W.J. (2008). The HMGA proteins: a myriad of functions (Review). Int J Oncol *32*, 289-305.
Cocka, L.J., and Bates, P. (2012). Identification of alternatively translated Tetherin isoforms with differing antiviral and signaling activities. PLoS Pathog *8*, e1002931.
Cockrell, A.S., Ma, H., Fu, K., McCown, T.J., and Kafri, T. (2006). A trans-lentiviral packaging cell line for high-titer conditional self-inactivating HIV-1 vectors. Mol Ther *14*, 276-284.
Coffin, J., Hughes, S., and Varmus, H. (1997a). Retroviruses (United States of America: Cold Spring Harbor Laboratory Press).

Coffin, J.M., Hughes, S.H., and Varmus, H.E. (1997b). The Interactions of Retroviruses and their Hosts. In Retroviruses, J.M. Coffin, S.H. Hughes, and H.E. Varmus, eds. (Cold Spring Harbor (NY)).
Coil, D.A., and Miller, A.D. (2004). Phosphatidylserine is not the cell surface receptor for vesicular stomatitis virus. Journal of virology *78*, 10920-10926.
Collins, M.K., and Cerundolo, V. (2004). Gene therapy meets vaccine development. Trends Biotechnol *22*, 623-626.
Collins, M.K.L., Ellard, F.M., Kingsman, S.M., Mitrophanous, K.A., and Takeuchi, Y. (2000). Packaging cells for retroviral vectors (Google Patents).
Compton, A.A., Bruel, T., Porrot, F., Mallet, A., Sachse, M., Euvrard, M., Liang, C., Casartelli, N., and Schwartz, O. (2014). IFITM proteins incorporated into HIV-1 virions impair viral fusion and spread. Cell Host Microbe *16*, 736-747.
Cook, J.D., and Lee, J.E. (2013). The secret life of viral entry glycoproteins: moonlighting in immune evasion. PLoS Pathog *9*, e1003258.
Cooper, A.R., Patel, S., Senadheera, S., Plath, K., Kohn, D.B., and Hollis, R.P. (2011). Highly efficient large-scale lentiviral vector concentration by tandem tangential flow filtration. J Virol Methods *177*, 1-9.
Coroadinha, A.S., Schucht, R., Gama-Norton, L., Wirth, D., Hauser, H., and Carrondo, M.J. (2006). The use of recombinase mediated cassette exchange in retroviral vector producer cell lines: predictability and efficiency by transgene exchange. J Biotechnol *124*, 457-468.
Cosset, F.L., Takeuchi, Y., Battini, J.L., Weiss, R.A., and Collins, M.K. (1995). High-titer packaging cells producing recombinant retroviruses resistant to human serum. Journal of virology *69*, 7430-7436.
Cronin, J., Zhang, X.Y., and Reiser, J. (2005). Altering the tropism of lentiviral vectors through pseudotyping. Curr Gene Ther *5*, 387-398.
Cundliffe, E. (1989). How antibiotic-producing organisms avoid suicide. Annu Rev Microbiol *43*, 207-233.
Davila, M.L., Riviere, I., Wang, X., Bartido, S., Park, J., Curran, K., Chung, S.S., Stefanski, J., Borquez-Ojeda, O., Olszewska, M.*, et al.* (2014). Efficacy and toxicity management of 19-28z CAR T cell therapy in B cell acute lymphoblastic leukemia. Sci Transl Med *6*, 224ra225.
Decroly, E., Vandenbranden, M., Ruysschaert, J.M., Cogniaux, J., Jacob, G.S., Howard, S.C., Marshall, G., Kompelli, A., Basak, A., Jean, F.*, et al.* (1994). The convertases furin and PC1 can both cleave the human immunodeficiency virus (HIV)-1 envelope glycoprotein gp160 into gp120 (HIV-1 SU) and gp41 (HIV-I TM). The Journal of biological chemistry *269*, 12240-12247.
Deeks, S.G., Autran, B., Berkhout, B., Benkirane, M., Cairns, S., Chomont, N., Chun, T.W., Churchill, M., Di Mascio, M., Katlama, C.*, et al.* (2012). Towards an HIV cure: a global scientific strategy. Nat Rev Immunol *12*, 607-614.
DePolo, N.J., Reed, J.D., Sheridan, P.L., Townsend, K., Sauter, S.L., Jolly, D.J., and Dubensky, T.W., Jr. (2000). VSV-G pseudotyped lentiviral vector particles produced in human cells are inactivated by human serum. Mol Ther *2*, 218-222.
Di Stasi, A., Tey, S.K., Dotti, G., Fujita, Y., Kennedy-Nasser, A., Martinez, C., Straathof, K., Liu, E., Durett, A.G., Grilley, B.*, et al.* (2011). Inducible apoptosis as a safety switch for adoptive cell therapy. N Engl J Med *365*, 1673-1683.
Dijkwel, P.A., and Hamlin, J.L. (1988). Matrix attachment regions are positioned near replication initiation sites, genes, and an interamplicon junction in the amplified dihydrofolate reductase domain of Chinese hamster ovary cells. Molecular and cellular biology *8*, 5398-5409.

Doms, R.W., Keller, D.S., Helenius, A., and Balch, W.E. (1987). Role for adenosine triphosphate in regulating the assembly and transport of vesicular stomatitis virus G protein trimers. J Cell Biol *105*, 1957-1969.
Donello, J.E., Loeb, J.E., and Hope, T.J. (1998). Woodchuck hepatitis virus contains a tripartite posttranscriptional regulatory element. Journal of virology *72*, 5085-5092.
Drummond, A.J., and Rambaut, A. (2007). BEAST: Bayesian evolutionary analysis by sampling trees. BMC Evol Biol *7*, 214.
Dull, T., Zufferey, R., Kelly, M., Mandel, R.J., Nguyen, M., Trono, D., and Naldini, L. (1998). A third-generation lentivirus vector with a conditional packaging system. Journal of virology *72*, 8463-8471.
Durand, S., Nguyen, X.N., Turpin, J., Cordeil, S., Nazaret, N., Croze, S., Mahieux, R., Lachuer, J., Legras-Lachuer, C., and Cimarelli, A. (2013). Tailored HIV-1 vectors for genetic modification of primary human dendritic cells and monocytes. Journal of virology *87*, 234-242.
Durrer, P., Gaudin, Y., Ruigrok, R.W., Graf, R., and Brunner, J. (1995). Photolabeling identifies a putative fusion domain in the envelope glycoprotein of rabies and vesicular stomatitis viruses. J Biol Chem *270*, 17575-17581.
Farmer, P.E. (2013). Shattuck Lecture. Chronic infectious disease and the future of health care delivery. N Engl J Med *369*, 2424-2436.
Farson, D., Witt, R., McGuinness, R., Dull, T., Kelly, M., Song, J., Radeke, R., Bukovsky, A., Consiglio, A., and Naldini, L. (2001). A new-generation stable inducible packaging cell line for lentiviral vectors. Hum Gene Ther *12*, 981-997.
Ferlin, A., Raux, H., Baquero, E., Lepault, J., and Gaudin, Y. (2014). Characterization of pH-sensitive molecular switches that trigger the structural transition of vesicular stomatitis virus glycoprotein from the postfusion state toward the prefusion state. Journal of virology *88*, 13396-13409.
Ferraresso, M. (2014). Construction of stable lentiviral vector packaging cell lines with different viral envelopes. In Faculty of Science and Technology (Italy: The University of Milan), pp. 55.
Finkelshtein, D., Werman, A., Novick, D., Barak, S., and Rubinstein, M. (2013). LDL receptor and its family members serve as the cellular receptors for vesicular stomatitis virus. Proc Natl Acad Sci U S A *110*, 7306-7311.
Fox, K.R., Grigg, G.W., and Waring, M.J. (1987). Sequence-selective binding of phleomycin to DNA. Biochem J *243*, 847-851.
Fredericksen, B.L., and Whitt, M.A. (1995). Vesicular stomatitis virus glycoprotein mutations that affect membrane fusion activity and abolish virus infectivity. Journal of virology *69*, 1435-1443.
Fredericksen, B.L., and Whitt, M.A. (1996). Mutations at two conserved acidic amino acids in the glycoprotein of vesicular stomatitis virus affect pH-dependent conformational changes and reduce the pH threshold for membrane fusion. Virology *217*, 49-57.
Fredericksen, B.L., and Whitt, M.A. (1998). Attenuation of recombinant vesicular stomatitis viruses encoding mutant glycoproteins demonstrate a critical role for maintaining a high pH threshold for membrane fusion in viral fitness. Virology *240*, 349-358.
Fribourgh, J.L., Nguyen, H.C., Matreyek, K.A., Alvarez, F.J., Summers, B.J., Dewdney, T.G., Aiken, C., Zhang, P., Engelman, A., and Xiong, Y. (2014). Structural insight into HIV-1 restriction by MxB. Cell Host Microbe *16*, 627-638.
Friedmann, T., and Roblin, R. (1972). Gene therapy for human genetic disease? Science *175*, 949-955.
Friedmann, T., and Yee, J.K. (1995). Pseudotyped retroviral vectors for studies of human gene therapy. Nat Med *1*, 275-277.

Ganser-Pornillos, B.K., Yeager, M., and Sundquist, W.I. (2008). The structural biology of HIV assembly. Current opinion in structural biology *18*, 203-217.
Gaspar, H.B., Cooray, S., Gilmour, K.C., Parsley, K.L., Adams, S., Howe, S.J., Al Ghonaium, A., Bayford, J., Brown, L., Davies, E.G.*, et al.* (2011a). Long-term persistence of a polyclonal T cell repertoire after gene therapy for X-linked severe combined immunodeficiency. Sci Transl Med *3*, 97ra79.
Gaspar, H.B., Cooray, S., Gilmour, K.C., Parsley, K.L., Zhang, F., Adams, S., Bjorkegren, E., Bayford, J., Brown, L., Davies, E.G.*, et al.* (2011b). Hematopoietic stem cell gene therapy for adenosine deaminase-deficient severe combined immunodeficiency leads to long-term immunological recovery and metabolic correction. Sci Transl Med *3*, 97ra80.
Gaudin, C., Mazauric, M.H., Traikia, M., Guittet, E., Yoshizawa, S., and Fourmy, D. (2005). Structure of the RNA signal essential for translational frameshifting in HIV-1. Journal of molecular biology *349*, 1024-1035.
Gaudin, Y., Ruigrok, R.W., Knossow, M., and Flamand, A. (1993). Low-pH conformational changes of rabies virus glycoprotein and their role in membrane fusion. Journal of virology *67*, 1365-1372.
Gaudin, Y., Tuffereau, C., Durrer, P., Flamand, A., and Ruigrok, R.W. (1995). Biological function of the low-pH, fusion-inactive conformation of rabies virus glycoprotein (G): G is transported in a fusion-inactive state-like conformation. Journal of virology *69*, 5528-5534.
Genovese, P., Schiroli, G., Escobar, G., Di Tomaso, T., Firrito, C., Calabria, A., Moi, D., Mazzieri, R., Bonini, C., Holmes, M.C.*, et al.* (2014). Targeted genome editing in human repopulating haematopoietic stem cells. Nature *510*, 235-240.
Geraerts, M., Michiels, M., Baekelandt, V., Debyser, Z., and Gijsbers, R. (2005). Upscaling of lentiviral vector production by tangential flow filtration. J Gene Med *7*, 1299-1310.
Girard-Gagnepain, A., Amirache, F., Costa, C., Levy, C., Frecha, C., Fusil, F., Negre, D., Lavillette, D., Cosset, F.L., and Verhoeyen, E. (2014). Baboon envelope pseudotyped LVs outperform VSV-G-LVs for gene transfer into early-cytokine-stimulated and resting HSCs. Blood *124*, 1221-1231.
Goff, S.P. (2001). Intracellular trafficking of retroviral genomes during the early phase of infection: viral exploitation of cellular pathways. The journal of gene medicine *3*, 517-528.
Goujon, C., Moncorge, O., Bauby, H., Doyle, T., Ward, C.C., Schaller, T., Hue, S., Barclay, W.S., Schulz, R., and Malim, M.H. (2013). Human MX2 is an interferon-induced post-entry inhibitor of HIV-1 infection. Nature *502*, 559-562.
Graham, F.L., Smiley, J., Russell, W.C., and Nairn, R. (1977). Characteristics of a human cell line transformed by DNA from human adenovirus type 5. The Journal of general virology *36*, 59-74.
Greene, M.R., Lockey, T., Mehta, P.K., Kim, Y.S., Eldridge, P.W., Gray, J.T., and Sorrentino, B.P. (2012). Transduction of human CD34+ repopulating cells with a self-inactivating lentiviral vector for SCID-X1 produced at clinical scale by a stable cell line. Hum Gene Ther Methods *23*, 297-308.
Grez, M., Reichenbach, J., Schwable, J., Seger, R., Dinauer, M.C., and Thrasher, A.J. (2011). Gene therapy of chronic granulomatous disease: the engraftment dilemma. Mol Ther *19*, 28-35.
Grupp, S.A., Kalos, M., Barrett, D., Aplenc, R., Porter, D.L., Rheingold, S.R., Teachey, D.T., Chew, A., Hauck, B., Wright, J.F.*, et al.* (2013). Chimeric antigen receptor-modified T cells for acute lymphoid leukemia. N Engl J Med *368*, 1509-1518.
Hacein-Bey Abina, S., Gaspar, H.B., Blondeau, J., Caccavelli, L., Charrier, S., Buckland, K., Picard, C., Six, E., Himoudi, N., Gilmour, K.*, et al.* (2015). Outcomes following gene therapy in patients with severe Wiskott-Aldrich syndrome. JAMA *313*, 1550-1563.

Hacein-Bey-Abina, S., Garrigue, A., Wang, G.P., Soulier, J., Lim, A., Morillon, E., Clappier, E., Caccavelli, L., Delabesse, E., Beldjord, K.*, et al.* (2008). Insertional oncogenesis in 4 patients after retrovirus-mediated gene therapy of SCID-X1. J Clin Invest *118*, 3132-3142.
Hacein-Bey-Abina, S., Hauer, J., Lim, A., Picard, C., Wang, G.P., Berry, C.C., Martinache, C., Rieux-Laucat, F., Latour, S., Belohradsky, B.H.*, et al.* (2010). Efficacy of gene therapy for X-linked severe combined immunodeficiency. N Engl J Med *363*, 355-364.
Hacein-Bey-Abina, S., Pai, S.Y., Gaspar, H.B., Armant, M., Berry, C.C., Blanche, S., Bleesing, J., Blondeau, J., de Boer, H., Buckland, K.F.*, et al.* (2014). A modified gamma-retrovirus vector for X-linked severe combined immunodeficiency. N Engl J Med *371*, 1407-1417.
Hakata, Y., Yamada, M., Mabuchi, N., and Shida, H. (2002). The carboxy-terminal region of the human immunodeficiency virus type 1 protein Rev has multiple roles in mediating CRM1-related Rev functions. Journal of virology *76*, 8079-8089.
Hanawa, H., Persons, D.A., and Nienhuis, A.W. (2005a). Mobilization and mechanism of transcription of integrated self-inactivating lentiviral vectors. Journal of virology *79*, 8410-8421.
Hanawa, H., Persons, D.A., and Nienhuis, A.W. (2005b). Mobilization and mechanism of transcription of integrated self-inactivating lentiviral vectors. J Virol *79*, 8410-8421.
Harris, R.S., Hultquist, J.F., and Evans, D.T. (2012). The restriction factors of human immunodeficiency virus. J Biol Chem *287*, 40875-40883.
Hershfield, M.S. (1998). Adenosine deaminase deficiency: clinical expression, molecular basis, and therapy. Semin Hematol *35*, 291-298.
Hilditch, L., and Towers, G.J. (2014). A model for cofactor use during HIV-1 reverse transcription and nuclear entry. Current opinion in virology *4*, 32-36.
Hirschberg, K., Miller, C.M., Ellenberg, J., Presley, J.F., Siggia, E.D., Phair, R.D., and Lippincott-Schwartz, J. (1998). Kinetic analysis of secretory protein traffic and characterization of golgi to plasma membrane transport intermediates in living cells. J Cell Biol *143*, 1485-1503.
Hoffmann, M., Wu, Y.J., Gerber, M., Berger-Rentsch, M., Heimrich, B., Schwemmle, M., and Zimmer, G. (2010). Fusion-active glycoprotein G mediates the cytotoxicity of vesicular stomatitis virus M mutants lacking host shut-off activity. The Journal of general virology *91*, 2782-2793.
Hoogerbrugge, P.M., van Beusechem, V.W., Fischer, A., Debree, M., le Deist, F., Perignon, J.L., Morgan, G., Gaspar, B., Fairbanks, L.D., Skeoch, C.H.*, et al.* (1996). Bone marrow gene transfer in three patients with adenosine deaminase deficiency. Gene Ther *3*, 179-183.
Howe, S.J., Mansour, M.R., Schwarzwaelder, K., Bartholomae, C., Hubank, M., Kempski, H., Brugman, M.H., Pike-Overzet, K., Chatters, S.J., de Ridder, D.*, et al.* (2008). Insertional mutagenesis combined with acquired somatic mutations causes leukemogenesis following gene therapy of SCID-X1 patients. J Clin Invest *118*, 3143-3150.
Hrecka, K., Hao, C., Gierszewska, M., Swanson, S.K., Kesik-Brodacka, M., Srivastava, S., Florens, L., Washburn, M.P., and Skowronski, J. (2011). Vpx relieves inhibition of HIV-1 infection of macrophages mediated by the SAMHD1 protein. Nature *474*, 658-661.
Hu, C., Saenz, D.T., Fadel, H.J., Walker, W., Peretz, M., and Poeschla, E.M. (2010). The HIV-1 central polypurine tract functions as a second line of defense against APOBEC3G/F. Journal of virology *84*, 11981-11993.
Iglesias, N., and Stutz, F. (2008). Regulation of mRNP dynamics along the export pathway. FEBS letters *582*, 1987-1996.

Ikeda, Y., Takeuchi, Y., Martin, F., Cosset, F.L., Mitrophanous, K., and Collins, M. (2003a). Continuous high-titer HIV-1 vector production. Nat Biotechnol *21*, 569-572.
Ikeda, Y., Takeuchi, Y., Martin, F., Cosset, F.L., Mitrophanous, K., and Collins, M. (2003b). Continuous high-titer HIV-1 vector production. In Nat Biotechnol (United States), pp. 569-572.
Ikeda, Y., Ylinen, L.M., Kahar-Bador, M., and Towers, G.J. (2004). Influence of gag on human immunodeficiency virus type 1 species-specific tropism. Journal of virology *78*, 11816-11822.
Isel, C., Ehresmann, C., and Marquet, R. (2010). Initiation of HIV Reverse Transcription. Viruses *2*, 213-243.
Janvier, K., Pelchen-Matthews, A., Renaud, J.B., Caillet, M., Marsh, M., and Berlioz-Torrent, C. (2011). The ESCRT-0 component HRS is required for HIV-1 Vpu-mediated BST-2/tetherin down-regulation. PLoS pathogens *7*, e1001265.
Jayakar, H.R., Jeetendra, E., and Whitt, M.A. (2004). Rhabdovirus assembly and budding. Virus Res *106*, 117-132.
Jeetendra, E., Ghosh, K., Odell, D., Li, J., Ghosh, H.P., and Whitt, M.A. (2003). The membrane-proximal region of vesicular stomatitis virus glycoprotein G ectodomain is critical for fusion and virus infectivity. Journal of virology *77*, 12807-12818.
Johannsdottir, H.K., Mancini, R., Kartenbeck, J., Amato, L., and Helenius, A. (2009). Host cell factors and functions involved in vesicular stomatitis virus entry. Journal of virology *83*, 440-453.
Johnson, L.A., Morgan, R.A., Dudley, M.E., Cassard, L., Yang, J.C., Hughes, M.S., Kammula, U.S., Royal, R.E., Sherry, R.M., Wunderlich, J.R.*, et al.* (2009). Gene therapy with human and mouse T-cell receptors mediates cancer regression and targets normal tissues expressing cognate antigen. Blood *114*, 535-546.
June, C.H., Blazar, B.R., and Riley, J.L. (2009). Engineering lymphocyte subsets: tools, trials and tribulations. Nat Rev Immunol *9*, 704-716.
June, C.H., Riddell, S.R., and Schumacher, T.N. (2015). Adoptive cellular therapy: A race to the finish line. Sci Transl Med *7*, 280ps287.
Kalos, M., Levine, B.L., Porter, D.L., Katz, S., Grupp, S.A., Bagg, A., and June, C.H. (2011). T cells with chimeric antigen receptors have potent antitumor effects and can establish memory in patients with advanced leukemia. Sci Transl Med *3*, 95ra73.
Kane, M., Yadav, S.S., Bitzegeio, J., Kutluay, S.B., Zang, T., Wilson, S.J., Schoggins, J.W., Rice, C.M., Yamashita, M., Hatziioannou, T.*, et al.* (2013). MX2 is an interferon-induced inhibitor of HIV-1 infection. Nature *502*, 563-566.
Kang, E.M., Choi, U., Theobald, N., Linton, G., Long Priel, D.A., Kuhns, D., and Malech, H.L. (2010). Retrovirus gene therapy for X-linked chronic granulomatous disease can achieve stable long-term correction of oxidase activity in peripheral blood neutrophils. Blood *115*, 783-791.
Kang, H.J., Bartholomae, C.C., Paruzynski, A., Arens, A., Kim, S., Yu, S.S., Hong, Y., Joo, C.W., Yoon, N.K., Rhim, J.W.*, et al.* (2011). Retroviral gene therapy for X-linked chronic granulomatous disease: results from phase I/II trial. Mol Ther *19*, 2092-2101.
Kao, S.Y., Calman, A.F., Luciw, P.A., and Peterlin, B.M. (1987). Anti-termination of transcription within the long terminal repeat of HIV-1 by tat gene product. Nature *330*, 489-493.
Kaplan, A.H., and Swanstrom, R. (1991). Human immunodeficiency virus type 1 Gag proteins are processed in two cellular compartments. Proc Natl Acad Sci U S A *88*, 4528-4532.
Karreman, S., Hauser, H., and Karreman, C. (1996). On the use of double FLP recognition targets (FRTs) in the LTR of retroviruses for the construction of high producer cell lines. Nucleic Acids Res *24*, 1616-1624.

Kaufmann, K.B., Buning, H., Galy, A., Schambach, A., and Grez, M. (2013). Gene therapy on the move. EMBO Mol Med *5*, 1642-1661.
Kay, M.A. (2011). State-of-the-art gene-based therapies: the road ahead. Nat Rev Genet *12*, 316-328.
Khan, M.A., Aberham, C., Kao, S., Akari, H., Gorelick, R., Bour, S., and Strebel, K. (2001). Human immunodeficiency virus type 1 Vif protein is packaged into the nucleoprotein complex through an interaction with viral genomic RNA. Journal of virology *75*, 7252-7265.
Kim, H., and Kim, J.S. (2014). A guide to genome engineering with programmable nucleases. Nat Rev Genet *15*, 321-334.
Kinomoto, M., Kanno, T., Shimura, M., Ishizaka, Y., Kojima, A., Kurata, T., Sata, T., and Tokunaga, K. (2007). All APOBEC3 family proteins differentially inhibit LINE-1 retrotransposition. Nucleic Acids Res *35*, 2955-2964.
Klages, N., Zufferey, R., and Trono, D. (2000). A stable system for the high-titer production of multiply attenuated lentiviral vectors. Mol Ther *2*, 170-176.
Klasse, P.J. (2012). The molecular basis of HIV entry. Cellular microbiology *14*, 1183-1192.
Knight, S. (2011). Lentiviral Vectors for Gene Therapy. In Division of Infection and Immunity (London, UK: University College London), pp. 349.
Knight, S., Bokhoven, M., Collins, M., and Takeuchi, Y. (2010). Effect of the internal promoter on insertional gene activation by lentiviral vectors with an intact HIV long terminal repeat. Journal of virology *84*, 4856-4859.
Kochenderfer, J.N., Dudley, M.E., Feldman, S.A., Wilson, W.H., Spaner, D.E., Maric, I., Stetler-Stevenson, M., Phan, G.Q., Hughes, M.S., Sherry, R.M.*, et al.* (2012). B-cell depletion and remissions of malignancy along with cytokine-associated toxicity in a clinical trial of anti-CD19 chimeric-antigen-receptor-transduced T cells. Blood *119*, 2709-2720.
Kochenderfer, J.N., Dudley, M.E., Kassim, S.H., Somerville, R.P., Carpenter, R.O., Stetler-Stevenson, M., Yang, J.C., Phan, G.Q., Hughes, M.S., Sherry, R.M.*, et al.* (2015). Chemotherapy-refractory diffuse large B-cell lymphoma and indolent B-cell malignancies can be effectively treated with autologous T cells expressing an anti-CD19 chimeric antigen receptor. J Clin Oncol *33*, 540-549.
Kochenderfer, J.N., and Rosenberg, S.A. (2013). Treating B-cell cancer with T cells expressing anti-CD19 chimeric antigen receptors. Nat Rev Clin Oncol *10*, 267-276.
Kochenderfer, J.N., Yu, Z., Frasheri, D., Restifo, N.P., and Rosenberg, S.A. (2010). Adoptive transfer of syngeneic T cells transduced with a chimeric antigen receptor that recognizes murine CD19 can eradicate lymphoma and normal B cells. Blood *116*, 3875-3886.
Kohn, D.B. (2008). Gene therapy for childhood immunological diseases. Bone Marrow Transplant *41*, 199-205.
Kohn, D.B., Hershfield, M.S., Carbonaro, D., Shigeoka, A., Brooks, J., Smogorzewska, E.M., Barsky, L.W., Chan, R., Burotto, F., Annett, G.*, et al.* (1998). T lymphocytes with a normal ADA gene accumulate after transplantation of transduced autologous umbilical cord blood CD34+ cells in ADA-deficient SCID neonates. Nat Med *4*, 775-780.
Kong, J., Kim, S.R., Binley, K., Pata, I., Doi, K., Mannik, J., Zernant-Rajang, J., Kan, O., Iqball, S., Naylor, S.*, et al.* (2008). Correction of the disease phenotype in the mouse model of Stargardt disease by lentiviral gene therapy. Gene Ther *15*, 1311-1320.
Koning, F.A., Newman, E.N., Kim, E.Y., Kunstman, K.J., Wolinsky, S.M., and Malim, M.H. (2009). Defining APOBEC3 expression patterns in human tissues and hematopoietic cell subsets. Journal of virology *83*, 9474-9485.

Kootstra, N.A., Navis, M., Beugeling, C., van Dort, K.A., and Schuitemaker, H. (2007). The presence of the Trim5alpha escape mutation H87Q in the capsid of late stage HIV-1 variants is preceded by a prolonged asymptomatic infection phase. Aids *21*, 2015-2023.
Kotwal, G.J., Capone, J., Irving, R.A., Rhee, S.H., Bilan, P., Toneguzzo, F., Hofmann, T., and Ghosh, H.P. (1983). Viral membrane glycoproteins: comparison of the amino terminal amino acid sequences of the precursor and mature glycoproteins of three serotypes of vesicular stomatitis virus. Virology *129*, 1-11.
Kuhlcke, K., Fehse, B., Schilz, A., Loges, S., Lindemann, C., Ayuk, F., Lehmann, F., Stute, N., Fauser, A.A., Zander, A.R.*, et al.* (2002). Highly efficient retroviral gene transfer based on centrifugation-mediated vector preloading of tissue culture vessels. Mol Ther *5*, 473-478.
Kumar, M.S., Armenteros-Monterroso, E., East, P., Chakravorty, P., Matthews, N., Winslow, M.M., and Downward, J. (2014). HMGA2 functions as a competing endogenous RNA to promote lung cancer progression. Nature *505*, 212-217.
Kutluay, S.B., and Bieniasz, P.D. (2010). Analysis of the initiating events in HIV-1 particle assembly and genome packaging. PLoS pathogens *6*, e1001200.
Kuzmin, I.V., Novella, I.S., Dietzgen, R.G., Padhi, A., and Rupprecht, C.E. (2009). The rhabdoviruses: biodiversity, phylogenetics, and evolution. Infect Genet Evol *9*, 541-553.
Laguette, N., Sobhian, B., Casartelli, N., Ringeard, M., Chable-Bessia, C., Segeral, E., Yatim, A., Emiliani, S., Schwartz, O., and Benkirane, M. (2011). SAMHD1 is the dendritic- and myeloid-cell-specific HIV-1 restriction factor counteracted by Vpx. Nature *474*, 654-657.
Lahouassa, H., Daddacha, W., Hofmann, H., Ayinde, D., Logue, E.C., Dragin, L., Bloch, N., Maudet, C., Bertrand, M., Gramberg, T.*, et al.* (2012). SAMHD1 restricts the replication of human immunodeficiency virus type 1 by depleting the intracellular pool of deoxynucleoside triphosphates. Nat Immunol *13*, 223-228.
Leboulch, P. (2013). Gene therapy: primed for take-off. Nature *500*, 280-282.
Leboulch, P., Huang, G.M., Humphries, R.K., Oh, Y.H., Eaves, C.J., Tuan, D.Y., and London, I.M. (1994). Mutagenesis of retroviral vectors transducing human beta-globin gene and beta-globin locus control region derivatives results in stable transmission of an active transcriptional structure. EMBO J *13*, 3065-3076.
Lee, D.W., Kochenderfer, J.N., Stetler-Stevenson, M., Cui, Y.K., Delbrook, C., Feldman, S.A., Fry, T.J., Orentas, R., Sabatino, M., Shah, N.N.*, et al.* (2015). T cells expressing CD19 chimeric antigen receptors for acute lymphoblastic leukaemia in children and young adults: a phase 1 dose-escalation trial. Lancet *385*, 517-528.
Levine, B.L., Humeau, L.M., Boyer, J., MacGregor, R.R., Rebello, T., Lu, X., Binder, G.K., Slepushkin, V., Lemiale, F., Mascola, J.R.*, et al.* (2006). Gene transfer in humans using a conditionally replicating lentiviral vector. Proc Natl Acad Sci U S A *103*, 17372-17377.
Li, M., Ablan, S.D., Miao, C., Zheng, Y.M., Fuller, M.S., Rennert, P.D., Maury, W., Johnson, M.C., Freed, E.O., and Liu, S.L. (2014). TIM-family proteins inhibit HIV-1 release. Proc Natl Acad Sci U S A *111*, E3699-3707.
Li, Y., Drone, C., Sat, E., and Ghosh, H.P. (1993). Mutational analysis of the vesicular stomatitis virus glycoprotein G for membrane fusion domains. Journal of virology *67*, 4070-4077.
Libersou, S., Albertini, A.A., Ouldali, M., Maury, V., Maheu, C., Raux, H., de Haas, F., Roche, S., Gaudin, Y., and Lepault, J. (2010). Distinct structural rearrangements of the VSV glycoprotein drive membrane fusion. J Cell Biol *191*, 199-210.
Linette, G.P., Stadtmauer, E.A., Maus, M.V., Rapoport, A.P., Levine, B.L., Emery, L., Litzky, L., Bagg, A., Carreno, B.M., Cimino, P.J.*, et al.* (2013). Cardiovascular toxicity and

titin cross-reactivity of affinity-enhanced T cells in myeloma and melanoma. Blood *122*, 863-871.
Liu, Z., Pan, Q., Ding, S., Qian, J., Xu, F., Zhou, J., Cen, S., Guo, F., and Liang, C. (2013). The interferon-inducible MxB protein inhibits HIV-1 infection. Cell Host Microbe *14*, 398-410.
Loew, R., Meyer, Y., Kuehlcke, K., Gama-Norton, L., Wirth, D., Hauser, H., Stein, S., Grez, M., Thornhill, S., Thrasher, A.*, et al.* (2010). A new PG13-based packaging cell line for stable production of clinical-grade self-inactivating gamma-retroviral vectors using targeted integration. Gene Ther *17*, 272-280.
Logan, A.C., Haas, D.L., Kafri, T., and Kohn, D.B. (2004). Integrated self-inactivating lentiviral vectors produce full-length genomic transcripts competent for encapsidation and integration. Journal of virology *78*, 8421-8436.
Lombardo, A., Cesana, D., Genovese, P., Di Stefano, B., Provasi, E., Colombo, D.F., Neri, M., Magnani, Z., Cantore, A., Lo Riso, P.*, et al.* (2011). Site-specific integration and tailoring of cassette design for sustainable gene transfer. Nat Methods *8*, 861-869.
Lombardo, A., and Naldini, L. (2014). Genome editing: a tool for research and therapy: targeted genome editing hits the clinic. Nat Med *20*, 1101-1103.
Lopes, L., Dewannieux, M., Gileadi, U., Bailey, R., Ikeda, Y., Whittaker, C., Collin, M.P., Cerundolo, V., Tomihari, M., Ariizumi, K.*, et al.* (2008). Immunization with a lentivector that targets tumor antigen expression to dendritic cells induces potent CD8+ and CD4+ T-cell responses. Journal of virology *82*, 86-95.
Louis, C.U., Savoldo, B., Dotti, G., Pule, M., Yvon, E., Myers, G.D., Rossig, C., Russell, H.V., Diouf, O., Liu, E.*, et al.* (2011). Antitumor activity and long-term fate of chimeric antigen receptor-positive T cells in patients with neuroblastoma. Blood *118*, 6050-6056.
Machen, T.E., Leigh, M.J., Taylor, C., Kimura, T., Asano, S., and Moore, H.P. (2003). pH of TGN and recycling endosomes of H+/K+-ATPase-transfected HEK-293 cells: implications for pH regulation in the secretory pathway. Am J Physiol Cell Physiol *285*, C205-214.
Malim, M.H. (2009). APOBEC proteins and intrinsic resistance to HIV-1 infection. Philos Trans R Soc Lond B Biol Sci *364*, 675-687.
Malim, M.H., and Bieniasz, P.D. (2012). HIV Restriction Factors and Mechanisms of Evasion. Cold Spring Harb Perspect Med *2*, a006940.
Mann, R., Mulligan, R.C., and Baltimore, D. (1983). Construction of a retrovirus packaging mutant and its use to produce helper-free defective retrovirus. Cell *33*, 153-159.
Marin, M., Tailor, C.S., Nouri, A., and Kabat, D. (2000). Sodium-dependent neutral amino acid transporter type 1 is an auxiliary receptor for baboon endogenous retrovirus. Journal of virology *74*, 8085-8093.
Marshall, H.M., Ronen, K., Berry, C., Llano, M., Sutherland, H., Saenz, D., Bickmore, W., Poeschla, E., and Bushman, F.D. (2007). Role of PSIP1/LEDGF/p75 in lentiviral infectivity and integration targeting. PloS one *2*, e1340.
Martin-Serrano, J., and Neil, S.J. (2011). Host factors involved in retroviral budding and release. Nature reviews Microbiology *9*, 519-531.
Martinez, I., and Wertz, G.W. (2005). Biological differences between vesicular stomatitis virus Indiana and New Jersey serotype glycoproteins: identification of amino acid residues modulating pH-dependent infectivity. Journal of virology *79*, 3578-3585.
Matrai, J., Chuah, M.K., and VandenDriessche, T. (2010). Recent advances in lentiviral vector development and applications. Mol Ther *18*, 477-490.
Matreyek, K.A., Wang, W., Serrao, E., Singh, P.K., Levin, H.L., and Engelman, A. (2014). Host and viral determinants for MxB restriction of HIV-1 infection. Retrovirology *11*, 90.

Maude, S.L., Frey, N., Shaw, P.A., Aplenc, R., Barrett, D.M., Bunin, N.J., Chew, A., Gonzalez, V.E., Zheng, Z., Lacey, S.F., *et al.* (2014). Chimeric antigen receptor T cells for sustained remissions in leukemia. N Engl J Med *371*, 1507-1517.
May, C., Rivella, S., Callegari, J., Heller, G., Gaensler, K.M., Luzzatto, L., and Sadelain, M. (2000). Therapeutic haemoglobin synthesis in beta-thalassaemic mice expressing lentivirus-encoded human beta-globin. Nature *406*, 82-86.
Mazurier, F., Gan, O.I., McKenzie, J.L., Doedens, M., and Dick, J.E. (2004). Lentivector-mediated clonal tracking reveals intrinsic heterogeneity in the human hematopoietic stem cell compartment and culture-induced stem cell impairment. Blood *103*, 545-552.
Merten, O.W. (2004). State-of-the-art of the production of retroviral vectors. J Gene Med *6 Suppl 1*, S105-124.
Merten, O.W., Charrier, S., Laroudie, N., Fauchille, S., Dugue, C., Jenny, C., Audit, M., Zanta-Boussif, M.A., Chautard, H., Radrizzani, M., *et al.* (2011). Large-scale manufacture and characterization of a lentiviral vector produced for clinical ex vivo gene therapy application. Hum Gene Ther *22*, 343-356.
Miller, A.D., Jolly, D.J., Friedmann, T., and Verma, I.M. (1983). A transmissible retrovirus expressing human hypoxanthine phosphoribosyltransferase (HPRT): gene transfer into cells obtained from humans deficient in HPRT. Proc Natl Acad Sci U S A *80*, 4709-4713.
Miller, A.D., and Metzger, M.J. (2011). APOBEC3-mediated hypermutation of retroviral vectors produced from some retrovirus packaging cell lines. Gene Ther *18*, 528-530.
Millevoi, S., and Vagner, S. (2010). Molecular mechanisms of eukaryotic pre-mRNA 3' end processing regulation. Nucleic acids research *38*, 2757-2774.
Mire, C.E., White, J.M., and Whitt, M.A. (2010). A spatio-temporal analysis of matrix protein and nucleocapsid trafficking during vesicular stomatitis virus uncoating. PLoS Pathog *6*, e1000994.
Mitchell, R.S., Beitzel, B.F., Schroder, A.R., Shinn, P., Chen, H., Berry, C.C., Ecker, J.R., and Bushman, F.D. (2004). Retroviral DNA integration: ASLV, HIV, and MLV show distinct target site preferences. PLoS Biol *2*, E234.
Miyoshi, H., Blomer, U., Takahashi, M., Gage, F.H., and Verma, I.M. (1998). Development of a self-inactivating lentivirus vector. Journal of virology *72*, 8150-8157.
Modlich, U., Navarro, S., Zychlinski, D., Maetzig, T., Knoess, S., Brugman, M.H., Schambach, A., Charrier, S., Galy, A., Thrasher, A.J., *et al.* (2009). Insertional transformation of hematopoietic cells by self-inactivating lentiviral and gammaretroviral vectors. Mol Ther *17*, 1919-1928.
Moiani, A., Paleari, Y., Sartori, D., Mezzadra, R., Miccio, A., Cattoglio, C., Cocchiarella, F., Lidonnici, M.R., Ferrari, G., and Mavilio, F. (2012). Lentiviral vector integration in the human genome induces alternative splicing and generates aberrant transcripts. J Clin Invest *122*, 1653-1666.
Montini, E., Cesana, D., Schmidt, M., Sanvito, F., Bartholomae, C.C., Ranzani, M., Benedicenti, F., Sergi, L.S., Ambrosi, A., Ponzoni, M., *et al.* (2009). The genotoxic potential of retroviral vectors is strongly modulated by vector design and integration site selection in a mouse model of HSC gene therapy. J Clin Invest *119*, 964-975.
Montini, E., Cesana, D., Schmidt, M., Sanvito, F., Ponzoni, M., Bartholomae, C., Sergi Sergi, L., Benedicenti, F., Ambrosi, A., Di Serio, C., *et al.* (2006). Hematopoietic stem cell gene transfer in a tumor-prone mouse model uncovers low genotoxicity of lentiviral vector integration. Nat Biotechnol *24*, 687-696.
Morgan, R.A., Dudley, M.E., Wunderlich, J.R., Hughes, M.S., Yang, J.C., Sherry, R.M., Royal, R.E., Topalian, S.L., Kammula, U.S., Restifo, N.P., *et al.* (2006). Cancer regression in patients after transfer of genetically engineered lymphocytes. Science *314*, 126-129.

Morgan, R.A., Yang, J.C., Kitano, M., Dudley, M.E., Laurencot, C.M., and Rosenberg, S.A. (2010). Case report of a serious adverse event following the administration of T cells transduced with a chimeric antigen receptor recognizing ERBB2. Mol Ther *18*, 843-851.
Mougel, M., Houzet, L., and Darlix, J.L. (2009). When is it time for reverse transcription to start and go? Retrovirology *6*, 24.
Mukherjee, S., and Thrasher, A.J. (2013). Gene therapy for PIDs: Progress, pitfalls and prospects. Gene.
Munch, R.C., Muhlebach, M.D., Schaser, T., Kneissl, S., Jost, C., Pluckthun, A., Cichutek, K., and Buchholz, C.J. (2011). DARPins: an efficient targeting domain for lentiviral vectors. Mol Ther *19*, 686-693.
Nabel, G., and Baltimore, D. (1987). An inducible transcription factor activates expression of human immunodeficiency virus in T cells. Nature *326*, 711-713.
Naciri, M., Kuystermans, D., and Al-Rubeai, M. (2008). Monitoring pH and dissolved oxygen in mammalian cell culture using optical sensors. Cytotechnology *57*, 245-250.
Naghavi, M.H., and Goff, S.P. (2007). Retroviral proteins that interact with the host cell cytoskeleton. Current opinion in immunology *19*, 402-407.
Naldini, L. (2011). Ex vivo gene transfer and correction for cell-based therapies. Nat Rev Genet *12*, 301-315.
Naldini, L., Blomer, U., Gallay, P., Ory, D., Mulligan, R., Gage, F.H., Verma, I.M., and Trono, D. (1996). In vivo gene delivery and stable transduction of nondividing cells by a lentiviral vector. Science *272*, 263-267.
Nayak, S., and Herzog, R.W. (2010). Progress and prospects: immune responses to viral vectors. Gene Ther *17*, 295-304.
Neagu, M.R., Ziegler, P., Pertel, T., Strambio-De-Castillia, C., Grutter, C., Martinetti, G., Mazzucchelli, L., Grutter, M., Manz, M.G., and Luban, J. (2009). Potent inhibition of HIV-1 by TRIM5-cyclophilin fusion proteins engineered from human components. J Clin Invest *119*, 3035-3047.
Negre, O., Bartholomae, C., Beuzard, Y., Cavazzana, M., Christiansen, L., Courne, C., Deichmann, A., Denaro, M., de Dreuzy, E., Finer, M.*, et al.* (2015). Preclinical evaluation of efficacy and safety of an improved lentiviral vector for the treatment of beta-thalassemia and sickle cell disease. Curr Gene Ther *15*, 64-81.
Neil, S.J. (2013). The antiviral activities of tetherin. Curr Top Microbiol Immunol *371*, 67-104.
Neil, S.J., Zang, T., and Bieniasz, P.D. (2008). Tetherin inhibits retrovirus release and is antagonized by HIV-1 Vpu. Nature *451*, 425-430.
Newrzela, S., Cornils, K., Li, Z., Baum, C., Brugman, M.H., Hartmann, M., Meyer, J., Hartmann, S., Hansmann, M.L., Fehse, B.*, et al.* (2008). Resistance of mature T cells to oncogene transformation. Blood *112*, 2278-2286.
Ni, Y., Sun, S., Oparaocha, I., Humeau, L., Davis, B., Cohen, R., Binder, G., Chang, Y.N., Slepushkin, V., and Dropulic, B. (2005). Generation of a packaging cell line for prolonged large-scale production of high-titer HIV-1-based lentiviral vector. J Gene Med *7*, 818-834.
Nie, Z., Phenix, B.N., Lum, J.J., Alam, A., Lynch, D.H., Beckett, B., Krammer, P.H., Sekaly, R.P., and Badley, A.D. (2002). HIV-1 protease processes procaspase 8 to cause mitochondrial release of cytochrome c, caspase cleavage and nuclear fragmentation. Cell Death Differ *9*, 1172-1184.
Nisole, S., Stoye, J.P., and Saib, A. (2005). TRIM family proteins: retroviral restriction and antiviral defence. Nat Rev Microbiol *3*, 799-808.
Notarangelo, L.D., Miao, C.H., and Ochs, H.D. (2008). Wiskott-Aldrich syndrome. Curr Opin Hematol *15*, 30-36.

O'Doherty, U., Swiggard, W.J., and Malim, M.H. (2000). Human immunodeficiency virus type 1 spinoculation enhances infection through virus binding. Journal of virology *74*, 10074-10080.
Ono, A., and Freed, E.O. (2001). Plasma membrane rafts play a critical role in HIV-1 assembly and release. Proc Natl Acad Sci U S A *98*, 13925-13930.
Onodera, M., Ariga, T., Kawamura, N., Kobayashi, I., Ohtsu, M., Yamada, M., Tame, A., Furuta, H., Okano, M., Matsumoto, S.*, et al.* (1998). Successful peripheral T-lymphocyte-directed gene transfer for a patient with severe combined immune deficiency caused by adenosine deaminase deficiency. Blood *91*, 30-36.
Ott, M.G., Schmidt, M., Schwarzwaelder, K., Stein, S., Siler, U., Koehl, U., Glimm, H., Kuhlcke, K., Schilz, A., Kunkel, H.*, et al.* (2006). Correction of X-linked chronic granulomatous disease by gene therapy, augmented by insertional activation of MDS1-EVI1, PRDM16 or SETBP1. Nat Med *12*, 401-409.
Overbaugh, J., Miller, A.D., and Eiden, M.V. (2001). Receptors and entry cofactors for retroviruses include single and multiple transmembrane-spanning proteins as well as newly described glycophosphatidylinositol-anchored and secreted proteins. Microbiology and molecular biology reviews : MMBR *65*, 371-389, table of contents.
Pak, C.C., Puri, A., and Blumenthal, R. (1997). Conformational changes and fusion activity of vesicular stomatitis virus glycoprotein: [125I]iodonaphthyl azide photolabeling studies in biological membranes. Biochemistry *36*, 8890-8896.
Palfi, S., Gurruchaga, J.M., Ralph, G.S., Lepetit, H., Lavisse, S., Buttery, P.C., Watts, C., Miskin, J., Kelleher, M., Deeley, S.*, et al.* (2014). Long-term safety and tolerability of ProSavin, a lentiviral vector-based gene therapy for Parkinson's disease: a dose escalation, open-label, phase 1/2 trial. Lancet *383*, 1138-1146.
Park, T.S., Rosenberg, S.A., and Morgan, R.A. (2011). Treating cancer with genetically engineered T cells. Trends Biotechnol *29*, 550-557.
Parkhurst, M.R., Yang, J.C., Langan, R.C., Dudley, M.E., Nathan, D.A., Feldman, S.A., Davis, J.L., Morgan, R.A., Merino, M.J., Sherry, R.M.*, et al.* (2011). T cells targeting carcinoembryonic antigen can mediate regression of metastatic colorectal cancer but induce severe transient colitis. Mol Ther *19*, 620-626.
Paruzynski, A., Arens, A., Gabriel, R., Bartholomae, C.C., Scholz, S., Wang, W., Wolf, S., Glimm, H., Schmidt, M., and von Kalle, C. (2010). Genome-wide high-throughput integrome analyses by nrLAM-PCR and next-generation sequencing. Nat Protoc *5*, 1379-1395.
Pauszek, S.J., Allende, R., and Rodriguez, L.L. (2008). Characterization of the full-length genomic sequences of vesicular stomatitis Cocal and Alagoas viruses. Arch Virol *153*, 1353-1357.
Pauszek, S.J., Barrera Jdel, C., Goldberg, T., Allende, R., and Rodriguez, L.L. (2011). Genetic and antigenic relationships of vesicular stomatitis viruses from South America. Arch Virol *156*, 1961-1968.
Perez-Caballero, D., Zang, T., Ebrahimi, A., McNatt, M.W., Gregory, D.A., Johnson, M.C., and Bieniasz, P.D. (2009). Tetherin inhibits HIV-1 release by directly tethering virions to cells. Cell *139*, 499-511.
Pertel, T., Hausmann, S., Morger, D., Zuger, S., Guerra, J., Lascano, J., Reinhard, C., Santoni, F.A., Uchil, P.D., Chatel, L.*, et al.* (2011a). TRIM5 is an innate immune sensor for the retrovirus capsid lattice. Nature *472*, 361-365.
Pertel, T., Reinhard, C., and Luban, J. (2011b). Vpx rescues HIV-1 transduction of dendritic cells from the antiviral state established by type 1 interferon. Retrovirology *8*, 49.
Pichlmair, A., Diebold, S.S., Gschmeissner, S., Takeuchi, Y., Ikeda, Y., Collins, M.K., and Reis e Sousa, C. (2007). Tubulovesicular structures within vesicular stomatitis virus G

protein-pseudotyped lentiviral vector preparations carry DNA and stimulate antiviral responses via Toll-like receptor 9. Journal of virology *81*, 539-547.
Pickl, W.F., Pimentel-Muinos, F.X., and Seed, B. (2001). Lipid rafts and pseudotyping. Journal of virology *75*, 7175-7183.
Pollard, V.W., and Malim, M.H. (1998). The HIV-1 Rev protein. Annu Rev Microbiol *52*, 491-532.
Porter, D.L., Levine, B.L., Kalos, M., Bagg, A., and June, C.H. (2011). Chimeric antigen receptor-modified T cells in chronic lymphoid leukemia. N Engl J Med *365*, 725-733.
Poznansky, M., Lever, A., Bergeron, L., Haseltine, W., and Sodroski, J. (1991). Gene transfer into human lymphocytes by a defective human immunodeficiency virus type 1 vector. Journal of virology *65*, 532-536.
Puigbo, P., Bravo, I.G., and Garcia-Vallve, S. (2008). CAIcal: a combined set of tools to assess codon usage adaptation. Biol Direct *3*, 38.
Pule, M.A., Savoldo, B., Myers, G.D., Rossig, C., Russell, H.V., Dotti, G., Huls, M.H., Liu, E., Gee, A.P., Mei, Z.*, et al.* (2008). Virus-specific T cells engineered to coexpress tumor-specific receptors: persistence and antitumor activity in individuals with neuroblastoma. Nat Med *14*, 1264-1270.
Ramezani, A., Hawley, T.S., and Hawley, R.G. (2000). Lentiviral vectors for enhanced gene expression in human hematopoietic cells. Molecular therapy : the journal of the American Society of Gene Therapy *2*, 458-469.
Rasaiyaah, J., Tan, C.P., Fletcher, A.J., Price, A.J., Blondeau, C., Hilditch, L., Jacques, D.A., Selwood, D.L., James, L.C., Noursadeghi, M.*, et al.* (2013). HIV-1 evades innate immune recognition through specific cofactor recruitment. Nature *503*, 402-405.
Rasko, J.E., Battini, J.L., Gottschalk, R.J., Mazo, I., and Miller, A.D. (1999). The RD114/simian type D retrovirus receptor is a neutral amino acid transporter. Proc Natl Acad Sci U S A *96*, 2129-2134.
Reeves, R.H., Nash, W.G., and O'Brien, S.J. (1985). Genetic mapping of endogenous RD-114 retroviral sequences of domestic cats. Journal of virology *56*, 303-306.
Reiser, J., Harmison, G., Kluepfel-Stahl, S., Brady, R.O., Karlsson, S., and Schubert, M. (1996). Transduction of nondividing cells using pseudotyped defective high-titer HIV type 1 particles. Proc Natl Acad Sci U S A *93*, 15266-15271.
Relander, T., Johansson, M., Olsson, K., Ikeda, Y., Takeuchi, Y., Collins, M., and Richter, J. (2005). Gene transfer to repopulating human CD34+ cells using amphotropic-, GALV-, or RD114-pseudotyped HIV-1-based vectors from stable producer cells. Mol Ther *11*, 452-459.
Riviere, L., Darlix, J.L., and Cimarelli, A. (2010). Analysis of the viral elements required in the nuclear import of HIV-1 DNA. Journal of virology *84*, 729-739.
Robbins, P.F., Morgan, R.A., Feldman, S.A., Yang, J.C., Sherry, R.M., Dudley, M.E., Wunderlich, J.R., Nahvi, A.V., Helman, L.J., Mackall, C.L.*, et al.* (2011). Tumor regression in patients with metastatic synovial cell sarcoma and melanoma using genetically engineered lymphocytes reactive with NY-ESO-1. J Clin Oncol *29*, 917-924.
Roberts, P.C., Kipperman, T., and Compans, R.W. (1999). Vesicular stomatitis virus G protein acquires pH-independent fusion activity during transport in a polarized endometrial cell line. Journal of virology *73*, 10447-10457.
Roche, S., Albertini, A.A., Lepault, J., Bressanelli, S., and Gaudin, Y. (2008). Structures of vesicular stomatitis virus glycoprotein: membrane fusion revisited. Cell Mol Life Sci *65*, 1716-1728.
Roche, S., Bressanelli, S., Rey, F.A., and Gaudin, Y. (2006). Crystal structure of the low-pH form of the vesicular stomatitis virus glycoprotein G. Science *313*, 187-191.

Roche, S., and Gaudin, Y. (2002). Characterization of the equilibrium between the native and fusion-inactive conformation of rabies virus glycoprotein indicates that the fusion complex is made of several trimers. Virology *297*, 128-135.
Roche, S., Rey, F.A., Gaudin, Y., and Bressanelli, S. (2007). Structure of the prefusion form of the vesicular stomatitis virus glycoprotein G. Science *315*, 843-848.
Rodrigues, A.F., Carmo, M., Alves, P.M., and Coroadinha, A.S. (2009). Retroviral vector production under serum deprivation: The role of lipids. Biotechnol Bioeng *104*, 1171-1181.
Rold, C.J., and Aiken, C. (2008). Proteasomal degradation of TRIM5alpha during retrovirus restriction. PLoS Pathog *4*, e1000074.
Rosenberg, S.A., Aebersold, P., Cornetta, K., Kasid, A., Morgan, R.A., Moen, R., Karson, E.M., Lotze, M.T., Yang, J.C., Topalian, S.L*., et al.* (1990). Gene transfer into humans--immunotherapy of patients with advanced melanoma, using tumor-infiltrating lymphocytes modified by retroviral gene transduction. N Engl J Med *323*, 570-578.
Rosenberg, S.A., and Restifo, N.P. (2015). Adoptive cell transfer as personalized immunotherapy for human cancer. Science *348*, 62-68.
Rossi, J.J., June, C.H., and Kohn, D.B. (2007). Genetic therapies against HIV. Nat Biotechnol *25*, 1444-1454.
Ryoo, J., Choi, J., Oh, C., Kim, S., Seo, M., Kim, S.Y., Seo, D., Kim, J., White, T.E., Brandariz-Nunez, A*., et al.* (2014). The ribonuclease activity of SAMHD1 is required for HIV-1 restriction. Nat Med *20*, 936-941.
Sainski, A.M., Natesampillai, S., Cummins, N.W., Bren, G.D., Taylor, J., Saenz, D.T., Poeschla, E.M., and Badley, A.D. (2011). The HIV-1-specific protein Casp8p41 induces death of infected cells through Bax/Bak. Journal of virology *85*, 7965-7975.
Sakuma, T., Barry, M.A., and Ikeda, Y. (2012). Lentiviral vectors: basic to translational. Biochem J *443*, 603-618.
Sambrook, J., Westphal, H., Srinivasan, P.R., and Dulbecco, R. (1968). The integrated state of viral DNA in SV40-transformed cells. Proc Natl Acad Sci U S A *60*, 1288-1295.
Sanber, K.S., Knight, S.B., Stephen, S.L., Bailey, R., Escors, D., Minshull, J., Santilli, G., Thrasher, A.J., Collins, M.K., and Takeuchi, Y. (2015). Construction of stable packaging cell lines for clinical lentiviral vector production. Sci Rep *5*, 9021.
Sandrin, V., Boson, B., Salmon, P., Gay, W., Negre, D., Le Grand, R., Trono, D., and Cosset, F.L. (2002). Lentiviral vectors pseudotyped with a modified RD114 envelope glycoprotein show increased stability in sera and augmented transduction of primary lymphocytes and CD34+ cells derived from human and nonhuman primates. Blood *100*, 823-832.
Schaller, T., Ocwieja, K.E., Rasaiyaah, J., Price, A.J., Brady, T.L., Roth, S.L., Hue, S., Fletcher, A.J., Lee, K., KewalRamani, V.N*., et al.* (2011). HIV-1 capsid-cyclophilin interactions determine nuclear import pathway, integration targeting and replication efficiency. PLoS Pathog *7*, e1002439.
Schambach, A., Bohne, J., Baum, C., Hermann, F.G., Egerer, L., von Laer, D., and Giroglou, T. (2006). Woodchuck hepatitis virus post-transcriptional regulatory element deleted from X protein and promoter sequences enhances retroviral vector titer and expression. Gene therapy *13*, 641-645.
Schlegel, R., Tralka, T.S., Willingham, M.C., and Pastan, I. (1983). Inhibition of VSV binding and infectivity by phosphatidylserine: is phosphatidylserine a VSV-binding site? Cell *32*, 639-646.
Scholler, J., Brady, T.L., Binder-Scholl, G., Hwang, W.T., Plesa, G., Hege, K.M., Vogel, A.N., Kalos, M., Riley, J.L., Deeks, S.G*., et al.* (2012). Decade-long safety and function of retroviral-modified chimeric antigen receptor T cells. Sci Transl Med *4*, 132ra153.

Schroder, A.R., Shinn, P., Chen, H., Berry, C., Ecker, J.R., and Bushman, F. (2002). HIV-1 integration in the human genome favors active genes and local hotspots. Cell *110*, 521-529.
Schucht, R., Coroadinha, A.S., Zanta-Boussif, M.A., Verhoeyen, E., Carrondo, M.J., Hauser, H., and Wirth, D. (2006). A new generation of retroviral producer cells: predictable and stable virus production by Flp-mediated site-specific integration of retroviral vectors. Mol Ther *14*, 285-292.
Segura, M.M., Mangion, M., Gaillet, B., and Garnier, A. (2013). New developments in lentiviral vector design, production and purification. Expert Opin Biol Ther *13*, 987-1011.
Sellers, S., Gomes, T.J., Larochelle, A., Lopez, R., Adler, R., Krouse, A., Donahue, R.E., Childs, R.W., and Dunbar, C.E. (2010). Ex vivo expansion of retrovirally transduced primate CD34+ cells results in overrepresentation of clones with MDS1/EVI1 insertion sites in the myeloid lineage after transplantation. Mol Ther *18*, 1633-1639.
Serra-Moreno, R., Zimmermann, K., Stern, L.J., and Evans, D.T. (2013). Tetherin/BST-2 antagonism by Nef depends on a direct physical interaction between Nef and tetherin, and on clathrin-mediated endocytosis. PLoS pathogens *9*, e1003487.
Shapiro, J., Machattie, L., Eron, L., Ihler, G., Ippen, K., and Beckwith, J. (1969). Isolation of pure lac operon DNA. Nature *224*, 768-774.
Sharp, P.M., and Li, W.H. (1987). The codon Adaptation Index--a measure of directional synonymous codon usage bias, and its potential applications. Nucleic Acids Res *15*, 1281-1295.
Shaw, G., Morse, S., Ararat, M., and Graham, F.L. (2002). Preferential transformation of human neuronal cells by human adenoviruses and the origin of HEK 293 cells. FASEB journal : official publication of the Federation of American Societies for Experimental Biology *16*, 869-871.
Shaw, K.L., and Kohn, D.B. (2011). A tale of two SCIDs. Sci Transl Med *3*, 97ps36.
Sheehy, A.M., Gaddis, N.C., Choi, J.D., and Malim, M.H. (2002). Isolation of a human gene that inhibits HIV-1 infection and is suppressed by the viral Vif protein. Nature *418*, 646-650.
Shokralla, S., Chernish, R., and Ghosh, H.P. (1999). Effects of double-site mutations of vesicular stomatitis virus glycoprotein G on membrane fusion activity. Virology *256*, 119-129.
Shokralla, S., He, Y., Wanas, E., and Ghosh, H.P. (1998). Mutations in a carboxy-terminal region of vesicular stomatitis virus glycoprotein G that affect membrane fusion activity. Virology *242*, 39-50.
Shou, Y., Ma, Z., Lu, T., and Sorrentino, B.P. (2006). Unique risk factors for insertional mutagenesis in a mouse model of XSCID gene therapy. Proc Natl Acad Sci U S A *103*, 11730-11735.
Sieczkarski, S.B., and Whittaker, G.R. (2003). Differential requirements of Rab5 and Rab7 for endocytosis of influenza and other enveloped viruses. Traffic *4*, 333-343.
Sleigh, M.J. (1976). The mechanism of DNA breakage by phleomycin in vitro. Nucleic Acids Res *3*, 891-901.
Sperling, J., Azubel, M., and Sperling, R. (2008). Structure and function of the Pre-mRNA splicing machine. Structure *16*, 1605-1615.
Stacey, G.N., and Merten, O.W. (2011). Host cells and cell banking. Methods Mol Biol *737*, 45-88.
Steffen, I., Liss, N.M., Schneider, B.S., Fair, J.N., Chiu, C.Y., and Simmons, G. (2013). Characterization of the Bas-Congo virus glycoprotein and its function in pseudotyped viruses. Journal of virology *87*, 9558-9568.
Stein, S., Ott, M.G., Schultze-Strasser, S., Jauch, A., Burwinkel, B., Kinner, A., Schmidt, M., Kramer, A., Schwable, J., Glimm, H.*, et al.* (2010). Genomic instability and

myelodysplasia with monosomy 7 consequent to EVI1 activation after gene therapy for chronic granulomatous disease. Nat Med *16*, 198-204.
Steven, A.C., and Spear, P.G. (2006). Biochemistry. Viral glycoproteins and an evolutionary conundrum. Science *313*, 177-178.
Stewart, H.J., Fong-Wong, L., Strickland, I., Chipchase, D., Kelleher, M., Stevenson, L., Thoree, V., McCarthy, J., Ralph, G.S., Mitrophanous, K.A.*, et al.* (2011). A stable producer cell line for the manufacture of a lentiviral vector for gene therapy of Parkinson's disease. Hum Gene Ther *22*, 357-369.
Stewart, H.J., Leroux-Carlucci, M.A., Sion, C.J., Mitrophanous, K.A., and Radcliffe, P.A. (2009). Development of inducible EIAV-based lentiviral vector packaging and producer cell lines. Gene Ther *16*, 805-814.
Stornaiuolo, A., Piovani, B., Bossi, S., Zucchelli, E., Corna, S., Salvatori, F., Mavilio, F., Bordignon, C., Rizzardi, G., and Bovolenta, C. (2013). RD2-MolPack-Chim3, a packaging cell line for stable production of lentiviral vectors for anti-HIV gene therapy. Hum Gene Ther Methods.
Strang, B.L., Ikeda, Y., Cosset, F.L., Collins, M.K., and Takeuchi, Y. (2004). Characterization of HIV-1 vectors with gammaretrovirus envelope glycoproteins produced from stable packaging cells. Gene Ther *11*, 591-598.
Stremlau, M., Owens, C.M., Perron, M.J., Kiessling, M., Autissier, P., and Sodroski, J. (2004). The cytoplasmic body component TRIM5alpha restricts HIV-1 infection in Old World monkeys. Nature *427*, 848-853.
Sun, X., Belouzard, S., and Whittaker, G.R. (2008). Molecular architecture of the bipartite fusion loops of vesicular stomatitis virus glycoprotein G, a class III viral fusion protein. J Biol Chem *283*, 6418-6427.
Sun, X., Roth, S.L., Bialecki, M.A., and Whittaker, G.R. (2010). Internalization and fusion mechanism of vesicular stomatitis virus and related rhabdoviruses. Future Virol *5*, 85-96.
Sunseri, N., O'Brien, M., Bhardwaj, N., and Landau, N.R. (2011). Human immunodeficiency virus type 1 modified to package Simian immunodeficiency virus Vpx efficiently infects macrophages and dendritic cells. Journal of virology *85*, 6263-6274.
Sutton, R.E., Reitsma, M.J., Uchida, N., and Brown, P.O. (1999). Transduction of human progenitor hematopoietic stem cells by human immunodeficiency virus type 1-based vectors is cell cycle dependent. Journal of virology *73*, 3649-3660.
Suzuki, T., Shen, H., Akagi, K., Morse, H.C., Malley, J.D., Naiman, D.Q., Jenkins, N.A., and Copeland, N.G. (2002). New genes involved in cancer identified by retroviral tagging. Nat Genet *32*, 166-174.
Svidritskiy, E., Ling, C., Ermolenko, D.N., and Korostelev, A.A. (2013). Blasticidin S inhibits translation by trapping deformed tRNA on the ribosome. Proc Natl Acad Sci U S A *110*, 12283-12288.
Tailor, C.S., Nouri, A., Zhao, Y., Takeuchi, Y., and Kabat, D. (1999). A sodium-dependent neutral-amino-acid transporter mediates infections of feline and baboon endogenous retroviruses and simian type D retroviruses. Journal of virology *73*, 4470-4474.
Tebas, P., Stein, D., Binder-Scholl, G., Mukherjee, R., Brady, T., Rebello, T., Humeau, L., Kalos, M., Papasavvas, E., Montaner, L.J.*, et al.* (2013). Antiviral effects of autologous CD4 T cells genetically modified with a conditionally replicating lentiviral vector expressing long antisense to HIV. Blood *121*, 1524-1533.
Tebas, P., Stein, D., Tang, W.W., Frank, I., Wang, S.Q., Lee, G., Spratt, S.K., Surosky, R.T., Giedlin, M.A., Nichol, G.*, et al.* (2014). Gene editing of CCR5 in autologous CD4 T cells of persons infected with HIV. N Engl J Med *370*, 901-910.
Thein, S.L. (2005). Pathophysiology of beta thalassemia--a guide to molecular therapies. Hematology Am Soc Hematol Educ Program, 31-37.

Thornhill, S.I., Schambach, A., Howe, S.J., Ulaganathan, M., Grassman, E., Williams, D., Schiedlmeier, B., Sebire, N.J., Gaspar, H.B., Kinnon, C.*, et al.* (2008). Self-inactivating gammaretroviral vectors for gene therapy of X-linked severe combined immunodeficiency. Mol Ther *16*, 590-598.
Thrasher, A.J. (2013). Progress in lentiviral vector technologies. Hum Gene Ther *24*, 117-118.
Thrasher, A.J., Hacein-Bey-Abina, S., Gaspar, H.B., Blanche, S., Davies, E.G., Parsley, K., Gilmour, K., King, D., Howe, S., Sinclair, J.*, et al.* (2005). Failure of SCID-X1 gene therapy in older patients. Blood *105*, 4255-4257.
Throm, R.E., Ouma, A.A., Zhou, S., Chandrasekaran, A., Lockey, T., Greene, M., De Ravin, S.S., Moayeri, M., Malech, H.L., Sorrentino, B.P.*, et al.* (2009). Efficient construction of producer cell lines for a SIN lentiviral vector for SCID-X1 gene therapy by concatemeric array transfection. Blood *113*, 5104-5110.
Tolar, J., Becker, P.S., Clapp, D.W., Hanenberg, H., de Heredia, C.D., Kiem, H.P., Navarro, S., Qasba, P., Rio, P., Schmidt, M.*, et al.* (2012). Gene therapy for Fanconi anemia: one step closer to the clinic. Hum Gene Ther *23*, 141-144.
Trobridge, G.D., Wu, R.A., Hansen, M., Ironside, C., Watts, K.L., Olsen, P., Beard, B.C., and Kiem, H.P. (2010). Cocal-pseudotyped lentiviral vectors resist inactivation by human serum and efficiently transduce primate hematopoietic repopulating cells. Mol Ther *18*, 725-733.
Turan, S., and Bode, J. (2011). Site-specific recombinases: from tag-and-target- to tag-and-exchange-based genomic modifications. FASEB journal : official publication of the Federation of American Societies for Experimental Biology *25*, 4088-4107.
Turan, S., Kuehle, J., Schambach, A., Baum, C., and Bode, J. (2010). Multiplexing RMCE: versatile extensions of the Flp-recombinase-mediated cassette-exchange technology. J Mol Biol *402*, 52-69.
Tuschong, L., Soenen, S.L., Blaese, R.M., Candotti, F., and Muul, L.M. (2002). Immune response to fetal calf serum by two adenosine deaminase-deficient patients after T cell gene therapy. Hum Gene Ther *13*, 1605-1610.
Uchida, N., Hsieh, M.M., Hayakawa, J., Madison, C., Washington, K.N., and Tisdale, J.F. (2011). Optimal conditions for lentiviral transduction of engrafting human CD34+ cells. Gene Ther *18*, 1078-1086.
Uchida, N., Sutton, R.E., Friera, A.M., He, D., Reitsma, M.J., Chang, W.C., Veres, G., Scollay, R., and Weissman, I.L. (1998). HIV, but not murine leukemia virus, vectors mediate high efficiency gene transfer into freshly isolated G0/G1 human hematopoietic stem cells. Proc Natl Acad Sci U S A *95*, 11939-11944.
van der Kuyl, A.C., Dekker, J.T., and Goudsmit, J. (1999). Discovery of a new endogenous type C retrovirus (FcEV) in cats: evidence for RD-114 being an FcEV(Gag-Pol)/baboon endogenous virus BaEV(Env) recombinant. Journal of virology *73*, 7994-8002.
van Rensburg, R., Beyer, I., Yao, X.Y., Wang, H., Denisenko, O., Li, Z.Y., Russell, D.W., Miller, D.G., Gregory, P., Holmes, M.*, et al.* (2013). Chromatin structure of two genomic sites for targeted transgene integration in induced pluripotent stem cells and hematopoietic stem cells. Gene Ther *20*, 201-214.
Vandepol, S.B., Lefrancois, L., and Holland, J.J. (1986). Sequences of the major antibody binding epitopes of the Indiana serotype of vesicular stomatitis virus. Virology *148*, 312-325.
Waheed, A.A., and Freed, E.O. (2010). The Role of Lipids in Retrovirus Replication. Viruses *2*, 1146-1180.
Wang, G.P., Berry, C.C., Malani, N., Leboulch, P., Fischer, A., Hacein-Bey-Abina, S., Cavazzana-Calvo, M., and Bushman, F.D. (2010). Dynamics of gene-modified progenitor

cells analyzed by tracking retroviral integration sites in a human SCID-X1 gene therapy trial. Blood *115*, 4356-4366.
Wanisch, K., and Yanez-Munoz, R.J. (2009). Integration-deficient lentiviral vectors: a slow coming of age. Mol Ther *17*, 1316-1332.
Waterhouse, A.M., Procter, J.B., Martin, D.M., Clamp, M., and Barton, G.J. (2009). Jalview Version 2--a multiple sequence alignment editor and analysis workbench. Bioinformatics *25*, 1189-1191.
Weiss, R.A., Boettiger, D., and Murphy, H.M. (1977). Pseudotypes of avian sarcoma viruses with the envelope properties of vesicular stomatitis virus. Virology *76*, 808-825.
Williams, D.A., and Thrasher, A.J. (2014). Concise review: lessons learned from clinical trials of gene therapy in monogenic immunodeficiency diseases. Stem Cells Transl Med *3*, 636-642.
Wirth, D., Gama-Norton, L., Riemer, P., Sandhu, U., Schucht, R., and Hauser, H. (2007). Road to precision: recombinase-based targeting technologies for genome engineering. Curr Opin Biotechnol *18*, 411-419.
Wu, C., Jares, A., Winkler, T., Xie, J., Metais, J.Y., and Dunbar, C.E. (2013). High efficiency restriction enzyme-free linear amplification-mediated polymerase chain reaction approach for tracking lentiviral integration sites does not abrogate retrieval bias. Hum Gene Ther *24*, 38-47.
Wu, X., Li, Y., Crise, B., and Burgess, S.M. (2003). Transcription start regions in the human genome are favored targets for MLV integration. Science *300*, 1749-1751.
Wu, X., Luke, B.T., and Burgess, S.M. (2006). Redefining the common insertion site. Virology *344*, 292-295.
Xu, K., Ma, H., McCown, T.J., Verma, I.M., and Kafri, T. (2001). Generation of a stable cell line producing high-titer self-inactivating lentiviral vectors. Mol Ther *3*, 97-104.
Xu, W., Russ, J.L., and Eiden, M.V. (2012). Evaluation of residual promoter activity in gamma-retroviral self-inactivating (SIN) vectors. Mol Ther *20*, 84-90.
Yamaguchi, I., Shibata, H., Seto, H., and Misato, T. (1975). Isolation and purification of blasticidin S deaminase from Aspergillus terreus. J Antibiot (Tokyo) *28*, 7-14.
Yang, Y., Vanin, E.F., Whitt, M.A., Fornerod, M., Zwart, R., Schneiderman, R.D., Grosveld, G., and Nienhuis, A.W. (1995). Inducible, high-level production of infectious murine leukemia retroviral vector particles pseudotyped with vesicular stomatitis virus G envelope protein. Hum Gene Ther *6*, 1203-1213.
Yee, J.K., Miyanohara, A., LaPorte, P., Bouic, K., Burns, J.C., and Friedmann, T. (1994). A general method for the generation of high-titer, pantropic retroviral vectors: highly efficient infection of primary hepatocytes. Proc Natl Acad Sci U S A *91*, 9564-9568.
Zagouras, P., Ruusala, A., and Rose, J.K. (1991). Dissociation and reassociation of oligomeric viral glycoprotein subunits in the endoplasmic reticulum. Journal of virology *65*, 1976-1984.
Zavada, J. (1982). The pseudotypic paradox. The Journal of general virology *63 (Pt 1)*, 15-24.
Zhang, L., and Ghosh, H.P. (1994). Characterization of the putative fusogenic domain in vesicular stomatitis virus glycoprotein G. Journal of virology *68*, 2186-2193.
Zhang, W., Du, J., Evans, S.L., Yu, Y., and Yu, X.F. (2012). T-cell differentiation factor CBF-beta regulates HIV-1 Vif-mediated evasion of host restriction. Nature *481*, 376-379.
Zufferey, R., Donello, J.E., Trono, D., and Hope, T.J. (1999). Woodchuck hepatitis virus posttranscriptional regulatory element enhances expression of transgenes delivered by retroviral vectors. Journal of virology *73*, 2886-2892.
Zufferey, R., Dull, T., Mandel, R.J., Bukovsky, A., Quiroz, D., Naldini, L., and Trono, D. (1998). Self-inactivating lentivirus vector for safe and efficient in vivo gene delivery. Journal of virology *72*, 9873-9880.

Zufferey, R., Nagy, D., Mandel, R.J., Naldini, L., and Trono, D. (1997). Multiply attenuated lentiviral vector achieves efficient gene delivery in vivo. Nat Biotechnol *15*, 871-875.
Zychlinski, D., Schambach, A., Modlich, U., Maetzig, T., Meyer, J., Grassman, E., Mishra, A., and Baum, C. (2008). Physiological promoters reduce the genotoxic risk of integrating gene vectors. Mol Ther *16*, 718-725.